Mathematical and fuzzy modelling of high-speed interconnections in integrated circuits.

AHMAD, Tahir.

R E F E R E N C E

Mathematical and Fuzzy Modelling of High-Speed Interconnections in Integrated Circuits

Tahir Ahmad

A thesis submitted in partial fulfilment of
the requirements of
Sheffield Hallam University
for the degree of Doctor of Philosophy

March 1998

To my parents, Hj. Ahmad b. Md. Esa & Hjh. Zauyah Bt. Budin

and my forever beloved wife who is also my best friend, Atie.

ACKNOWLEDGEMENTS

I would like to take this opportunity to extend my appreciation to several individuals who have contributed tremendously to this research.

Firstly, I would like to thank Faculty of Science, University of Technology Malaysia for sponsoring me.

Secondly, I am very grateful to my Director of Studies, Prof. A. Ray for giving me a chance to explore this new topic and for believing in me. Your encouragement, trust and friendship are really appreciated.

A salutation to my supervisor Prof. Z. Ghassemlooy who has guided me throughout my work and for being there whenever I need help and advice. My sincere gratitude to him for assisting me in every possible way.

I am debtful to Dr. Bruce Parker of Brunel University and Dr. N. Sarma of Regional Engineering College, India for their valuable assistance and discussions. The discussions were proved very useful.

I would like to thank the following students who I had supervised, Yann Michael Moyal (B. Com. Eng) and Ahmad Razzaly (M.Elec. & Elec. Eng) from France and Malaysia, respectively for their countless help and valuable suggestions .

To my dearest wife, Atie, I dedicate this achievement to her. Thank you for having the belief and confidence in me. She is the driving force throughout the entire period of my Ph.d and my life. Without your support this work might not be completed. I love you so much.

To all my colleagues in Harmer Building rooms 2413 and 2417, I would like to express my appreciation for all their supports directly and indirectly. The warm, friendly and amusing environment would certainly be missed.

To my parents and family your support and encouragement would not be forgotten.

Last but not least, my work could not be satisfied without encouragement from my "fuzzy" mentor, Prof. Lotfi Zadeh who I only met once in Aachen, Germany in 1997.

ABSTRACT

Microstrip line are the most popular interconnection type mainly due to its planar geometry. The mode of propagation is almost a transverse electromagnetic mode of wave propagation (TEM) and can be described by the Telegrapher's equations. These facts make mathematical and fuzzy modelling of microstrip lines possible.

Two types of nonuniformly coupled microstrip lines, namely, nonuniformly spaced and strictly nonuniform, are presented in this study. A new model of capacitance matrix was developed for nonuniformly spaced coupled microstrip lines. The model obtained was then translated into a Mathematica program in order to be utilised in real systems. Furthermore, a new matrix; mutual capacitance ratio matrix, was deduced from the previous model. A few valuable properties were then established from this matrix.

Novel concepts were introduced to approximate capacitance of strictly nonuniform coupled microstrip lines and Mathematica programs were coded to implement these methods. The study then continued with the development of new algorithms to calculate the time delay and characteristic impedance using capacitance matrices of both types of nonuniform lines. These algorithms finally became a generalised algorithm which could be used in any type of coupled microstrip lines, uniform and nonuniform. The time delay and characteristic impedance were later used as parameters to simulate crosstalk using SPICE.

Analysis of geometrical and electrical parameters of microstrip lines was performed mathematically and simulations modelled using the Mathematica package. Experimental work was also carried out to investigate the characteristic of crosstalk.

All information obtained from these analyses were then fed into the developed novel fuzzy model. The model was designed to minimise crosstalk and to optimise the geometrical and electrical parameters of coupled microstrip lines simultaneously. These models have the potential to become 'multi purpose on board designing tools' for a designer before the system is finally fabricated.

LIST OF FIGURES

LIST OF TABLES

LIST OF MATHEMATICAL DEFINITIONS

GLOSSARY OF SYMBOLS

$\{x_1, x_2, x_3, \ldots\}$	Set of elements $x_1, x_2, x_3, \ldots$
$\{x \mid p(x)\}$	Set determined by property p
$(x_1, x_2, x_3, \ldots, x_n)$	n-tuple
$i, j, k, \ldots$	Arbitrary identifiers (indices)
$I, J, K, \ldots$	General set of identifiers (indices)
$[x_{ij}]$	Matrix
N	Set of natural numbers / {1,2,3,...}
R	Set of real numbers
R^+	Set of positive real numbers
R^n	Set of n-tuple of real numbers
$[a,b]$	Closed interval of real numbers between a and b
$[a,b)$	Interval of real numbers closed in a and open in b
$[a,\infty)$	Set of real numbers greater than or equal to a
(a,b)	Open interval of real numbers between a and b
$(a,b]$	Interval of real numbers open in a and close in b
$(-\infty,a]$	Set of real numbers less than or equal to a
X	Univesal set
$A, B, C, \ldots$	Arbitrary sets (crisp or fuzzy)
$A=B$	Set equality
$A \neq B$	Set inequality
$A \setminus B$	Set difference

$A \subset B$	Proper set inclusion ($A \neq B$)
$A \subseteq B$	Set inclusion
$A \cap B$	Set intersection
$A \cup B$	Set union
$\varnothing$	Empty set
$f: X \to Y$	Function f from X into Y
$f^{-1}: Y \to X$	Inverse function of f from Y to X
$\Rightarrow$	Implies
$\Leftrightarrow$	If and only if
$\in$	Element of
$\notin$	Not an element of
$\ni$	Such that
$\exists$	There exist (at least one)
$\forall$	For all / for any
!.	Unique
min $[x_1, x_2, x_3, \ldots]$	Minimum of $x_1, x_2, x_3, \ldots$
max $[x_1, x_2, x_3, \ldots]$	Maximum of $x_1, x_2, x_3, \ldots$
sup A	Supremum of A
μ_A	Membership grade function of fuzzy set A
supp A	Support of fuzzy set A
α	Number in [0,1] employed to define an α - cut
$\wedge$	Intersection of two fuzzy sets
$\vee$	Union of two fuzzy sets
(D...)	Definition ...

TABLE OF CONTENTS

1. INTRODUCTION

Integrated circuit (IC) technology today is focusing on very large scale design of high-speed circuits. Research in interconnections has now become very important due to the rapid development of high speed, and high-density integrated circuits. A connection behaves like a transmission line and problems associated with transmission lines such as attenuations, distortions, signal delay, impedance matching, and particularly crosstalk arise for the interconnections. In order to understand these problems, an accurate mathematical modelling of interconnects is essential. To meet the expectations for speed and chip density, a number of issues, such as crosstalk and delay time, must be addressed before developing any design. A powerful tool available for the design engineers is mathematical modelling. This work addresses the issues involved in coupled microstrip lines and how they can be modelled, analysed and designed.

The thesis introduces the development of a mathematical model for coupled nonuniform microstrip lines in order to study their crosstalk. The theoretical basis for this development can be found in the work due to Romeo and Santomauro (1987) on time-domain simulation of n coupled transmission lines, and to Gao et al (1990) on modelling and simulation of interconnection delays and crosstalk in high speed integrated circuits.

The originality of the thesis lies in the derivation of expression for capacitance of n coupled nonuniform microstrip lines which have different dimensions and are differently spaced. The evaluation procedure is implemented using Mathematica computer packages and the effect of geometrical parameters on electrical characteristics of microstrip lines is investigated. The mathematical constraints on these geometrical parameters are then presented. A novel matrix is constructed from mutual capacitance ratios, giving physically valuable properties of eigenvalues and eigenvectors. Algorithms are developed in order to evaluate the time delay and characteristic impedance of different types of nonuniform lines. Optimisation of geometrical and electrical parameters of microstrip lines are carried out within the frame work of fuzzy logic in order to reduce the crosstalk. This model is useful for commercial implementation.

The approach adopted here is based on identifying relevant equations for the initiation of the models for coupled nonuniform microstrip lines. Geometrical and electrical parameters of the lines and crosstalk between them are investigated by performing experiments and simulation. The information obtained is analysed and then incorporated into a fuzzy model. Fuzzy modelling is undertaken in order to optimise the geometrical and electrical parameters for minimum crosstalk. The approach adopted for carrying this work is best illustrated in Figure 1.

^ *i* **aj**

=I

w 03

•— cn *an*

g

Figure 1 The Research.

The thesis is organised into nine chapters. Chapter 2 describes the structures of different types of microstrip lines with emphasis on specific applications. Necessary and important equations are written in explicit forms in Chapter 3. Mathematical notations are clearly explained. Chapter 4 introduces the concept of mathematical modelling of microstrip lines. A newly developed model for nonuniform coupled microstrip lines is presented and novel algorithms are included for computing time delay and characteristic impedance. The resulting physical parameters are then used to simulate the crosstalk between four nonuniform lines in Chapter 5. Analytical and simulated results for nonuniform lines are presented in this chapter. Experimental work on crosstalk between uniform lines is also included in this chapter and this information is used to predict the nature of crosstalk between nonuniform lines. Chapter 6 provides an overview of fuzzy set theory and presents the theoretical concepts required to develop a fuzzy model for design optimisation of microstrip lines. The formulation of fuzzy algorithms is explained in Chapter 7 as an optimisation design model with an aim to minimise crosstalk for microstrip lines. Chapter 8 presents the scope of applications of the fuzzy algorithms as a multi-purpose design tool for determining the geometrical and electrical parameters. Finally, Chapter 9 presents the conclusions of the present investigation and provides suggestions and guidelines for future work.

2. MICROSTRIP LINES

2.1 Introduction

Not many years ago electrical equipments were large physically, and constructed with electrically large discrete components. Nowadays equipments are becoming smaller and yet more efficient (Ruehli 1979), and as one can see the Japanese are in the forefront of this movement. They have developed products such as the micro walkman, the video camera, and the pocket television with physical sizes reducing each year.

This is partly due to the rapid development in technology of faster circuits (Schutt-Aine and Mittra 1989) and modern integrated circuits (Ruehli 1979). However, recent integrated circuits have delay times (signal speed) that are comparable to that of the interconnections, bringing the focus of investigation further by modelling them as transmission line (Parker 1994). Microstrip lines are the most popular interconnection methodology mainly due to their planar structure. The mode of propagation is almost a transverse electromagnetic mode of wave propagation (TEM) which may be described by Telegrapher's equations (Romeo and Santomauro 1987), making mathematical modelling of microstrip lines possible.

2.2 Microstrip Lines

Microstrip line may well become the most popular transmission line structure. The term "microstrip" is a abbreviated name for a microwave circuit configuration that is constructed by printed circuit techniques, modified where necessary to

reduce loss, reflections, and coupling. However it retains advantages in size, simplicity and reliability (Parker 1994). In general, a microstrip line is a transmission line deposited on a thin-film or thick film on dielectric substrates. Ease of fabrication by photolithographic techniques and a good range of impedances and couplings allow them to be used to interconnect a wide variety of circuit components. Harold Wheeler developed planar transmission lines (two coplanar strips) which could be rolled up in 1936 and a stripline-like structure in 1942 (Wadell 1991). Flat coaxial transmission line was first used by V.H. Rumsey and H.W. Jamieson for antenna systems during World War II (Barrett 1955). Coaxial cable was first adapted to a flat configuration using printed circuit techniques by Robert M. Barrett (Barrett 1955) at the Air Force Cambridge Research Centre, Cambridge, Massachusetts, USA. He successfully developed filters, directional couplers, matched loads and hybrids which were all constructed at 440 MHz. This technique evolved into stripline after W.W.II after the Telecommunications Division of the British Post Office issued a landmark paper with the title, "The Fundamental Research Problems of Telecommunications" in 1948 (Black and Higgins 1953). A major problem stressed in the paper was the difficulties in obtaining wire transmission lines of adequate performance in the portions of the frequency spectrum devoted to UHF television, radio relay and radar.

The first use of the microstrip line configuration was reported by engineers at the Federal Telecommunications Research Laboratories, a division of International Telephone and Telegraph Corporation sometime after 1949 (Barrett 1955). Microstrip lines have been increasingly and widely discussed ever since and

reported as early as the 1960's (Schneider 1969, Yamashita 1968). Their low-loss characteristics, compactness of structure, and ease of manufacture are particularly suited to low cost mass production techniques, especially for microwave applications where size reduction is important (Black and Higgins 1953).

Generally a microstrip line is characterised by conducting strips, large ground planes, dielectric-layer insulation, and planar geometry, as shown in Fig. 2.1. The most important geometrical parameters of a microstrip line are the width w and the height h (equal to the thickness of substrate). Also of critical importance is the relative permittivity of the dielectric substrate (sr). The thickness t of the metallic, top-conducting strip is generally of much lesser importance (Edwards 1992).

Microstrip Line

(lckness, t

Figure 2.1

A considerable amount of work has been done on the properties. classifications and applications of microstrip line and is discussed in the following subsections. Unfortunately, almost all of them dealt with uniform microstrip lines.

Recent trends in microelectronics have been driven by the need for increased packing density of devices and interconnects. The implementation of thin-film multilayer interconnects has caused the emergence of irregular geometries such as multilevel crossing metallic signal strips in orthogonal multilayer configurations. Recent developments in semiconductor manufacturing have also led to system level integration strategies allowing dense concentration of these interconnects on package and board level (Schutt-Aine 1992). Even though these interconnections are treated as uniform, the fact is they are usually nonuniform owing to physical geometrical constraints (Palusinski and Lee 1989) which are discussed in a later section. Only a small amount of theoretical work (Palusinski and Lee 1989, Schutt-Aine 1992, Protonotarios and Wing 1967, Curtins and Shah 1985, Chang 1994) have been devoted to nonuniform lines. Hence, insufficient reports are available and the majority of them only deal with a single (Schutt-Aine 1992, Curtins and Shah 1985) or 2 - coupled (Palusinski and Lee 1989) nonuniform microstrip line.

Furthermore, most of them are 'not really nonuniform' since all the lines have the same thickness (Palusinski and Lee 1989, Qian and Yamashita 1993, Curtins and Shah 1985, Orhanovic 1990). Therefore, as a result of these motivations, a new theoretical analysis on 'really nonuniform' (strictly nonuniform) is presented in Chapter 4. This is followed by a simulation to examine the crosstalk of 4 -

coupled. strictly nonuniform. microstrip lines in Chapter 5. The general classifications of microstrip lines may be described as follows.

2.2.1 Classification

There are eight basic types of microstrip transmission lines with one strip conductor supported by a dielectric substrate (Fig. 2.2). The most common is standard microstrip which is also known as open microstrip (Fig. 2.2.a).

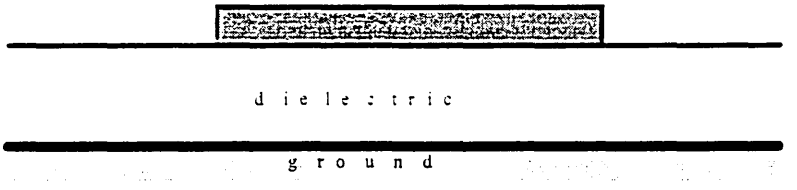

Figure 2.2.a Open microstrip.

The open microstrip line was soon abandoned by microwave designers because of the radiative nature of the open-strip line. However, the use of thin high-dielectric materials in open-strip lines greatly reduces the radiation and has been used for integrated microwave printed circuits (Stinehelfer 1968). Of the many configurations, the open microstrip appears to be the most convenient and inexpensive system for batch processing of microwave integrated circuits (Pucel et al 1968).

Proximity of the air-dielectric interface to the strip conductor can lead to excitation of plane-trapped surface waves. This problem can be solved by

utilising the embedded microstrip (Fig. 2.2.b) where the air-dielectric interface is moved into the far field region.

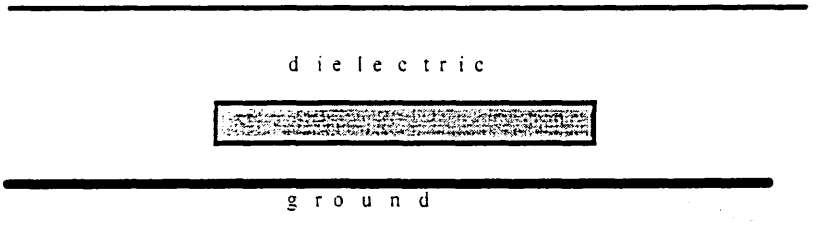

Figure 2.2.b Embedded microstrip.

If the substrate is a semiconductor, surface passivation(coating) may be necessary to protect against atmospheric contaminants. This can be achieved by a thin dielectric film as in a microstrip with an overlay (Fig. 2.2.c).

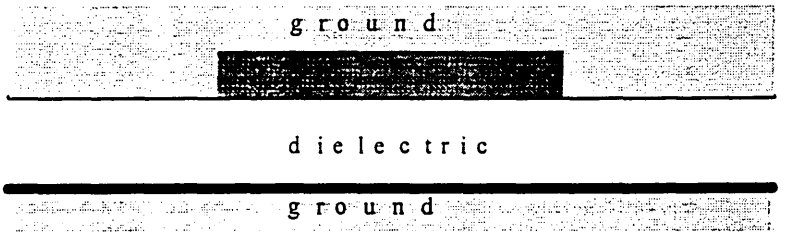

Figure 2.2.c Microstrip with overlay.

Solid-state devices with substantial heat dissipation such as IMPATT, GUNN, and LSA diodes as well as high-power varactor diodes have to be shunt-mounted in the microstrip in order to achieve a small thermal spreading resistance in the ground plane (Schneider 1969). A hole in the dielectric is required such as in the

microstrip with hole design (Fig. 2.2.d), for mounting a solid state device between the two microstrip conductors.

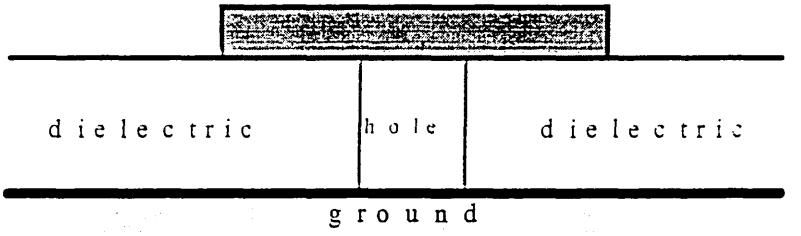

Figure 2.2.d Microstrip with hole

Other solid-state devices or materials which require shunt mounting are ferrites for circulators and isolators and high-Q dielectric resonators for microwave band-pass filters. Shunt mounting is facilitated in inverted microstrips, and suspended microstrips.

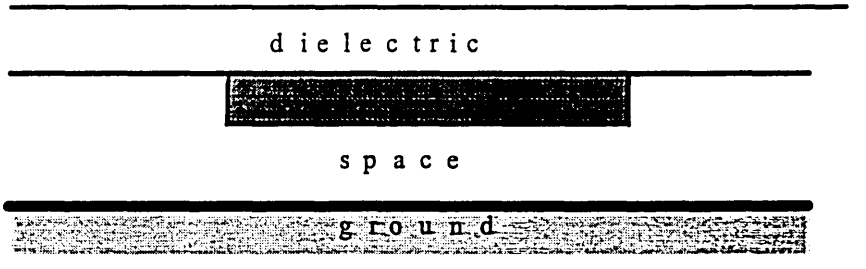

Figure 2.2.e Inverted microstrip.

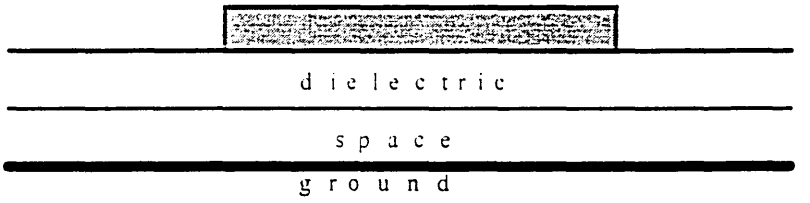

Figure 2.2.f Suspended microstrip.

Shielded microstrip or the slot transmission line can be coupled with open microstrip lines to give the widest possible choice of circuits to be built with existing hybrid integrated circuit technology.

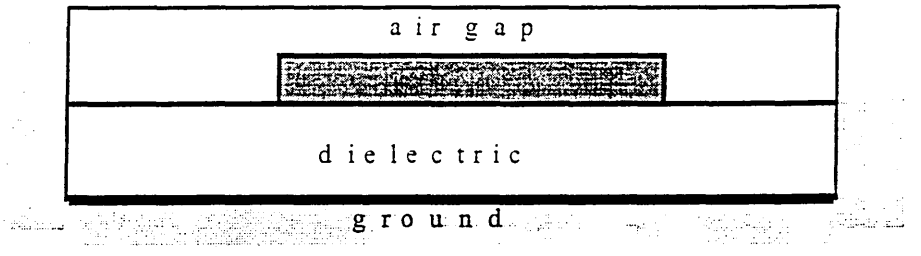

Figure 2.2.g Shielded microstrip.

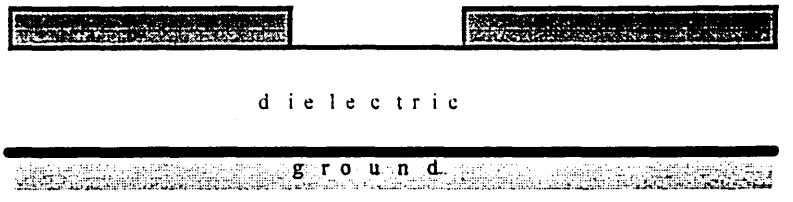

Figure 2.2.h Slot transmission line.

A major advantage of all microstrip configurations with an air gap is that the effective dielectric constant is small. This means that the effective dielectric loss tangent is substantially reduced, and since all circuit dimensions can be increased,

this leads to less stringent mechanical tolerances, better circuit reproducibility, and therefore lower production cost.

Even though microstrip line is a simple structure mechanically, it had not been analysed with reasonable accuracy until the introduction of modified conformal mapping (Wheeler 1965) and a variational method (Yamashita and Mittra 1968). The difficulties associated in modelling of this structure are:

- the dielectric boundary conditions restricting electric fields
- the electromagnetic wave cannot be considered a pure TEM because it extends over air and one or more dielectric substrates
- the circuitry may radiate at high frequencies
- if it is enclosed within a EM reflective enclosure, the waves reflect back to produce coupling and resonances.

The general classifications of microstrip lines have been deliberately tailored for certain applications as follows.

2.2.2 Application

The increasing importance of miniature planar microwave integrated circuits has renewed interest, on the part of microwave circuit designers, in the various forms of planar strip transmission line system; i.e. microstrip line. It has also been used in millimetre wave hybrid integrated circuits required for solid-state radio systems because of their simplicity and planar structure (Pucel et al 1968) and in many fast digital circuits (Djordjevic and Sarkar 1994).

Circuits built with microstrip transmission lines or microstrip components have three important advantages: (Schneider 1969)

(i) The complete conductor pattern can be deposited and processed on a single dielectric substrate which is supported by a single metal ground plane. Such a circuit can be fabricated at a substantially lower cost than waveguide or coaxial circuit configurations.

(ii) Beam-leaded active and passive devices can be bonded directly to metal stripes on the dielectric substrate.

(iii) Devices and components incorporated into hybrid integrated circuits are accessible for probing and circuit measurements (with some limitations imposed by external shielding requirements).

Double dielectric substrates have been used in the development of *large scale integrated circuits* (LSI) such as silicon-on-sapphire. Interest in insulating substrates as an alternative to silicon substrates increased considerably (Yuan et al 1982) during the early eighties to develop high-performance LSI and *very large scale integrated circuit* (VLSI) components. The widely used insulating substrates were sapphire and Cr-doped semi-insulating gallium arsenide.

2.2.3 Capacitance and inductance

The development of methods to evaluate the capacitance and inductance of microstrip lines is very closely related to the development of methods to calculate the characteristic impedance (Wheeler 1965, Wheeler 1977, Hill et al 1969, Cheng and Everard 1991, Farrar 1970, Bryant and Weiss 1968). Yamashita (1968) used the variational method in the Fourier transformed co-ordinate to calculate the

capacitance of microstrip lines. By this method, it is possible to take into account all the dielectric boundary conditions no matter how many planar boundaries exist in the lines. He started with investigating a shielded double-layer microstrip line and then derived simpler structures such as a double-layer microstrip line, a shielded microstrip line, and an ordinary open microstrip line.

Weeks (1970) refined the sub-areas method for the numerical determination of the coefficients of capacitance for a range of multiconductor transmission-line systems. His approach is purely mathematical in which basic numerical analysis tools such as the Simpson's rule has been applied to calculate the mutual and self capacitance of three different types of lines.

The problem of open-circuit capacitance was treated purely electrostatically by Silvester and Benedek (1972); Green's functions were constructed on the assumption that time retardation did not exist. In this technique, the formulation of the problem in a computable fashion resolves into two parts:

(i) determining the necessary integral equation to be solved and;

(ii) finding the Green's appropriate function.

A programme called TIC (thin-film and integrated-circuits capacitances) has been written and is based on the method of subdivisions of the conductors into rectangles (Balaban 1973). The method is very similar to that of sub-areas (Weeks 1970). A charge distribution with initial conditions (undefined parameters) is assumed over each rectangle. It is assumed that the potential is constant for each conductor and the self and mutual capacitances are computed

from the resultant charges and potentials. The programme is used to compute the capacitance values of geometrically complicated medium and high frequency circuits. Balaban (1973) introduced for the first time the lower and upper bound method for approximation of the capacitances.

A mixed order finite-element technique was used by Benedek (1976) to solve the integral equations governing the charge density distribution in a planar multiconductor configuration on a dielectric sheet. The method was then implemented in a package called PARCAP to calculate the capacitance, which were in agreement with measured values. Dividovitz (1991) further improved the technique by introducing the semidiscrete finite element method to compute the capacitance of multiconductor microstrip lines.

Harms and Mittra (1993) extended the T-equivalent circuit used for single-line microstrip bends to variable-angle, multiconductor, microstrip bend. These techniques were employed to obtain the capacitance and inductance matrices and at the same time effectively avoid the majority of numerical difficulties that occurred in accounting for the infinite extent of the microstrip lines making up bends with arbitrary bend angles. The study confirmed the effect of bend on capacitance and inductance of microstrip lines which in turn effects the digital pulse propagation along the line. On the other hand, quite recently Dinh et al (1992) revitalised the original concept based on an impedance-admittance transformation and on an equivalent circuit to calculate the capacitance and inductance of microstrip lines. It was assumed that the line has a lossless dielectric layer.

Capacitance and inductance are the main elements in determining the characteristic impedance of a microstrip line. These two parameters will be discussed in greater detail in the subsequent two chapters.

2.2.4 Characteristic impedance

There is a strong market demand for high speed communication links which require access to ultra-fast switching circuits with high density onchip and interchip interconnections. The recent advances in integrated circuit technology have increased the speed of a single device to the multi-giga hertz region. In such an environment the transmission line property of the IC interconnection plays a major role which cannot be ignored. In such conditions inter conductor crosstalk can cause false switching and, therefore, needs closer examination.

The calculation of crosstalk parameters, and the consequent determination of minimum acceptable line separation and/or line length, depend on a knowledge of the even-mode and odd-mode characteristic impedances of the lines concerned. The same data are also required in the closely related microwave problem of directional-coupler design.

There is a vast amount of literature leading to methods of calculating characteristic impedance. Wheeler (1965, 1977) introduced conformal mapping technique, Bryant and Weiss (1968) treated the problem by the use of a Green's function, Hill et al (1969) combined the Green function with a subinterval technique, Farrar (1970) used the method of moments, John and Arlett (1974) used Schwarzmann's equations to produce a very simple equation for

characteristic impedance, and Cheng and Everard (1991) recently pointed to a new method based on the spectral-domain approach.

The effect of strip thickness on characteristic impedances of a microstrip line must be taken into account when evaluating circuit performance such as crosstalk (Gunston and Weale 1969). The thickness affects both the impedance of the line and its time delay, both decreasing as the strip gets thicker. This relationship is explained by the fact that as the line gets thicker, the field is made to propagate on the surface of the line. This also increases the total capacitance of the line which in turn reduces the characteristic impedance. The loss per wavelength increases with thickness of the centre conductor (Stinehelfer 1968).

A new computational approximation method of characteristic impedance for coupled nonuniform microstrip lines is developed in Chapter 4. It is part of the mathematical modelling and will be used for simulation of microstrip lines in Chapter 5.

In any complex systems, static or dynamic, there are always constraints, which a designer has to deal with. The following sections discuss the sources of constraints associated with coupled microstrip lines.

2.3 Constraints

A coupled microstrip lines is a static system and will be discussed more elaborately in Chapter 4. Nevertheless, its constraints are mainly due to:

(i) general initial physical system lay out, and

(ii) crosstalk.

2.3.1 Physical

Some of the physical constraints when designing a microstrip line are:

- The thickness of the finished board is determined by system requirements (connectors, card guides, etc).
- The layers of the layout must be made symmetric about the centre line.
- Different thickness of dielectric or metallization on either side of the PC (printed circuit) board centre line can cause board warpage.
- Inner layer dielectric thickness must be at least 1.5 times as large as the sum of the opposing metallization thickness (Wadell 1991).
- The inner layers must also have sufficient space to fill the bumps created by the PC traces when the layers are compressed.
- Only a finite number of conducting and dielectric substrates materials are available off-the-shelf (Wadell 1991).

The main problem in all microstrip design is to evaluate the physical dimensions of width, length, height, and thickness of the microstrip lines (Edwards 1992) which will have a significant effect on crosstalk.

2.3.2 Crosstalk

Crosstalk by definition refers to *the unintended electromagnetic coupling between wires and PCB lands that are in close proximity.* Although the phenomenon is

due to the currents and voltages of the wires and is thus similar to the problem of antenna coupling. crosstalk is distinguished from the latter in that is a near-field coupling problem. Crosstalk between wires in cables or between lands in PCBs defines the intrasystem interference performance of the product; that is, the source of the electromagnetic emission and the receptor of this emission are within the same system (Paul 1992).

In designing interconnecting transmission lines, in particular microstrip lines, crosstalk is one of the three main characteristics that needs to be predicted and controlled. For example, in order to design an interconnection system for nanosecond-risetime logic circuitry, it is necessary to obtain a balance between impedance variations, propagation velocities and crosstalk. Therefore, it is essential to relate the electrical material properties as well as physical dimensions (configurations) of the connections to crosstalk phenomena.

A new computational method called multiple-image/subintervals (MISI) was introduced by Hill et-al (1969) to calculate the crosstalk coupling coefficients for open microstrip lines which can be also used for triplate line configurations. This technique avoids approximate boundary conditions and uses strictly Dirichlet boundary conditions. In this method, the coupling coefficient decreases as the line spacing-to-width ratio increases. This may also be interpreted as an increase in spacing causes a decrease in coupling, since the width of lines was constant. This result is confirmed by Seki and Hasegawa (1984). Qian and Yamashita (1993) showed that the crosstalk decreases when the width of the lines are nonuniform and widely spaced.

Assuming TEM mode propagation along microstrip lines, Stinehelfer (1968) suggested that the width of lines must be smaller than a half wavelength in order to minimise crosstalk.

Seki and Hasegawa (1984) concluded in their paper that the length, spacing, and termination conditions of interconnection, substrate thickness, and output impedance of gates have large and complicated effects on crosstalk. Shielded/screened lines may reduce crosstalk (Rizvi and Vetri 1996), but there is a risk of dynamic ringing , and limited wiring capacity since it doubles the spacing between lines. It can also imply a reaction of the shielded lines on the active lines and a distortion of the signals propagating on these lines (Chilo and Arnaud 1984).

A shielded multilevel interconnect (Seki and Hasegawa 1984) was then proposed to reduce crosstalk as well as ringing without reduction of wiring capacity. It also facilitates timing and layout design. Dielectric overlays (Fig. 2.2.c) are a further possible alternative to reduce crosstalk but, like close shielding (Fig. 2.2.g), can be difficult to design and control under production conditions (Edwards 1992). Rizvi and Vetri (1996) showed that selective use of a dielectric substrate (multiple dielectric substrates) beneath the microstrip lines also can reduce crosstalk. However, this technique is also difficult to produce. A possible solution to the problem of reflections is to decrease the length of the interconnections by increasing the system density. This trend toward greater density, however, increases the problem of crosstalk too (Palusinski and Lee 1989).

Parker et-al (1994) studied the crosstalk characteristics between the interconnection of eight uniform lines on high-speed digital circuits using the SPICE (Simulation Program with Integrated Circuit Emphasis), circuit simulator. They concluded that crosstalk decays gradually in a non-linear fashion with increasing distance from the activated lines, and supports the claim made earlier by Hill et al (1969), Seki and Hasegawa (1984). In the case of two lines being activated, an increase in crosstalk is seen on the lines between them, but little or no change in crosstalk is seen on the other lines, when compared to the case of a single line.

There has been further work on minimisation of crosstalk. Coekin (1975) has pointed out that crosstalk can be halved if a grounded conductor strip can be interposed between two signal carrying runs of microstrip lines. Further halving crosstalk can be achieved if the interposed strip can actually be connected through to the ground plane via close-spaced plated-through holes (Edwards 1992). This fact is confirmed in Chapter 5.

Porthecary and Railton (1991) proposed the finite difference technique to produce pulse shaping as an alternative way of reducing crosstalk. However, the work is at an early stage and requires a large number of different pulses to be further investigated.

Zhang et al (1992) introduced an optimisation technique to minimise crosstalk, delay and reflection simultaneously in high-speed VLSI interconnects. This technique demonstrates significant reductions of crosstalk, delay, distortion and

reflection at all vital connection ports. It is an important step towards optimal design of circuit interconnects for high-speed digital computers and communication systems.

Crosstalk is getting ever harder to eliminate because of the increasing number of interconnections on a chip. Other than the optimisation described above, another way to alleviate this would be to have several small, simple processors on a chip instead of one big, intricate one, but in the end more basic redesign; i.e. modelling may be needed (Science and Technology 1998).

In order to model crosstalk, it is important to understand the analysis of two-conductor transmission lines (Fig 2.3) since for such a transmission line there is no crosstalk. In order to have crosstalk, we must have three or more conductors (Paul 1992). Therefore in our studies, we must have two or more parallel microstrip lines.

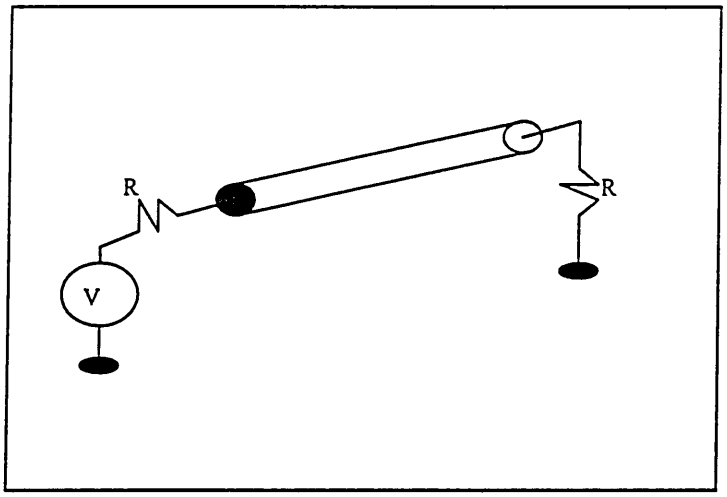

Figure 2.3 A two-conductor line.

Several researchers (Edwards 1992. Okugawa and Hagiwara 1970) have advocated the use of the well-established expression (2.1) to model crosstalk:

$$C_T = \frac{Z_{0e} - Z_{0o}}{Z_{0e} + Z_{0o}} \qquad (2.1)$$

where Z_{0e}. Z_{0o} are the even and odd modes of characteristic impedance used to model crosstalk. However, there are two problems in using the model:

(i) data for Z_{0e} and Z_{0o} are difficult to obtain; and

(ii) even if these data can be obtained, notably by computer-oriented work of Bryant and Weiss (1968), there has been some debate about their accuracy.

Therefore, for these reasons, the expression for crosstalk used by Parker et al (1994) is adopted in the studies. The remaining part of this chapter discusses microstrip line design structure, a topic researched by many workers (Akhtarzad et al 1975, Kajfez and Govind 1975, Kirschning and Jansen 1984, Lange 1969, Dydyk 1990).

2.4 Structure Design

The design of the structure is centred around the mid-band coupling factor (Edwards 1992);

$$C' = 20\log\left|\frac{Z_{0e} - Z_{0o}}{Z_{0e} + Z_{0o}}\right| \qquad (2.2)$$

and impedance relationship;

$$Z_0^2 \approx Z_{0e} Z_{0o} . \qquad (2.3)$$

From equations 2.2 and 2.3 the even and odd characteristic impedances are given by;

$$Z_{0e} \approx Z_0 \sqrt{\frac{1+10^{C'/20}}{1-10^{C'/20}}} \qquad (2.4)$$

$$Z_{0o} \approx Z_0 \sqrt{\frac{1-10^{C'/20}}{1+10^{C'/20}}} . \qquad (2.5)$$

The outline of design procedures are summarised as follows:

2.4.1 $C' \leq -3$ dB

(a) Provided the coupling is loose enough for eqn. 2.3 to hold with sufficient accuracy, then eqns. 2.4 and 2.5 give the required characteristic impedances (Edwards 1992):

Even mode: $$Z_{0e} = Z_0 \sqrt{\frac{H}{Q}} \qquad (2.6)$$

Odd mode: $$Z_{0o} = Z_0 \sqrt{\frac{Q}{H}} \qquad (2.7)$$

where $H = 1 + 10^{C'/20}$ and $Q = 1 - 10^{C'/20}$, and the coupling factor C' is directly substituted as '-C' dB' since eqn. 2.2 is always positive because of its absolute value. The substitution is necessary to produce the correlation with crosstalk which is always measured and expressed in negative dB in value.

(b) An approximate synthesis is then performed using the method proposed by Akhtarzad et al (1975). It is likely that the discrepancies in the region of 10 % will arise in this process, which yields initial values of the 'shape ratios' w/h and s/h.

(c) These initial values can then be used to determine the corresponding impedances, Z_{0e} and Z_{0o}. If higher accuracy is required, then the computational method developed by Bryant and Weiss (1968) may be used. Some adjustment for finite conductor thickness may sometimes be necessary.

(d) The new values obtained in (c) are then compared with the original requirements, determined at stage (a), and discrepancies are noted. Shape ratios w/h and s/h can now be adjusted slightly to correct the impedances, and hence the coupling factor C', to the desired values. It will usually be best if spacing, s, alone is slightly altered, since the resulting mismatch to the feed lines will be small.

Spacing affects the odd mode more than the even mode; increasing s means that more field is within the (air) coupling gap and Z_{0o}. As a rough approximation

x % change in s results in $x/10$ % change in Z_{0o}. Finally, the value of the mid-band coupling factor given by eqn. 2.2 must be checked for accuracy (Edwards 1992).

2.4.2 $C' \geq -3$ dB

The problems of unequal even and odd mode wave velocities worsen rapidly as the coupling increases, e.g. the approximation of eqn. 2.3 becomes poor when $C' > -3$ dB. There is an exact expression for Z_0 which takes into account the even and odd modes electrical lengths θ_e and θ_o, respectively, given as (Edwards 1992):

$$Z_0^2 = Z_{0e} Z_{0o} \frac{Z_{0e} \sin\theta_e + Z_{0o} \sin\theta_o}{Z_{0e} \sin\theta_o + Z_{0o} \sin\theta_e} \tag{2.8}$$

However, in order to find θ_e and θ_o one needs to know the geometry of the structure. One approach could be:

(a) Carry through a rough, first order synthesis using eqn. 2.3, hence determining an initial value of w/h and s/h.

(b) Calculate approximate values of θ_e and θ_o and effective microstrip permittivities, $\varepsilon_{effe,o}$, (Edwards 1992) using the values obtained in step (a). The electrical length ($\theta_{e,o}$) of a microstrip line is given by:

$$\theta_{e,o} = \frac{2\pi l}{\lambda_g}\sqrt{\varepsilon_{effe,o}} \qquad (2.9)$$

where l is the physical length of the microstrip and λ_g is the wavelength.

An approximate value of Z_0 is then obtained using eqn. 2.8. If Z_0 differs from that of the feed lines by an unacceptable amount, then the width w of the microstrip lines should be altered to compensate. However, altering w will alter Z_{0e}, Z_{0o}, θ_e and θ_o; thus the procedure must be iterated to find the optimum value of w.

(c) The evaluation of w must also ensure that the required mid-band coupling factor (2.2) is obtained.

(d) Having used the above procedure and obtained the parameter values, the final values of Z_{0e} and Z_{0o} are then used for the synthesis.

(e) Finally, for close coupling, the effect of finite microstrip thickness which is often significant should be taken into account.

2.4.3 Wavelength

In a directional coupler the coupled region extends for one quarter of a wavelength at mid-band and the designer requires the physical length of this region. Since, in a microstrip, we are faced with the problem of different phase velocities,

applicable to both even and odd modes. then the wavelengths associated with these modes must be considered as given below:

$$\lambda_{ge} \approx \frac{300}{F}\frac{Z_{0e}}{Z_{01e}} \tag{2.10}$$

and

$$\lambda_{go} \approx \frac{300}{F}\frac{Z_{0o}}{Z_{01o}} \tag{2.11}$$

where F is the frequency in megahertz and Z_{0e} and Z_{0o} are the even and odd mode characteristic impedances for the coupled microstrips with a substrate respectively. Z_{01e} and Z_{01o} are the even and odd mode characteristic impedances for the air-spaced microstrips respectively. The average value of wavelength is given as (Edwards 1992):

$$\lambda_{gm} \approx \frac{1}{2}(\lambda_{ge} + \lambda_{go}) \tag{2.12}$$

However, a weighted-average method (Kajfez and Govind 1975) can be used for further improved accuracy of the wavelength estimation.

2.4.4 Frequency characteristics

There are two fundamental effects governing the frequency dependent behaviour of coupled microstrips:

a) the basic frequency response of any pair of parallel-coupled lines (neglecting any dispersion)

b) the effect of microstrip dispersion (Edwards 1992).

Great care must be taken when using the fairly complicated expressions involving effective permmitivity (ε_{effe}) given as:

$$\varepsilon_{effe}(f) = \varepsilon_r - \frac{\varepsilon_r - \varepsilon_{effe}}{1 + G_e(f / f_{pe})^2} \tag{2.13}$$

with

$$f_{pe} = \frac{Z_{0e}}{4\mu_0 h} \tag{2.14}$$

and

$$G_e = 0.6 + 0.0045 Z_{0e}\,. \tag{2.15}$$

f, μ_0, ε_r and h are the frequency, permeability of vacuum, dielectric constant and height of dielectric substrate respectively.

Although it appears that the even mode electrical length θ_e may be evaluated 'fairly accurately' using (2.13) and

$$\theta_e = 2\pi l / \lambda_{ge}, \tag{2.16}$$

there is evidence that the odd-mode calculation overestimates changes in $\varepsilon_{effe}(f)$ (Edwards 1992). For better accuracy, particularly for high frequencies (0 - 30 MHz) the equations proposed by Kirchning and Jansen should be adopted (Kirschning and Jansen 1984).

2.4.5 Crosstalk and coupling factor

The expression for crosstalk (2.1) is identical to the coupling factor. Although several alternative methods to reduce crosstalk have been reported and are discussed in Section 2.3.2, the technique invented by Lange (1969) still yields an electrical performance which is generally superior to that of its closest rivals. The main disadvantage is the requirement for short wire connections. A design procedure now exists for the 'Lange coupler' and combinations of Lange couplers have been built covering a wide frequency range of 2 - 18 GHz. The design repeatability of such couplers is generally ± 0.05 dB, on the coupling factor, that is $\pm 2.5\mu m$ excursions in coupling gaps which results in $\pm$ 0.1dB changes in the coupling factor.

Of the other techniques which have been developed the end-connected compensating lumped capacitor is possibly the next best (Dydyk 1990). However, when a tight or fairly tight coupling factor is required (i.e. $C' \geq -3$dB) the already narrow coupling gap makes it difficult to incorporate the lumped capacitive structures.

Closely shielded (Fig. 2.2.g) couplers may be used in some instances but, to achieve good compensation, the close proximity of the shield to the circuit can cause ringing and distortion of signals.

2.4.6 Post manufacture adjustment

If a completed coupled line circuit requires adjustment, then this can be achieved by etching or laser trimming. However, changing s or w slightly will alter the impedances and hence the coupling factor. It will generally be necessary to alter both w and s at the same time so that the correct impedance relationships are preserved. For example, if s is increased by 1 % then Z_{0o} will also increase by approximately 0.1 %. Therefore w/h should be increased slightly by less than 1 % to reduce the impedance again (Edwards 1992).

These design procedures are complicated. Therefore the need for a new and revolutionary method to evaluate the physical/geometrical characteristics is of prime importance. This work has set out to produce such a novel method based on fuzzy logic which is explained in later chapters.

3. MATHEMATICAL BACKGROUND

3.1 Introduction

This chapter introduces relevant mathematical equations required throughout this work. These equations represent the physical meaning of the lines, i.e. electrical and geometrical parameters, which have been rewritten as mappings. These mappings are compact and will give significant clarity and precision to the equations. The chapter begins with an expression for the impedance of a single microstrip line and then moves on to coupled microstrip line.

3.2 Impedance of a Single Microstrip Line

The earlier published works on a single microstrip line show the characteristic impedance Z_{om} in terms of line width w, dielectric constant ε_r, and the height of the line above the ground plane h, as (Schneider 1969, Wheeler 1965, Parker 1994, Hammerstad 1975):

$$Z_{om} = \frac{60}{\sqrt{\varepsilon_{re}}} \ln\left(\frac{8h}{w} + 0.25\frac{w}{h}\right) \quad \text{for } \frac{w}{h} \leq 1 \tag{3.1}$$

$$Z_{om} = \frac{120\pi}{\sqrt{\varepsilon_{re}}}\left[\frac{w}{h} + 1.393 + 0.667\ln\left(\frac{w}{h} + 1.444\right)\right]^{-1} \quad \text{for } \frac{w}{h} \geq 1 \tag{3.2}$$

where the effective dielectric constant ε_{re} is

$$\varepsilon_{re} = \frac{\varepsilon_r + 1}{2} + \frac{\varepsilon_r - 1}{2} f(w/h) \tag{3.3}$$

$$\text{and } f(w/h) = \begin{cases} (1+12h/w)^{-1/2} + 0.04(1-w/h)^2 & \text{for } \dfrac{w}{h} \geq 1 \\ (1+12h/w)^{-1/2} & \text{for } \dfrac{w}{h} \leq 1 \end{cases}. \tag{3.4}$$

Recently published materials have also included the line thickness t in the impedance equation given as (Bahl and Garg 1977):

$$Z_{om} = \frac{60}{\sqrt{\varepsilon_{re}}} \ln\left(\frac{8h}{W_e} + 0.25\frac{W_e}{h}\right) \quad \text{for } \frac{w}{h} \leq 1 \tag{3.5}$$

$$Z_{om} = \frac{120\pi}{\sqrt{\varepsilon_{re}}}\left[\frac{W_e}{h} + 1.393 + 0.667\ln\left(\frac{W_e}{h} + 1.444\right)\right]^{-1} \quad \text{for } \frac{w}{h} \geq 1 \tag{3.6}$$

where the effective width, W_e is

$$\frac{W_e}{h} = \begin{cases} \dfrac{w}{h} + \dfrac{1.25t}{\pi h}\left(1 + \ln\left(4\pi w/t\right)\right); & \text{for } \dfrac{w}{h} \leq \dfrac{1}{2\pi} \\ \dfrac{w}{h} + \dfrac{1.25t}{\pi h}\left(1 + \ln\left(2h/t\right)\right); & \text{for } \dfrac{w}{h} \geq \dfrac{1}{2\pi} \end{cases} \tag{3.7}$$

and

$$\varepsilon_{re} = \frac{\varepsilon_r + 1}{2} + \frac{\varepsilon_r - 1}{2} f(w/h) - E \tag{3.8}$$

such that

$$E = \frac{\varepsilon_r - 1}{4.6}\frac{t/h}{\sqrt{w/h}} = \frac{t(\varepsilon_r - 1)}{4.6\sqrt{hw}}. \tag{3.9}$$

The inclusion of the thickness of microstrip line, t, contributes to accuracy in evaluation of all electrical parameters since the characteristic impedance is one of the main elements in them. The electrical parameters of microstrip lines are fringe capacitance, gap capacitance in air, capacitance value due to electric flux, gap capacitance, modified fringe capacitance and mutual capacitance.

3.3 Fringe Capacitance

The fringe capacitance of the microstrip and the ground plane is given as (Gupta et al 1979) (Figure 3.0):

$$C_f = 0.5\left[\frac{\sqrt{\varepsilon_{re}}}{cZ_{om}} - \varepsilon_0\varepsilon_r\frac{w}{h}\right] \tag{3.10}$$

where ε_0 is permittivity of free space (Wadell 1991):

$$\varepsilon_0 = 8.854183\times10^{-12}\ \text{F/m} \tag{3.11}$$

All the geometrical parameters are parameters of fringe capacitance except the spacing of lines, s. The equations for impedance and fringe capacitance are functions, and they are the main elements in other electrical parameter equations.

Magnetic Wall

(a) Even mode capacitances.

Electric Wall

(b) Odd mode capacitances.

Figure 3.0 Electrical parameters (a) even mode capacitances (b) odd mode capacitances.

Keys for figure 3:

Er	Dielectric
cf	Fringe capacitance with no neighbouring line
CP	Parallel plate capacitance
c>	Modified fringe capacitance
Cga	Gap capacitance in air
Cgd	Capacitance due to electric flux

The modified fringe capacitance is a fringe capacitance which takes into account the spacing between lines.

3.4 Modified Fringe Capacitance

Let R denotes a set of all real numbers and R^n is a set of all n tuples of real numbers, ie; $R^n = \{(a_1, a_2, \ldots, a_n): a_i \text{ is a real number}\}$. The modified fringe capacitance of a single line due to the presence of another line can be considered as a mapping (Gupta et al 1979) (Figure 3.0):

$C'_f : R^5 \rightarrow R$ such that

$$C'_f(\varepsilon_r, t, w, h, s) = \frac{C_f}{1 + A(h/s)\tanh(10s/h)}\sqrt{\frac{\varepsilon_r}{\varepsilon_{re}}} \tag{3.12}$$

where the fringe capacitance with no neighbouring line C_f, is

$$C_f = \frac{1}{2}\left[\frac{\sqrt{\varepsilon_{re}}}{cZ_{om}} - \varepsilon_0\varepsilon_r\frac{w}{h}\right] \tag{3.13}$$

$$A = e^{-0.1e^{2.33-2.53w/h}}$$

with c is the speed of light in a vacuum taken as $c = 2.99792456 \times 10^8\,\mathrm{m/s}$.

3.5 Gap Capacitance in Air

The gap capacitance in air of microstrip lines can be considered as a mapping (Gupta et al 1979) (Figure 3.0):

$C_{ga}: R^3 \rightarrow R$ such that

$$C_{ga}(s,h,w) = \begin{cases} \frac{\varepsilon_0}{\pi} \ln\left(2\frac{1+\sqrt{k'}}{1-\sqrt{k'}}\right) & \text{for } 0 \le k^2 \le 0.5 \\ \pi\varepsilon_0 / \ln\left(2\frac{1+\sqrt{k'}}{1-\sqrt{k'}}\right) & \text{for } 0.5 \le k^2 \le 1 \end{cases} \quad (3.14)$$

where

$$k = \frac{s/h}{(s/h)+2(w/h)} \text{ and } k'^2 = 1-k^2 \quad (3.15)$$

It is clear from (3.14) that C_{ga} depends on the spacing, height and the width of lines.

3.6 Capacitance Value due to the Electric Flux

The capacitance due to electric flux can be considered as a mapping (Gupta et al 1979) (Fig. 3.0):

$C_{gd}: R^5 \rightarrow R$ such that

$$C_{gd}(\varepsilon_r,t,w,h,s) = \frac{\varepsilon_0\varepsilon_r}{\pi} \ln\left[\coth\left(\frac{\pi s}{4h}\right)\right] + 0.65C_f\left[\frac{0.02}{s/h}\sqrt{\varepsilon_r} + (1-\frac{1}{\varepsilon_r^2})\right] \quad (3.16)$$

3.7 Gap Capacitance

The gap capacitance of microstrip lines can be considered as a mapping (Gupta et al 1979):

$C_{gt}: R^2 \rightarrow R$ such that

$$C_{gt}(t,s) = 2\varepsilon_0 \frac{t}{s} \tag{3.17}$$

3.8 Mutual Capacitance

Finally, the mutual capacitance of a coupled microstrip lines is a composition of equations (3.12) - (3.17):

$C_{ij}: R^5 \rightarrow R$ such that

$$C_{ij}(\varepsilon_r, t, w, h, s) = \frac{1}{2}\left[C_{ga} + C_{gd} + C_{gt} - C'_f\right] \tag{3.18}$$

All the electrical parameters are composed into a matrix which we may call the capacitance matrix, C. The inductance matrix is then deduced from the capacitance matrix, followed by the characteristic impedance and time delay matrices. The next section introduces some general features of matrices.

3.9 Matrix

Some of classifications of matrices which will be used in both the C and L matrices and fuzzy theory are outlined as follows:

(D 3.1) A square matrix $A=[c_{ij}]$ is a tridiagonal matrix if $c_{ij}=0$ for $|i-j|>1$

(D 3.2) A square matrix A is called a symmetric matrix if $A^T = A$

(D 3.3) A square matrix $A=[a_{ij}]$ is called a Toeplitz matrix if each entry is equal diagonally.

i.e.
$$a_{11}=a_{22}=\ldots=a_{nn};$$
$$a_{12}=a_{23}=\ldots=a_{(n-1)n};$$
$$a_{21}=a_{32}=\ldots=a_{n(n-1)};$$
$$\ldots$$

(D 3.4) The symmetric matrix A and the corresponding quadratic form $Q(x)=x'Ax$ are said to be:

1. positive definite if (any of the conditions)

   $Q(x)>0, x \neq 0 \Leftrightarrow$ all eigenvalues, $\lambda_K > 0 \Leftrightarrow$ all $\det A_k \geq 0$;

2. positive semidefinite if $Q(x) \geq 0 \Leftrightarrow$ all $\lambda_K \geq 0$;

3. indefinite if Q assumes positive and negative values $\Leftrightarrow A$ has positive and negative eigenvalues;

4. A and Q are negative definite $\Leftrightarrow -A$ and $-Q$ are positive definite (Rade and Westergren 1988).

3.9.1 Capacitance and inductance matrices

With the assumptions of the *transverse electromagnetic mode* (TEM) of wave propagation, the distribution of voltages and currents along a set of n coupled

lossless microstrip lines is given by the generalized Telegrapher's equations earlier in thesis:

$$\begin{bmatrix} v^x(x,t) \\ i^x(x,t) \end{bmatrix} = -\begin{bmatrix} 0 & L \\ C & 0 \end{bmatrix} \begin{bmatrix} v^t(x,t) \\ i^t(x,t) \end{bmatrix} \tag{3.19}$$

where vectors $v(x.t)$ and $i(x.t)$ denote voltages and currents, respectively. L is the per unit length (PUL) inductance matrix and C is the PUL capacitance matrix. Superscripts x and t denote differentiation of signals with respect to space and time, respectively. Distance and time are denoted by x and t and the capacitance matrix is given as (Romeo and Santomauro 1987):

$$C = \begin{bmatrix} c_{11} & -c_{12} & \cdots & -c_{1n} \\ -c_{21} & c_{22} & \cdots & -c_{2n} \\ \vdots & \vdots & \vdots & \vdots \\ -c_{n1} & -c_{n2} & \cdots & c_{nn} \end{bmatrix} \text{ with } c_{ii} = c_{i0} + \sum_{\substack{j=1 \\ j \neq i}}^{n} c_{ij} \tag{3.20}$$

where c_{i0} is the capacitance PUL of line i with respect to ground, c_{ij} is the capacitance PUL between line i and j, i.e. mutual capacitance, and c_{ii} is the self-capacitance PUL of line i.

The inductance matrix of the lines is given as below (Romeo and Santomauro 1987):

$$L = \mu_0 \varepsilon_0 C_0^{-1} \tag{3.21}$$

where C_0 is the capacitance matrix for the same set of lines with dielectric replaced by a vacuum and $\mu_0 = 4\pi \times 10^{-7} H/m$ is the permeability of free space (Wadell 1991).

4 MATHEMATICAL MODELLING OF MICROSTRIP LINES

4.1 Introduction

Current mathematical equations for uniform microstrip lines have been explained systematically in Chapter 3. The purpose of this chapter is to propose a generalised model for a coupled microstrip lines system, both uniform and non-uniform. It will be used as a foundation for the present study.

The chapter begins with a brief review of the concepts of a system and its model. Microstrip lines are then introduced as a physical model and relevant mathematical equations are written in order to simulate crosstalk. The chapter concludes by presenting a novel algorithm to compute time delay and the characteristic impedance of coupled microstrip lines of different types.

4.2 System

A system is *a collection of things which are related in such a way that it makes sense to think of them as a whole* (Dorny 1975). A set of coupled microstrip lines (Fig. 4.3) is an example of a system. Microstrip lines have constraints as discussed in Chapter 2. These constraints lead to modelling (Carlin 1973). A model itself is neither science nor mathematics, but a way of putting all the constraints together (Bender 1978, Wang 1997) and mimics relevant features of the system, the microstrip system, being studied.

4.3 Modelling

The principal rationale for modelling a system is a desire to determine the method for the system design and predict its performance characteristic without experimenting upon with the actual system. Then a designer may use models to modify the design in order to meet a required set of specifications, and to evaluate the nature of the interaction of the system with other systems. No model is truly a perfect one unless all parameters of a real system are taken into account. In some models, certain simplifying assumptions can be made provided their effects are insignificant (Bender 1978).

There are three main stages in building a model of a system.

i) Problem formulation.

ii) Model formulation.

iii) Application of the model.

In the first stage, a designer formulates all questions related to the system that needs to be answered by the model. The model information is then identified in three parts: information which need to be neglected (unimportant), information as input (exogenous) and the output (endogenous) of the model. These are illustrated in Fig. 4.1.

At the second stage, a designer may reduce the number of different concepts by making assumptions in order to conceive the system in simpler terms. A complex system will necessitate a vast number of assumptions. If the assumptions are too arbitrary, the model gets divorced from reality and if it is too precise the solution

of the model become unrealitiscally difficult. Models depending only on special assumptions are, on the other hand, very fragile.

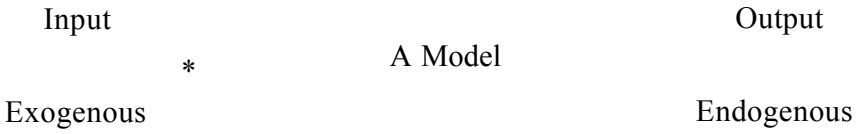

Figure 4.1 Components of a model.

Basically, there are two classes of models: physical and mathematical. They will be used to represent an actual microstrip lines as shown in Fig. 4.2. In the former model the system is presented in a simplified form, e.g. a set of coupled microstrip lines, see Fig. 4.3. System descriptions and all its constraints are carried out mathematically in the second model.

4.4 Mathematical Modelling

There are several advantages in modelling a system mathematically (Bender 1978):

a) ability to manipulate the mathematical language;

b) availability of large number of theorems;

c) availability of high speed computers.

It is the clearest of all models used in science and technology that follow physical laws (Terano et al 1987). Statistical, structural and predicate logic are three

widely used types of mathematical models. However, a statistical model requires a large amount of data and for this reason, only the later two are adopted in this work.

4.4.1 Structural modelling

A structural model is usually presented graphically. It is also sometimes called a logical model. This model is suitable for handling complex and ambiguous systems. Expert intuition and interpretation as well as written description of the system are necessary for the development of this type of the model (Terano et al 1987). This model is adopted to perform simulation. The results with supporting experimental data are given in Chapter 5.

4.4.2 Predicate logic

Predicate logic forms the basis of knowledge engineering (Terano et al 1987). It is usually expressed by a short and compact sentence called propositions (theorems). A proposition is a written model which has been proven analytically. It can be used for ambiguous objects or situations as long as they fulfil the definition and meaning.

This type of model produces results which tend to move far away from the actual system or reality. However, it admits examination of the reasoning, evaluation, extension, combination and co-ordination among the propositions themselves.

Predicate logic or theorems are effectively used to explain some of the important results obtained for modelling a microstrip system.

4.5 Microstrip System

Figure 4.2 illustrates an ideal and a real microstrip line. The reason for the difference lies in the method of line etching and fabrication. The lines will never have ideal sharp edges, i.e. there always will be a certain amount of undeterminininistic aspects of the microstrip line, even when the most simple fabrication process is used. The degree of deviation is negligible when $\delta w < w$. However when $\delta w \geq w$, then the result would have a significant impact on the effective width of the microstrip line. This becomes a totally different modelling problem, which goes much further into the physics of the structure and not of our interest in this work.

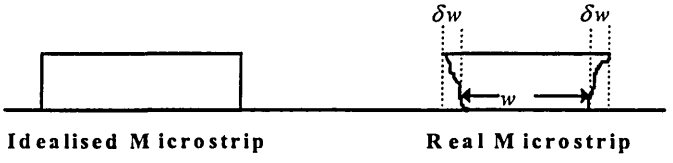

Figure 4.2 Microstrip line.

Idealised (see Fig. 4.2) or physical models (Bender 1978) of microstrip lines are subject to several assumptions which are necessary for building the mathematical models.

4.5.1 Assumptions

To simplify both mathematical and fuzzy models, several general assumptions have been made.

Asp.1- ***Each transmission line is coupled directly only with the immediate neighbouring lines.***

This assumption will make matrices C and L to be tridiagonal matrices (Gao et al 1990).

Asp.2- ***The lines are neither identical nor equally spaced.***

This assumption will lead to nonuniform coupling between the lines.

Asp.3- ***The effects of length on the coupling is negligible.***

Asp.4- ***The lengths of all lines are equal***

This assumption is made in order to have the same reference point for a specific set of microstrip lines, see Fig. 4.3.

Asp.5- ***The dielectric constant, ε_r, and height, h, of the substrate is the same.***

This assumption refers to a specific set of coupled microstrip lines.

Asp.6- ***The material of the microstrip lines are common between the coupled lines.***

Asp.7- ***The number of lines must be greater or equal than three.***

The purpose of this assumption is to ensure that the capacitance matrix is tridiagonal.

Assumptions 1 -7 are part of the constraints in our models and are used unless otherwise stated. They are applied to the uniform as well as the nonuniform models of a set of coupled microstrip lines. Let us first consider the former lines.

4.5.2 Uniform lines

A uniform microstrip assembly is a set of microstrip lines in which all the geometrical configurations, namely the width, w, thickness, t, and spacing, s, the same for each of the lines. The dimensions are shown in Fig. 4.3. This is mainly due to simplicity of its capacitance matrix which is tridiagonal, symmetric and Teoplitz as:

$$C = \begin{pmatrix} a_{11} & a_{12} & 0 \\ a_{12} & a_{22} & a_{12} \\ 0 & a_{12} & a_{33} \end{pmatrix} \qquad (4.1)$$

Figure 4.3 Uniform lines.

4.5.2.1 Time delay and characteristic impedance

Time delay, *W,* and characteristic impedance, Z, of uniform coupled microstrip lines depend on the diagonalisation of matrices C and *L* (Romeo and Santomauro 1987). For a given set of *n* uniform coupled microstrip lines, the voltages v and currents / of the lines are given as (Fig. 4.4):

$$\begin{bmatrix} v_1 \\ v_2 \\ v_3 \\ \bullet \\ J\,V \end{bmatrix} = M_{vvd} = \begin{bmatrix} \cdots & \cdots & \cdots \\ \cdots & \cdots & \cdots \\ \cdots & \cdots & \cdots \\ \cdots & \cdots & \cdots \\ \cdots & \cdots & M_{ntt} \end{bmatrix} \begin{bmatrix} V_{d1} \\ V_{d2} \\ V_{d3} \\ \bullet \\ V_{dn} \end{bmatrix}$$

$$i = \begin{bmatrix} i_1 \\ i_2 \\ i_3 \\ . \\ . \\ . \\ i_n \end{bmatrix} = M_i i_d = \begin{bmatrix} M^i{}_{11} & . & . & . & M^i{}_{1n} \\ . & . & . & . & . \\ . & . & . & . & . \\ . & . & . & . & . \\ M^i{}_{n1} & . & . & . & M^i{}_{nn} \end{bmatrix} \begin{bmatrix} i_{d_1} \\ i_{d_2} \\ i_{d_3} \\ . \\ . \\ . \\ i_{d_n} \end{bmatrix}. \qquad (4.3)$$

Note, the change of notation from v to v_d and i to i_d: as the transformation matrices M_v and M_i are applied to the parameters respectively.

The voltage and current of the kth line are given as:

$$v_k = \sum_{j=1}^{n} M_{kj} v_{d_j} \quad \text{and} \quad i_k = \sum_{j=1}^{n} M^i{}_{kj} i_{d_j} \quad \text{for } k = 1, 2, 3, \ldots, n. \qquad (4.4)$$

Differentiating (4.4) with respect to space, x and time, t results in:

$$\frac{\partial}{\partial x} v_k(x,t) = \sum_{j=1}^{n} M_{kj} \frac{\partial}{\partial x} v_{d_j}(x,t) \qquad (4.5)$$

and

$$\frac{\partial}{\partial x} i_k(x,t) = \sum_{j=1}^{n} M^i{}_{kj} \frac{\partial}{\partial x} i_{d_j}(x,t); \qquad (4.6)$$

$$\frac{\partial}{\partial t} v_k(x,t) = \sum_{j=1}^{n} M_{kj} \frac{\partial}{\partial t} v_{d_j}(x,t) \qquad (4.7)$$

and

$$\frac{\partial}{\partial t} i_k(x,t) = \sum_{j=1}^{n} M^i{}_{kj} \frac{\partial}{\partial t} i_{d_j}(x,t). \tag{4.8}$$

Simplifying (4.5) and (4.7) and then rewriting $\sum_{j=1}^{n} M_{kj}$ as a square matrix $M_v = [M_{kj}]$ where $k, j = 1,2,3,\ldots,n$ (see eqn. 4.2):

$$\frac{\partial}{\partial x} v(x,t) = M_v \frac{\partial}{\partial x} v_d \tag{4.9}$$

and

$$\frac{\partial}{\partial t} v(x,t) = M_v \frac{\partial}{\partial t} v_d \tag{4.10}$$

Similarly (4.6) and (4.8) will give:

$$\frac{\partial}{\partial x} i(x,t) = M_i \frac{\partial}{\partial x} i_d \tag{4.11}$$

and

$$\frac{\partial}{\partial t} i(x,t) = M_i \frac{\partial}{\partial t} i_d \tag{4.12}$$

where $M_i = [M^i_{kj}]$ is a square matrix (see eqn. 4.3) where $k, j = 1,2,3,\ldots,n$.

Differentiating eqn. (3.19) with respect to x:

$$\frac{\partial}{\partial x} v(x,t) = -L \frac{\partial}{\partial t} i(x,t) \tag{4.13a}$$

and

$$\frac{\partial}{\partial x} i(x,t) = -C \frac{\partial}{\partial t} v(x,t) \tag{4.13b}$$

Substituting (4.12) into the right hand side of (4.13a):

$$\begin{aligned} \frac{\partial}{\partial x} v(x,t) &= -LM_i \frac{\partial}{\partial t} i_d \\ &= M_v \frac{\partial}{\partial x} v_d \quad \text{because of the equivalence of (4.13a) and (4.9)} \end{aligned} \tag{4.14}$$

Thus (4.14) implies that,

$$\frac{\partial}{\partial x} v_d = -M_v^{-1} L M_i \frac{\partial}{\partial t} i_d . \tag{4.15}$$

Similarly

$$\frac{\partial}{\partial x} i(x,t) = -CM_v \frac{\partial}{\partial t} v_d = M_i \frac{\partial}{\partial x} i_d \tag{4.16}$$

which implies that

$$\frac{\partial}{\partial x} i_d = -M_i^{-1} C M_v \frac{\partial}{\partial t} v_d . \tag{4.17}$$

The new Telegrapher's equations with respect to the change of basis is written as:

$$\begin{bmatrix} v_d^x(x,t) \\ i_d^x(x,t) \end{bmatrix} = -\begin{bmatrix} 0 & M_v^{-1}LM_i \\ M_i^{-1}CM_v & 0 \end{bmatrix}\begin{bmatrix} v_d^t(x,t) \\ i_d^t(x,t) \end{bmatrix}$$

$$= -\begin{bmatrix} 0 & L_d \\ C_d & 0 \end{bmatrix}\begin{bmatrix} v_d^t \\ i_d^t \end{bmatrix} \tag{4.18}$$

The time delay matrix is given as:

$$W = (L_d C_d)^{1/2} \tag{4.19}$$

and the characteristic impedance matrix is:

$$Z = (L_d C_d)^{1/2} C_d^{-1} = W_d C_d^{-1} \tag{4.20}$$

such that $C_d = M_i^{-1}CM_v$ and $L_d = M_v^{-1}LM_i$.

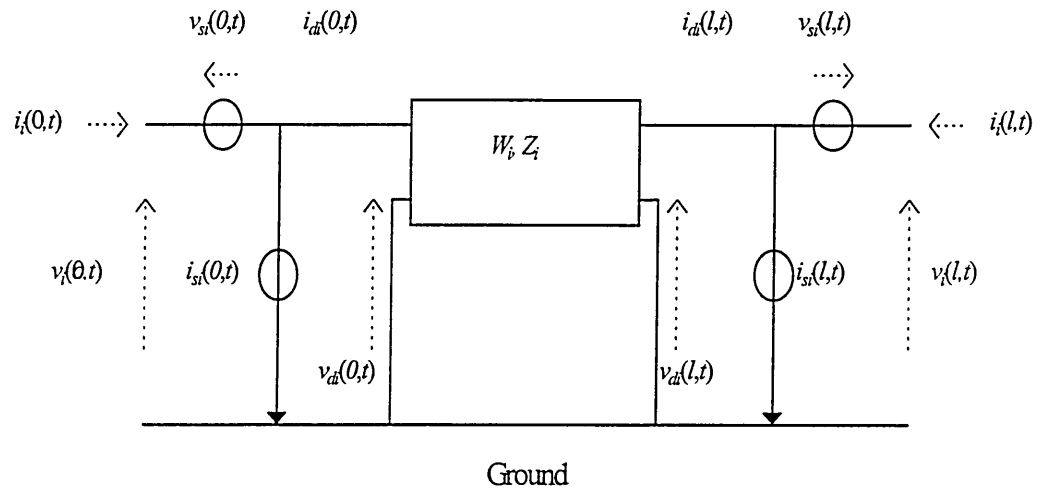

Figure 4.4 Detailed model for the *i* th line.

The theoretical aspects (time delay and characteristic impedance) of the uniform coupled microstrip lines described above can be extended to nonuniform coupled microstrip lines. Here, we shall look at all types of nonuniform lines and their corresponding capacitance matrices and mathematical properties before the extension is finally made at the end of this chapter.

4.5.3 Nonuniform lines

In this work, nonuniform microstrip lines are divided into two types; nonuniformly spaced and strictly nonuniform. The former is a set of microstrip lines having the same geometrical configurations except the spacing between the lines, see Fig. 4.5.

Figure 4.5 Nonuniformiy spaced microstrip lines.

Coupled microstrip lines, nonuniformiy spaced, will have a nonuniformiy spaced capacitance matrix *(C*,s) as:

$$K_{ns} = \begin{matrix} a_n & & a_0 \\ a_{12} & a_{22} & a_{23} \\ 0 & a_{23} & a_{33} \end{matrix} \qquad (4.21)$$

The nonuniformiy spaced capacitance matrix is tridiagonal, symmetric and non-Teoplitz.

In strictly nonuniform microstrip lines, all geometrical configurations are different from one another, see Fig. 4.6. This is the most non-ideal set of microstrip lines.

Figure 4.6 Strictly nonuniform microstrip lines.

This type of lines has a strictly nonuniform capacitance matrix *(Csn)* which is tridiagonal, non-symmetric and non-Teoplitz.

$$K_{sn} = \begin{bmatrix} ran & au & 0 \\ a21 & a22 & a23 \\ V\ 0 & a32 & \end{bmatrix} \qquad (4.22)$$

Since strictly nonuniform microstrip lines result in a very unstable (non-symmetric and non-Teoplitz) capacitance matrix, it is very hard to work on especially in deducing time delay and characteristic impedance. Therefore for this reason, several methods have been devised to approximate the mutual capacitance of each

4.5.3.1 Bound capacitances

Three methods have been designed and named to estimate the capacitance of strictly nonuniform coupled microstrip lines (Fig. 4.6). Those methods are:

method 1: *general bound*

This is a method which computes the minimum and maximum mutual capacitances of a given set of coupled lines. The computation is based on comparing values of each the geometrical parameter of the lines (see Fig. 4.5). It is defined in the following manner.

For n- strictly nonuniform coupled microstrip lines, the capacitance matrix, $C(n)_{sn}$, is subject to the inequality relation below:

$$C(n)_{sn\min} \le C(n)_{sn} \le C(n)_{sn\max} \quad \text{where} \tag{4.23}$$

$$C(n)_{sn\min} = \begin{cases} \min(w_1, w_2, w_3, \ldots, w_{n-1}, w_n) \\ \min(t_1, t_2, t_3, \ldots, t_{n-1}, t_n) \\ s_1, s_2, s_3, \ldots, s_{n-2}, s_{n-1} \end{cases} \tag{4.24}$$

and

$$C(n)_{sn\max} = \begin{cases} \max(w_1, w_2, w_3, \ldots, w_{n-1}, w_n) \\ \max(t_1, t_2, t_3, \ldots, t_{n-1}, t_n) \\ s_1, s_2, s_3, \ldots, s_{n-2}, s_{n-1} \end{cases} \tag{4.25}$$

method 2: *intermediate bound*

Contrary to general bound, this method defines the minimum and maximum capacitances by comparing values of mutual capacitances of neighbouring lines. It is defined formally as below:

For n strictly nonuniform coupled microstrip lines, the capacitance matrix, $C(n)_{sn}$, is subject to the inequality relation below:

$C(n)_{sn\min} \le C(n)_{sn} \le C(n)_{sn\max}$ where

$C(n)_{sn\min} = [c_{ij_{\min}}]$ and $C(n)_{sn\max} = [c_{ij_{\max}}]$. (4.26)

$c_{ij_{\min}} = \min(c_{ij}, c'_{ij})$ *and* $c_{ij_{\max}} = \max(c_{ij}, c'_{ij})$ such that (4.27)

c_{ij} = mutual capacitance of coupled microstrip lines taking line i as their parameters

and

c'_{ij} = mutual capacitance of coupled microstrip lines taking line j as their parameters.

method 3: *focus bound*

The focus bound is treated in more detailed than the previous two methods. Minimum and maximum values of geometrical parameters for any two pairs of lines are determined at a time. These parameters are then used to calculate the minimum and maximum mutual capacitances, respectively.

For n strictly nonuniform coupled microstrip lines, the capacitance matrix, $C(n)_{sn}$, is subject to the approximate relation below:

$$C(n)_{sn\min} \approx C(n)_{sn} \approx C(n)_{sn\max} \quad \text{such that} \tag{4.28}$$

$$C(n)_{sn\min} = [c_{ij_{\min}}] \text{ and } C(n)_{sn\max} = [c_{ij_{\max}}] \text{ where} \tag{4.29}$$

$$c_{ij_{\min}} = \left\{ \begin{array}{c} \min(w_i, w_j) \\ \min(t_i, t_j) \\ s = \sum_{p=i}^{j-1} s_p + \sum_{p=i+1}^{j-1} w_p \end{array} \right\} = c_{ji_{\min}} \tag{4.30}$$

$$\text{and } c_{ij_{\max}} = \left\{ \begin{array}{c} \max(w_i, w_j) \\ \max(t_i, t_j) \\ s = \sum_{p=i}^{j-1} s_p + \sum_{p=i+1}^{j-1} w_p \end{array} \right\} = c_{ji_{\max}} \tag{4.31}$$

The first method will give minimum and maximum capacitance matrices with respect to all the parameters of lines. On the other hand, the second method will give minimum and maximum capacitance matrices with respect to the mutual capacitance of the immediate adjacent line. The second method is expected to give a better estimation than the general bound. Nevertheless, the third (focus bound) is the best of the three methods because it compares the geometrical configurations a line to its adjacent before the mutual capacitance is finally calculated.

The intermediate and focus methods have been coded as a program using Mathematica software, see Appendix A.3. To illustrate its application, an example of a strictly nonuniform set of 4-coupled lines is presented, see Fig. 4.7.

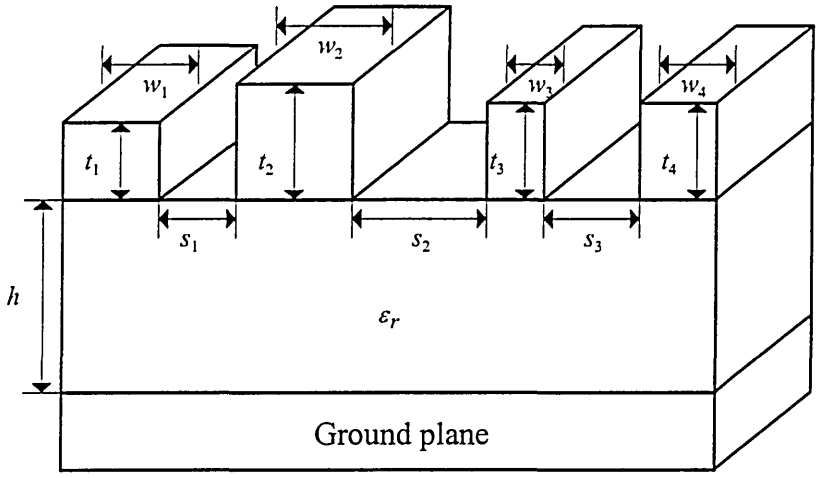

$w_1 = 2.3\mu m$, $w_2 = 3\mu m$, $w_3 = 1\mu m$, $w_4 = 2\mu m$,
$t_1 = 2\mu m$, $t_2 = 5\mu m$, $t_3 = 3.3\mu m$, $t_4 = 4\mu m$,
$s_1 = 3\mu m$, $s_2 = 15\mu m$, $s_3 = 7\mu m$, $h = 16\mu m$
and $\varepsilon_r = 12$.

Figure 4.7 4 strictly nonuniform coupled lines, (dimension in μ m).

By ignoring assumption 1 of section 4.5.1, the capacitance matrix of the set (see Fig. 4.7) is calculated as follows:

general bound

$$C(4)_{sn\min} = \begin{bmatrix} 123.571 & -48.4587 & 0.182353 & 5.3854 \\ -48.4587 & 130.195 & -4.29158 & 3.23531 \\ 0.182353 & -4.29158 & 107.627 & -22.8375 \\ 5.3854 & 3.23531 & -22.8375 & 94.8966 \end{bmatrix} pF \qquad (4.32)$$

and

$$C(4)_{sn\max} = \begin{bmatrix} 154.225 & -60.2384 & 0.415477 & 6.5392 \\ -60.2384 & 164.526 & -6.80597 & 3.45963 \\ 0.415477 & -6.80597 & 135.932 & -28.6009 \\ 6.5392 & 3.45963 & -28.6009 & 119.543 \end{bmatrix} pF \qquad (4.33)$$

intermediate bound

$$C(4)_{sn\min} = \begin{bmatrix} 144.173 & -60.2384 & 0.842355 & 5.60243 \\ -60.2384 & 154.126 & -6.80597 & 2.06533 \\ 0.842355 & -6.80597 & 99.0632 & -26.1078 \\ 5.60243 & 2.06533 & -26.1078 & 105.136 \end{bmatrix} pF \qquad (4.34)$$

and

$$C(4)_{sn\max} = \begin{bmatrix} 154.434 & -51.8617 & 2.01309 & 6.3153 \\ -51.8617 & 165.92 & -4.2729 & 2.94949 \\ 2.01309 & -4.2729 & 105.406 & -23.4684 \\ 6.3153 & 2.94949 & -23.4684 & 109.372 \end{bmatrix} pF\,. \qquad (4.35)$$

focus

$$C(4)_{sn\min} = \begin{bmatrix} 144.8696 & -51.8617 & 1.84727 & 5.78479 \\ -51.8617 & 154.1261 & -4.2729 & 2.94949 \\ 1.84727 & -4.2729 & 99.2290 & -23.4684 \\ 5.78479 & 2.94949 & -23.4684 & 105.6666 \end{bmatrix} pF \qquad (4.36)$$

and

$$C(4)_{sn\max} = \begin{bmatrix} 153.614 & -60.2384 & 1.10189 & 6.16282 \\ -60.2384 & 165.9200 & -6.80597 & 2.06533 \\ 1.10189 & -6.80597 & 105.406 & -26.1078 \\ 6.16282 & 2.06533 & -26.1078 & 108.812 \end{bmatrix} pF \qquad (4.37)$$

The focus method is superior since most of its mutual/self capacitance difference values (∇c_{ij}) are smaller than values given by the other two methods, see Table

4.1. The smaller the value of the difference, the better is the approximation for the capacitance of coupled strictly nonuniform microstrip lines.

$\nabla c_{ij} = \left\| c_{ij_{\max}} - c_{ij_{\min}} \right\|$ pF	**Gen. Bound**	**Inter. Bound**	**Foc. Bound**
∇c_{11}	30.654	10.261	8.7444
∇c_{12}	11.7797	8.3767	8.3767
∇c_{13}	0.233124	1.170735	0.74538
∇c_{14}	1.1538	0.71287	0.37803
∇c_{22}	34.331	11.794	11.7939
∇c_{23}	2.51439	2.53307	2.53307
∇c_{24}	0.22432	0.88416	0.88416
∇c_{33}	28.305	6.3428	6.177
∇c_{34}	5.7634	2.6394	2.6394
∇c_{44}	24.6464	4.236	3.1454

Table 4.1 Comparison of methods of bound capacitances.

One main beauty of the methods of bound capacitance is that it will transform the strictly nonuniform capacitance matrices to 'look a like' nonuniformly spaced capacitance matrices. In other word, they are tridiagonal, symmetric and non-Teoplitz. The matrices are easier to work with than the strictly nonuniform matrices and most of all, the transformed matrices also behave as any nonuniformly spaced capacitance matrices. This simply implies that any general mathematical properties (matrices) that the nonuniformly spaced capacitance

matrices possesses are also applicable to the transform strictly nonuniform capacitance matrix. These properties are discussed at the end of the following section.

4.5.3.2 Theorems

Let us consider a set of any three coupled nonuniformly spaced microstrip lines, say $s_1 \neq s_2$; where s_1 is the spacing between line 1 and line 2 and s_2 is the spacing between line 2 and line 3.

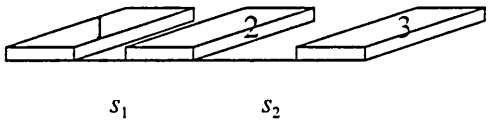

Figure 4.8 3-coupled nonuniformly spaced microstrip lines.

With the assumptions of the *transverse electromagnetic mode* (TEM) of wave propagation as described in Section 3.9.1, the distribution of voltages and currents along the lines is given by the generalized telegrapher equations:

$$\begin{bmatrix} v^x(x,t) \\ i^x(x,t) \end{bmatrix} = -\begin{bmatrix} 0 & L \\ C & 0 \end{bmatrix} \begin{bmatrix} v^t(x,t) \\ i^t(x,t) \end{bmatrix} \tag{4.38}$$

where vectors $v(x,t)$ and $i(x,t)$ denote voltages and currents, respectively. L is the PUL (per unit length) inductance matrix and C is the PUL capacitance matrix. Superscripts x and t denote differentiation of signals with respect to space and

time, respectively. Distance and time are denoted by x and t and (Romeo and Santomauro 1987):

$$C = \begin{bmatrix} c_{11} & -c_{12} & \cdots & -c_{1n} \\ -c_{21} & c_{22} & \cdots & -c_{2n} \\ \vdots & \vdots & \vdots & \vdots \\ -c_{n1} & -c_{n2} & \cdots & c_{nn} \end{bmatrix} \text{ such that } c_{ii} = c_{i0} + \sum_{\substack{j=1 \\ j \neq i}}^{n} c_{ij} \tag{4.39}$$

where c_{i0} is the capacitance per unit length (PUL) of line i with respect to ground, c_{ij} is the capacitance PUL between line i and c_{ii} is the self capacitance PUL of line i. Thus the capacitance matrix C may be written as:

$$C = \begin{bmatrix} a_{11} & -a_{12} & 0 \\ -a_{12} & a_{22} & -a_{23} \\ 0 & -a_{23} & a_{33} \end{bmatrix} \tag{4.40}$$

where

(i) each line is coupled directly only to adjacent line, (see Asp. 1)

(ii) all lines are identical, not equally spaced and side effects are negligible,

(iii) the length of the lines are equal and have the same reference point,

(iii) the dielectric and the material of the lines are the same, (see Asp. 5-6)

All the minus signs in C can be ignored since they do not affect calculations and proofs.

From (4.39) and (4.40) we have;

$a_{11} = a_{10} + a_{12} + a_{13} = a_{10} + a_{12} + 0$, $a_{22} = a_{20} + a_{21} + a_{23} = a_{10} + a_{12} + a_{23}$,
and $a_{33} = a_{30} + a_{31} + a_{32} = a_{10} + 0 + a_{23}$.

Furthermore, we can simplify

$a_{22} = a_{11} + a_{23}$, and $a_{10} = a_{11} - a_{12}$
thus $a_{33} = a_{10} + a_{23} = (a_{11} - a_{12}) + a_{23} = (a_{11} + a_{23}) - a_{12}$

Therefore, the new C matrix is represented as:

$$C = \begin{bmatrix} a_{11} & -a_{12} & 0 \\ -a_{12} & a_{11} + a_{23} & -a_{23} \\ 0 & -a_{23} & a_{11} + a_{23} - a_{12} \end{bmatrix} \tag{4.41}$$

which is tridiagonal and symmetric.

Eqn. 4.41 indicates that:

- the self capacitance of line 2 depends only on the self capacitance of line 1 and the mutual capacitance of line 2 and 3,
- the self capacitance of line 3 depends only on the self capacitance of line 1, the mutual capacitance of line 2 and 3, and the mutual capacitance of line 1 and line 2.

Therefore we can put the result formally as a theorem.

Theorem 4.1: For n-coupled identical microstrip lines with different spacing such that $n \geq 3$, see Fig. 4.5, the capacitance matrix can be written as:

$$C = \begin{bmatrix} a_{11} & -a_{12} & 0 & \dots & 0 & 0 \\ -a_{12} & a_{22} & -a_{23} & \dots & 0 & 0 \\ . & . & . & . & . & . \\ . & . & . & . & . & . \\ 0 & 0 & 0 & \dots & -a_{n(n-1)} & a_{nn} \end{bmatrix} \tag{4.42}$$

where $a_{11} = a_{10} + a_{12}$, and $a_{ii} = a_{(i-1)(i-1)} - a_{(i-2)(i-1)} + a_{i(i+1)}$

for $2 \leq i \leq n$.

proof:

The theorem can be proved by a mathematical induction (Grossman 1984).

For n=2,

$a_{22} = a_{11} - a_{01} + a_{23} = a_{11} + a_{23}$.

a_{01}= 0 since this term does not exist.

Thus,

$$a_{22} = a_{10} + a_{12} + a_{23} \tag{4.43}$$

Suppose that $a_{nn} = a_{(n\text{-}1)(n\text{-}1)} - a_{(n\text{-}2)(n\text{-}1)} + a_{n(n+1)}$, then we need to show

$$a_{(n+1)(n+1)} = a_{nn} - a_{(n\text{-}1)n} + a_{(n+1)(n+2)} = a_{nn} - a_{(n-1)n} \tag{4.44}$$

since $a_{(n+1)(n+2)} = 0$ and it does not exist for

$$C = \begin{bmatrix} a_{11} & -a_{12} & 0 & 0 & \cdots & 0 & 0 \\ -a_{12} & & & & & & \vdots \\ 0 & & & & & -a_{(n-1)n} & 0 \\ \vdots & \vdots & \vdots & & -a_{(n-1)n} & a_{nn} & -a_{n(n+1)} \\ 0 & 0 & 0 & \cdots & 0 & -a_{n(n+1)} & a_{(n+1)(n+1)} \end{bmatrix} \tag{4.45}$$

Now,

$$\begin{aligned} a_{(n+1)(n+1)} &= a_{(n+1)0} + 0 + \ldots\ldots\ldots + 0 + a_{(n+1)n} \\ &= a_{(n+1)0} + a_{(n+1)n} = a_{10} + a_{n(n+1)} \\ &= a_{10} + a_{(n+1)n} = a_{10} + a_{nn} - a_{(n-1)(n-1)} + a_{(n-2)(n-1)} \\ &= a_{nn} + a_{10} - a_{(n-1)(n-1)} + a_{(n-2)(n-1)} \end{aligned} \tag{4.46}$$

and since

$$\begin{aligned} a_{(n-1)(n-1)} &= a_{(n-1)0} + a_{(n-1)1} + \ldots\ldots\ldots + a_{(n-1)(n-2)} + a_{(n-1)n} \\ &= a_{10} + 0 + \ldots\ldots\ldots 0 + a_{(n-1)(n-2)} + a_{(n-1)n} \\ &= a_{10} + a_{(n-1)(n-2)} + a_{(n-1)n} \end{aligned} \tag{4.47}$$

then

$$\begin{aligned} a_{(n+1)(n+1)} &= a_{nn} + a_{10} - (a_{10} + a_{(n-1)(n-2)} + a_{(n-1)n}) + a_{(n-2)(n-1)} \\ &= a_{nn} - a_{(n-1)n} \end{aligned} \tag{4.48}$$

because $a_{(n-1)(n-2)} = a_{(n-2)(n-1)}$.

We have just shown that the self capacitance of line i, where $2 \le i \le n$, of n-coupled microstrip lines with different spacing is given by

$$a_{ii} = a_{(i-1)(i-1)} - a_{(i-2)(i-1)} + a_{i(i+1)}. \qquad (4.49)$$

A modified Mathematica (Wolfram 1991) program of Parker (1994) is developed (Appendix A.1) and used to verify the above theorem. Below are two examples of coupled microstrip lines with different spacing. In both examples, different values are used to generate the capacitance matrices. The matrices obtained are then compared to those predicted by the theorem.

Geometrical parameters	**3-coupled nonuniformly spaced microstrip lines**	**10-coupled nonuniformly spaced microstrip lines**
Dielectric	12	12
Thickness (μm)	0.01	0.01
Width (μm)	2	2
Height (μm)	20	20
s_1 (μm)	3	0.3
s_2	4	4.114
s_3		5.002
s_4		6
s_5		4.7
s_6		8
s_7		9.2
s_8		5.0343
s_9		0.004

Table 4.2 Parameters for coupled nonuniformly spaced microstrip lines.

The parameters used to calculate and simulate the capacitance matrices are listed in Table 4.2 for 3 and 10 coupled nonuniformly spaced microstrip lines. The results obtained are shown below.

$$C = \begin{bmatrix} 155.2(133.4) & -50(-50) & -21.79(0) \\ -50(-50) & 175.8(175.8) & -42.4(42.4) \\ -217.9(0) & -42.44(-42.4) & 147.6(125.8) \end{bmatrix} \text{ pF} \qquad (4.50)$$

$$C = \begin{bmatrix} 245(226) & -143 & -30.2 & -12.5 & -3.30 & 0.948 & 4.52 & 6.60 & 7.39 & 75.7 \\ -143 & 266(268) & -41.7 & -16.7 & -5.34 & -0.281 & 3.89 & 6.27 & 7.16 & 7.37 \\ -30.2 & -41.7 & 189(161) & -36.6 & -13.2 & -4.78 & 1.68 & 5.17 & 6.41 & 6.68 \\ -12.5 & -16.7 & -36.6 & 183(151) & -31.9 & -13.7 & -2.31 & 3.29 & 5.18 & 5.58 \\ -3.30 & -5.34 & -13.2 & -31.9 & 179(153) & -38.2 & -10.5 & -0.232 & 2.96 & 3.63 \\ 0.948 & -0.281 & -4.78 & -13.7 & -38.2 & 168(146) & -24.6 & -5.26 & -4.20 & 1.00 \\ 4.52 & 3.89 & 1.68 & -2.31 & -10.5 & -24.6 & 146(129) & -21.2 & -8.52 & -6.23 \\ 6.60 & 6.27 & 5.17 & 3.29 & -0.232 & -5.26 & -21.2 & 153(141) & -36.4 & -27.8 \\ 7.39 & 7.16 & 6.41 & 5.18 & 2.96 & -0.0420 & -8.52 & -36.4 & 4380(4400) & -4280 \\ 7.57 & 7.37 & 6.68 & 5.58 & 3.63 & 1.00 & -6.23 & -27.8 & -4280 & 4370(4360) \end{bmatrix}$$

pF.

(4.51)

In both cases, the self capacitances, a_{ii}, are very close to the values predicted by theorem 4.1 (listed in brackets). The calculated and simulated self capacitances

of the 10 coupled lines are further compared in Fig. 4.9. The difference is found to be extremely small.

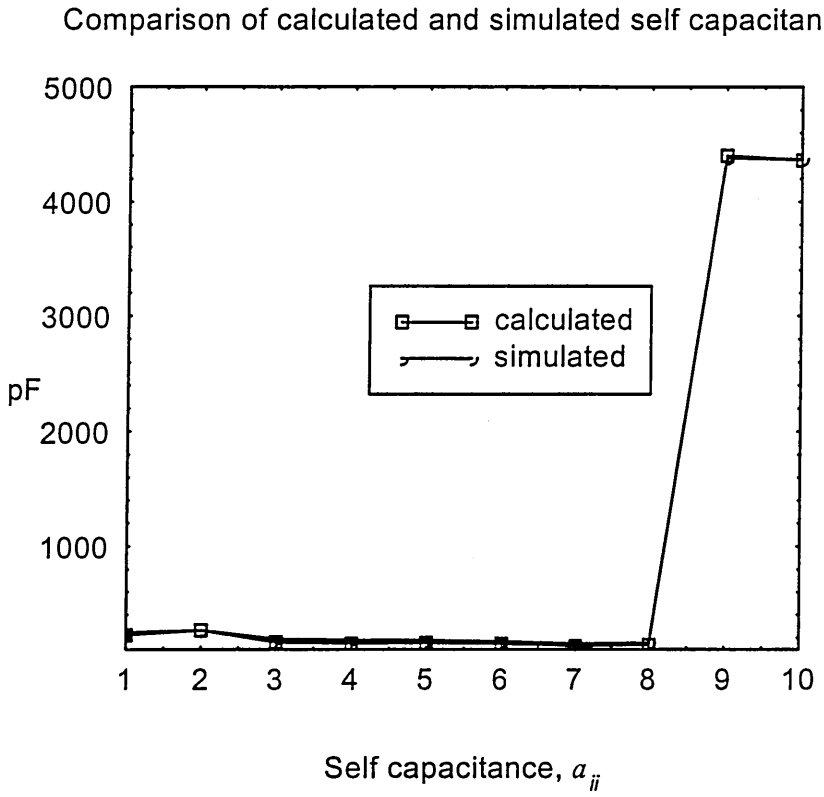

Figure 4.9 Comparison of calculated and simulated self capacitances of 10 - coupled nonuniformly spaced microstrip lines.

Even though, the main purpose of the theorem is to calculate capacitance matrix of nonuniformly spaced, because of its generality, it can also be applied to any uniformly coupled microstrip lines. The new capacitance matrix, C, (4.42) can be written as composition of two matrices; namely the identity matrix and the mutual capacitance ratio matrix. The composition is presented in the following section.

4.5.3.2.1 *Mutual capacitance ratio matrix*

The new matrix C given in (4.42) can be written as:

$$C = \begin{bmatrix} a_{10}+a_{12} & a_{12} & 0 & \dots & 0 & 0 \\ a_{12} & a_{10}+a_{12}+a_{23} & a_{23} & \dots & 0 & 0 \\ . & . & . & . & . & . \\ . & . & . & . & . & . \\ 0 & 0 & 0 & \dots & a_{n(n-1)} & a_{(n-1)(n-1)} - a_{(n-2)(n-1)} + a_{n(n+1)} \end{bmatrix}$$

(4.52)

by applying the theorem. By substituting $a_{i(i+1)} = b_i a_{12}$ for $i = 2,\dots,n$, then

(4.52) is transformed as:

$$C = \begin{bmatrix} a_{10}+a_{12} & a_{12} & 0 & \dots & 0 & 0 \\ a_{12} & a_{10}+a_{12}+b_2 a_{12} & b_2 a_{12} & \dots & 0 & 0 \\ . & . & . & . & . & . \\ . & . & . & . & . & . \\ 0 & 0 & 0 & \dots & b_{n-1}a_{12} & a_{10}+b_{n-1}a_{12} \end{bmatrix}$$

(4.53)

By factoring the common terms; i.e. a_{12}, C becomes:

$$C = \begin{bmatrix} a_{10}+a_{12} & a_{12} & 0 & \dots & 0 & 0 \\ a_{12} & a_{10}+a_{12}(1+b_2) & b_2 a_{12} & \dots & 0 & 0 \\ . & . & . & . & . & . \\ . & . & . & . & . & . \\ 0 & 0 & 0 & \dots & b_{n-1}a_{12} & a_{10}+b_{n-1}a_{12} \end{bmatrix}.$$

(4.54)

and can be generalised as a composition of two matrices as follows:

$$C = a_{10}\begin{bmatrix} 1 & 0 & 0 & . & . & . & 0 \\ 0 & 1 & 0 & . & . & . & 0 \\ . & . & . & . & . & . & . \\ . & . & . & . & . & . & . \\ . & . & . & . & . & . & . \\ 0 & 0 & 0 & . & . & 1 & 0 \\ 0 & 0 & 0 & . & . & 0 & 1 \end{bmatrix} + a_{12}\begin{bmatrix} 1 & 1 & 0 & . & . & . & 0 \\ 1 & (1+b_2) & b_2 & . & . & . & 0 \\ 0 & b_2 & (b_2+b_3) & b_3 & . & . & 0 \\ . & . & . & . & . & . & . \\ . & . & . & . & . & . & . \\ 0 & 0 & 0 & . & . & . & b_{n-1} \\ 0 & 0 & 0 & . & . & b_{n-1} & b_{n-1} \end{bmatrix}$$

(4.55)

Formally,

$C = a_{10}I + a_{12}S_n$; such that I and S_n are identity and mutual capacitance ratio matrices, respectively. The entries of S_n, b_i, are defined as $b_i = \frac{a_{i(i+1)}}{a_{12}}$ for $i = 2,\ldots,n$.

The eigenvalues and eigenvectors of a system are very valuable information. They give, or lead to, many physical interpretations of a system. This particular structure of C allows for the relatively easy computation of eigenvalues and eigenvectors. They can be deduced directly from the mutual capacitance ratio matrix, S_n.

4.5.3.2.2 *Eigenvalues*

Theorem 4.2: For n-coupled identical microstrip lines with different spacing such that $n \geq 3$, see Fig.4.5, the eigenvalues of C are given by;

$$\lambda_j = a_{10} + a_{12}\theta_j(S_n) \qquad (4.56)$$

$$\text{where } S_n = \begin{bmatrix} 1 & 1 & 0 & . & . & . & 0 \\ 1 & (1+b_2) & b_2 & . & . & . & 0 \\ 0 & b_2 & (b_2+b_3) & b_3 & . & . & 0 \\ . & . & . & . & . & . & . \\ . & . & . & . & . & . & . \\ 0 & 0 & 0 & . & . & . & b_{n-1} \\ 0 & 0 & 0 & . & . & b_{n-1} & b_{n-1} \end{bmatrix} \tag{4.57}$$

such that $b_i = \dfrac{a_{i(i+1)}}{a_{12}}$ and $\theta_j(S_n)$ is the eigenvalue of S_n for $i, j = 2,\ldots,n$.

proof:

$\det\ (C - \lambda_j I) = \det\ (a_{10} I + a_{12} S_n - \lambda_j I)$ by applying the composition.

$$= \det\ (\left[a_{10} - \lambda_j\right] I + a_{12} S_n) \text{ by factoring the common term.}$$

$$= \det\ a_{12} (\frac{\left[a_{10} - \lambda_j\right]}{a_{12}} I + S_n). \tag{4.58}$$

Let $\lambda_j = a_{10} + a_{12}\theta_j(S_n)$ where $\theta_j(S_n)$ is the eigenvalue of S_n for

$i, j = 2,\ldots,n$.

$$= \det\ a_{12}\left[\frac{\left(a_{10} - a_{10} - a_{12}\theta_j(S_n)\right)}{a_{12}} I + S_n\right] \tag{4.59}$$

$$= \det\ a_{12}\left[\frac{\left(-a_{12}\theta_j(S_n)\right)}{a_{12}} I + S_n\right] \tag{4.60}$$

$$= \det\ a_{12}\left[-\theta_j(S_n) I + S_n\right] \tag{4.61}$$

$$= a_{12} \det (S_n - \theta_j(S_n) I) = 0 \qquad (4.62)$$

The result of (4.62) leads immediately to the following corollary. It is the application of theorem to any 3-coupled nonuniformly spaced microstrip lines.

Corollary 4.3: For any three nonuniformly spaced coupled microstrip lines such that $C = \begin{bmatrix} a_{11} & a_{12} & 0 \\ a_{12} & a_{22} & ba_{12} \\ 0 & ba_{12} & a_{33} \end{bmatrix}$, then its eigenvalues are

$$\lambda = a_{10} + a_{12}\left\{0, (b+1) \pm \sqrt{b^2 - b + 1}\right\} \qquad (4.63)$$

where $b = \frac{a_{23}}{a_{12}}$.

Another striking result from the new capacitance matrix is that its eigenvectors are similar to S_n.

4.5.3.2.3 *Eigenvectors*

Theorem 4.4: The capacitance matrix C and the mutual ratio matrix S_n have the same eigenvectors.

proof:

$$(C - \lambda I)\mathrm{x} = (a_{10} I + a_{12} S_n - \lambda I)\mathrm{x}$$

$$= (a_{12} S_n - [\lambda - a_{10}] I)\mathrm{x}$$

$$= a_{12}(S_n - \frac{[\lambda - a_{10}]}{a_{12}} I)\mathrm{x}$$

$$= a_{12}(S_n - \theta\ (S_n)I)\mathrm{x}\,. \qquad (4.64)$$

Corollary 4.5: For any three nonuniformly spaced coupled microstrip lines such that $C = a_{10}I + a_{12}S_n$, then eigenvalues of C are given by $\lambda_i = a_{11} + a_{12}(J_3)$ and eigenvectors J_3 are the same as eigenvectors of C where

$$J_3 = \begin{bmatrix} 0 & 1 & 0 \\ 1 & b_2 & b_2 \\ 0 & b_2 & b_2 - 1 \end{bmatrix};\ b_2 = \frac{a_{23}}{a_{12}}. \qquad (4.65)$$

proof:

By (4.56), the capacitance matrix of three non-uniform coupled microstrip lines of different spacing can be written as $C = a_{10}I + a_{12}S_3$ where

$$S_3 = \begin{bmatrix} 1 & 1 & 0 \\ 1 & (1+b_2) & b_2 \\ 0 & b_2 & b_2 \end{bmatrix}. \qquad (4.66)$$

By theorem 4.2, eigenvalues of C and S_3 are given by $\lambda_j = a_{10} + a_{12}\theta_j(S_3)$ and $\theta_j(S_3)$, respectively. From theorem 4.4, C and S_3 have the same eigenvectors.

The mutual capacitance ratio matrix can be written as:

$$S_3 = \begin{bmatrix} 1 & 0 & 0 \\ 0 & 1 & 0 \\ 0 & 0 & 1 \end{bmatrix} + \begin{bmatrix} 0 & 1 & 0 \\ 1 & b_2 & b_2 \\ 0 & b_2 & b_{2-1} \end{bmatrix} = I + J_3 . \tag{4.67}$$

Using theorem 4.2 the eigenvalues of S_3 are given by $\theta_j(S_3) = 1 + 1\delta_i(J_3)$ where $\delta_i(J_3)$ is eigenvalues of J_3.

Therefore,

$$\lambda_j = a_{10} + a_{12}(1 + 1\delta_i(J_3)) = a_{10} + a_{12} + a_{12}\delta_i(J_3) = a_{11} + a_{12}\delta_i(J_3) . \tag{4.68}$$

The new capacitance matrix is expected to alter the inductance matrix introduced in Sect. 3.9.1. The new inductance matrix is presented formally in the following section.

4.5.3.2.4 *Inductance matrix*

The inductance matrix for nonuniformly coupled microstrip lines is given as:

$$L = \mu_0 \varepsilon_0 C_0^{-1} \tag{4.69}$$

where C_0^{-1} = the inverse of capacitance matrix of coupled nonuniform microstrip lines with the dielectric replaced by vacuum,

ε_0 = 8.854183×10^{-12} F/m; permittivity of free space,

μ_0 = $4\pi \times 10^{-7}$ H / m; the permeability of free space.

The new inductance (eqn. 4.69) and capacitance matrices structures (eqn. 4.42) have been written as Mathematica programs. They are listed in Appendix A.4 and A.5 respectively. These programs allow one to calculate the capacitance and inductance matrices of nonuniformly spaced as well as strictly nonuniform coupled microstrip lines. The information obtained is essential to determine other parameters in later sections, i.e. time delay and characteristic impedance.

Before that, there are some special features of the new capacitance and inductance matrices. These features are established by the following theorems:

Theorem 4.6: If C_0 is symmetric, then C_0^{-1} is also symmetric

proof:

Since C_0 is symmetric, then $C_0 = C_0^T$.

But, $I = C_0\ C_0^{-1}$

$$= C_0^T\ C_0^{-1} \tag{4.70}$$

$$= C_0^T\ (C_0^T)^{-1} \qquad \text{by the fact above} \tag{4.71}$$

$$= C_0^T\ (C_0^{-1})^T \qquad \text{since } (A^{-1})^T = (A^T)^{-1} \tag{4.72}$$

$$= C_0\ (C_0^{-1})^T \tag{4.73}$$

Since C_0^{-1} is symmetric, then L is also symmetric (see eqn. 4.69).

Because of the symmetry of the new capacitance and inductance matrices, the following theorem follows immediately.

Theorem 4.7: $CL = (LC)^T$

proof:

$CL = C^T L^T$ because of the symmetry of C and L. (4.74)

$= (LC)^T$ by a property of transposition (Rade and Westergren 1988) (4.75)

Equivalence of eigenvalues of LC and CL (Romeo and Santomauro 1987) is conformed by a corollary below.

Corollary 4.8: Matrices LC and CL share the same eigenvalues

proof:

Since $L = L^T$ and $C = C^T$, then $LC = (L^T C^T) = (CL)^T$. (4.76)

Now,

$\det (LC - \lambda I) = \det ((CL)^T - \lambda I)$ since $LC = (CL)^T$ (4.77)

$= \det ((CL)^T - \lambda I)^T$ since $\det(A) = \det(A^T)$ (4.78)

$= \det (CL - (\lambda I)^T)$ since $(A+B)^T = A^T + B^T$ (4.79)

$= \det (CL - \lambda I)$ (4.80)

All the above properties will be used in developing algorithms for modelling and simulating time delay, $W(n)_{ns}$, and characteristic impedance, $Z(n)_{ns}$, for nonuniform coupled microstrip lines as outlined below.

4.5.3.3 $W(n)_{ns}$ and $Z(n)_{ns}$ of nonuniform spacing

Using equations 4.2 - 4.20, 4.42 and an algorithm proposed by Romeo and Santomauro (1987), which only deals with uniform lines, an algorithm has been developed to calculate $W(n)_{ns}$ and $Z(n)_{ns}$. The steps required for this development are as follows:-

Step 1: Given a set of n coupled microstrip lines with different spacing.

Step 2: The capacitance matrix, C, is given by (4.42).

Step 3: Calculate C_0.

Step 4: Calculate the inductance matrix, L.

Step 5: Find eigenvectors of LC and CL

Step 6: Find normalised eigenvectors of LC; M_v, and CL; M_I, using the Gramm-Schmidt method (Rade and Westergren 1988).

Step 7: Find $M_V{}^{-1}$, $M_v{}^T$ and $M_I{}^{-1}$ such that $M_v{}^T = M_I{}^{-1}$. (4.81)

Step 8: Find $C_d = M_I^{-1}.C.M_v$ and $L_d = M_v^{-1}.L.M_I$.

Step 9: Time delay, $W(n)_{ns} = \sqrt{L_d.C_d}$ and characteristic impedance, $Z(n)_{ns} = W_d.C_d^{-1}$.

Both Romeo and Santomauro (1987) and Parker (1994) mentioned matrices M_v and M_I in their algorithms, but they did not emphasise the importance of normality of these matrices. The normality of these matrices is crucial in order to establish the relation given in (4.81), which enables one to diagonalize matrices C and L. The diagonalisation of these matrices is denoted as C_d and L_d. Moreover the diagonal elements of C_d and L_d are eigenvalues of C and L,

respectively. The following outlines the procedure for executing the developed algorithm for determining time delay and characteristic impedance for 3 coupled nonuniformly spaced microstrip lines with parameters as listed in Table 4.2. Mathematica program Mat 2 (see Appendix A.4) was used to calculate C and L matrices, and the results are:

$$C = \begin{bmatrix} 133.4 & -50 & 0 \\ -50 & 175.8 & -42.4 \\ 0 & -42.4 & 125.8 \end{bmatrix} \text{pF} \tag{4.82}$$

and

$$L = \begin{bmatrix} 592980 & 168634 & 0 \\ 168634 & 551567 & 153391 \\ 0 & 153391 & 608223 \end{bmatrix} \text{pH} \tag{4.83}$$

$$\text{Then, } LC = \begin{bmatrix} 7.06718 & -3.1428\times10^{-4} & -7.15008\times10^{-1} \\ -5.08257\times10^{-1} & 8.203 & -4.08985\times10^{-1} \\ -7.66955\times10^{-1} & 1.17748\times10^{-1} & 7.00107 \end{bmatrix} \times 10^{-17} \tag{4.84}$$

and

$$CL = (LC)^T = \begin{bmatrix} 7.06718 & -5.08257\times10^{-1} & -7.66955\times10^{-1} \\ -3.1428\times10^{-4} & 8.203 & 1.17748\times10^{-1} \\ -7.15008\times10^{-1} & -4.08985\times10^{-1} & 7.00107 \end{bmatrix} \times 10^{-17} \tag{4.85}$$

by theorem 4.7. Eigenvectors of LC and CL are;

$$\begin{bmatrix} 0.167489 & -0.963 & -0.211137 \\ 0.963124 & -0.148629 & -0.22428 \\ 1 & 0 & 0 \end{bmatrix} \tag{4.86}$$

and

$$\begin{bmatrix} 0.201858 & -0.927212 & 0.315485 \\ 1 & 0 & 0 \\ -0.996293 & -0.0000378129 & -0.0860268 \end{bmatrix}. \tag{4.87}$$

However, the calculated normalised eigenvectors of LC and CL are:

$$M_{v_{LC}} = \begin{bmatrix} -0.119768 & -0.688709 & -0.715078 \\ 0.986475 & -0.00137018 & -0.163904 \\ -0.111902 & 0.725037 & -0.679558 \end{bmatrix} \tag{4.88}$$

and

$$M_{I_{CL}} = \begin{bmatrix} -0.14156 & -0.701285 & 0.698685 \\ 0.98993 & -0.100263 & 0.0999325 \\ 0.0000288901 & -0.705795 & -0.708416 \end{bmatrix} \tag{4.89}$$

The diagonalization of the capacitance and inductance matrices are in the form:

$$C_d = M_V^T C M_v \approx \begin{bmatrix} 1.95741\times10^{-10} & 0 & 0 \\ 0 & 1.29395\times10^{-10} & 0 \\ 0 & 0 & 1.09864\times10^{-10} \end{bmatrix} \quad (4.90)$$

and

$$L_d = M_v^{-1} L (M_V^{-1})^T \approx \begin{bmatrix} 4.79158\times10^{-7} & 0 & 0 \\ 0 & 6.01006\times10^{-7} & 0 \\ 0 & 0 & 6.72606\times10^{-7} \end{bmatrix}. \quad (4.91)$$

Thus, the time delay of the set is given as:

$$W(3)_{ns} = \sqrt{L_d C_d}$$

$$= \begin{bmatrix} 9.07966 & 0.772113 & 1.80724 \\ 0.99804 & 8.81603 & 0.899562 \\ 0 & 0.599349 & 7.90884 \end{bmatrix} ns$$

$$\approx \begin{bmatrix} 9.07966 & 0 & 0 \\ 0 & 8.81603 & 0 \\ 0 & 0 & 7.90884 \end{bmatrix} ns \quad (4.92)$$

and the characteristic impedance is given as:

$$Z(3)_{ns} = W_d C_d^{-1}$$

$$= \begin{bmatrix} 48.4332 & 4.58151 & -7.70452 \\ 2.1953 & 67.9386 & 5.20651 \\ -23.3102 + 11.9255i & 3.41272 - 0.246282i & 83.4564 - 5.90914i \end{bmatrix} \Omega$$

$$\approx \begin{bmatrix} 48.4332 & 0 & 0 \\ 0 & 67.9386 & 0 \\ 0 & 0 & 83.4564 \end{bmatrix} \Omega. \qquad (4.93)$$

The results obtained using Parker's algorithm (1994) are different as presented below:

$$W'(3)_{ns} = \begin{bmatrix} 9.27065 & 6.78319 \times 10^{-8} & 1.03595 \\ 1.56044 & 9.51151 & 2.91816 \\ 1.74216 & 3.32388 & 8.2234 \end{bmatrix} ns \qquad (4.94)$$

and

$$Z'(3)_{ns} = \begin{bmatrix} 50.5752 & -24.8496 & -4.15538 \\ -56.0597 & 308.339 & 337.996 \\ -44.3265 & 283.764 & 369.011 \end{bmatrix} \Omega. \qquad (4.95)$$

As can be seen from eqns. 4.94 and 4.95, the matrices are not diagonal and most of all the values are inconsistent when compared to (4.92) and (4.93). The novel algorithm can be generalised to apply to strictly nonuniform types of coupled microstrip lines.

4.5.3.4 $W(n)_{sn}$ and $Z(n)_{sn}$ of strictly nonuniform

The algorithm used to calculate time delay $W(n)_{sn}$ and characteristic impedance $Z(n)_{sn}$ of any n-coupled strictly nonuniform microstrip lines is based mainly on the value of its capacitance matrix. The capacitance matrix can be evaluated by the bound capacitance methods, see section 4.6.3.2. Once this is achieved, the rest follows steps 4 to 9 of the algorithm for nonuniformly spaced coupled microstrip lines.

As a sample of the execution of the algorithm, the time delay, $W(4)_{sn}$, and the characteristic impedance, $Z(4)_{sn}$, of 4 coupled strictly nonuniform microstrip lines of 4.5.3.1 (see Fig. 4.6) are presented. The capacitance and inductance matrices of this set are calculated with respect to the focus method by using a developed Mathematica program Matrdiff (see Appendix A.5). The calculation of the mutual capacitance in the program is simplified by taking assumption 1 of section 4.5.1, i.e.

$$c_{ij\,\max,\min} = \begin{cases} 0 & \text{for } j-i>1 \\ c^*_{ij\max,\min} & \text{for } j-i=1 \end{cases} \tag{4.96}$$

such that (4.30) simplifies to

$$c^*_{ij\min} = \left\{ \begin{matrix} \min(w_i, w_j) \\ \min(t_i, t_j) \\ s_i \end{matrix} \right\} = c^*_{ji\min} \tag{4.97}$$

and (4.31) changes to

$$c^*_{ij\max} = \begin{Bmatrix} \max(w_i, w_j) \\ \max(t_i, t_j) \\ s_i \end{Bmatrix} = c^*_{ji\max} \tag{4.98}$$

The capacitance matrix for the set is taken to be $C_{\max}$ for this purpose, and the values for C, L, LC and CL are given as:

$$C = \begin{bmatrix} 160.878 & -60.2384 & 0 & 0 \\ -60.2384 & 167.684 & -6.80597 & 0 \\ 0 & -6.80597 & 133.554 & -26.1078 \\ 0 & 0 & -26.1078 & 126.748 \end{bmatrix} \text{pF} \tag{4.99}$$

and

$$L = \begin{bmatrix} 463.168 & 153.128 & 0 & 0 \\ 153.128 & 383.396 & 27.3842 & 0 \\ 0 & 27.3842 & 505.843 & 122.789 \\ 0 & 0 & 122.789 & 492.088 \end{bmatrix} n\text{H}. \tag{4.100}$$

Then

$$LC = \begin{bmatrix} 65.2894 & -2.22338 & -1.04218 & 0 \\ 1.53976 & 54.8788 & 1.04789 & -0.714941 \\ -1.64958 & 1.14914 & 64.1652 & 2.35681 \\ 0 & -0.835698 & 3.55163 & 59.1654 \end{bmatrix} \times 10^{-18} \tag{4.101}$$

and

$$CL = (LC)^T = \begin{bmatrix} 65.2894 & 1.53976 & -1.64958 & 0 \\ -2.22338 & 54.8788 & 1.14914 & -0.835698 \\ -1.04218 & 1.04789 & 64.1652 & 3.55163 \\ 0 & -0.714941 & 2.35681 & 59.1654 \end{bmatrix} \times 10^{-18} \tag{4.102}$$

by theorem 4.7. The eigenvectors for LC and CL are:

$$\begin{bmatrix} 1 & 0 & 0 & 0 \\ -0.0433443 & 0.345748 & -0.904037 & -0.247581 \\ -0.114657 & -0.677855 & 0.7262 & 0 \\ -0.179376 & -0.576042 & 0.00462638 & 0.797483 \end{bmatrix} \tag{4.103}$$

and

$$\begin{bmatrix} 1 & 0 & 0 & 0 \\ -0.329175 & -0.28647 & -0.897906 & -0.0578155 \\ -0.00832446 & -0.685032 & -0.672763 & 0.279377 \\ 0.0875933 & -0.901983 & -0.422794 & 0 \end{bmatrix}. \tag{4.104}$$

However, the calculated normalised eigenvectors of LC and CL are

$$M_{v_{LC}} = \begin{bmatrix} -0.977204 & 0.0423562 & 0.112043 & 0.175287 \\ 0.168612 & -0.374934 & 0.701415 & 0.582247 \\ -0.127924 & -0.746156 & 0.158136 & -0.63394 \\ 0.0166955 & 0.548526 & 0.685898 & -0.477895 \end{bmatrix} \tag{4.105}$$

and

$$M_{I_{CL}} = \begin{bmatrix} -0.946561 & 0.311585 & 0.00787961 & -0.0829125 \\ -0.0161027 & -0.239939 & -0.586304 & -0.773574 \\ 0.314226 & 0.844083 & 0.172244 & -0.398896 \\ -0.0708834 & -0.364511 & 0.791528 & -0.485376 \end{bmatrix} \quad (4.106)$$

Furthermore

$$M_I^{-1} = \begin{bmatrix} -0.946562 & -0.01610285 & 0.314226 & -0.0708833 \\ 0.311585 & -0.239939 & 0.844083 & -0.364511 \\ 0.00787954 & -0.586305 & 0.172244 & 0.791529 \\ -0.0829125 & -0.773575 & -0.398896 & -0.485377 \end{bmatrix} \quad (4.107)$$

and

$$M_v^T = \begin{bmatrix} -0.977204 & 0.168612 & -0.127924 & 0.0166955 \\ 0.0423562 & -0.374934 & -0.746156 & 0.548526 \\ 0.112043 & 0.701415 & 0.158136 & 0.685898 \\ 0.175287 & 0.582247 & -0.63394 & -0.477895 \end{bmatrix} \quad (4.108)$$

Note that $M_I^{-1} \approx M_v^T$, as expected.

The diagonalization of the capacitance and inductance matrices are:

$$C_d = M_V^T C M_v$$

$$\approx \begin{bmatrix} 1.80871 & 0 & 0 & 0 \\ 0 & 1.55829 & 0 & 0 \\ 0 & 0 & 1.30845 & 0 \\ 0 & 0 & 0 & 1.21319 \end{bmatrix} \times 10^{-10} \quad (4.109)$$

$$L_d = M_v^{-1} L (M_V^{-1})^T$$

$$\approx \begin{bmatrix} 4.09439 & 0 & 0 & 0 \\ 0 & 3.94362 & 0 & 0 \\ 0 & 0 & 4.95374 & 0 \\ 0 & 0 & 0 & 5.4532 \end{bmatrix} \times 10^{-7} \qquad (4.110)$$

.

Therefore, the time delay and the characteristic impedance of the set are given as:

$$W(4)_{sn} = \sqrt{L_d C_d} = \begin{bmatrix} 8.0427 & 0 & 0.306727 & 0 \\ 0 & 7.74394 & 0 & 1.54731 \\ 0 & 0 & 7.56938 & 0 \\ 0 & 1.89675 & 0 & 7.84535 \end{bmatrix} \times 10^{-9}\,\text{s}$$

$$\approx \begin{bmatrix} 8.0427 & 0 & 0 & 0 \\ 0 & 7.74394 & 0 & 0 \\ 0 & 0 & 7.56938 & 0 \\ 0 & 0 & 0 & 7.84535 \end{bmatrix} n\text{s} \qquad (4.111)$$

$$Z(4)_{sn} = W_d C_d^{-1} = \begin{bmatrix} 50.4407 & 7.74007 & -13.0882 & -10.5483 \\ 5.64082 & 50.8527 & -5.70573 & 13.0876 \\ -14.7634 & -4.09359 & 64.1231 & -7.42468 \\ -8.13146 & 12.0362 & -8.72116 & 68.457 \end{bmatrix}$$

$$\approx \begin{bmatrix} 50.4407 & 0 & 0 & 0 \\ 0 & 50.8527 & 0 & 0 \\ 0 & 0 & 64.1231 & 0 \\ 0 & 0 & 0 & 68.457 \end{bmatrix} \Omega. \qquad (4.112)$$

All off-diagonal elements (eqns. 4.111 and 4.112) can be neglected and use only the diagonal elements. Although this approach may appear to be very crude,

simulation results obtained by using a wide range of different parameters indicated that the induced error is small. Moreover, since C_d and L_d were diagonal matrices, this made the computation of W_{sn} and Z_{sn} trivial. For these reasons, both W_{sn} and Z_{sn} were also diagonal as appeared above. Similar observations were true for the case of nonuniformly spaced coupled microstrip lines, i.e. W_{ns} and Z_{ns}.

The difference of the values of characteristic impedance between line 1 and 2 is small. However, the value of the characteristic impedance of line 3 is drastically bigger than line 2 because the lines are quite far apart ($s_2 = 15\mu m$). This shows immediately that the spacing has a significant effect on the characteristic impedance of a coupled microstrip line.

Even though, the main purpose of the algorithm is to calculate time delay and characteristic impedance of strictly nonuniform coupled microstrip lines, because of its generality and the fact that $C(n)_{sn_{\min}} = C(n)_{sn} = C(n)_{sn_{\max}}$ (see Sect. 4.5.3.1) for bound capacitances of n coupled uniform lines, therefore, the algorithm can also be applied to any kind of coupled microstrip lines; uniform and nonuniform.

The generalisation of the time delay and characteristic impedance algorithms for any type of n coupled lines (Sect. 4.5.3.4) introduces its very own unique problems. One of these is that the calculation of the eigenvalues and eigenvectors which is not a trivial since for a quite large matrices, Mathematica may introduce

errors which then propagate rapidly through to the final evaluation of the time delay and characteristic impedance. For the same reason, Parker (1994) limited his calculation to only three coupled uniform microstrip lines.

Simulations were succesfully carried out on three or more nonuniform coupled lines using the novel algorithms of time delay and characteristic impedance. However, time delay and characteristic impedance values for 8 nonuniform coupled lines were quite inconsistent probably due to the same problem as mentioned above.

Finally the set of n nonuniformly spaced or strictly nonuniform coupled microstrip lines can be represented by n single line parameters by applying the algorithms. These parameters are then used to simulate crosstalk using the coupled lines SPICE model as described in the next chapter.

5. ANALYSIS BY SIMULATION AND EXPERIMENTAL

5.1 Introduction

The central idea of Chapter 4 was to develop a mathematical model of a microstrip system. The model was then used to determine the performance characteristics of the system, namely; geometrical parameters, electrical parameters and in particular crosstalk.

This chapter presents all the experimental and simulation results based on the model. It is divided into three major sections:

- geometrical parameters,
- electrical parameters and
- crosstalk analysis.

The analysis of geometrical parameters was only done analytically, whereas the analysis of electrical parameters was carried out using both simulation and analysis. Finally, the crosstalk analysis was carried out by experimentation and simulation. These analyses led to important conclusions which were used in developing a fuzzy model of the system, as outlined in Chapter 7.

5.2 Analysis of the Geometrical Parameters

The investigation of the geometrical parameters was carried out analytically. A thorough examinations of the mathematical expressions of microstrip lines, introduced in Chapter 3, led to a few mathematical constraints. These constraints are described in the following subsection.

5.2.1 Thickness (t)

The capacitance matrix cannot have complex number entries because it must be definitely positive as well as diagonally dominant (Romeo and Santomauro 1987).

For example, let us suppose

$$C = \begin{pmatrix} a_{11} & a+ib & 0 \\ a+ib & a_{22} & a_{23} \\ 0 & a_{23} & a_{33} \end{pmatrix} \tag{5.1}$$

and let

$$C_1 = \begin{pmatrix} a_{11} & a+ib \\ a+ib & a_{22} \end{pmatrix} \tag{5.2}$$

$$\text{Thus det } (C_k) = \begin{vmatrix} a_{11} & a+ib \\ a+ib & a_{22} \end{vmatrix}$$

$$= a_{11}a_{22} - (a+ib)^2$$

$$= a_{11}a_{12} - a^2 + b^2 - i2ab \tag{5.3}$$

which is a complex number (see D 3.4).

Therefore, in order to prevent the capacitance matrix from having complex numbers as its entries, the mutual capacitance (see. eqn. 3.18) must not produce any complex number. This is true if any of its components which have a square

root within their expressions, i.e. ε_{re}, (see eqns. 3.5, 3.6, 3.10, 3.12, 3.3.13, 3.16), is positive as below:

$$\varepsilon_{re} = \frac{\varepsilon_r + 1}{2} + \frac{\varepsilon_r - 1}{2} f(w/h) - E > 0 \qquad (5.4)$$

where $f(w/h)$ and E are defined in eqns. 3.4 and 3.9, respectively.

Using (5.4) , then (3.9), it can be deduced that

$$\frac{e_r + 1}{2} + \frac{e_r - 1}{2} f(w/h) - \frac{t(e_r - 1)}{4.6\sqrt{hw}} > 0 \qquad (5.7)$$

or

$$\frac{t(e_r - 1)}{4.6\sqrt{hw}} < \frac{1}{2}\left[e_r + 1 + (e_r - 1) f(w/h)\right]. \qquad (5.8)$$

For $e_r > 1$, (5.8) can be rewritten as:

$$t < \frac{2.3\sqrt{hw}}{e_r - 1}\left[e_r\left(1 + f(w/h)\right) + (1 - f(w/h))\right] \qquad (5.9)$$

Since the thickness, t, of a microstrip line is always positive, (5.9) can be rewritten as:

$$0 < t < \frac{2.3\sqrt{hw}}{e_r - 1}\left[e_r\left(1 + f(w/h)\right) + (1 - f(w/h))\right] \qquad (5.10)$$

The other possibility of having complex numbers as the entries of the capacitance matrix comes from eqn. 3.7. This equation must be positive in order to avoid this problem. Therefore the restrictions of t in terms of w and h are as given below:

For $\frac{w}{h} \leq \frac{1}{2\pi}$ and $\frac{w}{h} \geq \frac{1}{2\pi}$ the restrictions on the thickness are $t \leq 4\pi w$ and $t \leq 2h$, respectively. In summary, the thickness of coupled microstrip lines must fulfil all the conditions listed below:

1) $0 < t < \frac{2.3\sqrt{hw}}{e_r - 1}\left[e_r\left(1 + F(w/h)\right) + (1 - F(w/h))\right]$ where $e_r > 1$

2) $t \leq 4\pi w$ for $\frac{w}{h} \leq \frac{1}{2\pi}$

3) $t \leq 2h$ for $\frac{w}{h} \geq \frac{1}{2\pi}$

The application of these inequalities is illustrated using set of geometrical parameters taken from Belahrach (1990) and reproduced below:

Width	Spacing	Thickness	Height	Dielectric
405 μm	285 μm	16 μm	1060 μm	12

These parameters must fulfil all the conditions listed above. Let us look at the width to height ratio:

$$\frac{w}{h} = 405/1060 = 0.382075471. \qquad (5.11)$$

From (5.11) $\frac{w}{h} \geq \frac{1}{2\pi}$, therefore the thickness of the line must satisfy the third condition:

$$t < 2(1060) \qquad (5.12)$$

The thickness must also satisfy the first condition:

$$t < 136.9984316[12(1+0.175662013)+(1-0.175662013)] \\ = 2045.693184\mu m \qquad (5.13)$$

Eqns. 5.12 and 5.13 impose different values on the constraint on t. This deadlock can be solved by taking the minimum of the two constraint values which is $t < \min[2120, 2045.693184]$ μm. This simply implies that as long as $t < 2045.693\mu m$, the mutual capacitances are not complex numbers, and in this case Belahrach (1990) has taken $t = 16\mu m$.

The restriction on t has been coded as part of the Mathematica program Travail (Appendix A.2) for electrical parameters analysis in Section 5.3.

5.2.2 Spacing (s), Height (h) and Width (w)

No obvious mathematical restrictions exist for spacing, height and width of microstrip lines. This can be observed in eqn. 3.14 as,

$$\sqrt{k'} \neq 1 \text{ which implies } k' \neq 1. \qquad (5.14)$$

Eqn. 5.14 leads to a restriction on eqn. 3.15 as follows:

$$1-k^2 \neq 1 \text{ which implies } k \neq 0 \qquad (5.15)$$

and

$$\frac{s/h}{(s/h)+2(w/h)} \neq 0; \tag{5.16}$$

Eqn. 5.16 implies:

$$\frac{s}{h} \neq 0 \tag{5.17}$$

, thus $s,\ h \neq 0$ and similarly for w. (5.18)

Thus $s, w, h \in R^{+} \setminus \{0\}$, in other words the width and the height of the lines can have any positive values. A similar open condition also applies to the spacing.

5.3 Analysis of the Electrical Parameters

Here electrical parameters are analysed both analytically and by computer simulation. The latter is carried out using the Mathematica software package; see Appendix A.1 and A.2.

5.3.1 Impedance vs. *w/h*

Parker (1994) has shown by simulation that increasing *w/h* for a microstrip line, decreases its characteristic impedance. This can be proved analytically by observing eqns. 3.1 to 3.4 (excluding the thickness) where the impedance should approach zero as *w/h* tends to infinity. His results are only valid for a specific set

of 8 -coupled microstrip lines. Here, an attempt has been made to generalise the result so as to apply to any microstrip line with a configuration which excludes its thickness. This is done by a theorem and subsequent proof as outlined below.

Theorem 5.1: For a single microstrip line the characteristic impedance is as

$$\text{If } Z_{om} = \begin{cases} \dfrac{60}{\sqrt{\varepsilon_{re}}} \ln\left(\dfrac{8h}{w} + 0.25\dfrac{w}{h}\right) & \text{for } \dfrac{w}{h} \le 1 \\ \dfrac{120\pi}{\sqrt{\varepsilon_{re}}\left[\dfrac{w}{h} + 1.393 + 0.667\ln\left(\dfrac{w}{h} + 1.444\right)\right]^{-1}} & \text{for } \dfrac{w}{h} \ge 1 \end{cases} \tag{5.19}$$

where ε_{re} and $F(w/h)$ are defined as in eqns. 3.3 and 3.4, respectively.

$$\text{Then } \lim_{w/h \to \infty} Z_{om} = 0. \tag{5.20}$$

proof:

Let $\dfrac{w}{h} = a \in R$, thus (3.3) can be simplified to

$$\begin{aligned} \varepsilon_{re} &= \frac{\varepsilon_r + 1}{2} + \frac{\varepsilon_r - 1}{2}\left[\left(1 + \frac{12}{a}\right)^{-\frac{1}{2}} + 0.04(1-a)^2\right] \\ &= \frac{\varepsilon_r + 1}{2} + \frac{\varepsilon_r - 1}{2}\left[\frac{1}{\sqrt{1 + \dfrac{12}{a}}} + 0.04(1-a)^2\right]. \end{aligned} \tag{5.21}$$

The proof of this theorem is divided into two parts:

i) when $\dfrac{w}{h} \le 1$.

$$\lim_{a\to 1} Z_{om} = \lim_{a\to 1} \frac{60}{\sqrt{\varepsilon_{re}}} \ln[8a^{-1} + 0.25a] = \frac{\lim_{a\to 1} 60\ln[8a^{-1} + 0.25a]}{\lim_{a\to 1} \sqrt{\varepsilon_{re}}} \tag{5.22}$$

$$= \frac{60\ln[8 + 0.25]}{\lim_{a\to 1} \sqrt{\varepsilon_{re}}} = \frac{126.612792}{\lim_{a\to 1} \sqrt{\varepsilon_{re}}} \tag{5.23}$$

$$= \frac{126.612792}{\sqrt{\frac{\varepsilon_r + 1}{2} + \frac{\varepsilon_r - 1}{2}[\frac{1}{\sqrt{1 + \frac{12}{1}}} + 0.04(1-1)^2]}} \tag{5.24}$$

$$= \frac{126.612792}{\sqrt{\frac{\varepsilon_r + 1}{2} + \frac{\varepsilon_r - 1}{2}[\frac{1}{\sqrt{1+12}}]}} = \frac{126.612792}{\sqrt{\frac{\varepsilon_r + 1}{2} + \frac{\varepsilon_r - 1}{2}[\frac{1}{\sqrt{13}}]}} \tag{5.25}$$

$$= \frac{126.612792}{\sqrt{\frac{\sqrt{13}(\varepsilon_r + 1) + (\varepsilon_r - 1)}{2\sqrt{13}}}} = \frac{\sqrt{2\sqrt{13}}(126.612792)}{\sqrt{\sqrt{13}(\varepsilon_r + 1) + (\varepsilon_r - 1)}} \tag{5.26}$$

$$= \frac{339.9996122}{\sqrt{\varepsilon_r(\sqrt{13} + 1) + (\sqrt{13} - 1)}}. \tag{5.27}$$

ii) when $\frac{w}{h} \geq 1$.

$$\lim_{a=1\to\infty} Z_{om} = \lim_{a=1\to\infty} \frac{120\pi}{\sqrt{\varepsilon_{re}}}[a + 1.393 + 0.667\ln(a + 1.444)]^{-1} \tag{5.28}$$

$$= \frac{\lim_{a\to\infty} 120\pi}{\lim_{a=1\to\infty} \sqrt{\varepsilon_{re}}\left[a + 1.393 + 0.667\ln(a + 1.444)\right]} \tag{5.29}$$

$$= \frac{120\pi}{\lim_{a=1\to\infty} \sqrt{\varepsilon_{re}}\left[a + 1.393 + 0.667\ln(a + 1.444)\right]} \tag{5.30}$$

$$= 120\pi \frac{1}{\lim_{a=1\to\infty} \sqrt{\varepsilon_{re}}\left[a + 1.393 + 0.667\ln(a + 1.444)\right]} = 0 \tag{5.31}$$

Notice, $\varepsilon_{re} \to \infty$ and $\left[a + 1.393 + 0.667\ln(a + 1.444)\right] \to \infty$ as $a = 1 \to \infty$, which implies that the denominator will become larger and larger. Therefore $\lim_{a=\frac{w}{h}\to\infty} Z_{om} = 0$ as claimed earlier.

The geometrical parameters of coupled microstrip lines have a significant effect on their electrical parameters. These effects can be best discovered by applying the developed Travail program (Appendix A.2). Below are some numerical simulations of the electrical parameters using this program.

5.3.2 Gap capacitance

The geometrical parameters for the gap capacitance (see eqn. 3.17) are the thickness and the spacing between the lines. Therefore, the gap capacitance for different line thicknesses and spacings are simulated and shown in Fig. 5.1. The capacitance increases linearly with the thickness of line and decreases as the

spacing between the lines increases, as one would have expected. The gap capacitance almost approaches zero when the spacing between the lines is >1.0 μm. This can be proven as follows:

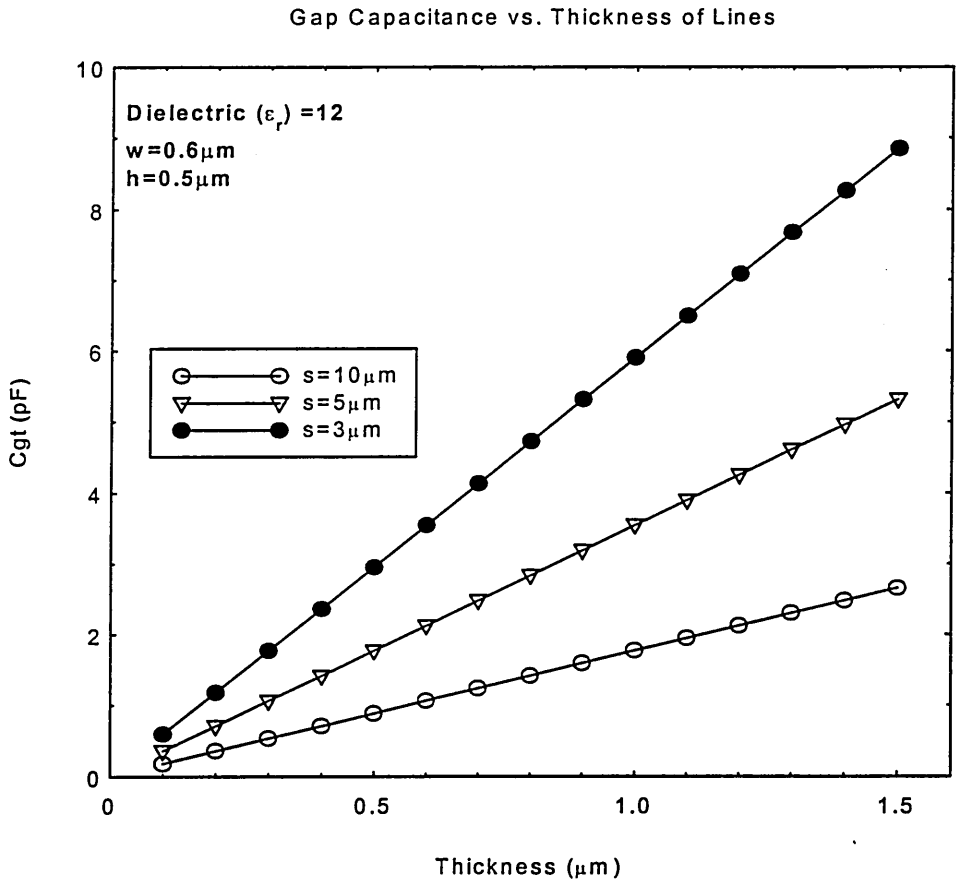

Fig. 5.1(a)

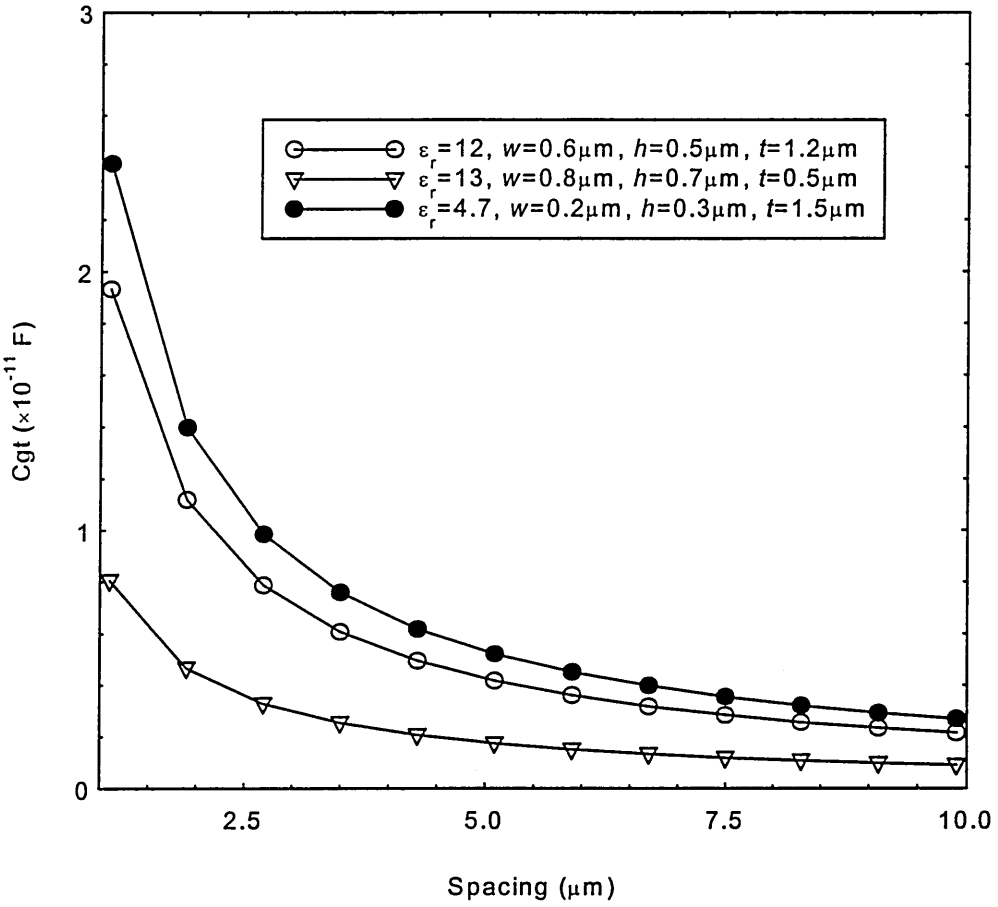

Fig. 5.1(b)

Figure 5.1 Microstrip line gap capacitance vs. (a) thickness

(b) spacing.

Theorem 5.2:

From eqn. 3.17;

$$\text{If } C_{gt}(t,s) = 2\varepsilon_0 \frac{t}{s}, \text{ then } \lim_{s\to\infty} C_{gt} = 0. \tag{5.32}$$

proof:

$$\lim_{s\to\infty} C_{gt} = \lim_{s\to\infty} 2\varepsilon_0 \frac{t}{s}. \tag{5.33}$$

$$= 2\varepsilon_0 t \lim_{s\to\infty} \frac{1}{s} \tag{5.34}$$

$$= 2\varepsilon_0 t(0) = 0 \tag{5.35}$$

5.3.3 Gap capacitance in air

Using the eqn. 3.14, the gap capacitance in air versus the height, spacing, width and thickness are simulated and the results are plotted in Fig. 5.2. The height of the line from the ground plane has no effect on the gap capacitance in air. This result can be explained directly from eqn 3.15 because:

$$k = \frac{s/h}{(s/h)+2(w/h)} \tag{5.36}$$

$$= \frac{s/h}{\frac{s+2w}{h}} = \frac{s}{s+2w} \tag{5.37}$$

where h is deleted.

The capacitance increases as the width of lines increases (Fig. 5.2.c) and it decreases as the spacing between the lines increases (Fig. 5.2.b). Therefore, the need to strike a balance between the width and spacing of lines is necessary when considering the gap capacitance of microstrip lines.

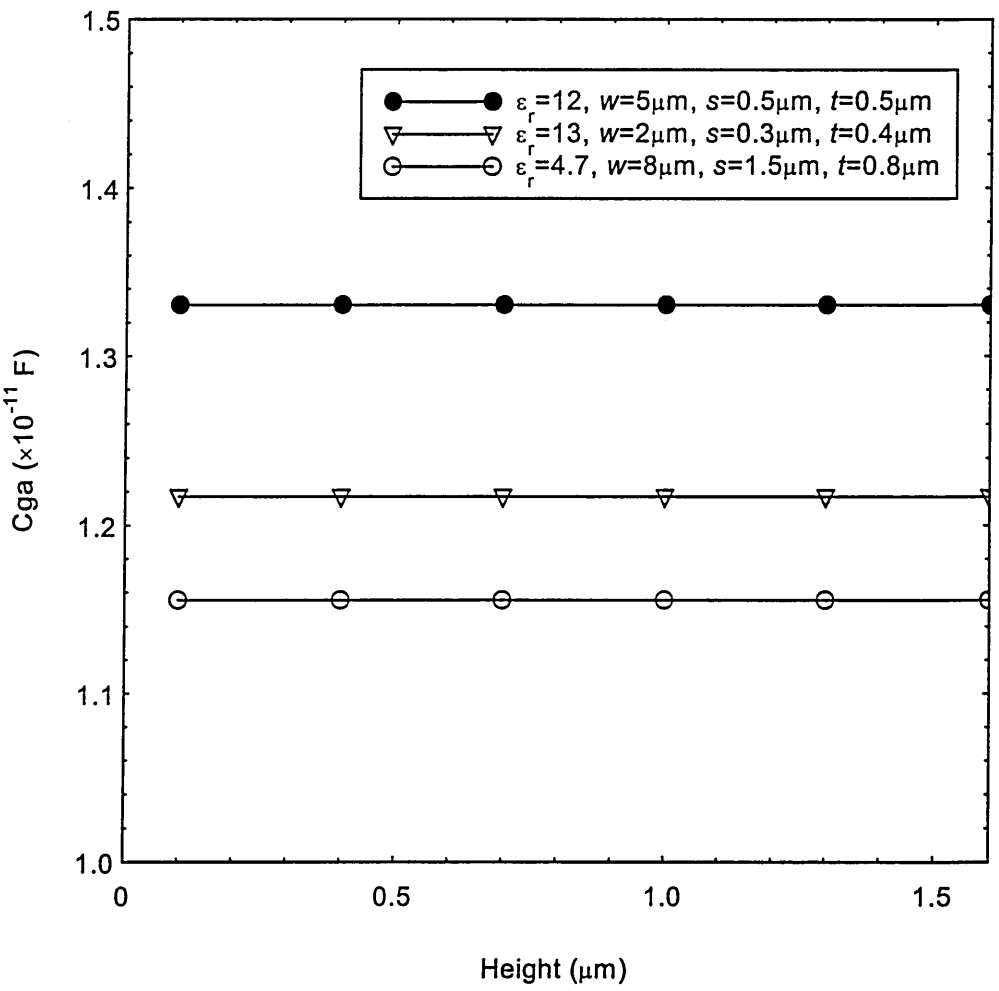
Gap Capacitance in Air vs. Height of Lines
1.5
1.4
1.3
1.2
1.1
1.0
Cga (x10^-11 F)
0
0.5
1.0
1.5
Height (μm)
εr=12, w=5μm, s=0.5μm, t=0.5μm
εr=13, w=2μm, s=0.3μm, t=0.4μm
εr=4.7, w=8μm, s=1.5μm, t=0.8μm

Fig. 5.2(a)

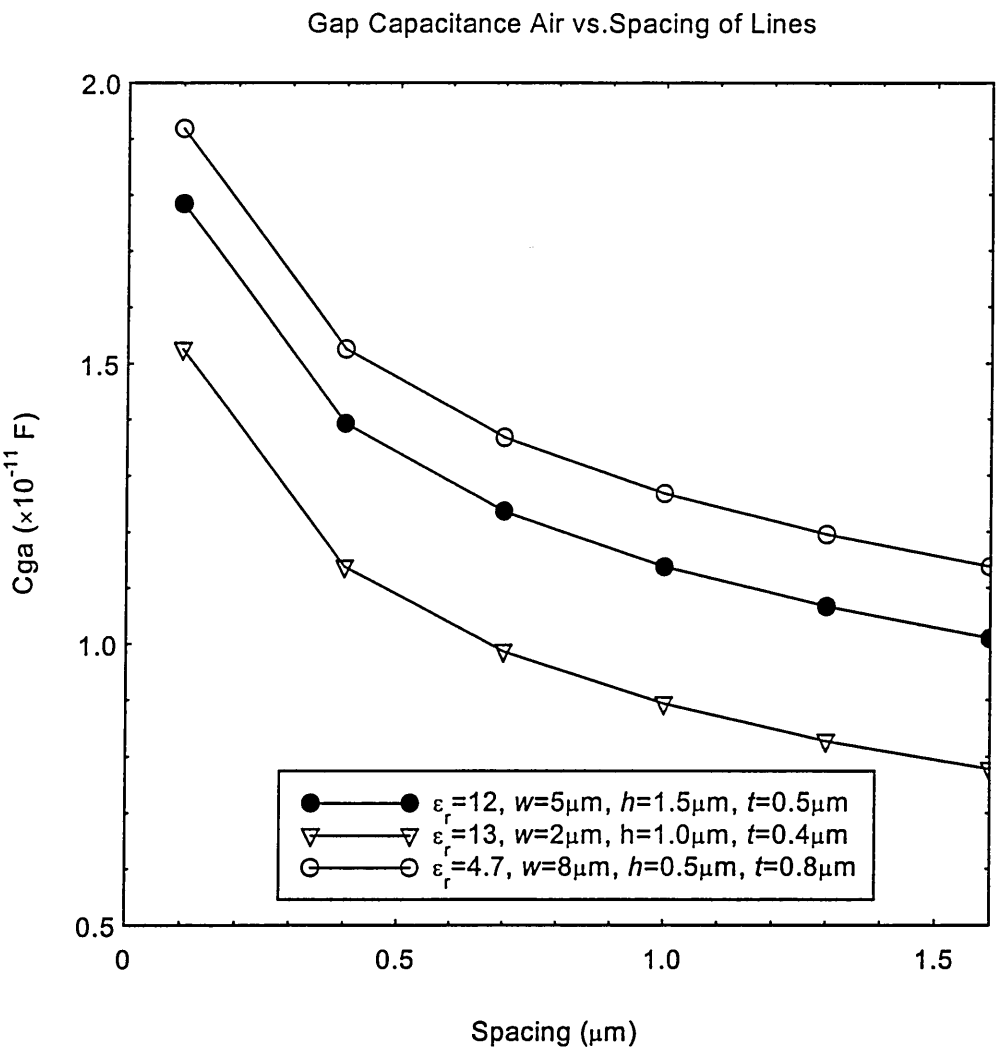
Gap Capacitance Air vs.Spacing of Lines
2.0
1.5
1.0
0.5
Cga (×10^-11 F)
0
0.5
1.0
1.5
Spacing (μm)
εr=12, w=5μm, h=1.5μm, t=0.5μm
εr=13, w=2μm, h=1.0μm, t=0.4μm
εr=4.7, w=8μm, h=0.5μm, t=0.8μm

Fig. 5.2(b)

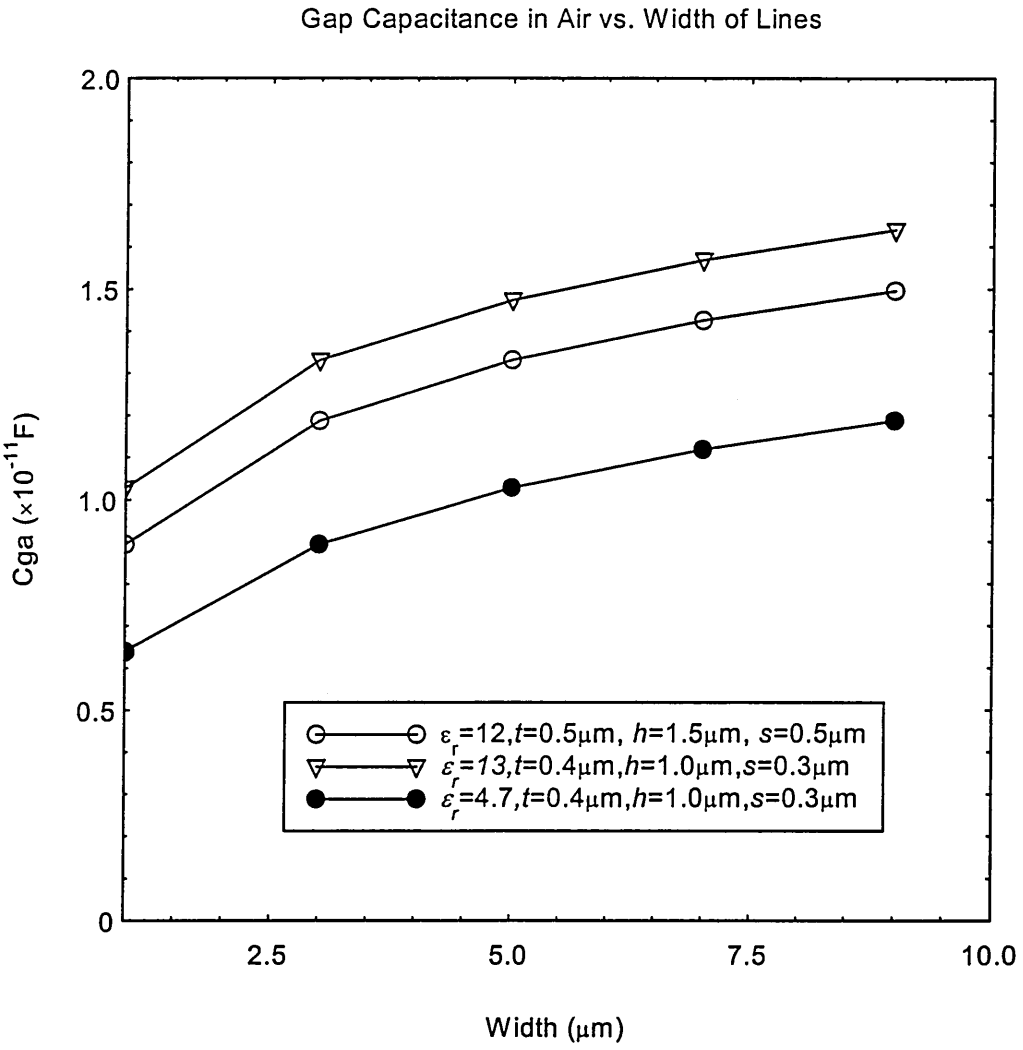
Gap Capacitance in Air vs. Width of Lines
2.0
1.5
1.0
0.5
0
Cga (x10^-11 F)
2.5
5.0
7.5
10.0
Width (μm)
ε_r=12,t=0.5μm, h=1.5μm, s=0.5μm
ε_r=13,t=0.4μm,h=1.0μm,s=0.3μm
ε_r=4.7,t=0.4μm,h=1.0μm,s=0.3μm

Fig. 5.2(c)

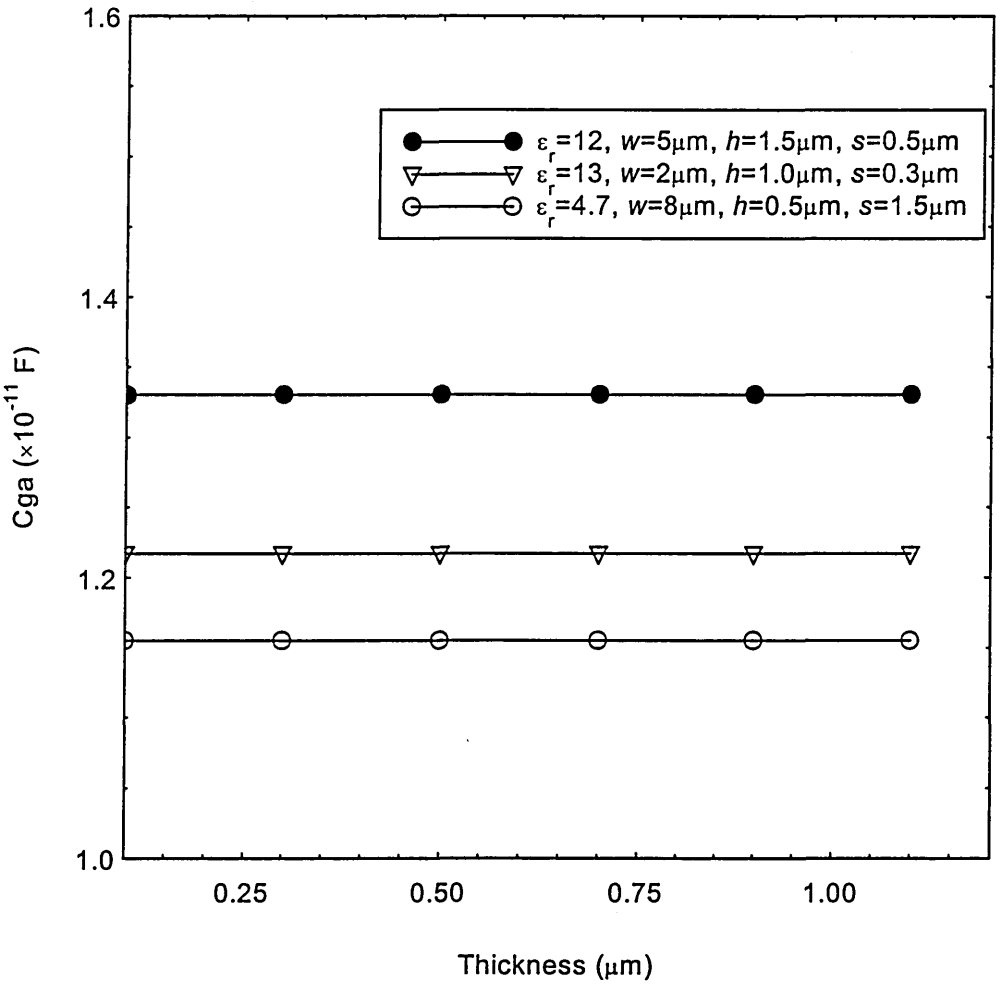

Fig. 5.2(d)

Figure 5.2 Microstrip line gap capacitance in air vs. (a) height (b) spacing (c) width (d) thickness.

The graphs in Fig. 5.2.d (C_{ga} vs. t) are identical to the graphs in Fig. 5.2.a (C_{ga} vs. h) due to the fact that thickness is not a parameter of the gap capacitance in air.

5.3.4 Capacitance due to electric flux

Using the eqn. 3.16, the capacitance due to electric flux versus the spacing, height, width and thickness of the lines is shown in Fig 5.3. The capacitance decreases exponentially (Fig. 5.3.a) as the spacing increases and the capacitance drop is large when the height of the lines increases (Fig. 5.3.b), to a threshold value of h = 0.4 um. It increases very slightly (almost negligibly) when the height of the lines is above the threshold value.

The capacitance increases steadily, almost linearly, as the width increases; see Fig. 5.3.c. On the contrary, the capacitance decreases steadily as the thickness increases (Fig. 5.3.d). These phenomenon (constraints) place demands on a design of any novel 'tool' which can calculate the set of geometrical parameters that can make compromises between all the constraints when designing microstrip lines. Such a novel tool is introduced in Chapter 7.

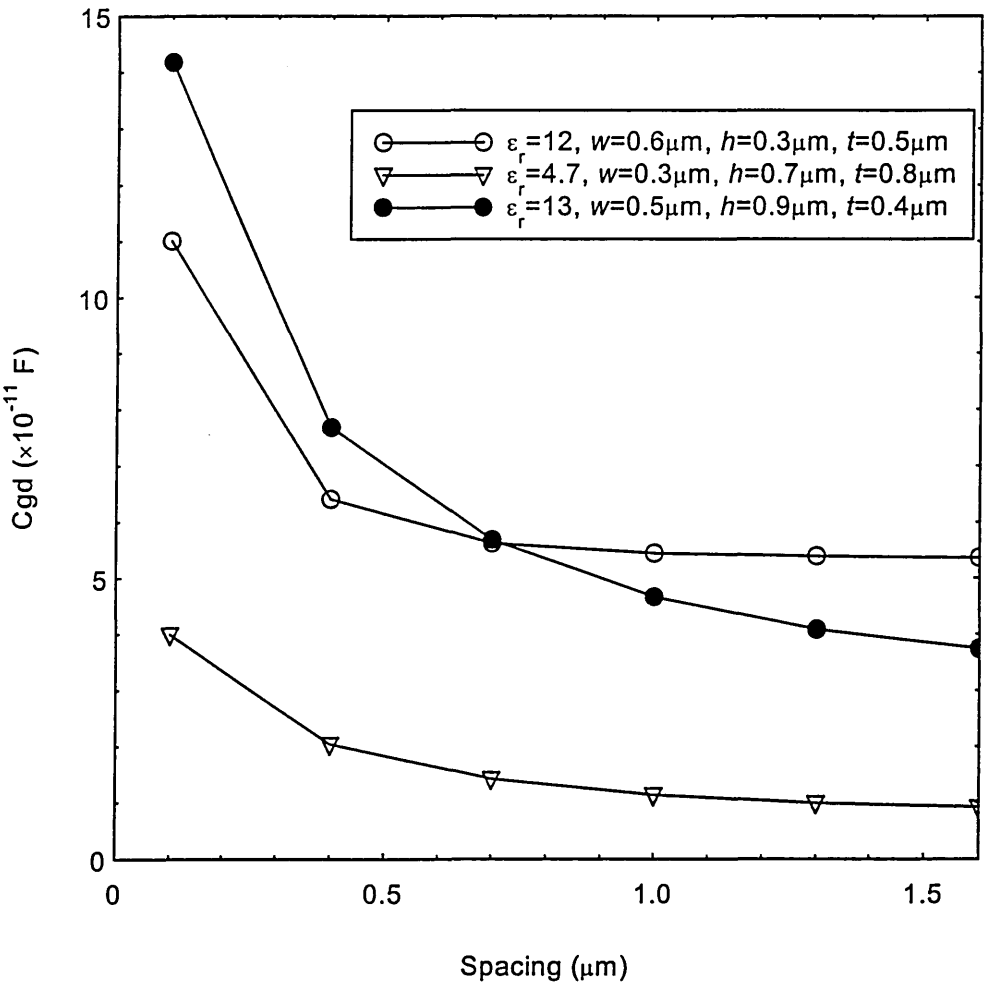
Capacitance Due to Electric Flux vs.Spacing of Lines
15
10
5
0
0
0.5
1.0
1.5
Cgd (×10^-11 F)
Spacing (μm)
εr=12, w=0.6μm, h=0.3μm, t=0.5μm
εr=4.7, w=0.3μm, h=0.7μm, t=0.8μm
εr=13, w=0.5μm, h=0.9μm, t=0.4μm

Fig. 5.3(a)

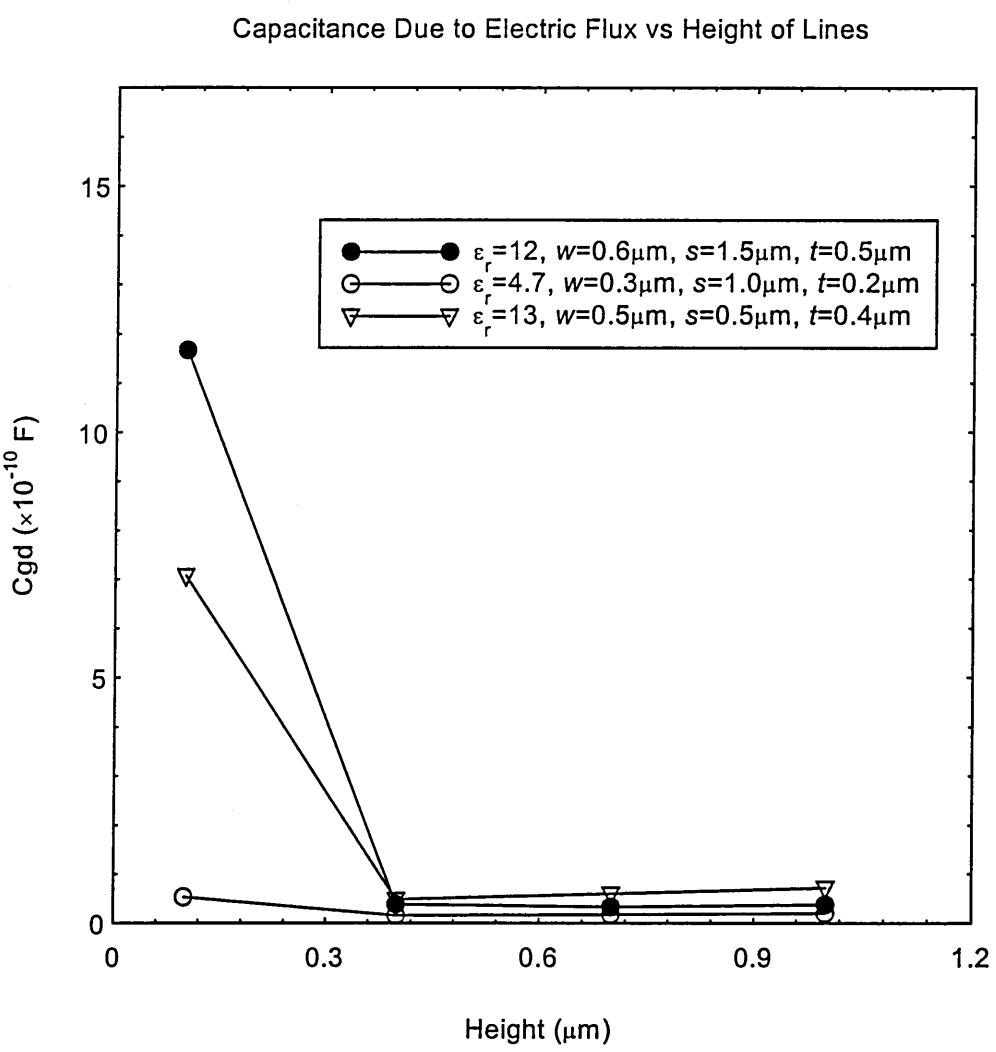
Capacitance Due to Electric Flux vs Height of Lines
15
10
5
0
0
0.3
0.6
0.9
1.2
Cgd (×10^-10 F)
Height (μm)
εr=12, w=0.6μm, s=1.5μm, t=0.5μm
εr=4.7, w=0.3μm, s=1.0μm, t=0.2μm
εr=13, w=0.5μm, s=0.5μm, t=0.4μm

Fig. 5.3(b)

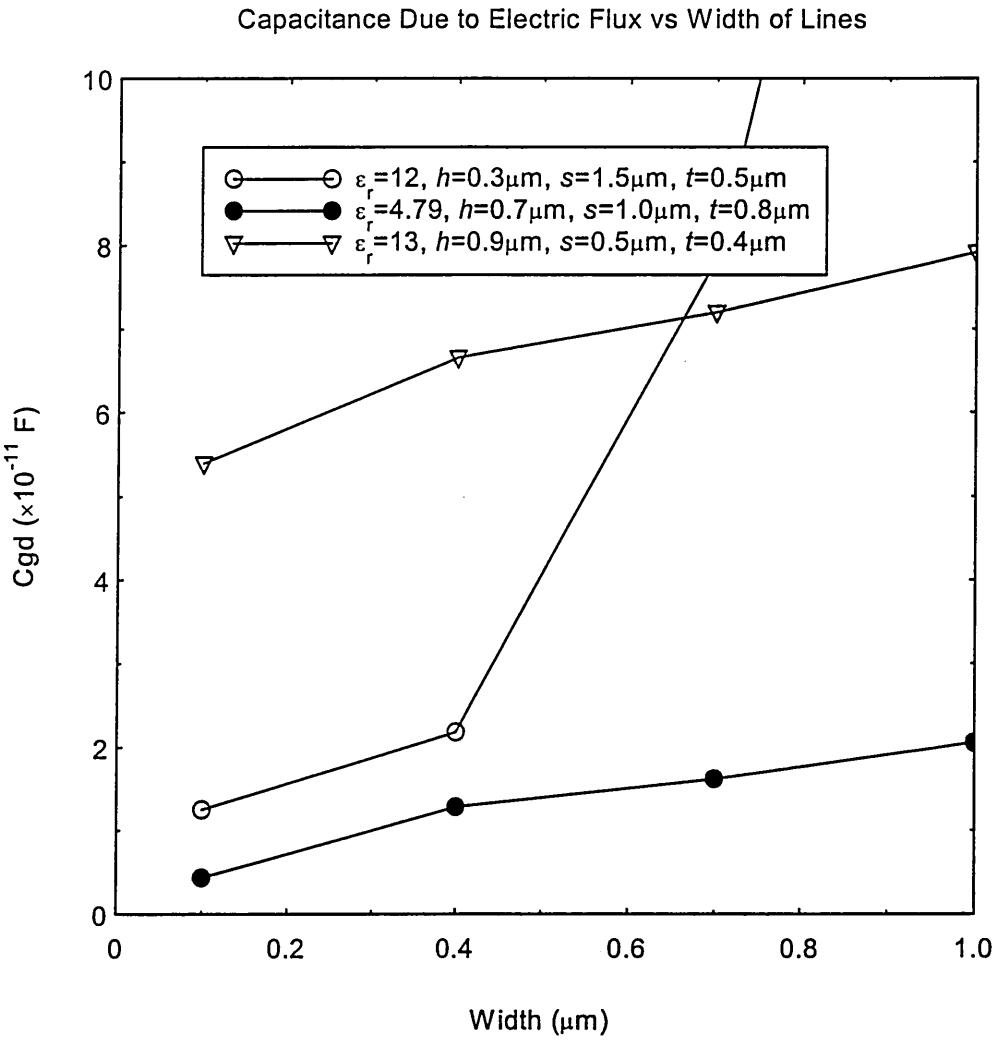
Capacitance Due to Electric Flux vs Width of Lines
εr=12, h=0.3μm, s=1.5μm, t=0.5μm
εr=4.79, h=0.7μm, s=1.0μm, t=0.8μm
εr=13, h=0.9μm, s=0.5μm, t=0.4μm
Cgd (×10^-11 F)
Width (μm)
0
2
4
6
8
10
0
0.2
0.4
0.6
0.8
1.0

Fig. 5.3(c)

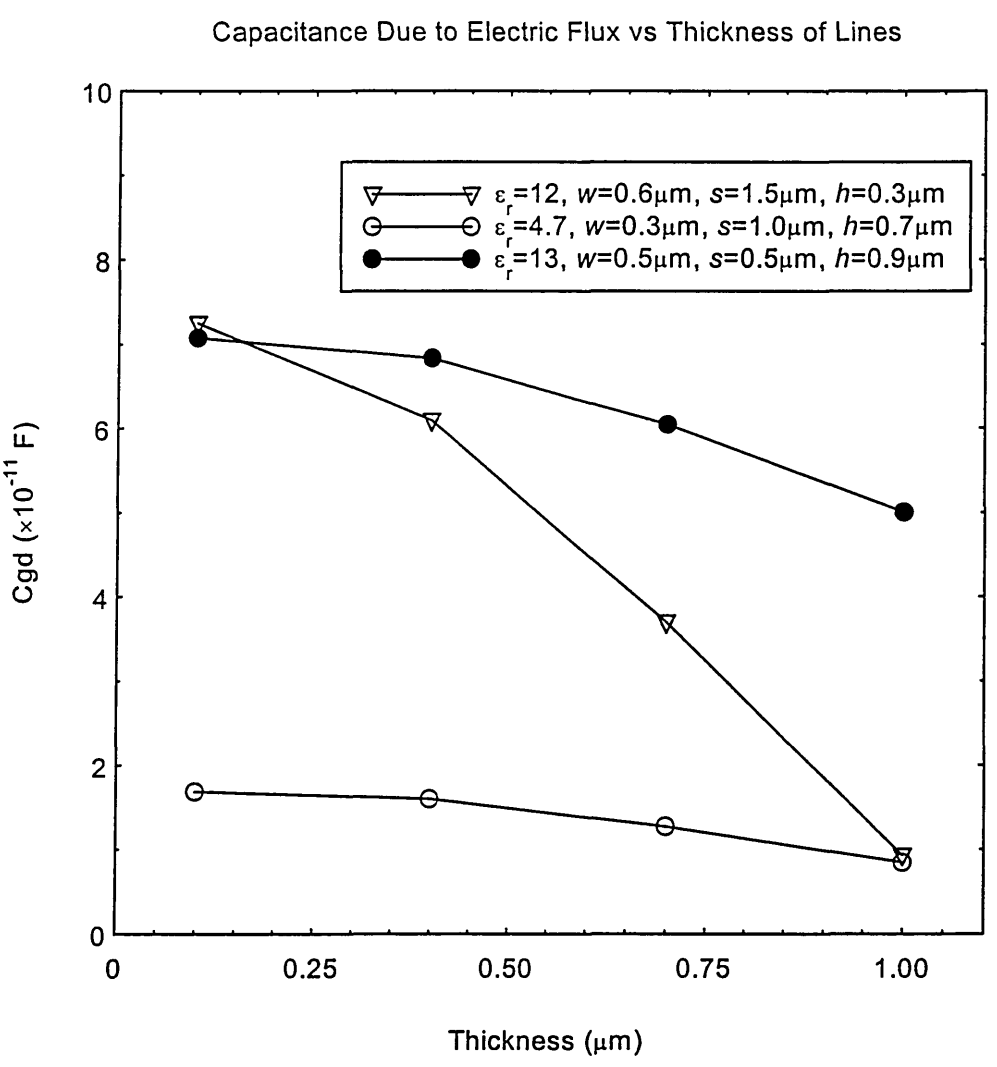

Fig. 5.3(d)

Figure 5.3 Microstrip line capacitance due to electric flux vs. (a) spacing (b) height (c) width (d) thickness.

5.3.5 Modification of fringe capacitance

Using the eqn. 3.12 the modifications of fringe capacitance versus spacing, height, width and thickness are presented in Fig 5.4. The capacitance decreases rapidly as the height of the lines increases, see Fig. 5.4.a, reaching a threshold value (~ h =

0.4 μm) beyond which very little changes take place. Therefore, lines with the height of 0.4 μm seem to be the most appropriate to use for the given samples.

Fringe capacitance also decreases steadily as the line thickness increases, reaching a value of zero at $t \approx 1.5$ μm (see Fig. 5.4.b) in two of the samples. It increases as the lines are placed further apart (see Fig. 5.4.c) which is in close agreement with experimental results obtained by Cottrell and Buturla (1985). However, the graphs of fringe capacitance vs. width are inconsistent, see Fig. 5.4.d. Therefore their profile cannot be easily generalised.

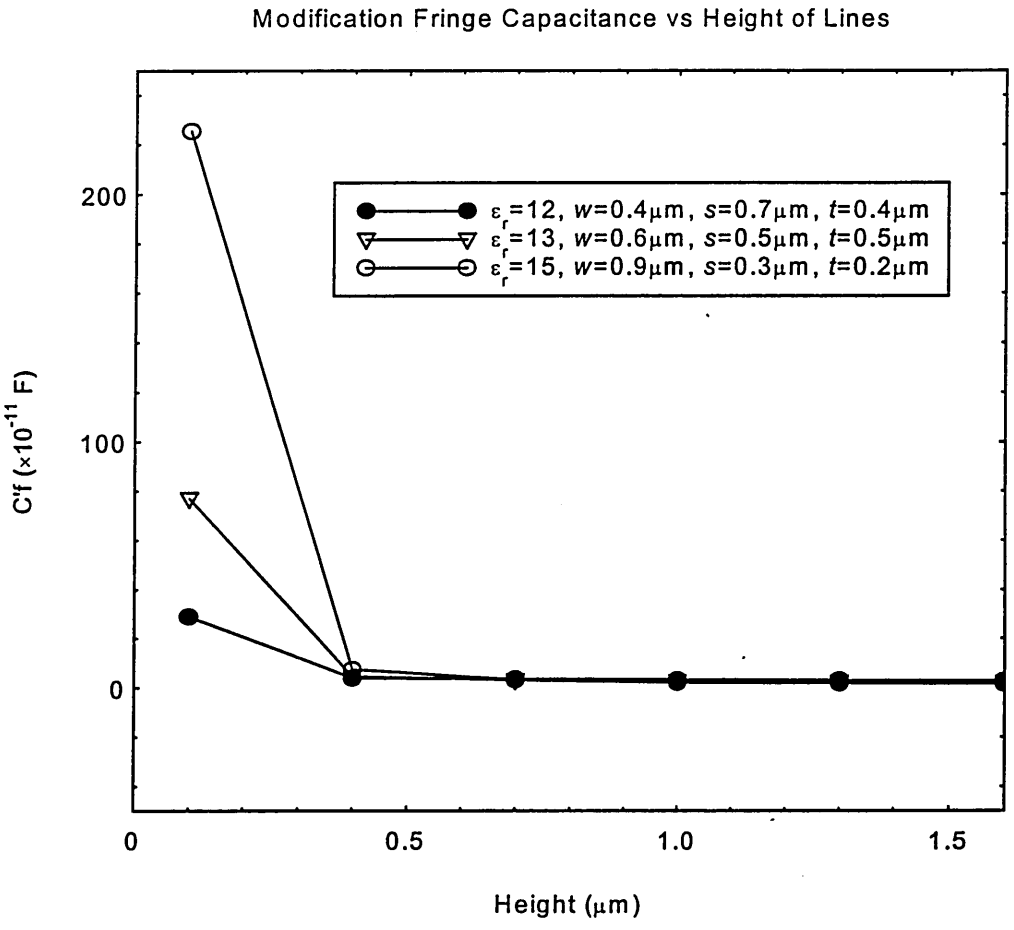

Fig. 5.4(a)

Modification Fringe Capacitance vsThickness of Lines

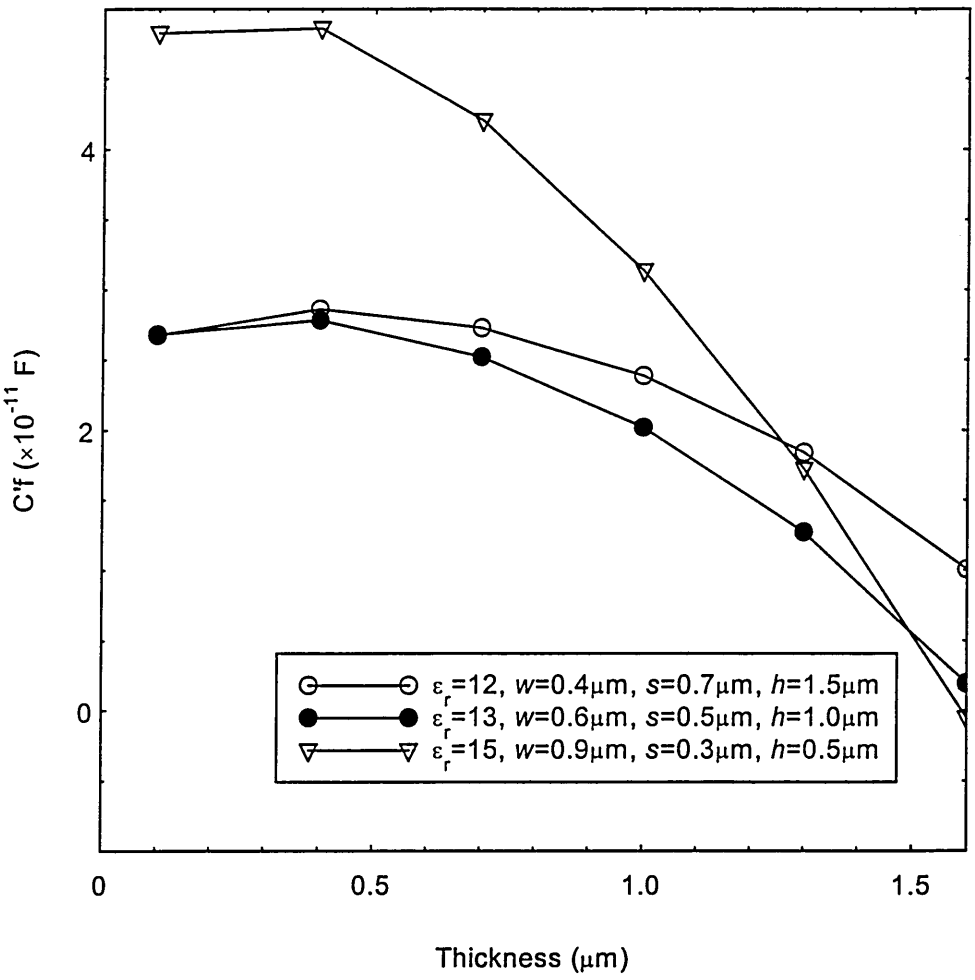

Fig. 5.4(b)

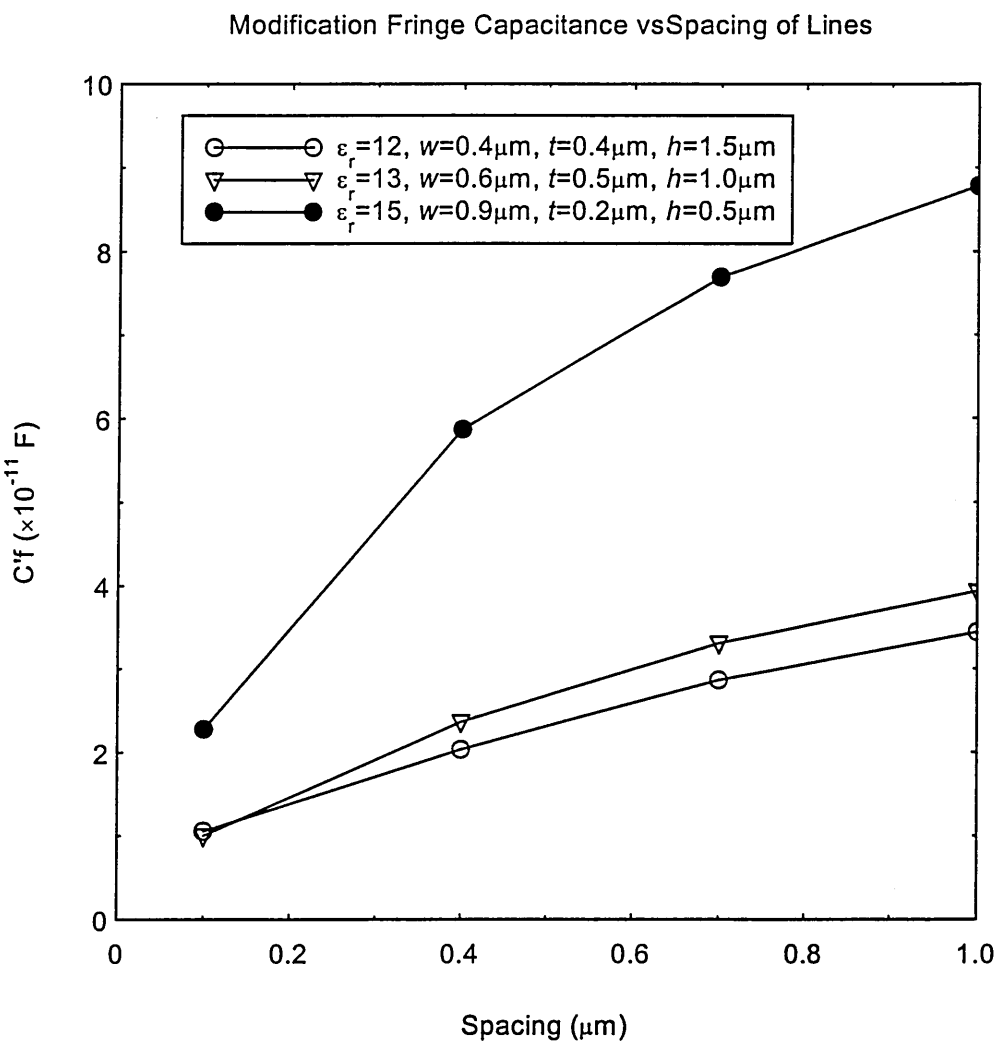
Modification Fringe Capacitance vsSpacing of Lines
εr=12, w=0.4μm, t=0.4μm, h=1.5μm
εr=13, w=0.6μm, t=0.5μm, h=1.0μm
εr=15, w=0.9μm, t=0.2μm, h=0.5μm
C'f (×10^-11 F)
Spacing (μm)
0
2
4
6
8
10
0
0.2
0.4
0.6
0.8
1.0

Fig. 5.4(c)

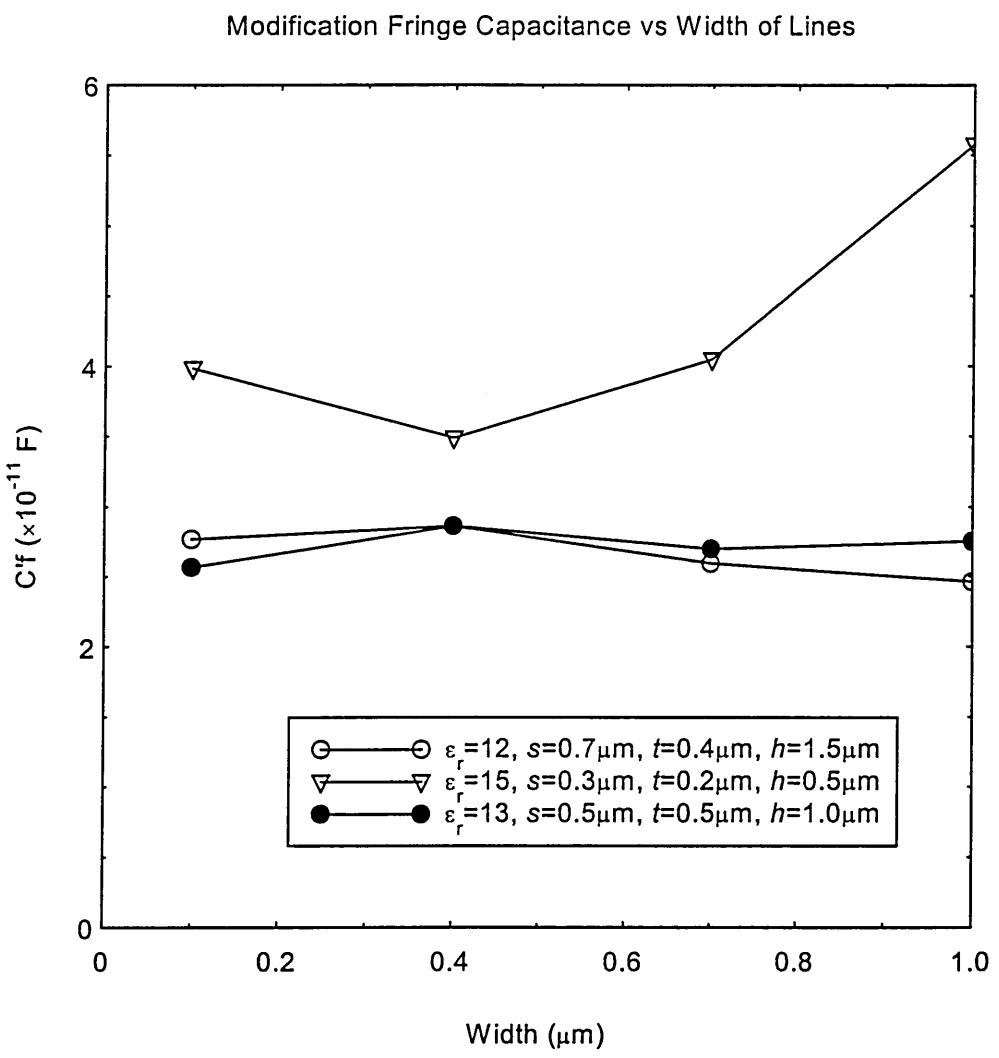

Fig. 5.4(d)

Figure 5.4 Microstrip line modification fringe capacitance vs. (a) height (b) thickness (c) spacing (d) width.

5.3.6 Mutual capacitance

Using eqn. 3.18 the graphs showing the mutual capacitance versus the height, thickness, spacing and width are shown in Fig. 5.5. The capacitance increases steadily as the width and height increases in all samples, see Fig. 5.5.a and Fig. 5.5.b.

The mutual capacitance increases only very slightly, as the thickness of lines increases (Fig. 5.5.d). On the other hand, it decreases exponentially as the spacing between the lines increases (Fig. 5.5.c). This fact has been confirmed by Parker's (1994) simulation as well as by the experimentation of Cottrell and Buturla (1985) and can be proven analytically (by contradiction). This can be explained as follows:

If C_{ij} (see eqn. 3.18) is linear with respect to spacing, then $C_{ij}(ks)$ is equal to $kC_{ij}(s)$ for $k \in R^+$, hence all of its components are also linear. However, the capacitance due to the electric flux (see eqn. 3.16) is not linear ($C_{gd}(ks) \neq kC_{gd}(s)$) since $\coth(2s) \neq 2\coth(s)$. If that is the case then C_{ij} is not linear with respect to s either.

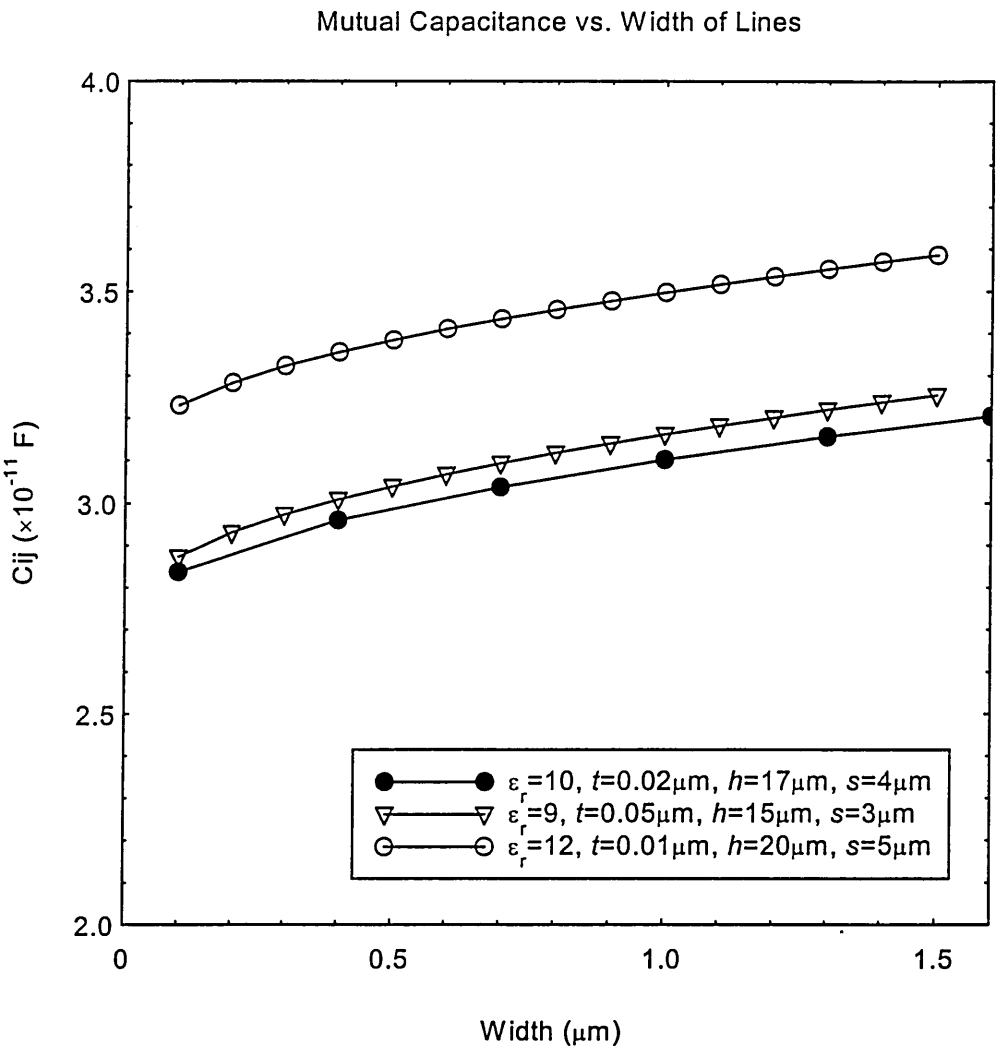
Mutual Capacitance vs. Width of Lines
4.0
3.5
3.0
2.5
2.0
Cij (×10^-11 F)
0
0.5
1.0
1.5
Width (μm)
εr=10, t=0.02μm, h=17μm, s=4μm
εr=9, t=0.05μm, h=15μm, s=3μm
εr=12, t=0.01μm, h=20μm, s=5μm

Fig. 5.5(a)

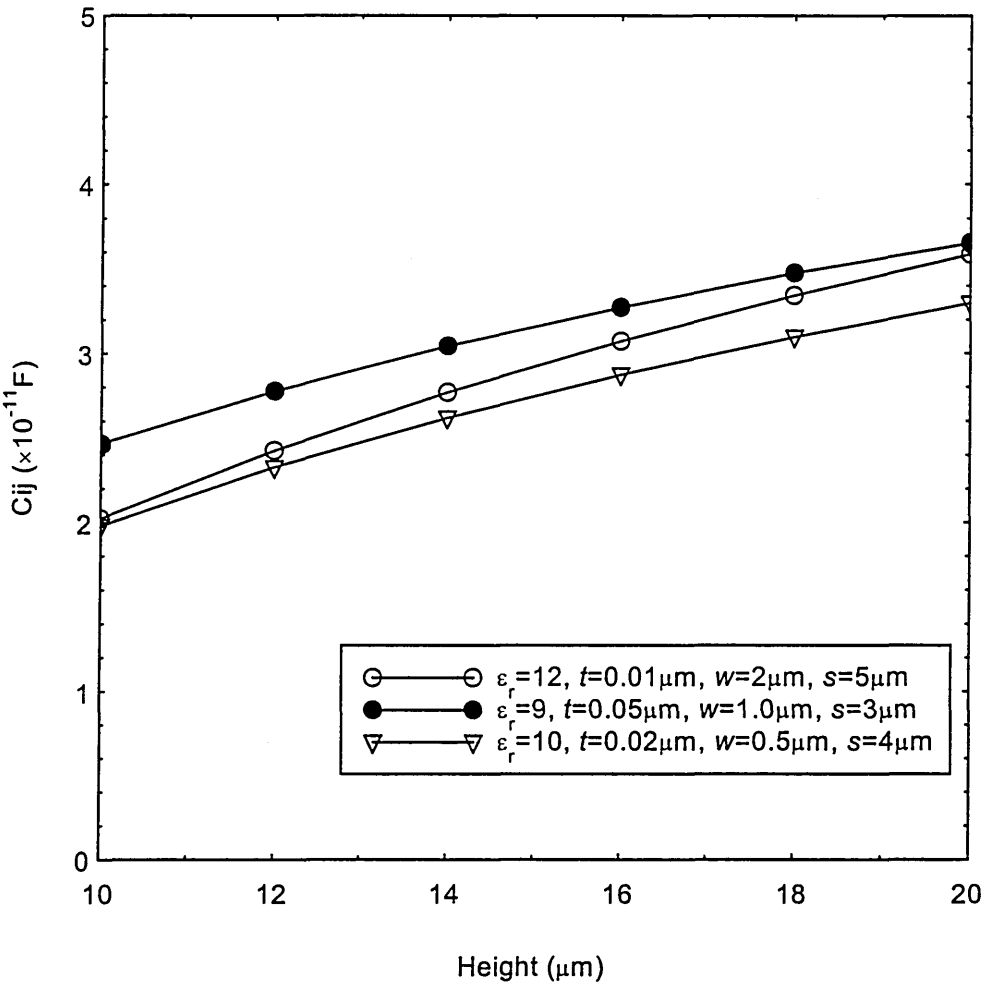
Mutual Capacitance vs. Height of Lines
Cij (×10^-11 F)
Height (μm)
0
1
2
3
4
5
10
12
14
16
18
20
εr=12, t=0.01μm, w=2μm, s=5μm
εr=9, t=0.05μm, w=1.0μm, s=3μm
εr=10, t=0.02μm, w=0.5μm, s=4μm

Fig. 5.5(b)

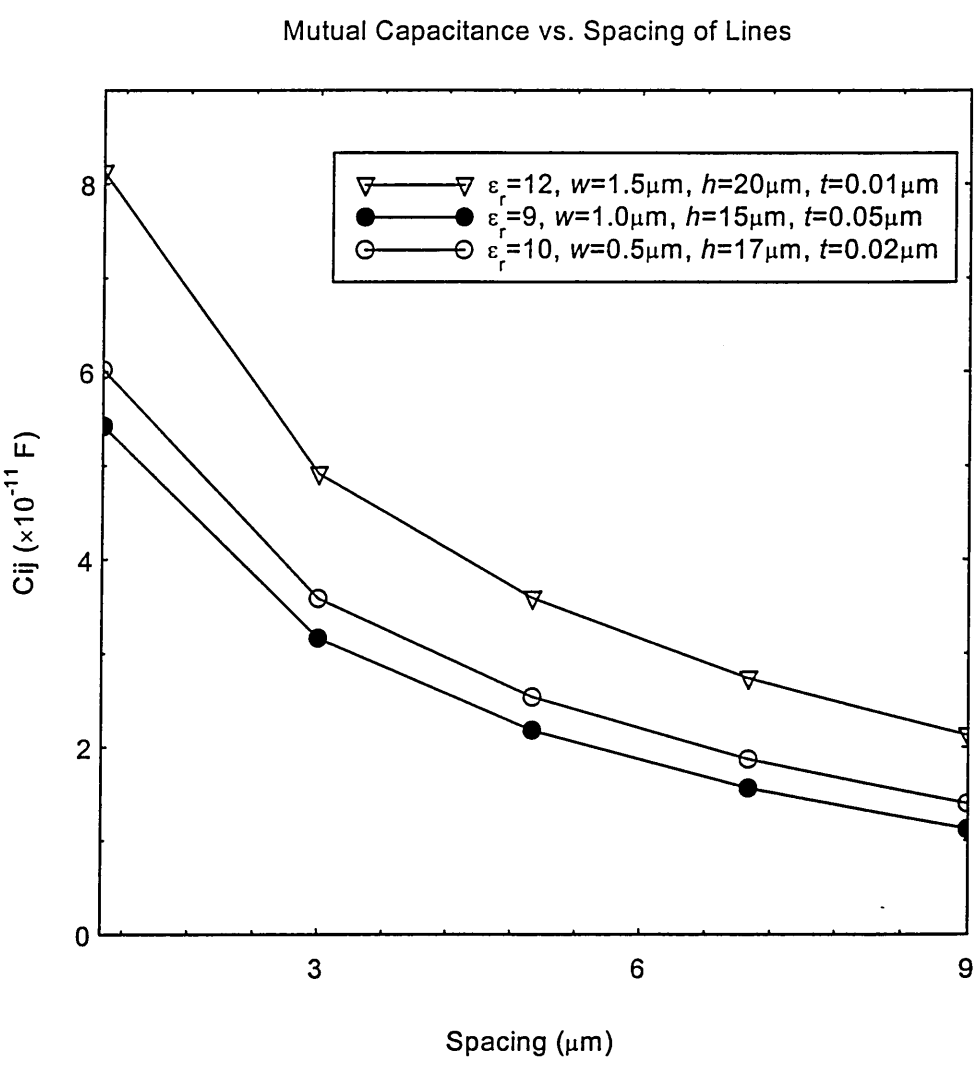
Mutual Capacitance vs. Spacing of Lines
εr=12, w=1.5μm, h=20μm, t=0.01μm
εr=9, w=1.0μm, h=15μm, t=0.05μm
εr=10, w=0.5μm, h=17μm, t=0.02μm
Cij (×10-11 F)
0
2
4
6
8
3
6
9
Spacing (μm)

Fig. 5.5(c)

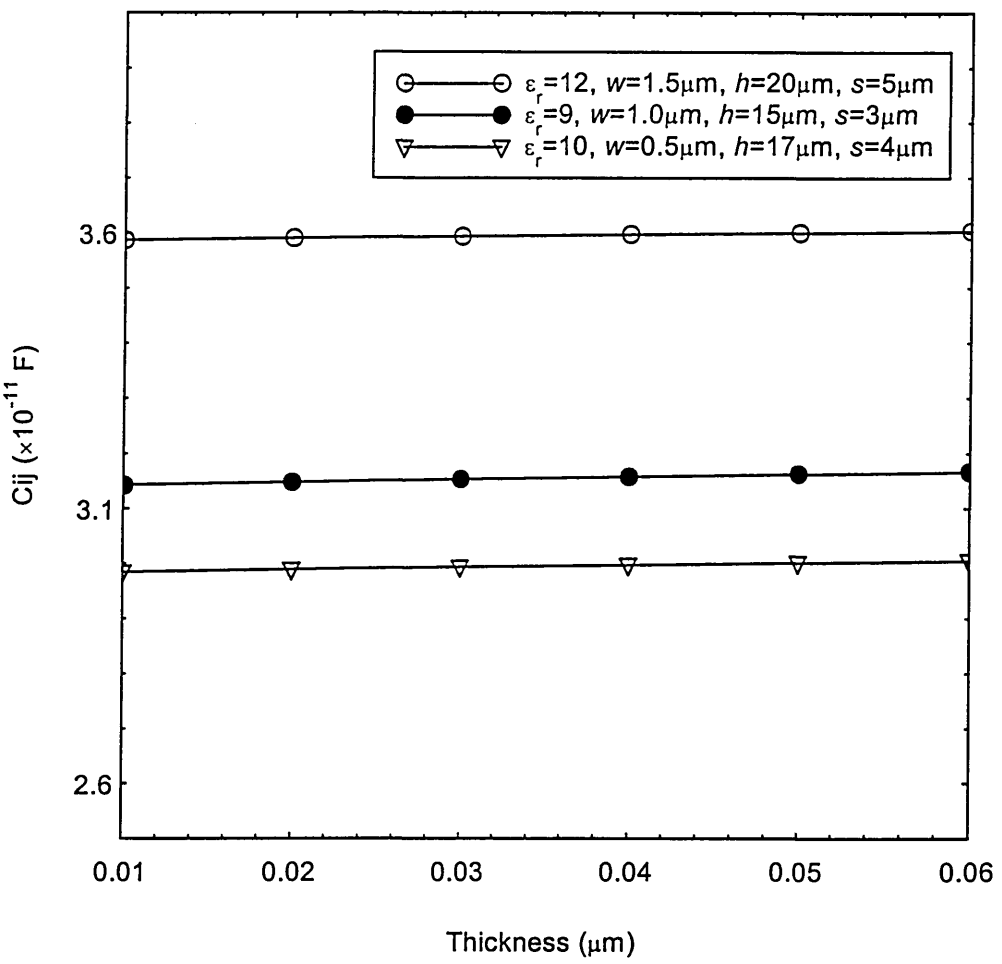

Fig. 5.5(d)

Figure 5.5 Microstrip line mutual capacitance vs. (a) width (b) height (c) spacing (d) thickness.

The effect of the geometrical parameters of microstrip lines on crosstalk has been noted by various researchers (Gunston and Weale 1969, Seki and Hasegawa 1984, Zhang et al 1992, Palusinski and Lee 1989, Qian and Yamashita 1993) and discussed in Chapter 2. However, one can suspect from these results, that there is a relationship between mutual capacitance and crosstalk itself via geometrical parameters. The increased magnitudes of the width and thickness of coupled lines will increase the mutual capacitance, hence the crosstalk. On the other hand, the increased spacing between coupled lines will decrease the mutual capacitance and

the crosstalk. These important relations are very beneficial in developing a fuzzy model of microstrip lines in Chapter 7.

5.4 Analysis of the Crosstalk

The objective in crosstalk analysis is to determine the near-end and far-end voltages of the line for given cross-sectional dimensions (Paul 1992). The far end crosstalk is measured at the end of line whereas the near end crosstalk is measured at the beginning of line. However, "crosstalk" normally refers to the far end side.

There are two types of crosstalk analysis: frequency-domain analysis (Snelson 1971, Seki and Hasegawa 1984) and time-domain analysis (Grifith and Nakhla 1990, Zounon et al 1990). Frequency-domain analysis is the determination of the magnitude and phase of the receptor terminal phasor voltages $\hat{V}_{NE}(j\omega)$ and $\hat{V}_{FE}(j\omega)$ for a sinusoidal source voltage $V_s(t) = V_s \cos(\omega t + \phi)$. Frequency-domain analysis presumes a steady state. On the other hand time-domain analysis is the determination of the time form of the receptor terminal voltages $V_{NE}(t)$ and $V_{FE}(t)$ for some general time form of the source voltage $V_s(t)$ (Paul 1992). Here the latter type is adopted for experimentation as well as simulations. The parameters for the simulation are based on the algorithms presented in Chapter 4.

5.4.1 Experimentation

Tests carried out using the experimental technique were aimed at studying the characteristics and behaviour of microstrip lines, particularly the occurrence of crosstalk in coupled microstrip lines. These experiments were undertaken

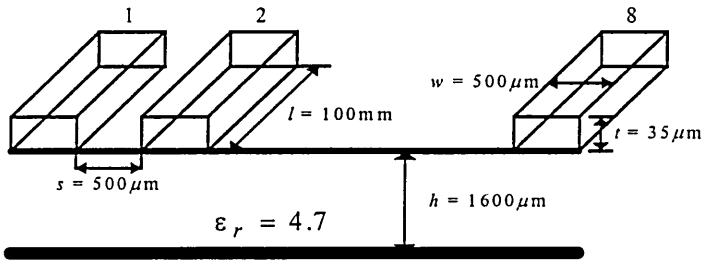

Figure 5.6 Eight coupled microstrip lines ($s = w = 500$ μm)

using four sets of 8 parallel lines, which had equal lengths of 100mm. The sets of microstrip lines were different in width(spacing) of 1000 μm, 750 μm, 500 μm (see Fig. 5.6), and 250 μm. Some of the experiments were deliberately designed to verify the simulation made by Parker (1994). The following are details of the equipment used, specifications of the microstrip lines and general procedures used during the experiments.

Equipments used:

i. Oscilloscope Hewlett Packard (54520A) 500 Msa/s, 500MHz.

ii. Synthesised Function Generator (30MHz.) model DS 345X2.

iii. Microstrip lines.

iv. Generated signals were connected to the microstrip lines using braid screened (50 Ω) cable with screw coupling connector.

Specifications of the microstrip lines:

Base material:	FR4 epoxy all woven glass laminated to BS 4584 Part 3
Thickness:	1/6" (1.6mm)
Copper foil cladding per square ft:	1oz (35microns)
Water absorption:	0.10 %
Specific gravity:	1.85 - 1.9
Dielectric constant ε_r *at 1MHz*:	5.0 ($\approx$ 4.7)
Dissipation factor tan 0 at 1MHz:	0.020
Flex strength length wise:	550N/mm^2
Surface resistance:	$10^{11}\Omega$
Volume resistivity:	$10^{14}\Omega$
Foil pull off strength:	140N
Photoresist:	Positive working
Sensitivity:	Ultra violet
Coating thickness:	7microns $\pm$ 0.7micron

General procedures:

- The output from the function generator was set to produce a square wave output to simulate the digital input applied to the source input of microstrip lines.
- The frequency was set to 10MHz and 50% duty cycle with peak-to-peak voltages ranging from 1V to 5V.
- All the lines, except the feeder lines(s) were terminated with 50Ω resistors.

- Reading of steady state voltage was needed for the calculation of the crosstalk, and the probe positions were placed at the near end and far end of microstrip lines.
- An oscilloscope with digital storage for up to four (4) memories was used. If there was an indication of signal modulation, several readings were taken and the maximum reading was taken as the valid result. Measurement of peak-to-peak (p-p) voltage was done automatically.
- Other parameters that can be obtained from the utilisation of the Oscilloscope, and were useful for the purpose of these experiments are: rise time, fall time, pulse width and frequency of signal monitored.
- Two function generators were used when two (2) input signals were required for investigating the effects of superimposition or cancellation of signals.
- In probing the signals, a barrel insulator and a grounding spanner were used to avoid possible shorting of other circuitry. With these two pieces of equipment the probe was in its sub-miniature mode of operation and a very short ground lead was required.

Further exploration was achieved by applying varied input lines, frequencies and voltages in these experiments. Through these detailed explorations, the behaviour of the microstrip lines will be more clearly understood.

5.4.1.1 The experiments

Seven experiments were performed to study the characteristics and behaviour of microstrip lines, mainly the occurrence of crosstalk, when different voltages and

frequencies were applied to the input. These experiments were conducted on four sets of eight parallel microstrip lines, where all the sets were similar in length but different in width and spacing.

These experiments, with one or two input signals applied, were measured at the near end and far end of each set of microstrip lines. In collecting data, the voltages of each point were measured twice and results were identified from readings of the highest voltage. Voltage readings captured at the near and far ends of each line were calculated in dB and compared. The crosstalk (ξ) in dB is defined as:

$$\xi = 20\log_{10}[V_e(t) / V_i(t)] \qquad (5.38)$$

where V_i is the voltage source on the activated line at time t, and V_e is the voltage at any location along the line at the same time t (Parker et al 1994, Parker 1994). The results were then plotted using EASY-PLOT.

Experiment 1: (*line inputs*)

Experiment 1 was carried out to study the profile of crosstalk when the same input voltage (5 V p-p) was applied to different lines.

Set up no.1

Input applied to Line #4 :

- microstrip lines with $s = w = 750\ \mu$m and $s = w = 1000\ \mu$m.
- with frequency of 10MHz.

Set up no.2

Input applied to Line #5 :

- microstrip lines with $s = w = 250\ \mu m$ and $s = w = 500\ \mu m$.
- with frequency of 10MHz.

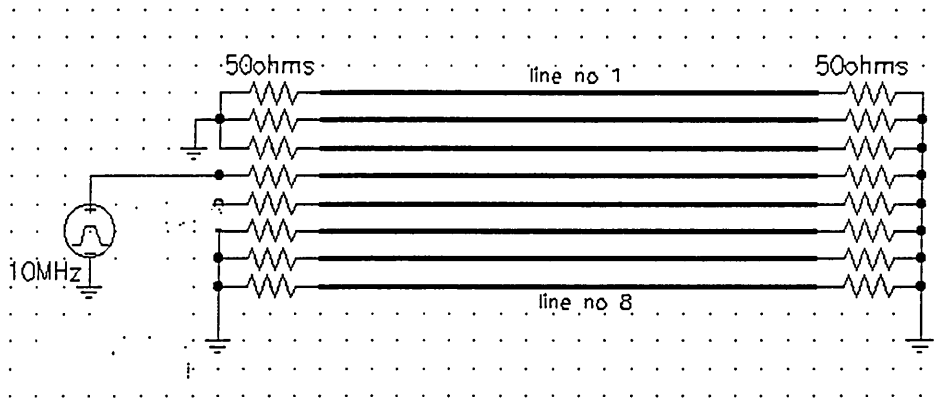

Figure 5.7 Experimental set up no. 1.

Results

The crosstalk levels measured at the near and far ends for the first and second arrangements are shown in Fig. 5.8.a. and b, respectively. In Fig. 5.8.a, the crosstalk is the highest (-30 dB) at lines 3 and 5, reducing further by 8 dB when measured at lines 1 and 7 for the near end. Crosstalk at the far end is lower by 3 dB compared to the near end crosstalk when measured at lines 3 and 5.

Figure 5.8.b shows the crosstalk at both ends when the same input signal is applied to line 5. The crosstalk profile is very similar to Fig. 5.8.a, with the near end crosstalk being higher (~ 3 - 4 dB) in comparison with the far end crosstalk.

As shown in both figures the crosstalk at the far ends is lower than the crosstalk at the near ends. The essential features of crosstalk remain the same in both figures whether line 4 or 5 were activated. This fact is confirmed by Parker et al (1994).

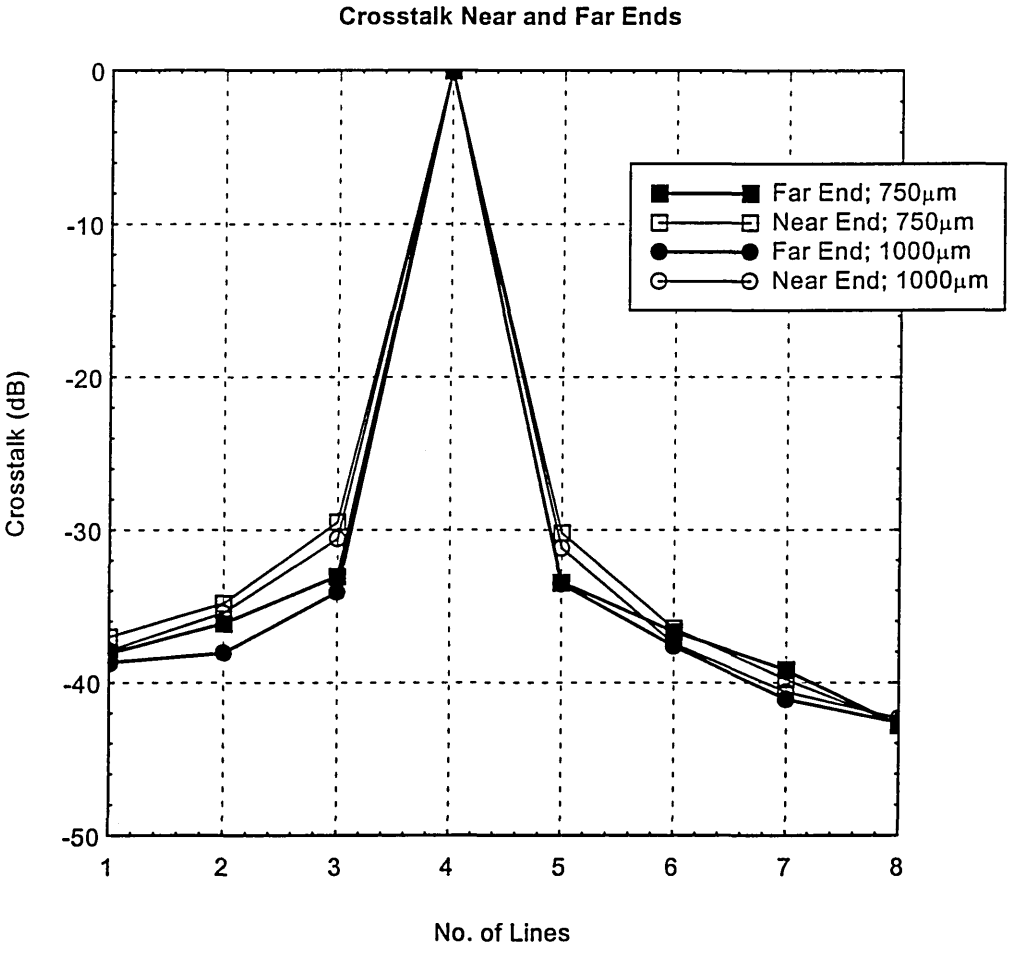

(a) Crosstalk of set up no. 1.

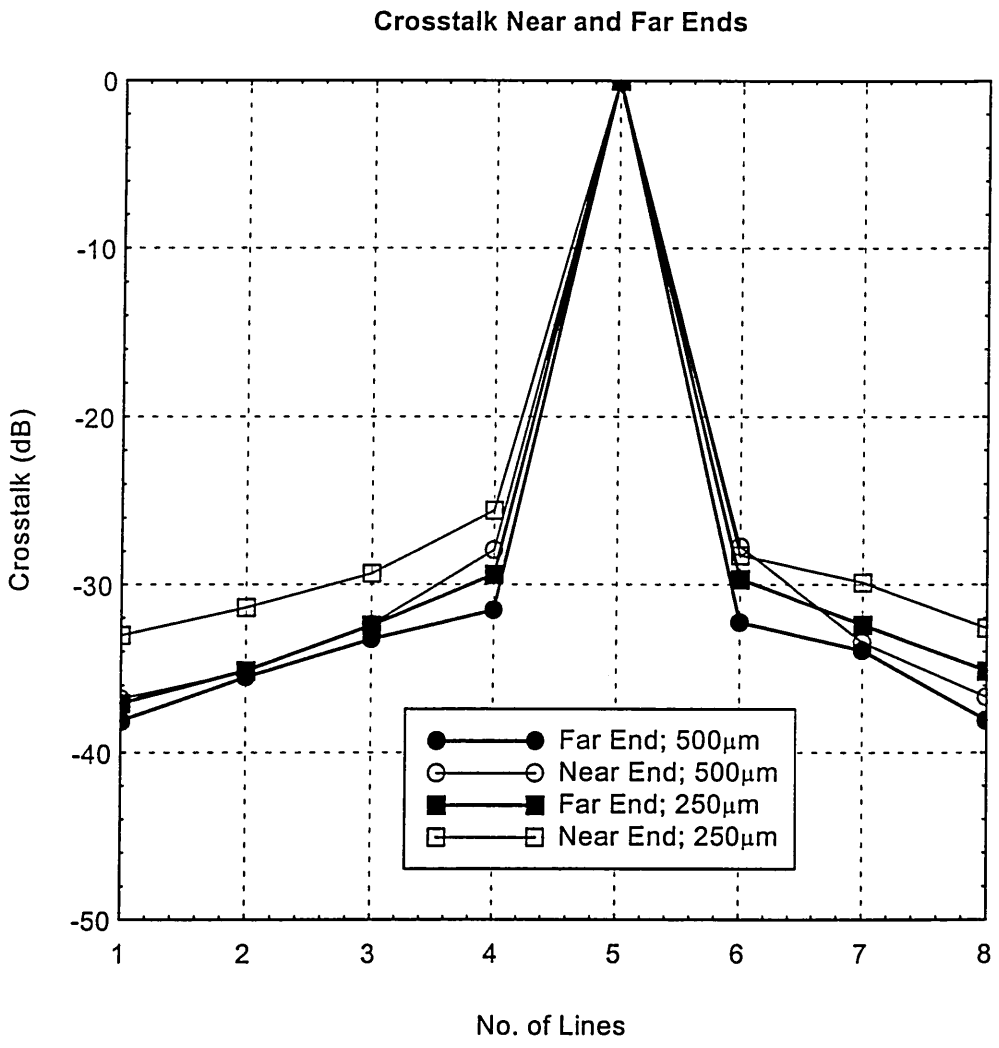

(b) Crosstalk of set up no. 2

Figure 5.8 **Crosstalk at near and far ends of (a) set up no. 1; $s = w =$ 750 μm and $s = w =$1000 μm (b) set up no. 2; $s = w =$ 250 μm and $s = w =$ 500 μm; microstrip lines with input signal 5V p-p and frequency of 10 MHz.**

Experiment 2: (*input voltages*)

Experiment 2 was carried out to study the changes in crosstalk magnitude when different input voltages were applied to the microstrip lines.

Set up

Inputs applied to Line #4 were:

- of the same direction.
- varied at 1Vp-p to 5Vp-p.
- with frequency of 10MHz.

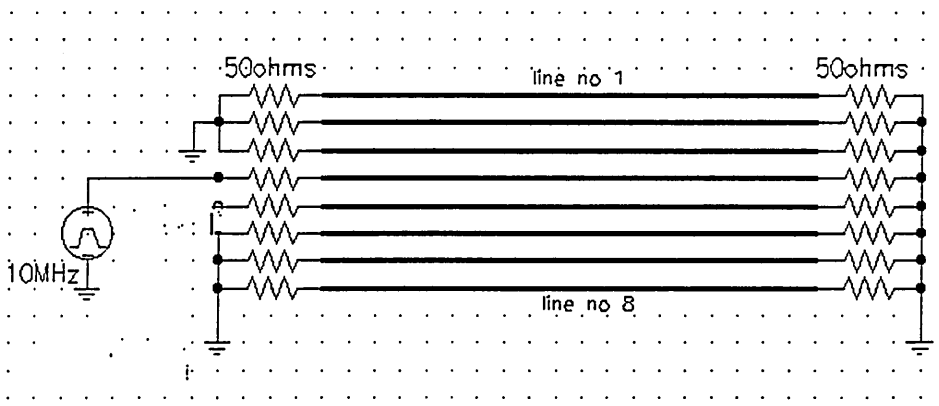

Figure 5.9 Experimental set up with input to line #4.

Results

Figure 5.10 shows the measured crosstalk at near and far ends for a set of microstrip lines with $s = w = 1000\,\mu m$ over a range of input voltages Therefore the crosstalk is unaffected by the range of input voltages, which is in agreement with the claim made by Parker et al (1994).

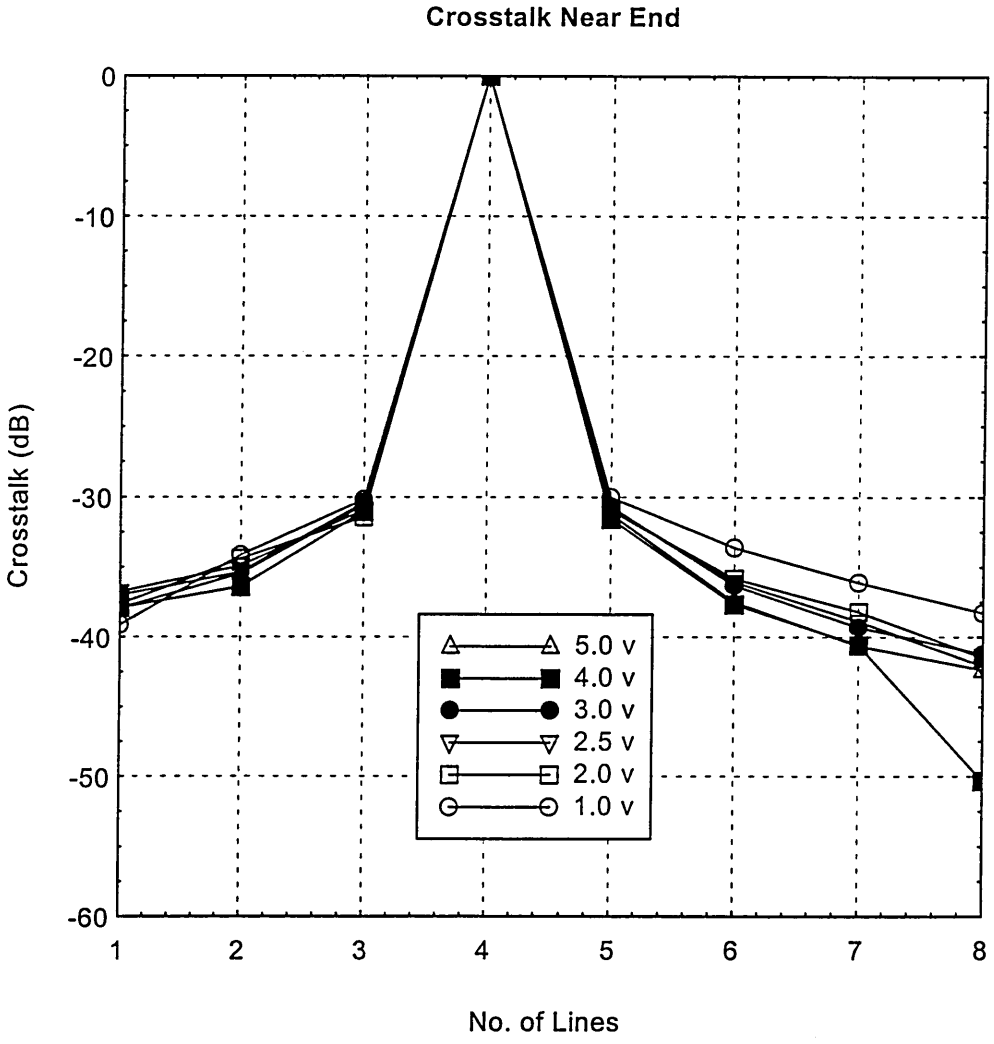

(a) Crosstalk at near end.

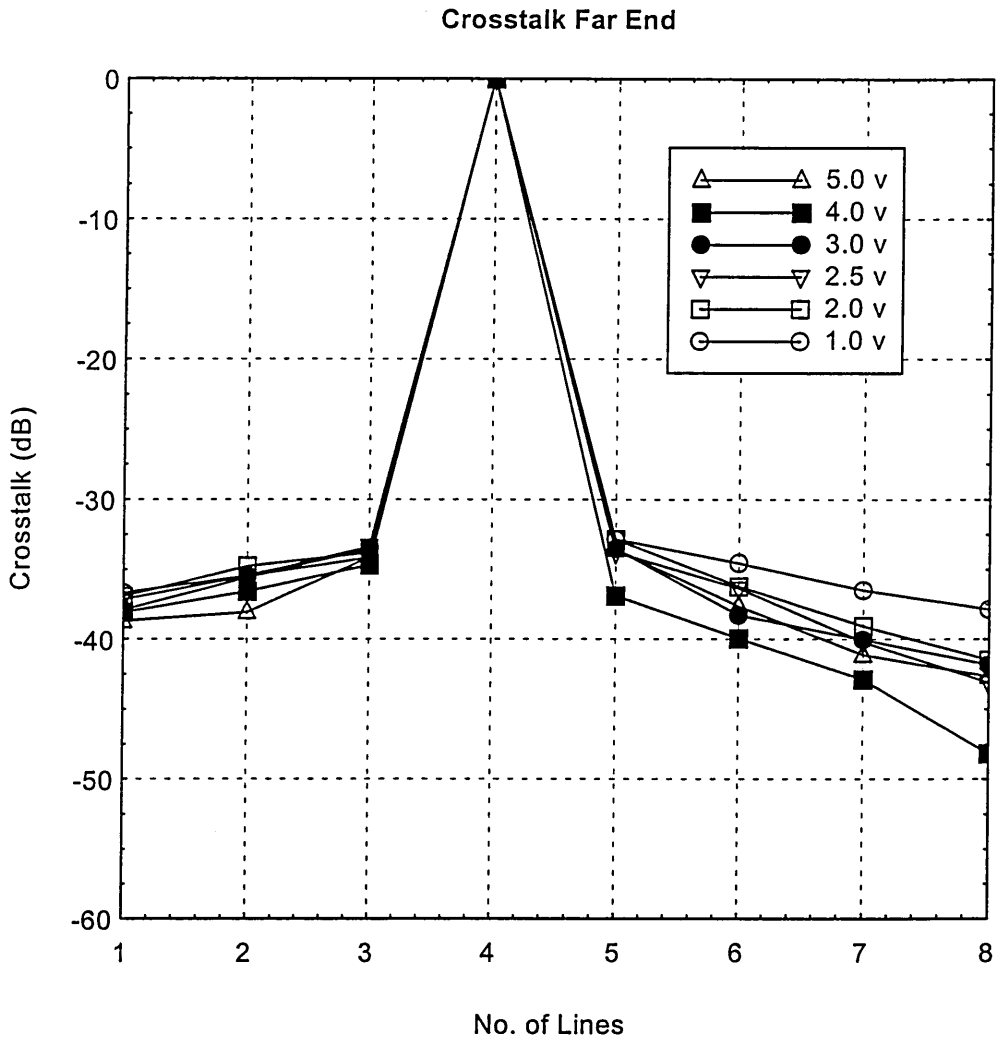

(b) Crosstalk at far end.

Figure 5.10 Crosstalk at (a) near end (b) far end; of 1000 μm microstrip lines with input signals 1V - 5V p-p and frequency of 10 MHz.

Experiment 3: (*frequency*)

Experiment 3 was carried out to study how crosstalk was affected by increasing the input frequency.

Set up

Input applied to Line #4 :

- microstrip lines with $s = w = 250\ \mu m$ and $s = w = 500\ \mu m$.
- 1 V p-p
- with frequency of 0.25, 0.5, 1.0, 2.5, 5, 10, 20 and 30 MHz..

Results

Figure 5.11 shows that the crosstalk at both ends increased steadily as the frequency increased. This result also confirms recent findings of Son et al (1993), Van Deventer and Katehi (1994), and Linares y M et al (1995). For $s = w = 250\ \mu m$ and at 30 MHz the crosstalk is measured as being -26.5 dB and -29.5 dB for near and far ends, respectively. The results decreased by a further ~ -1.5 to -2.0 dB for $s = w = 500\ \mu m$.

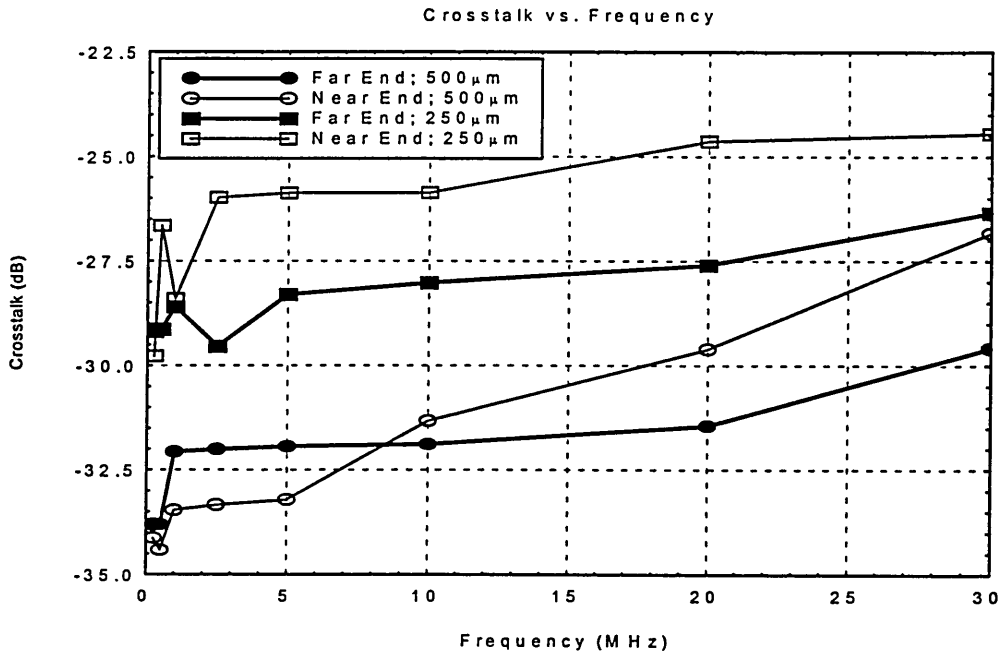

Figure 5.11 Crosstalk at different frequencies.

Experiment 4: (*spacing*)

Experiment 4 was carried out to study the effect of spacing on crosstalk.

Set up

Inputs applied to Line #1:

- of 1Vp-p.
- with frequency of 10MHz.

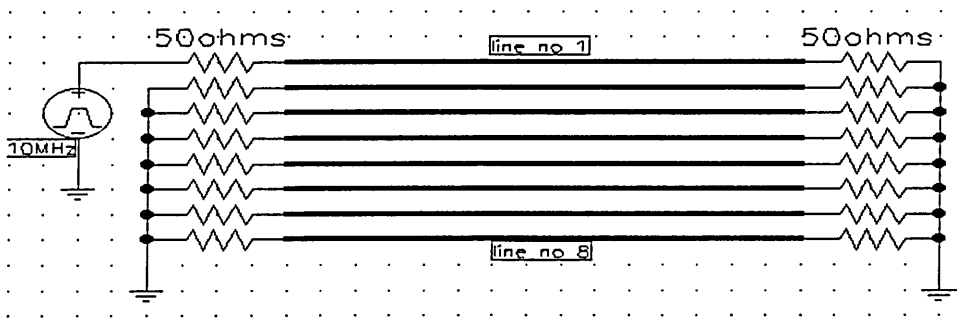

Figure 5.12 Experimental set up with input to line #1.

Results

Further crosstalk measurements were carried out using sets with different spacings and widths and the results are shown in Fig. 5.14. Both graphs indicate that the crosstalk decays exponentially with increasing distance from the feeder line. As expected the crosstalk in line 2 is measured as being -30 dB, decreasing to ~ -40 dB in line 8. Crosstalk for the set with $s = w = 1000\,\mu m$ is the lowest followed by the sets $s = w = 750\,\mu m$, $s = w = 500\,\mu m$ and $s = w = 250\,\mu m$ respectively. This demonstrates that the effect of spacing on crosstalk is significant.

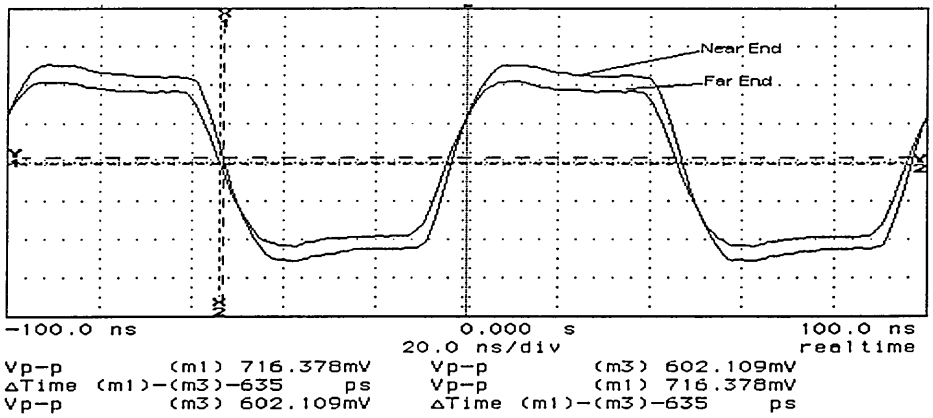

Figure 5.13 Input signals showing Vp-p at near and far ends of microstrip line #1(250μm).

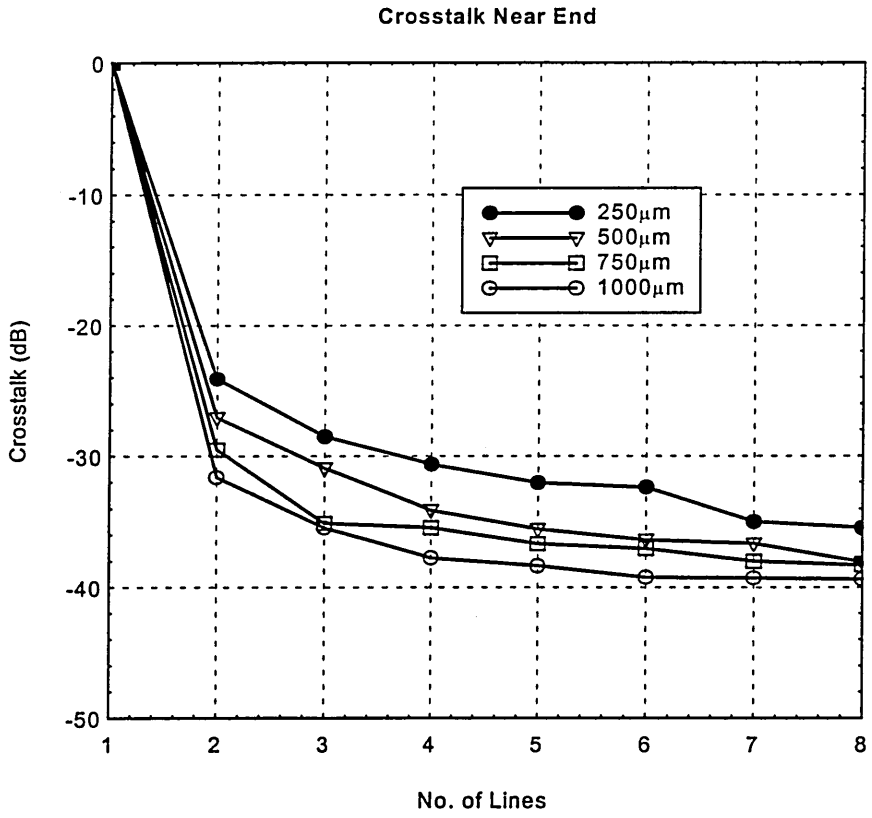

(a) Crosstalk at near end.

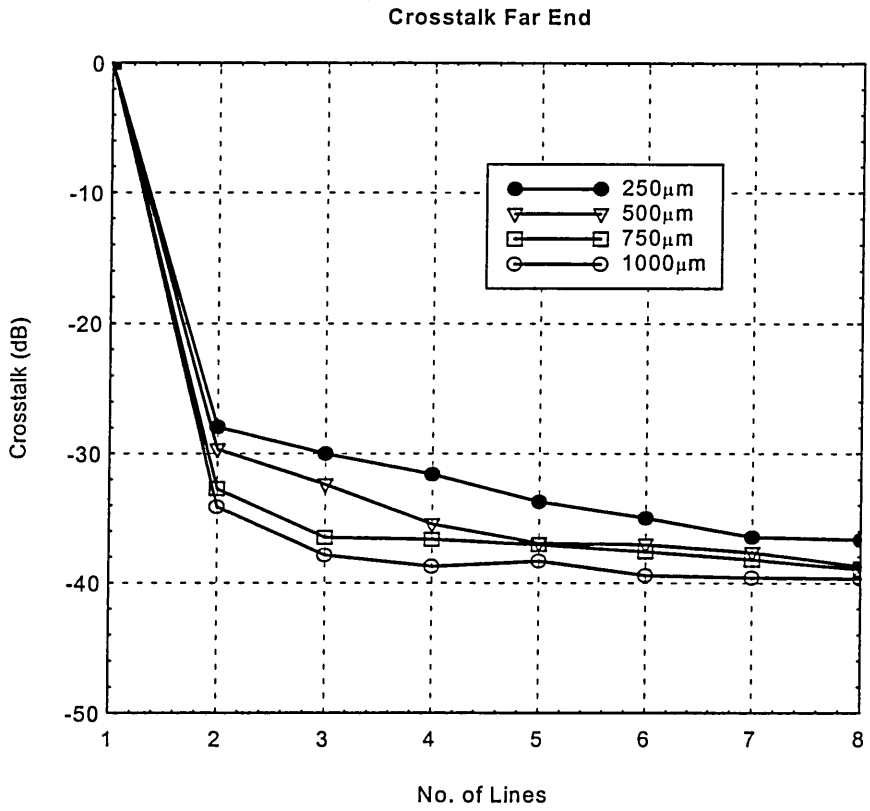

(b) Crosstalk at far end.

Figure 5.14 Crosstalk of different spacings (a) near end (b) far end.

The effect that spacing has on the electrical parameters of coupled microstrip lines alone has been shown by simulation; see Sect. 5.3 and experiment (Cottrell and Buturla 1985). The effect of spacing on crosstalk has also been studied by various researchers (Seki and Hasegawa 1984, Zhang et al 1992, Parker et al 1994) mainly by simulation. However, the direct relation between the line spacing and crosstalk (crosstalk as a function of spacing) has not been dealt extensively and therefore requires further investigation. This is described in Chapter 7.

Experiment 5: (*between two signals*)

Experiment 5 was carried out to study the crosstalk between two signals in the same direction.

Set up

Inputs applied to Line #3 and #5:

- of the same direction
- of 1Vp-p.
- microstrip lines with $s = w = 500$ μm (see Fig. 5.6).
- with frequency of 10MHz.

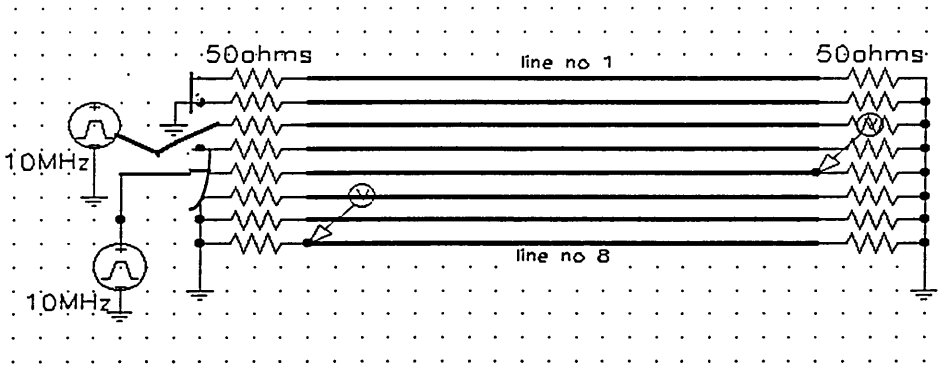

Figure 5.15 Experimental set up with input to line #3 and #5.

Results

As can be seen from Fig. 5.16, the near end crosstalk ~-18 dB observed in line 4 is only 2 dB higher than that of lines 2 and 5, confirming the simulation results reported by Parker et al (1994). The crosstalk taken at the far end of lines 2, 4 and 6 is approximately 2 - 3 dB lower than the near ends'. This is mainly due to mutual field attraction. However, when further away from the feeder lines, measurements of the crosstalk from the far end are higher than at the near end for lines 1 and 7 and beyond. As the spacing increases, crosstalk at the near end

drops drastically. For example, crosstalk at the near end of line 6 drops to 7.84% compared to 30.92% at line 7. On the other hand, crosstalk at the far end drops steadily by about 2% when moving from one line to the next.

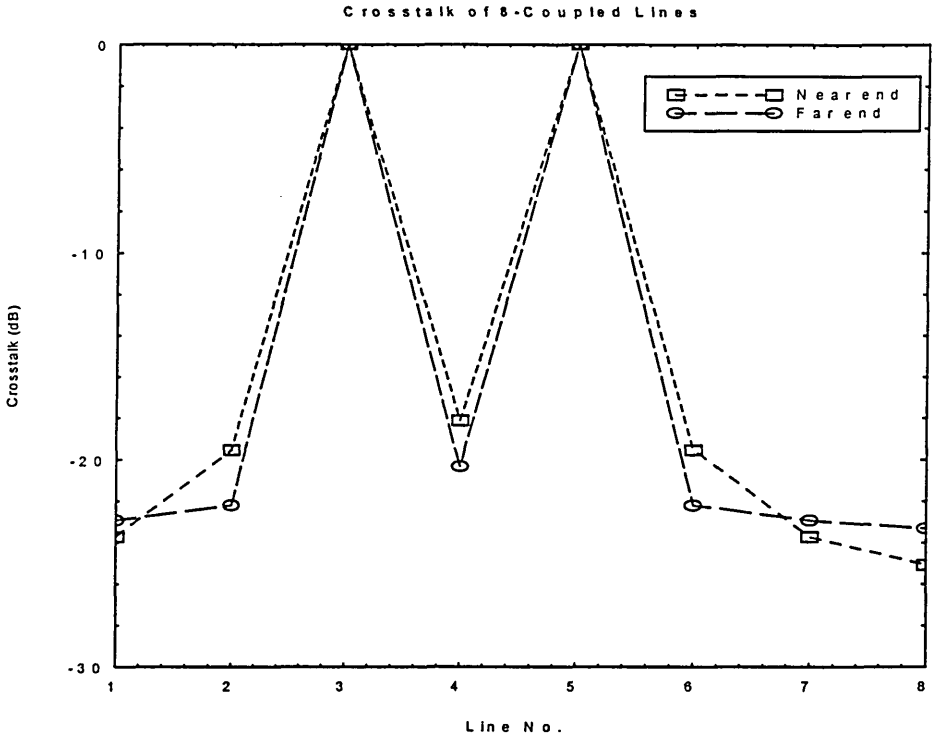

Figure 5.16 Crosstalk for 8-coupled lines with double inputs.

Experiment 6: (*length*)

The effect of the length of microstrip lines on crosstalk has been discussed briefly by several authors (Gunston and Weale 1969, Zhang et al 1992). Some of them even consider it as negligible (Seki and Hasegawa 1984, Parker et al 1994, Gao et al 1990, Qian and Yamashita 1993) due to the fact that the length (l) is not one of the variables (see eqns. 3.1 - 3.18) in any electrical parameters of microstrip lines. *Experiment 6* was designed to study the effect of length on crosstalk.

Set up no.1

Inputs applied to Line #4:

- of 1Vp-p.
- microstrip lines with $s = w = 500$ μm and $l = 100$ mm(see Fig. 5.6).
- with frequency of 10MHz.

Set up no.2

Inputs applied to Line #4:

- of 1Vp-p.
- microstrip lines with $s = w = 500$ μm and $l = 200$ mm(see Fig. 5.11).
- with frequency of 10MHz.

Results

The far end crosstalk (Fig. 5.17.a) measured at the adjacent lines 3 and 5 is the same for both length. However, it drops by 1 dB per line away from the lines 3 and 5 for longer lengths. For line 7, the drops are 1 and 3 dB, respectively. On the other hand, the near end crosstalk (Fig. 5.17.b) increases as the length increases, in particular at the adjacent lines (3 and 5). This result has shown that as the length increases, mutual field interaction (proximity effect) between the lines increases, thus effecting the crosstalk at both ends of the line.

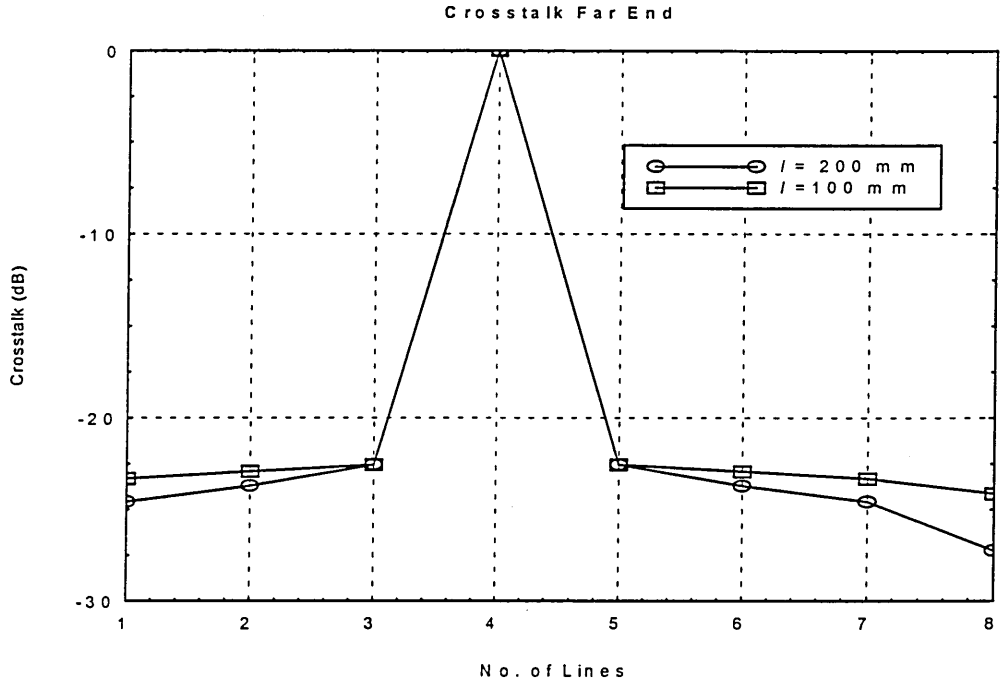

(a) Crosstalk at far ends.

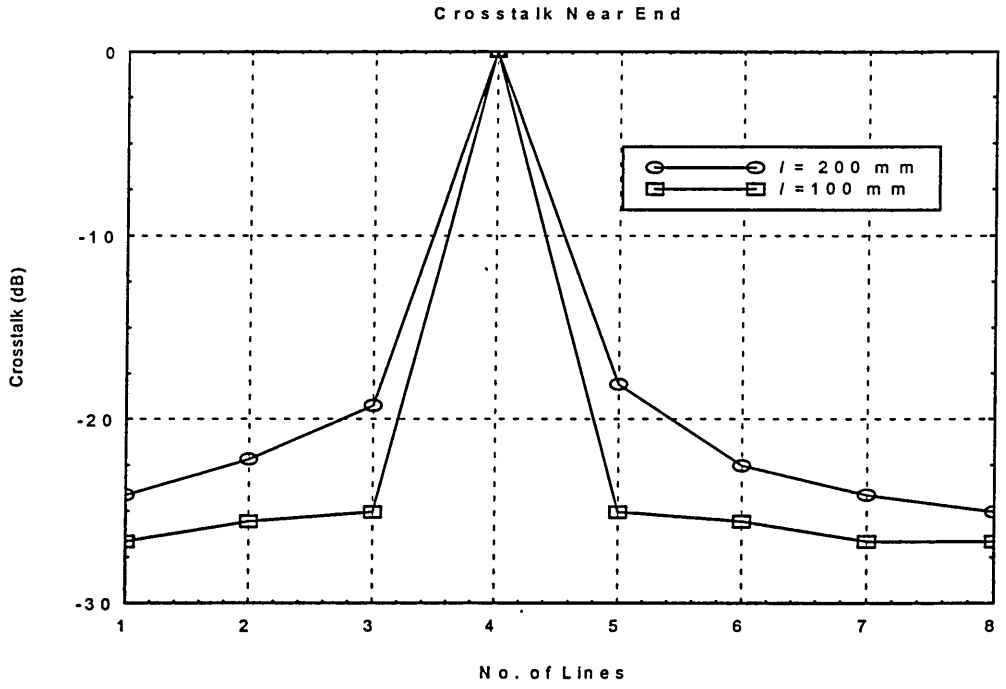

(b) Crosstalk at near ends.

Figure 5.17 Crosstalk at (a) far ends (b) near ends of 8-coupled lines with $s = w = 500$ μm, $l = 100$ mm and $l = 200$ mm.

Experiment 7: (*shielded line*)

Experiment 7 was carried out to reproduce the effects of shielded lines on crosstalk. Only the first three lines of Fig. 5.6 were involved in the investigation.

Set up

Inputs applied to Line #1:

- were of 5Vp-p.
- microstrip lines with $s = w = 500\ \mu m$ and $l = 100$ mm(see Fig. 5.6).
- had a frequency of 10MHz.
- line #2 was grounded and line #3 was monitored.

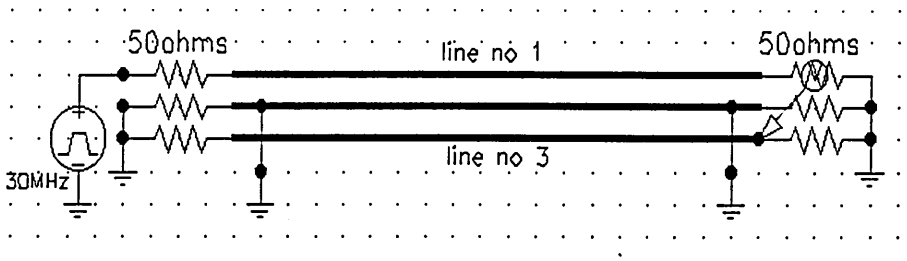

Figure 5.18 Shielded line.

Results

Lines	Not Grounded	Grounded
Line 1	3037 mV	3037 mV
Line 2	163.697 mV	-
Line 3	81.2282 mV	42.9241 mV

Table 5.0 Measurement for shielded line.

Results of this experiment show that by grounding the in-between lines, the voltage at line #3 was reduced from 81.2282mV to 42.9241mV, i.e. by 50% as also found by Coekin (1975). To find out more about the main source of crosstalk, readings of the ungrounded line #2 (163.697mV) were picked as the input source. It was observed that the voltage reading of the immediate neighbouring line was only 14.575mV. From the results of these experiments, one can conclude that the effects of crosstalk originated mainly from the source (input) line and that the second generation crosstalk can be ignored or taken as negligible. This important conclusion is further applied in the next section during the simulation of the crosstalk of nonuniform coupled microstrip lines. This simulation used SPICE (Simulation Program with Integrated Circuit Emphasis), by monitoring only the mutual capacitance between the source and the line.

5.4.2 Simulation

This section presents simulations of the crosstalk of nonuniformly spaced and strictly nonuniformly coupled microstrip lines, using the novel algorithms developed in Chapter 4. The resulting parameters from the algorithms are used to simulate crosstalk using the coupled lines SPICE model (see Fig. 5.19).

PARAMETERS:

CVAL 1pF

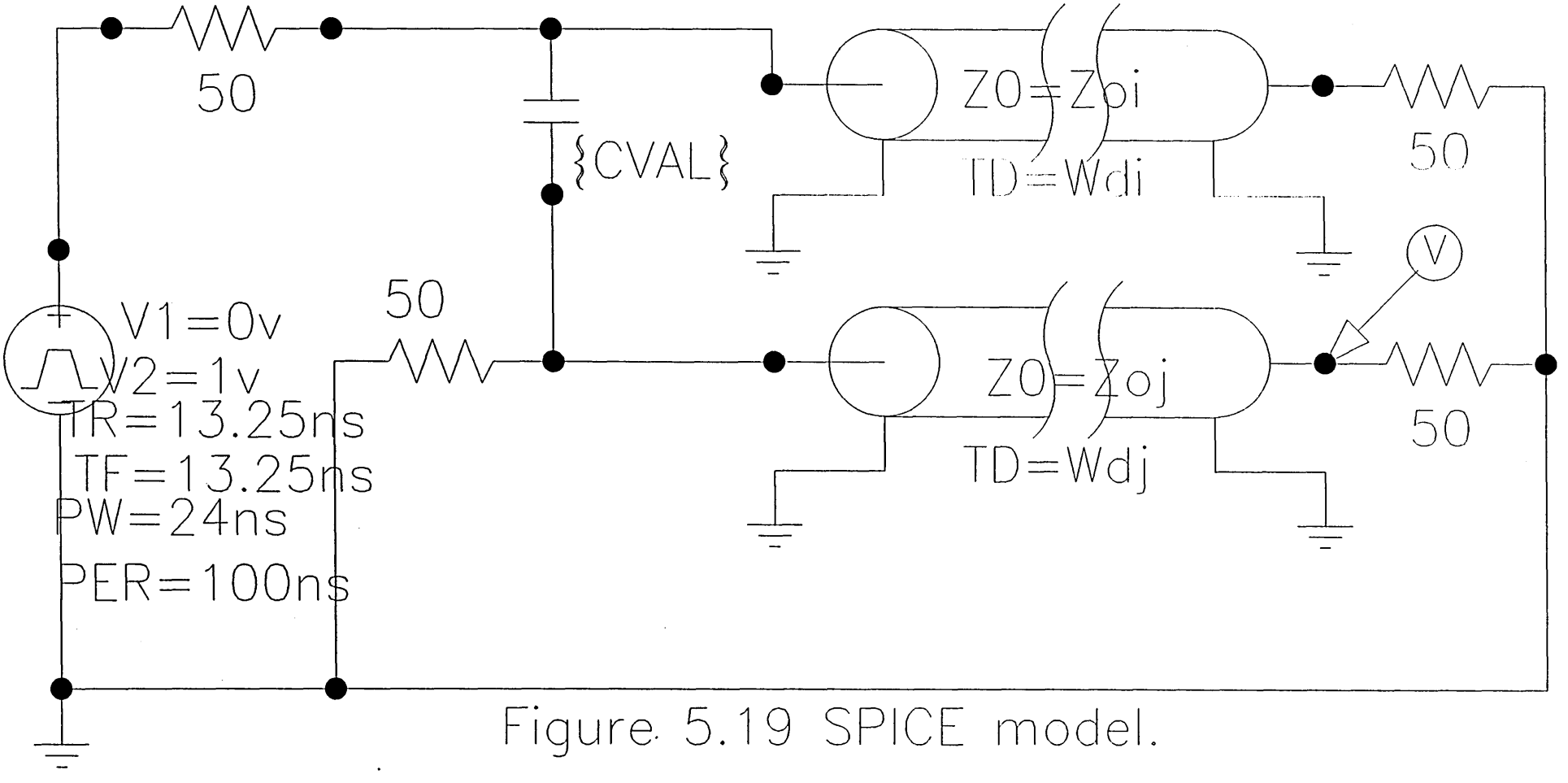

Figure 5.19 SPICE model.

5.4.2.1 Nonuniform spacing

A set of 3 nonuniformly spaced coupled microstrip lines, as described in Section 4.5.3.2 was used for the simulation of crosstalk. The time delay (eqn. 4.92) and characteristic impedance (eqn. 4.93) for the set were calculated as in Section 4.5.3.4. Three distinct simulations were performed on the sample. A pulse train of 1 V amplitude, was first applied to line 1 and then to line 2 and finally line 3. All the other lines were terminated with 50Ω resistors. The crosstalk were measured at both ends of the lines and are presented in Figure 5.20.

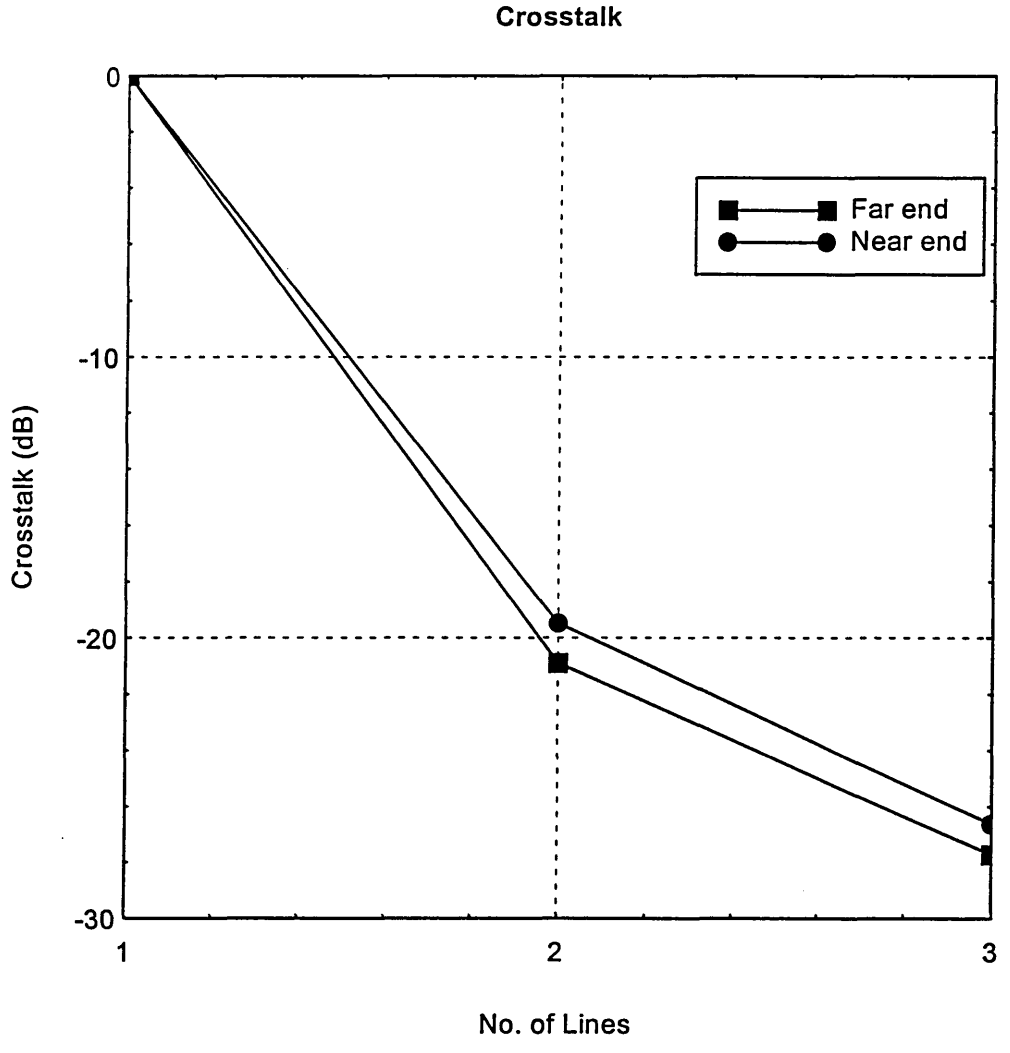

Fig. 5.20(a)

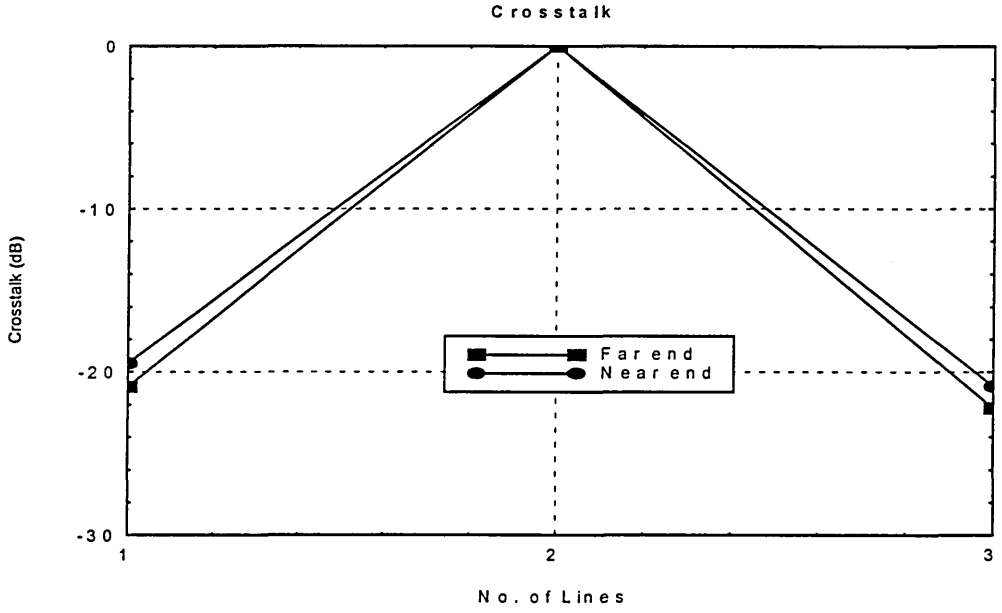

Fig. 5.20(b)

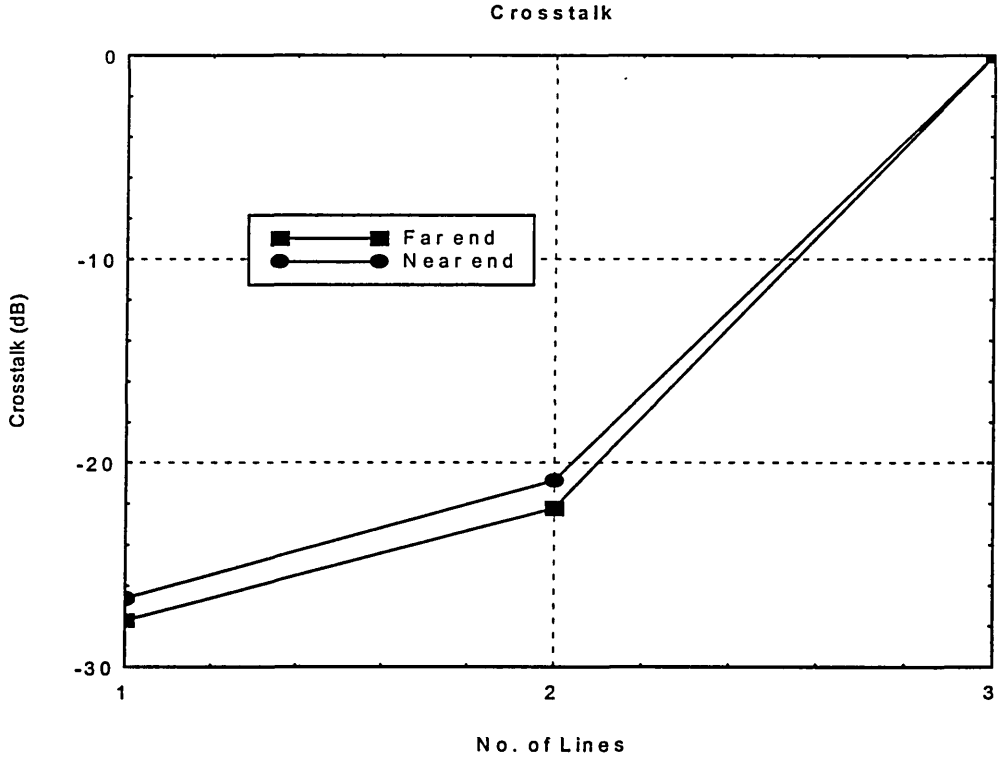

Fig. 5.20(c)

Figure 5.20 Crosstalk vs. line numbers for 3-coupled nonuniformly spaced microstrip lines with (a) feeder line 1 (b) feeder line 2 and (c) feeder line 3.

In Fig. 5.20.a, the near end crosstalk of lines 2 and 3 is ~ -19 dB and ~ -26 dB, whereas the far end is ~ -21 dB and ~ -28 dB, respectively. In Fig. 5.20.c, the near end crosstalk of lines 2 and 1 is ~ -21 dB and ~ -27 dB, whereas the far end is ~ -22 dB and ~ -28 dB, respectively. The near and far end crosstalk of the third simulation drops 2 dB more than the third simulation at line 2 as shown in Fig. 5.21. This is due to the fact that the spacing between lines 3 and 2 is 1 μm more than the spacing between lines 1 and 2. In the other words, the crosstalk decreases as the spacing increases, which is in agreement with experimental results (see Exp. 4) in Section 5.4.1.1.

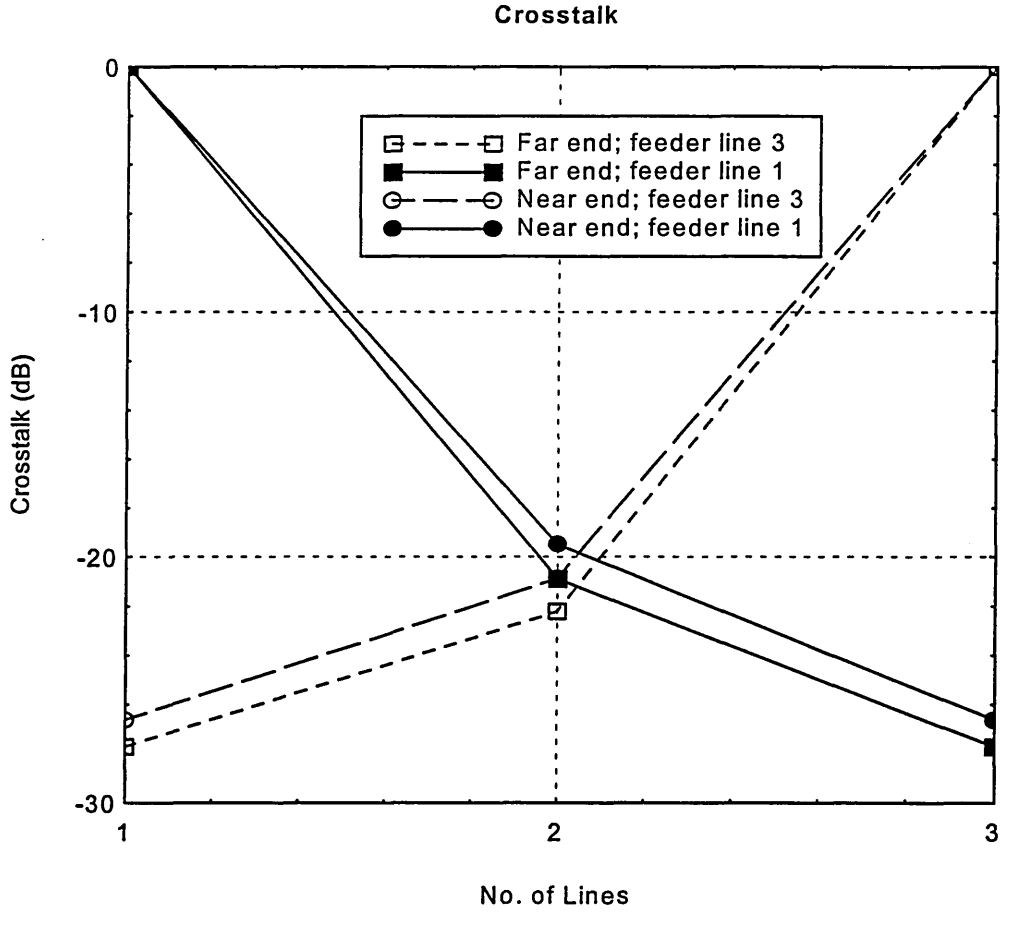

Figure 5.21 Comparison of crosstalk when the feeder line is line 1 and line 3.

The second simulation; see Fig. 5.20.b, also indicated the same results. Both the near and far ends of line 3 drop about 2 dB in comparison to line 1. It is also important to note that the drop of the far ends is slightly lower than that of the near ends in all simulations. This is mainly due to an increase in crosstalk in neighbouring lines as the input signals propagate along the feeder line for corresponding time delays.

5.4.2.2 Strictly nonuniform

A set of 4 - strictly nonuniform coupled microstrip lines introduced in Chapter 4, (see Fig. 4.7) was adopted for the simulation of crosstalk. The time delay (eqn. 4.111) and characteristic impedance (eqn. 4.112) for the set were calculated in Section 4.5.3.4. A pulse train of 1 V amplitude, was applied to line 1 and then to line 4. With all the other lines terminated with 50Ω resistors the crosstalk results are measured at both ends of the lines, are shown in Figure 5.22.

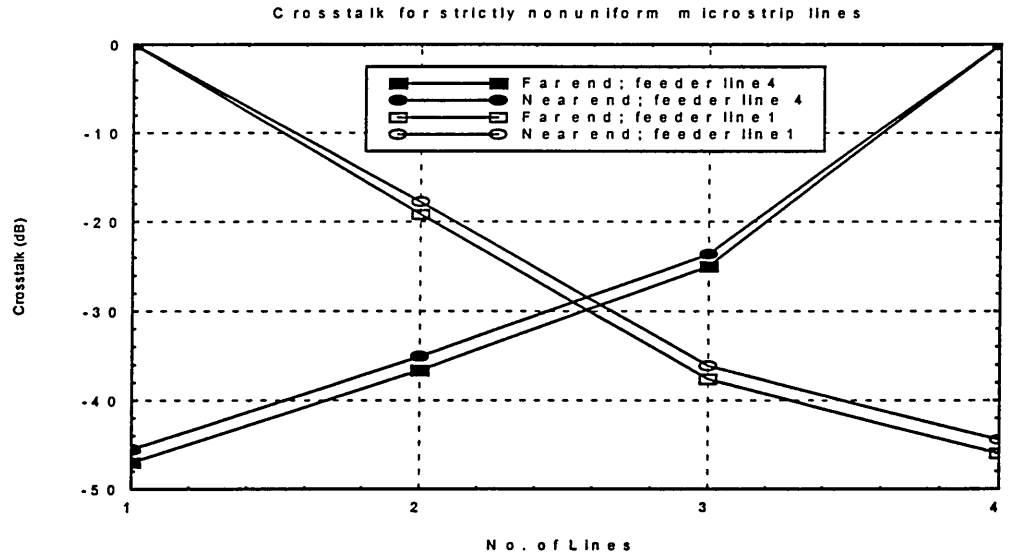

Figure 5.22 Crosstalk vs. line number of coupled 4-strictly nonuniform microstrip lines with input signal applied to line 1 and 4.

The far end crosstalk of lines 2 and 3 is ~ - 19 dB and ~ -38 dB, respectively, for feeder line 1, whereas the far ends crosstalk is ~ -37 dB and ~ -25 dB, respectively, for feeder line 4. The difference in these results is due to the fact that the spacing between lines 2 and 3 is the largest ($s_2 = 15\mu m$) compared to the spacing between the other two lines; i.e. $s_1 = 3\mu m$ and $s_3 = 7\mu m$. These important results indicate that the line spacing plays an important role in crosstalk even for strictly nonuniform coupled microstrip lines, which is in agreement with the findings of Orhanovic et al (1990) and Mao and Li (1991). However the findings are more significant compared to them because their results were based on nonuniform microstrip lines which had the same thickness. Furthermore crosstalk of the last lines is approximately the same in both cases. This is best illustrated in Fig. 5.23, where line 1 is the feeder line.

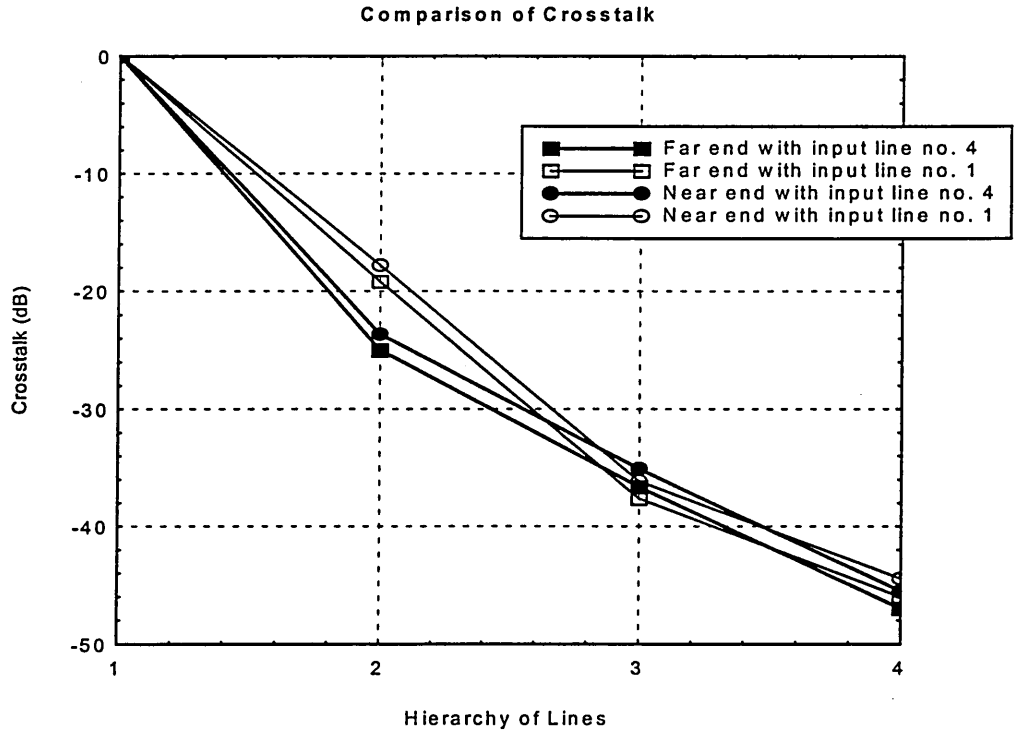

Figure 5.23 Comparison on both simulations.

Finally, crosstalk from the first simulation is not linear with respect to that of the second simulation; see Fig. 5.23, which confirms that the simulated set of coupled microstrip lines was indeed strictly nonuniform.

6. FUZZY LOGIC

6.1 Introduction

In the previous chapter, experiments were performed to investigate the effects of geometric configurations on crosstalk. The outcome of this work is to develop a method in order to achieve a compromise between different constraints. This will lead to production of the best possible design of microstrip lines having a considerable reduction in crosstalk.

This chapter serves as an overview of the topics providing theoretical background for the construction of fuzzy modelling of microstrip lines. It consists of three sections: crisp set theory, fuzzy set theory and fuzzy systems. It starts with an introduction of crisp set theory (ordinary set theory) and its common algebraic operations. The chapter then introduces the fuzzy set theory with its principal operations. An overview of a fuzzy system relevant to this work is also presented.

6.2 Crisp Set Theory

The ordinary or crisp set theory is the foundation of all branches of modern mathematics. The crisp set is defined in such a way as to dichotomise the individuals in a universe into two groups: members (those who certainly belong to the set) and nonmembers (those who certainly do not) (Klir and Folger 1988). However, the basic concept of a fuzzy set is, in essence, the generalisation of a crisp set.

(D 6.1) Generally, the letter X denotes the universal set. To indicate that an individual object x is a member of the set A, we write

$$x \in A.$$

(D 6.2) Whenever x is not an element of A, we write

$$x \notin A.$$

(D 6.3) The set A the members of which are $a_1, a_2, a_3, \ldots, a_n$ is usually written as

$$A = \{a_1, a_2, a_3, \ldots, a_n\}.$$

The process by which individuals make the universal set X is determined by the condition that either members or nonmembers of a set can be defined by a characteristic function (Klir and Folger 1988).

(D 6.4) For a given set A, the characteristic function assigns a value $\mu_A(x)$ to every $x \in X$ such that

$$\mu_A(x) = \begin{cases} 1 \text{ if and only if } x \in A \\ 0 \text{ if and only if } x \notin A \end{cases}.$$

(D 6.5) The set A the members of which satisfy property P is usually written as

$$A' = \{a \in A | a \text{ has property P}\}.$$

The property P has to be satisfied in total or not at all, i.e. it is either true or false for each of the elements of A. It works well as long as the objects are well defined.

For example a set A of positive natural numbers which is less than 10 is

$$A = \{a \in N | a < 10\} = \{1,2,3,4,5,6,7,8,9\}.$$

(D 6.6) A set whose elements are themselves sets is called a family of sets. It is denoted in the form

$$\{A_i | i \in I\}$$

where i and I are called the set identifier and the identification set, respectively. The identification set is usually the set of natural numbers, N.

An important set which is frequently used in this work is the set of all points in the n-dimensional Euclidean space, R^n (i.e.: all n-tuples of real numbers). Sets

defined in terms of R^n are often required to possess a property known as convexity.

(D 6.7) A set A in R^n is called convex if, for every pair of elements

$$r = (r_i | i \in N) \in A,\ s = (s_i | i \in N) \in A$$

and every real number $\lambda \in [0,1]$, exclusively, then the element t

$$t = (\lambda r_i + (1-\lambda) s_i | i \in N) \in A.$$

In other words, a set A in R^n is convex if, for every pair of points r and s in A, all points located on the straight line segment connecting r and s are also in A. This is explained in Fig. 6.1.

Figure 6.1 Crisp set (a) convex (b) nonconvex.

6.2.1 Crisp set operations

Operations in the ordinary set theory are used to represent relationships between elements of two sets.

(D 6.8) If every member of set A is also a member of set B, that is, if $a \in A$ implies $a \in B$, then A is called a subset of B (Fig. 6.2.a), and this is written in the form

$$A \subseteq B .$$

(D 6.9) If $A \subseteq B$ and $B \subseteq A$, then these sets are equal sets; this is denoted by the following equation:

$$A = B .$$

(D 6.10) If every member of a set A is not a member of set B, then set A and B are not equal, we write

$$A \neq B .$$

(D 6.11) A is called a proper subset of B when $A \subseteq B$ and $A \neq B$, which is denoted by

$$A \subset B .$$

(D 6.12) The relative complement of a set A with respect to set B is the set containing all the elements of B that are not elements of A (Fig. 6.2.b). This set is denoted as

$$B \setminus A = \{b \in B | b \notin A\} .$$

(D 6.13) The union of sets A and B is the set containing all the elements that belong either to set A or B or both of them (Fig. 6.2.c). This set is written as

$$A \cup B = \{x | x \in A \text{ or } x \in b\} .$$

(D 6.14) The union operation can be generalised for any number of sets. For a family of sets $\{A_i | i \in I\}$, this is defined as

$$\bigcup_{i \in I} A_i = \{x | x \in A_i \text{ for some } i \in I\} .$$

(D 6.15) The intersection of sets A and B is the set containing all the elements belonging to both set A and B (Fig. 6.2.d). It is denoted as a logic equation

$$A \cap B = \{x | x \in A \text{ and } x \in b\} .$$

(D 6.16) The intersection operation can be generalised for any number of sets. For a family of sets $\{A_i | i \in I\}$, this is defined as

$$\bigcap_{i \in I} A_i = \{x | x \in A_i \text{ for all } i \in I\} .$$

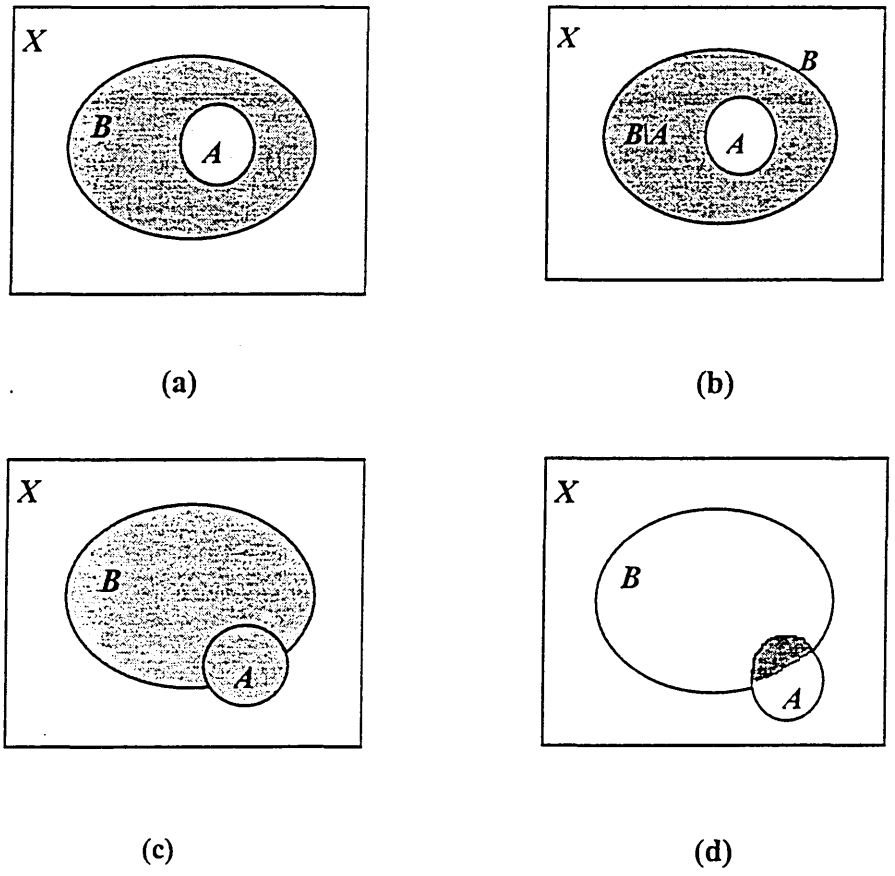

Figure 6.2 **a)** $A \subseteq B$; **b)** $B \setminus A$; **c)** $A \cup B$; **d)** $A \cap B$.

(D 6.17) A Cartesian product of two crisp sets X and Y, denoted by $X \times Y$, is the crisp set of all ordered pairs such that the first element in each pair is a member of X and the second element is a member of Y. Formally,

$$X \times Y = \{(x, y) | x \in X \text{ and } y \in Y\}.$$

It should be noted that if $X \neq Y$, then $X \times Y \neq Y \times X$.

(D 6.18) The Cartesian product of n crisp sets $\{X_i | i \in N\}$ are set of n-tuples defined in this form;

$\underset{i \in N}{\times} X_i = \{(x_1, x_2, ..., x_n) | x_i \in X_i \text{ for all } i \in N\}$.

(D 6.19) A relation among crisp sets X_1, X_2, ..., X_n is a subset of the Cartesian product $\underset{i \in N}{\times} X_i$ such that

$$R(X_1, X_2, ..., X_n) \subset X_1 \times X_2 \times ... \times X_n .$$

(D 6.20) A crisp relation $R(X \times X)$ is reflexive if and only if $(x,x) \in R$, $\forall x \in X$, otherwise it is called antireflexive if $(x,x) \notin R$, $\forall x \in X$.

(D 6.21) A crisp relation $R(X \times X)$ is symmetric if and only if $(x,y) \in R \Rightarrow (y,x) \in R$ for $x, y \in X$. On the other hand if $(x,y) \in R$ and $(y,x) \in R \Rightarrow x = y$, the relation is called antisymmetric.

(D 6.22) A crisp relation $R(X \times X)$ is transitive if and only if $(x,y),(y,z) \in R \Rightarrow (x,z) \in R$ for $x, y, z \in X$. On the other hand if $(x,y),(y,z) \in R \Rightarrow (x,z) \notin R$, the relation is called antitransitive.

(D 6.23) A crisp binary relation $R(X \times X)$ that is reflexive, antisymmetric, and transitive is partially ordered.

(D 6.24) Let X be a partially ordered relation and $A \subseteq X$. $x \in X$ is called a lower bound of A if $x \leq y$, $y \in A$.

(D 6.25) Let X be a partially ordered relation and $A \subseteq X$. $x \in X$ is called an upper bound of A if $y \leq x$, $y \in A$.

(D 6.26) Let X be a partially ordered relation and $A \subseteq X$. $x \in X$ is called an infimum (greatest lower bound) of A, written as $\inf A$ if and only if:

(i) x is a lower bound of A

(ii) if y is another lower bound of A, then $y < x$

(D 6.27) Let X be a partially ordered relation and $A \subseteq X$. $x \in X$ is called a supremum (least upper bound) of A, written as $\sup A$ if and only if:

(i) x is an upper bound of A

(ii) if y is another upper bound of A, then $y > x$

(D 6.28) Let X be a partially ordered relation and $A \subseteq X$. $x \in X$ is called a minimum of A, written as $\min A$ if and only if:

(i) x is a lower bound of A

(ii) $x \in A$

Clearly a minimum of a set is also the infimum.

(D 6.29) Let X be a partially ordered relation and $A \subseteq X$. $x \in X$ is called a maximum of A, written as max A if and only if:

(i) x is an upper bound of A

(ii) $x \in A$

Clearly a maximum of a set is also the supremum.

The ordinary or crisp set theory was critically reviewed by mathematicians and philosophers including Betrand Russell. It is pointed out that the sets cannot be defined in an arbitrary way without producing paradoxes. The problem is observed as coming from the real world situations. Axioms of specifications cannot be used to build the sets in a consistent way (Birkhoff and Bartee 1970). That is, there are meaningful properties that cannot be used to define sets uniquely (Kosanovic et al 1994).

The application of a crisp set (see D 5) fails when one attempts to define a set for objects which are not well defined. The examples of cases may be based on meaningful properties, but the sets cannot be uniquely determined. The reason is that the properties involved do not precisely describe the situation as in a crisp set.

6.3 Fuzzy Set Theory

As mentioned earlier, before the beginning of 19th century, the field of science and engineering was known for precision, specificity, sharpness, consistency and speciality. This view was adopted mainly due to the fact that mathematics, i.e.

crisp set theory, was the main tool of science. The technique was considered as being precise and consisted of two logical values: yes or no. However, this view was finally challenged by L. Zadeh (1965) in his revolutionary paper, *Fuzzy Sets*. In this paper, the concept of degree of membership for a set was introduced in a closed unit interval [0,1]. The extreme values in the interval, 0 and 1 represent the total denial and affirmation of the membership in a set, respectively. On the other hand, all the values between these values represent gradual transitions from membership to nonmembership of the set. This ground breaking concept provides meaningful and powerful representation of measurement of uncertainties, and also gives a meaningful representation of vague expression in natural language.

The purpose of fuzzy set theory is to bring mathematics closer to reality. Being a constitutive part of modern mathematics, fuzzy sets are not intended to replace crisp set theory. It will however provide a formal way of describing the real-world phenomena (Kosanòvic 1995). It is a theory in which everything is a matter of degree, i.e. everything has elasticity (Zimmermann 1991).

Formally, a fuzzy set may be defined as follows:

(D 6.30) Let X be the universal set with its element denoted by x. A fuzzy set F in X is characterised by a membership function $\mu_F: X \rightarrow [0,1]$, with the value $\mu_F(x)$ representing the grade of membership of x in F.

Fuzzy sets are always mappings from a universal set into [0,1]. Conversely, every function $\mu: X \rightarrow [0,1]$ may be considered as a fuzzy set (Kruse et al 1994).

For example, one can define a set $F_1 = \{x \in R | x \text{ is about between 5 and 8}\}$ with a membership function

$$\mu_{F_1}(x) = \begin{cases} x-4, & x \in [4,5) \\ 1, & x \in [5,8] \\ -x+9, & x \in (8,9] \\ 0, & \text{otherwise} \end{cases}$$

The above relation for the intervals (see Glossary of Symbols) can be represented graphically in Figure 6.3

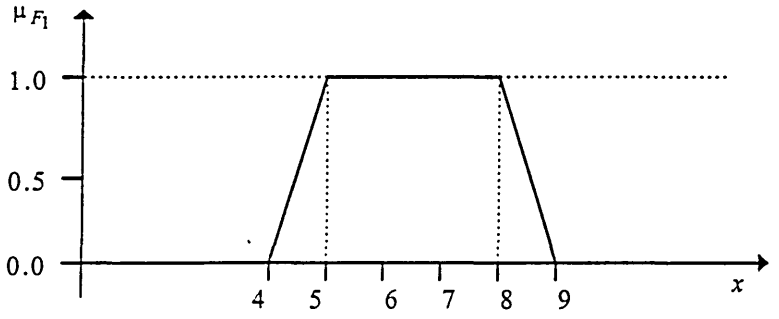

Figure 6.3 Membership function of fuzzy set

$F_1 = \{x \in R | x \text{ is about between 5 and 8}\}$.

Thus a membership function μ_F measures the extent to which the property of 'about between 5 and 8' established by F is valid for each of the elements in $X = R$.

Another example is $F_2 = \{x \in R | x \text{ is about 4}\}$. The membership function for the set is written below

$$\mu_{F_2}(x) = \begin{cases} x-3, & x \in [3,4) \\ 1, & x = 4 \\ -x+5, & x \in (4,5] \\ 0, & \text{otherwise} \end{cases}$$

The graphical description is given in Fig. 6.4.

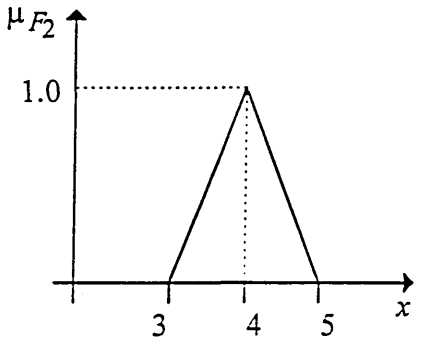

Figure 6.4 **Fuzzy number** $F_2 = \{x \in R | x \text{ is about } 4\}$.

(D 6.31) Since a function can be represented by a set of ordered pairs, any fuzzy set F can written as

$$F = \{(x, \mu_F(x)) | x \in X\}.$$

6.3.1 Fuzzy set operations

Since the membership function completely characterises a fuzzy set, the operations with fuzzy sets are defined based on membership functions (Klir and Folger 1988). The basic set operations of crisp set theory (D 6.8-D 6.16), may be extended to fuzzy set theory.

(D 6.32) If the membership function of each element of the universal set X in fuzzy set A is less than or equal its membership function in fuzzy set B, then A is called a subset of B or vice versa, i.e.

$$A \subseteq B \Leftrightarrow \mu_A(x) \leq \mu_B(x).$$

(D 6.33) Fuzzy sets A and B are equal if and only if all the membership functions for every element are equal.

$$A = B \Leftrightarrow \mu_A(x) = \mu_B(x), \ \forall x \in X.$$

Consequently, if $A = B$, then $A \subseteq B$ and $B \subseteq A$.

(D 6.34) Fuzzy sets A and B are not equal if there is one element which has a different membership function.

$$A \neq B \Leftrightarrow \mu_A(x) \neq \mu_B(x), \text{ for some } x \in X.$$

(D 6.35) Fuzzy set A is a proper subset of B when A is a subset of B but not equal

$$A \subset B \Leftrightarrow \mu_A(x) \leq \mu_B(x), \ \forall x \in X \text{ and } \exists x \in X \text{ such that } \mu_A(x) < \mu_B(x).$$

(D 6.36) The complement of fuzzy set A (Fig. 6.4 b), $\tilde{A}$, is the fuzzy set defined as

$$\tilde{A} = \{(x, \mu_{\tilde{A}}(x)) | \mu_{\tilde{A}}(x) = 1 - \mu_A(x),\ x \in A\}.$$

(D 6.37) The union of fuzzy sets A and B (Fig. 6.2.c), $A \cup B$, is the fuzzy set defined by the following membership function:

$$\mu_{A \cup B}(x) = \mu_A(x) \vee \mu_B(x) = \max[\mu_A(x), \mu_B(x)].$$

(D 6.38) The union operation for fuzzy sets can be generalised for a finite number of sets. For a family of fuzzy sets $\{A_i | i \in \{1,2,...,n\}\}$, the union is defined by a membership function:

$$\mu_{\bigcup_{i=1}^{n} A_i} = \mu_{A_1}(x) \vee \mu_{A_2}(x) \vee ... \vee \mu_{A_n}(x) = \max[\mu_{A_1}(x), \mu_{A_2}(x), ..., \mu_{A_n}(x)]$$

(D 6.39) The intersection of fuzzy sets A and B (Fig. 6.2.d), $A \cap B$, is the fuzzy set defined by the following membership function:

$$\mu_{A \cap B}(x) = \mu_A(x) \wedge \mu_B(x) = \min[\mu_A(x), \mu_B(x)].$$

(D 6.40) Similar to the union, the intersection operation for fuzzy sets can be generalised for a finite number of sets. For a family of fuzzy sets $\{A_i | i \in \{1,2,...,n\}\}$, the union is defined with the membership function

$$\mu_{\bigcap_{i=1}^{n} A_i} = \mu_{A_1}(x) \wedge \mu_{A_2}(x) \wedge ... \wedge \mu_{A_n}(x) = \min[\mu_{A_1}(x), \mu_{A_2}(x), ..., \mu_{A_n}(x)].$$

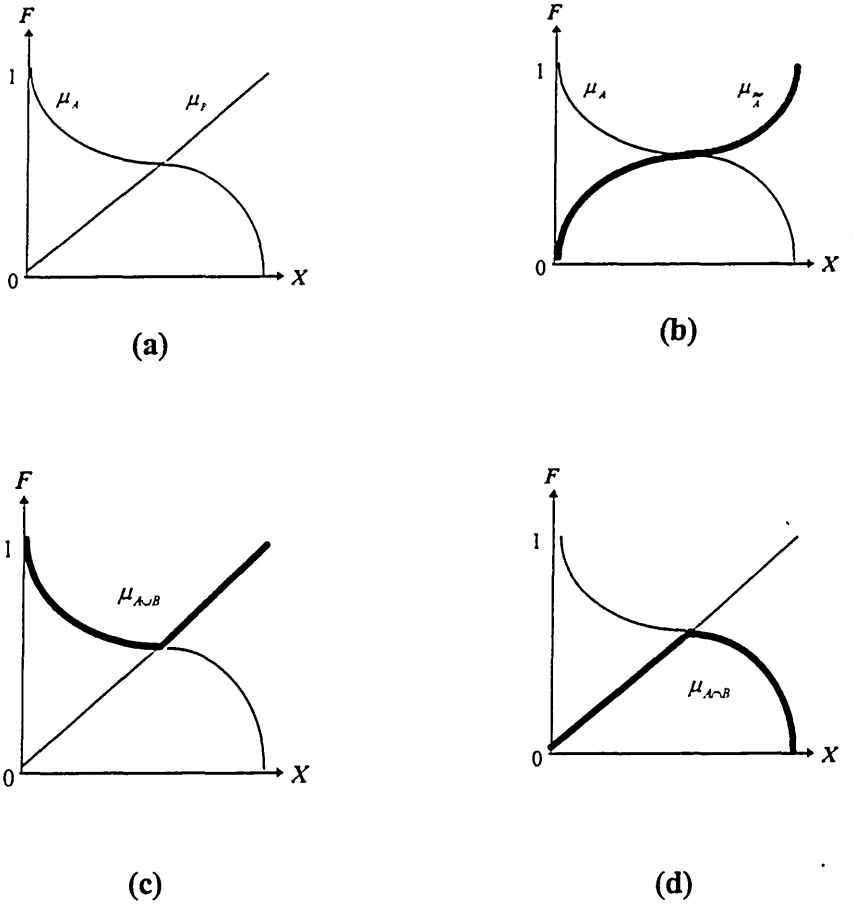

Figure 6.5 a) Fuzzy sets *A* and *B*; b) Fuzzy complement of *A*; c) Fuzzy union of *A* and *B*; d) Fuzzy intersection of *A* and *B*.

(D 6.41) A fuzzy relation is a fuzzy set defined on the Cartesian product of crisp sets $X_1, X_2, ..., X_n$; $R(X_1, X_2, ..., X_n)$ where tuples $(x_1, x_2, ..., x_n)$ may have varying degrees of membership within the relation.

(D 6.42) A fuzzy relation $R(X, X)$ is reflexive if and only if $\mu_R(x,x) = 1, \forall x \in X$. The relation is called irreflexive if $\exists x \in X \ni \mu_R(x,x) \neq 1$ and antireflexive if $\mu_R(x,x) \neq 1, \forall x \in X$.

(D 6.43) A fuzzy relation $R(X, X)$ is symmetric if and only if $\mu_R(x,y) = \mu_R(y,x), \forall x,y \in X$. The relation is called asymmetric if $\exists x,y \in X \ni \mu_R(x,y) \neq \mu_R(y,x)$ and strictly antisymmetric if $\mu_R(x,y) \neq \mu_R(y,x), \forall x,y \in X$.

(D 6.44) A fuzzy relation $R(X,X)$ is transitive if and only if $\mu_R(x,z) \geq \max_{y \in Y} \min[\mu_R(x,y), \mu_R(y,z)]$ is satisfied for each pair $(x,z) \in X \times X$. The relation is called nontransitive if $\exists (x,z) \in X \times X \ni \mu_R(x,z) < \max_{y \in Y} \min[\mu_R(x,y), \mu_R(y,z)]$ and antitransitive if $\mu_R(x,z) < \max_{y \in Y} \min[\mu_R(x,y), \mu_R(y,z)], \forall (x,z) \in X \times X$.

(D 6.45) A fuzzy binary relation R on a set X is a fuzzy partial ordering if and only if it is reflexive, antisymmetric, and transitive under some form of fuzzy transitivity.

Any fuzzy partial ordering can be transformed into a series of crisp partial orderings by taking a series of α - cuts that produce increasing levels of refinement.

6.3.2 Alpha cut (α-cut)

The alpha cut (α-cut) is one of the main ingredients in building the fuzzy model. It is a procedure of creating the fuzzy environment as well as defuzzification.

(D 6.46) The support of a fuzzy A in the universal set X is the crisp set containing all the elements of X with nonzero membership function in A (Klir and Folger 1988).

$$\text{supp } A = \{x \in X | \mu_A(x) > 0\}.$$

In Figure 6.3, supp A = (4,9).

A more general notion of the support is the α - cut.

(D 6.47) An α - cut, A_α, is a crisp set which contains all the elements of the universal set X that have a membership functions at least to the degree of α (Fig. 6.6):

$$A_\alpha = \{x \in X | \mu_A(x) \geq \alpha\}.$$

and the set $A'_\alpha = \{x \in X | \mu_A(x) > \alpha\}$ is called the strong α - cut.

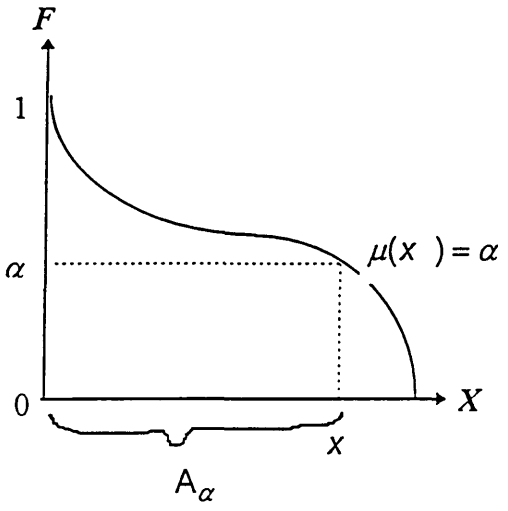

Figure 6.6 α - cut

6.3.3 Fuzzy numbers

An important feature of a fuzzy set which will be used extensively in the next chapter is fuzzy numbers.

(D 6.48) Let $F = \{(x, \mu_F(x)) | x \in X\}$ be a fuzzy set. F is called convex fuzzy set (see Fig. 6.7) if

$$\mu_F(\lambda x_1 + (1-\lambda)x_2) \geq \min[\mu_F(x_1), \mu_F(x_2)], \ \forall x_1, x_2 \in X \text{ and } \forall \lambda \in [0,1].$$

Clearly, a fuzzy set F is convex if and only if each F_α is a convex set.

(D 6.49) A fuzzy set F is normal if $\exists x \in X$ such that $\mu_F(x) = 1.0$ (see Fig. 6.3)

A fuzzy set is normal if there exist at least an element with a membership grade of 1.

(D 6.50) A convex and normalised fuzzy set F with the membership function that is piecewise continuous (Grossman 1984) is called a fuzzy number (see Fig. 6.4).

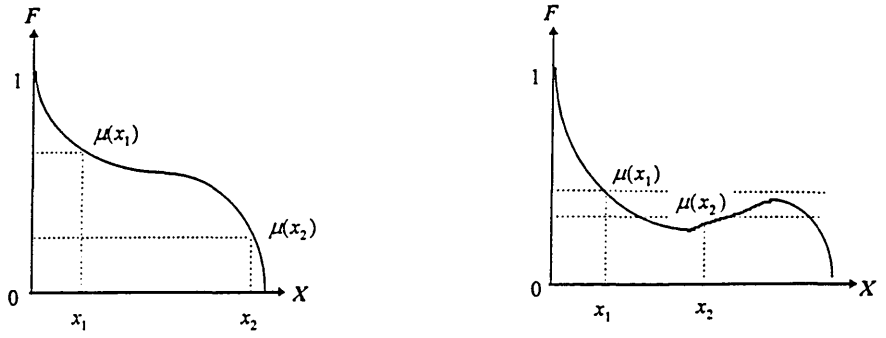

(a) (b)

Figure 6.7 Fuzzy set (a) convex b) nonconvex.

6.3.4 Fuzzy sets induced by mappings

Like any other branches of mathematics, mappings between two spaces are very crucial. This is especially valid when they can preserve some topological properties (Dugundji 1966). Therefore, the identification of these special functions which have the necessary characteristics is very important in fuzzy set theory, i.e. fuzzy sets induced by mappings. One of them is the inverse principle of set theory (Kosanovic 1995).

(D 6.51) Let Q be a mapping from X to space Y. Let A be a fuzzy set in X with membership function $\mu_A(x)$. The mapping Q induces a fuzzy set B in Y whose membership function is defined by

$$\mu_A(x) = \mu_B(y), \quad y \in Y$$

for all $x \in X$ that are mapped by Q into y, i.e. $\forall x \in Q^{-1}(y)$ (inverse image of y).

Another important mapping is the extension principle. It was introduced by Zadeh (1965) and was finally elaborated by Yager (1986). It is a building block of the model in the next chapter. It is defined formally as (Kruse et al 1994) in the following.

(D 6.52) Let $\phi: X^n \rightarrow Y$ be a mapping. The extension of ϕ is given by:

$\phi^n: (F(X))^n \rightarrow F(Y)$ with

$$\phi^n(\mu_1, \mu_2, \ldots, \mu_n)(y) = \sup\{\min\{\mu_1, \mu_2, \ldots, \mu_n\} | (x_1, x_2, \ldots, x_n) \in X^n \text{ and } y = \phi(x_1, x_2, \ldots, x_n)\}$$

i.e.

A function $\phi: X^n \rightarrow Y$, which maps the tuples $(x_1, x_2, \ldots, x_n)$ of X^n to the crisp value $\phi(x_1, x_2, \ldots, x_n)$ of Y, can be extended in a suitable way to a function $\phi^n: (F(X))^n \rightarrow F(Y)$. This maps a vague description $(\mu_1(x_1), \mu_2(x_2), \ldots, \mu_n(x_n)) \in (F(X))^n$ to the fuzzy value $\phi^n(\mu_1, \mu_2, \ldots, \mu_n)$.

6.3.5 Methods of fuzzification

The process of fuzzification, i.e. the process of determining the membership function for a set varies. This largely depends on quantity as well as quality of information of its elements. These factors make fuzzy set theory very suitable for a wide range of applications. The determination methods break down into the following categories.

1. Subjective evaluation and elicitation

As fuzzy sets are usually intended to model people's cognitive states, they can be determined from either simple or sophisticated elicitation procedures. At the very least, subjects simply draw or otherwise specify different membership curves appropriate to a given problem. These subjects are typically experts in the problem area or they are given a more constrained set of possible curves from which they choose. Under more complex methods, users can be tested using psychological methods. This is a very popular approach in signal and system analysis especially in the interpretation of psychological problems such as sleeping disorder (Kosanovic 1995). It involves a lot of random collection of data.

2. Ad-hoc forms

While there is a vast (hugely infinite) array of possible membership function forms, most actual fuzzy control operations draw from a very small set of different curves, for example simple forms of fuzzy numbers. This simplifies the problem, for example to choose a just central value and the slope on either side.

This is a fairly simple but yet an effective means of determining membership function. It is widely used in a control system involving container crane control in shipping ports (Altrock 1996). One of the main features of this approach is to provide normal and convex fuzzy sets immediately. This approach will be widely used to fuzzify most of the input parameters in the proposed model for microstrip lines.

3. *Converted frequencies or probabilities*

Information taken in the form of frequency histograms or other probability curves is occasionaly used as the basis for the construction of the membership function. There are a variety of possible conversion methods, each with its own mathematical and methodological strengths and weaknesses. However, it should always be remembered that membership functions are not necessarily probabilities.

4. *Physical measurement*

Many applications of fuzzy logic use physical measurement, but none of them measures the membership grade directly. It is widely used in the chemical industry and in engineering where a vast amount of raw information is available from experiments. Mostly a membership function is provided by an independent method, and individual membership grades of data are then calculated from it. This approach is adopted for fuzzification of crosstalk in the proposed model.

5. *Learning and adaptation*

This technique is called neurofuzzy (Brown and Harris 1994). It is a combination of neural network and fuzzy set theory. Several alternative methods of integrating neural nets and fuzzy logic have been proposed in the literature (Yager 1992). One major milestone in the development of neural net technology is the application of the error back propagation (see Fig. 6.8). Firstly, it selects one of the examples of the training data set. Secondly, it computes the neural output values for the current training example inputs. Then, it compares these output values with the desired output value of the training example. The difference, called the error, determines the neurone in the net to be modified. The mathematical mapping of the error back into the neurones of the net is called error back propagation. The fuzzy logic is used in building the error back propagation algorithm (see Fig. 6.8). This particular approach is widely used in medical and industrial sectors such as in the design of a recycling glass classifier (Altrock 1996).

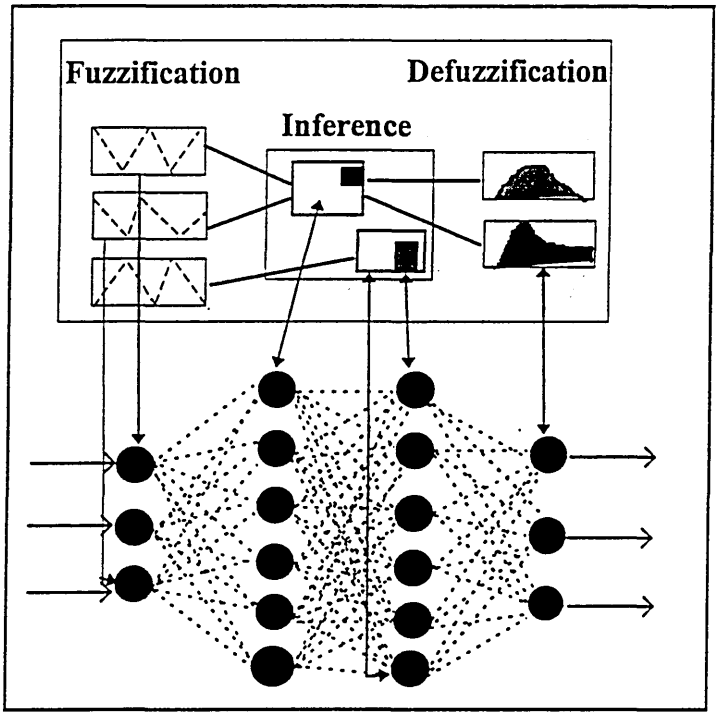

Figure 6.8 Back propagation.

6.4 Fuzzy System

In science a gradual transition from the traditional view demands that uncertainty is undesirable and needs to be avoided by all possible means. An alternative view tolerant to uncertainty is that science cannot avoid the occurrence of uncertainty. This transition of view is then followed in engineering and in several other areas. Needless to say, most of the current systems are so complex that the complexity frequently leads to a degree of uncertainty and the development of illogicality, ambiguity and subjectivity of the systems. A model of this kind is not expected to fulfil logical, objective, qualitative, precision of the system. An example of such a complex system is a set of coupled microstrip lines (Fig. 4.3, 4.5, 4.6).

Fuzzy logic can deal with the majority of the problems arising from a complex system because it is designed to measure uncertainties. From this point of view, it has branched out into several domains of mathematics such as a fuzzy algebra, fuzzy topology, and fuzzy modelling.

6.4.1 Fuzzy modelling

A complex system such as an array of microstrip line is not straight forward to model. The challenge is to develop a model where an optimal level of allowable uncertainty, vagueness and imprecision can be estimated. A uniform calculus is incapable of integrating the above three variables. Fuzzy theory, on the other hand, is a suitable tool for the task.

The basic principles of fuzzy modelling was laid down by Zadeh (1973). It has been argued that fuzzy modelling *'provide an approximate and yet effective means of describing the behaviour of systems which are too complex or too ill-defined to admit use of precise mathematical analysis'*.

In the case of the microstrip lines, the problem of delay and reflections can be solved by decreasing the length of the lines. This will increase the density of the circuits. However, the solution of this type will increase the problem of crosstalk between adjacent lines. Therefore, a designer must make proper trade-offs between conflicting factors, large numbers of circuit parameters and design specifications.

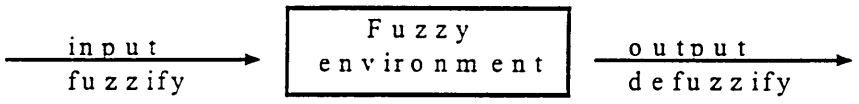

Figure 6.9 Fuzzy model.

Fuzzy modelling is believed to be flexible and it can accommodate these criteria. Therefore, a future improvement in the numerical equations, specifications of system designers and consumers and experimental results for crosstalk of microstrip lines can be easily incorporated into the model.

6.4.1.1 Methods

There are three principles in developing fuzzy modelling:

a) The use of linguistics variables in place of or in addition to numerical variables;

b) The characterisation of simple relations between variables by conditional fuzzy statements;

c) The characterisation of complex relations by fuzzy algorithms (Yager and Filev 1994).

These principles form the basis of two methods used for fuzzy modelling:

i) Direct approach and

ii) System identification.

In the first method, the system is first described linguistically using terms from natural language and then translated into the formal structure of a fuzzy system. The description is taken solely from the knowledgeable expert of the system.

The second method is more objective than the first method. Its development consists of two stages:

- structure identification and
- parameter identification (Yager and Filev 1994).

It is also called method of transition and rely on the use of extension principle of fuzzy set theory (Terano et al 1987). Since our work involves in the decision making for parameters of microstrip lines, the process has to be very objective. For this reason, the system identification is the most suitable method adopted and its development is presented in next chapter.

7. FUZZY MODELLING OF MICROSTRIP LINES

7.1 Introduction

This chapter describes the application of fuzzy theory as an optimisation tool to the design and modelling of microstrip lines with an aim to minimise crosstalk. This procedure is essentially a fuzzy model taken in three phases. The first phase is the fuzzification of all the input parameters required for the model. Then, all the fuzzified parameters are processed in the fuzzy environment. The third phase consists of the defuzzification of processed data.

7.2 Fuzzy Flow Chart

As shown in Fig. 7.1, the three phases of our fuzzy model are best described by a flow chart. Geometrical and electrical parameters and information obtained from the mathematical analysis on crosstalk are defined in 'crisp set' form and then fuzzified. Data obtained from the fuzzification are:

- fuzzified geometrical/electrical parameters and
- fuzzified intersection of parameters.

The fuzzified data are treated in a fuzzy environment where all the parameters are defined in a fuzzy set. The fuzzified data in the environment are finally defuzzified in order to obtain crisp results. The whole process is grouped into three algorithm blocks namely; induced performance parameter, the process and defuzzification. These are explained in Fig. 7.2. These algorithms are described in detail in Sect. 7.4.1.

7.3 Fuzzifications

Variables involved in an engineering design are usually referred to as parameters. These parameters are input, output and performance parameters (Kruse et al 1994). The specifications of different types of parameters are presented in Table 7.0:

Input Parameters (design parameters)	*Output Parameters*	*Performance Parameters*
• independent • values are determined during the design process	• involved in design process • functionally dependent on the input parameters and possibly on some performance parameters • not subject to any specified functional requirement	• subject to some functional requirement

Table 7.0 Design parameters.

The functional requirement may take on a value or a range of values specified for a performance parameter. These values are, however, independent of the design process.

The input parameters of our model are geometrical parameters of microstrip lines (see Fig. 2.1). On the other hand, all the electrical parameters (see eqns. 3.12 - 3.18) of microstrip lines are regarded as being performance parameters or output parameters. The fuzzification of these parameters is the first phase of the model. It is divided into three parts:

i) fuzzification of geometrical, performance and crosstalk parameters;

ii) intersection of fuzzified crosstalk and corresponding fuzzified input parameters:

iii) evaluation of induced performance parameters.

7.3.1 Fuzzy geometrical parameters

All geometrical parameters of microstrip lines are input parameters. They are predetermined by the designer, consumer or the current state of technology. Under these circumstances, the ad-hoc form is the best suitable method of fuzzification. The fuzzy sets must be normal as well as convex.

7.3.2 Fuzzy crosstalk

The complex phenomenon of crosstalk depends on various factors (Seki and Hasegawa 1984, Zhang et al 1992). Therefore the scope of obtaining sufficient information from measurement alone is difficult and it is also fairly complex to find a mathematical expression for crosstalk. In order to assist designers in overcoming these difficulties, an alternative approach based on fuzzy logic may be adopted. This is because the choice of a certain precise membership function (i.e. line parameters) is less significant in fuzzy applications since only the qualitative properties of functions are generally needed (Terano et al 1987).

The spacing between the microstrip lines influences the crosstalk (see Sect. 5.4). The following statements need to be included:

(i) $$\lim_{s\to\infty} \xi(s) = -\infty \qquad (7.1)$$

(ii) crosstalk between lines decreases monotically as spacing increases;

i.e. $\xi(a) \geq \xi(s) \geq \xi(b), \ \forall s \in [a,b]$ (7.2)

(iii) all the values of ξ appear in the fourth quadrant

(iv) crosstalk is symmetrical about the feeder line (line 4)

These properties are employed in order to derive the membership function of fuzzy crosstalk. This may be achieved by a direct physical measurement (Wheeler 1965). For a given line spacing $S = [a,b]$, where a and b are the possible range of values for line spacing, the crosstalk for such a configuration is given as $\xi(s)$. This is valid for the interval ($\forall s \in S$). The crosstalk preference membership function μ mapped over $S \rightarrow [0,1]$ is defined with respect to the spacing between lines and initial conditions in the following form:

$$\mu_{\xi}(s) = \begin{cases} 1, & s = b \\ \dfrac{\xi(s)}{\xi(b)}, & s \neq b \end{cases} \qquad (7.3)$$

and a set of fuzzified crosstalk is also defined as $F_{\xi} = \{(s, \mu_{\xi}) : s \in S\}$. (7.4)

By the property of (iv), the crosstalk versus line spacing is shown in Fig. 7.3(a). Due to the symmetry, the spacing between lines 4 to 8 is shown. Using the defined membership function (7.3), the measured value of crosstalk for experimental data of Exp. 4 ($s = w = 500\mu m$), as given in Fig 7.3(a) is then transformed into the fuzzified crosstalk. Corresponding results are presented in Fig. 7.3(b). Generally, it is an induced crosstalk versus line spacing, generated

by reflection with respect to the x - axis. It is normal and convex ,and these properties are essential for our fuzzy model.

The novel fuzzified crosstalk always carries the factor of preference with respect to spacing. This indicates that as the spacing between the lines increases the crosstalk decreases and the fuzzy value approaches unity. A fuzzy value of unity is the goal for a designer to achieve. Therefore, fuzzified results, obtained from a single set of practical measurement, can be employed for further design of microstrip lines subject to the condition that the values of physical parameters are within the fuzzy set.

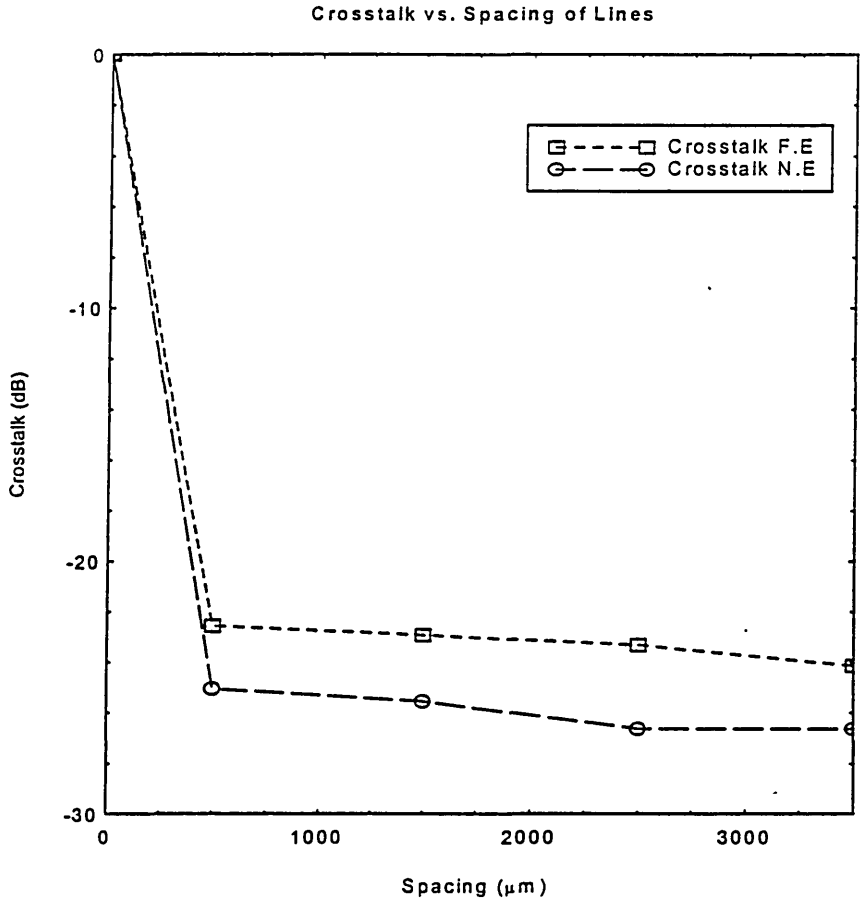

Fig. 7.3(a)

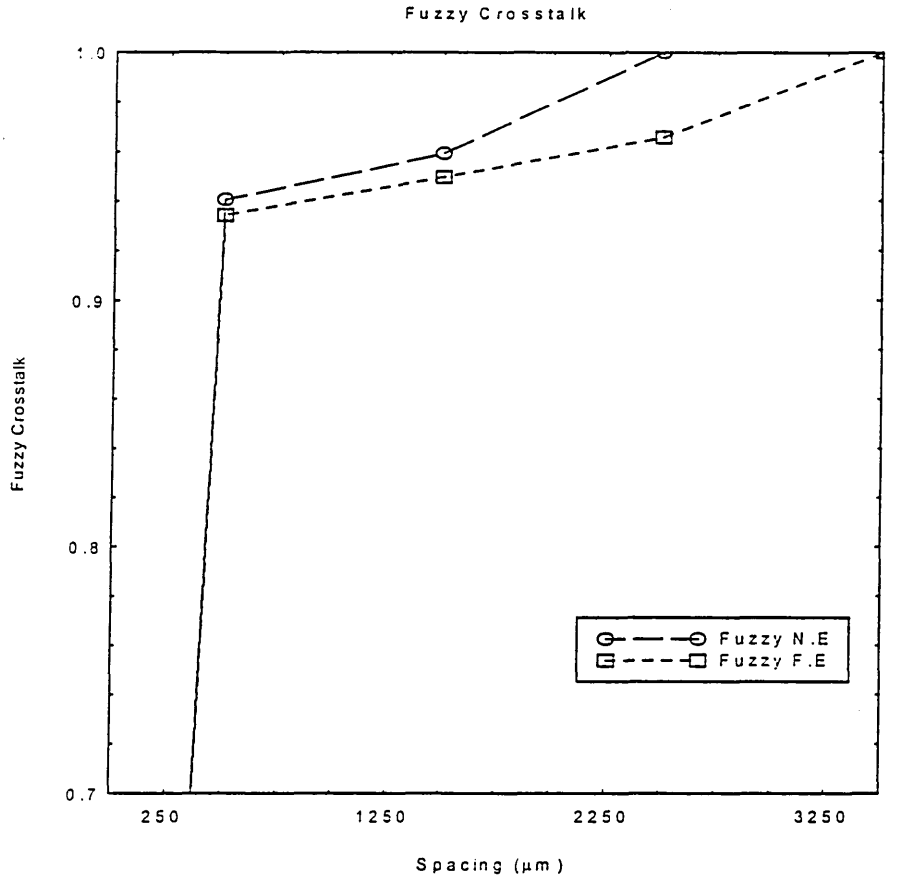

Fig. 7.3(b)

Figure 7.3 Crosstalk versus line spacing (a) measured (b) fuzzified.

7.3.3 Fuzzified constrained optimisation

The process of fuzzified constrained optimisation is the intersection of fuzzified crosstalk and its respective fuzzified geometrical parameters within the same size of interval domains. In addition, it is possible that they are normal and convex. The fuzzified geometrical parameter is a preferred parameter and the fuzzified crosstalk contains its respective parameter within an allowed limit.

The resulting intersection contains an optimised allowable parameter involving crosstalk. The collective intersection with other fuzzified geometrical parameters are then used to estimate the induced performance parameter.

7.4 Fuzzy Environment

In a fuzzy environment, all the parameters (input and induced) have been completely fuzzified. They are then used to determine the induced performance parameter.

7.4.1 Algorithm I (induced performance parameter)

The induced fuzzified performance parameter, $F_{j_{ind}}$, plays an important role as a reference set for optimisation of input parameters. It is produced by applying extension principle (D 6.52) to the performance and input parameters.

All the fuzzy sets F_{I_i} expressing preferences of all input parameters $g_i \in I_i \subset R^+$ $(i \in N)$ are determined, normalised and convex. I is a close interval of positive real numbers. C_g is a performance parameter which considers all input parameters as its variables and it can be presented within a fuzzy set F_{C_g}.

The algorithm to determine a fuzzy set induced on C_g, F_{ind}, has the following steps:

Step 1. Let $C_g: I_1 \times I_2 \times ... \times I_i \rightarrow R$ is the performance parameter $(i \in N)$ such that $r = C_g(g_1, g_2, g_3, ..., g_n)$.

In this step, a designer is able to determine the most suitable performance parameter for the whole process. The performance parameter contains all input parameters as its variables.

Step2. Select appropriate values for α- cut, such that $\alpha_1,\alpha_2,\alpha_3,...,\alpha_k \in (0.1]$ **which are equally spaced.**

The values of α- cut for the process are determined. The smaller the value, the resolution of output will be finer. This implies an improved degree of accuracy for the final result.

Step 3. Determine all the α_k- cuts for all F_{I_i} $(i \in N)$.

Once the value is determined, all α- cuts of the input parameters are calculated.

Step 4. Generate all 2^n combinations of the endpoints of intervals representing α_k- cuts for all F_{I_i} $(i \in N)$. Each combination is an n-tuple $(g_1,g_2,g_3,...,g_n)$.

Combinations of the end points of intervals for all input parameters with respect to each particular value of α- cut are determined. The smaller of the value of α- cut, the larger of the number of combinations.

Step 5. Determine $r_j = C_g(g_1,g_2,g_3,...,g_n)$ for each n-tuple $j \in 1,2,3,...,2^n$.

Find the corresponding performance parameter for each of the combinations with respect to each particular value of α- cut.

Step 6. Set $F_{jind} = [\min r_j, \max r_j]$ **for all** $j \in 1,2,3,....2^n$.

Find minimum and maximum values of performance parameters with respect to each value of α - cut. Then plot graph of fuzzy induced performance parameter, F_{jind}. Normal and convex fuzzified input parameters will produce normal and convex fuzzy induced performance parameter.

7.4.2 Algorithm II (the process)

Step 7. Set $F_{C_g} \cap F_{ind}$.

Find the intersection of the fuzzified performance parameter; F_{C_g}, with the fuzzy induced performance parameter; F_{ind}. This can be performed by superimposing one graph on to the other.

Step 8. Find the membership value of supremum of step 1, say f^* = sup $[F_{C_g} \cap F_{ind}]$.

Determine the largest fuzzy membership value for the intersection.

Step 9. Find the C_g value of f^*, say C_g^*.

Determine its corresponding value of the performance parameter.

Once all the fuzzified parameters have been processed by the above short algorithm, they are ready to undergo the final phase of the model.

7.5 Inherited Constrained Defuzzification

The process of inherited and constrained defuzzification starts when the membership value of intersection, f^*, is applied to every fuzzified input parameters by f^* - cuts. These fuzzy values have inherited all the constraints described earlier in Section 7.3. It is simply a repetition of Step 3 to 5 given in Section 7.4.1. The folowing theorems are then used to determine a most appropriate/optimised value of generated combination data.

7.5.1 Theorems of optimised defuzzified values

The proof of theorems forms the main part of the final phase of defuzzifications. This will enable one to identify the best optimised value from theoreticaly predicated results in the final phase.

Theorem 7.1: If $C_g^* = r_j^* = \max\ r_j$ such that $\mu(r_j^*) = f^*$, for some $(r_j, f^*) \in F_{ind}$, then

$$r_j^* = C_g^* = \max[C_g(g_1^*, g_2^*, \ldots, g_n^*)] \text{ where } \mu(g_i^*) = f^*. \qquad (7.5)$$

proof:

Suppose $C_g^* = r_j^* = \max\ r_j$ such that $\mu(r_j^*) = f^*$, for some $(r_j, f^*) \in F_{ind}$.

Find all the f cuts of all F_{I_i} $(i \in N)$ to create all n-tuples of $(g_1^*, g_2^*, ..., g_n^*)$ such that $\mu(g_i^*) = f^*$ and $(g_i^*, f^*) \in F_{I_i}$.

Set $r_j = \max[C_g(g_1^*, g_2^*, ..., g_n^*)]$, therefore $(r_j, f^*) \in F_{ind}$. However, since F_{ind} is normal and convex, therefore $r_j = r_j^*$.

Corollary 7.2: If $C_g^* = r_j^* = \min r_j$ such that $\mu(r_j^*) = f^*$, for some $(r_j, f^*) \in F_{ind}$, then

$$r_j^* = C_g^* = \min[C_g(g_1^*, g_2^*, ..., g_n^*)] \text{ where } \mu(g_i^*) = f^*. \quad (7.6)$$

The theorems are very important since they encompass the whole algorithms and hence the model. Theorem 1 (see Fig. 7.4.a) indicates that if the preferred fuzzy intersects on the maximum side of the fuzzy induced, then the set of optimised parameters is the set for the maximum induced values. On the other hand, Corollary 2 (see Fig. 7.4.b) points out that if the preferred fuzzy intersects on the minimum side of the fuzzy induced, the set of optimised parameters is the set for the minimum induced values.

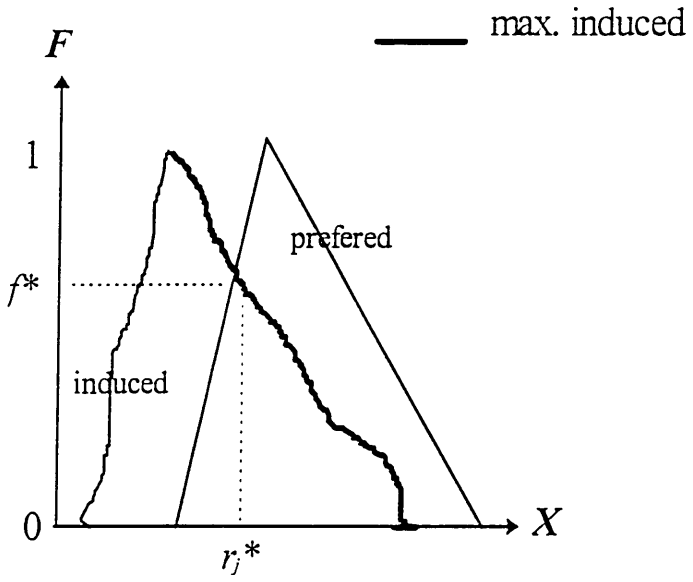

(a)

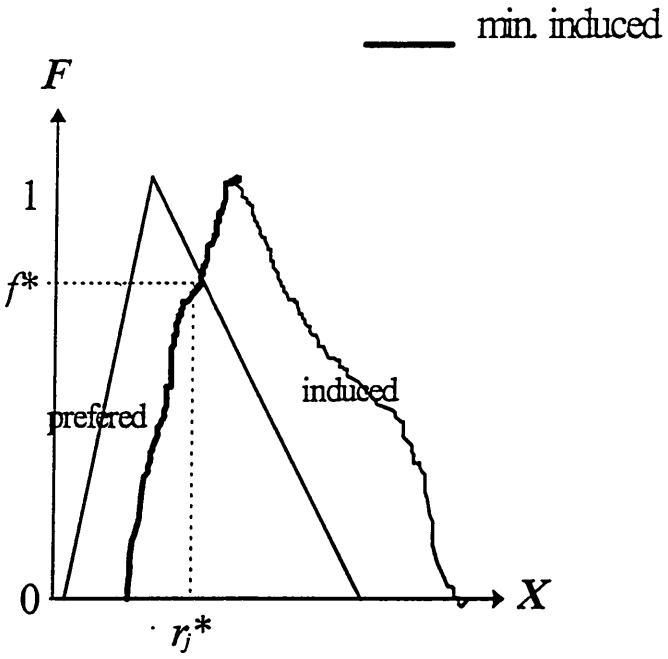

(b)

Figure 7.4 Optimised defuzzified values (a) maximum (b) minimum sides.

An algorithm to simplify the process of defuzzification is presented.

7.5.2 Algorithm III (defuzzify)

Step 10. Find f^*- cut of all F_{I_i} $(i \in N)$.

Determine all α - cuts of the fuzzified input parameters by using the highest fuzzy membership value of the intersection in Step 8; f^*, as its α - cut value.

Step 11. Generate all 2^n combinations of the endpoints of interval representing f^*- cut of all F_{I_i} $(i \in N)$. Each combination is an *n*-tuple $(g_1^*, g_2^*, g_3^*, ..., g_n^*)$.

Similar to Step 4, find all combinations of endpoints of intervals for the f^*- cuts.

Step 12. Determine $C_g(g_1^*, g_2^*, g_3^*, ..., g_n^*)$ for each *n*-tuple $j \in 1,2,3,...,2^n$.

Calculate all performance parameters for each of the combinations.

Step 13. If $C_g^* = r_j^* = \max r_j$ such that $\mu(r_j^*) = f^*$, for some $(r_j, f^*) \in F_{ind}$, then $r_j^* = C_g^* = \max[C_g(g_1^*, g_2^*, ..., g_n^*)]$ where $\mu(g_i^*) = f^*$ (by theorem 7.1)

If the preferred fuzzy intersects on the maximum side of the fuzzy induced, then optimised parameters are the performance parameters with the largest values. These have been determined in Step 12.

Step 14. If $C_g^* = r_j^* = \min r_j$ **such that** $\mu(r_j^*) = f^*$, **for some** $(r_j, f^*) \in F_{ind}$, **then**

$r_j^* = C_g^* = \min[C_g(g_1^*, g_2^*, ..., g_n^*)]$ **where** $\mu(g_i^*) = f^*$ **(by Corollary 7.2)**

Otherwise, if the preferred fuzzy intersects on the minimum side of the fuzzy induced, then the optimised parameters are the performance parameters with the smallest values. These have been determined in Step 12.

These algorithms can be applied easily for determining the electrical and geometrical parameters of microstrip lines with respect to a wide range of initial constraints or specifications. These applications are presented in the following chapter.

8. IMPLEMENTATION RESULTS

8.1 Introduction

The central theme of *'fuzzy modelling'* is to develop a decision making model/tool for designing microstrip lines. This will assist designers in choosing the most appropriate parameters of microstrip lines in order to reduce the crosstalk.

In this chapter, the method of employing the algorithms is described in order to determine geometrical and electrical parameters of microstrip lines. Firstly, these parameters are simulated in order to test our model under some initial constraints. Later, the fuzzified crosstalk is incorporated into these algorithms. Finally the parameters obtained are simulated for crosstalk using the mathematical model developed in Chapter 4 for cross-reference.

8.2 Determination of Geometrical Parameters

In order to illustrate the first application of the algorithms, the value of capacitance due to the electric flux (eqn. 3.16) is used as the performance parameter. The domains and values of input parameters are given in Table 8.1. A suggested values can be any value within the domains.

Parameters	Domain	Suggested
C_{gd} (x 10^{-11})F	3 - 9	5
Dielectric constant (ε_r)	3 - 10	9
Thickness, t (μm)	3 - 7	5
Width, w (μm)	4 - 9	6
Height, h (μm)	8 - 10	9
Spacing, s (μm)	1 - 5	3

Table 8.1 Input parameters.

Fuzzified values of the input parameters are shown in Fig. 8.1. These figures represent simple fuzzy numbers. The two limits of the domain will have the lowest fuzzy values whereas the suggested value will be assigned to the highest fuzzy value.

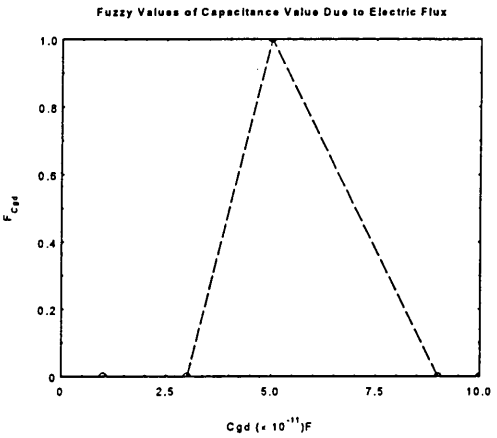

Fig. 8.1(a)

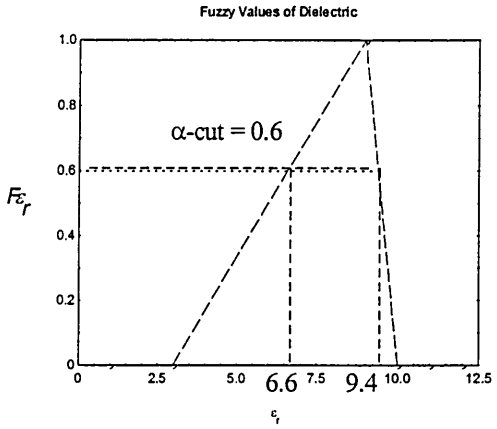

Fig. 8.1(b)

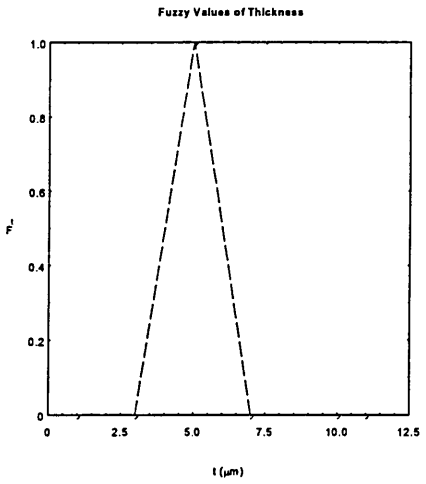

Fig. 8.1(c)

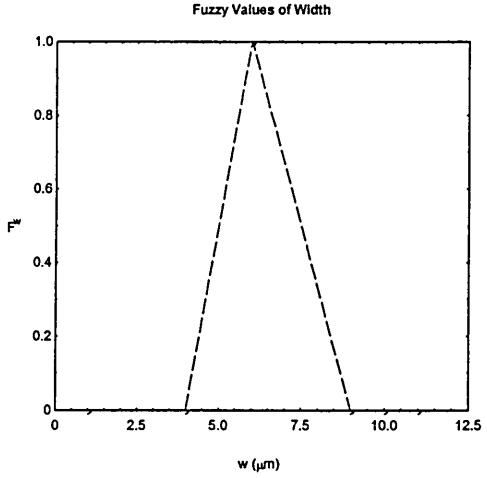

Fig. 8.1(d)

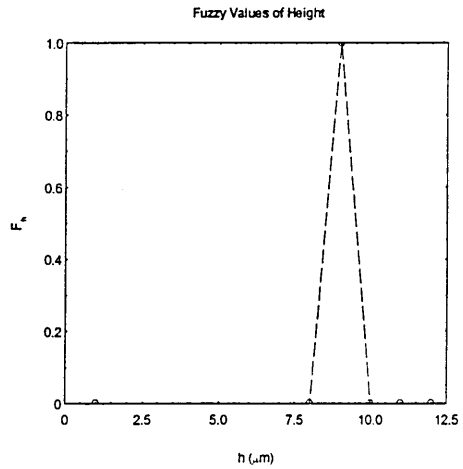

Fig. 8.1(e)

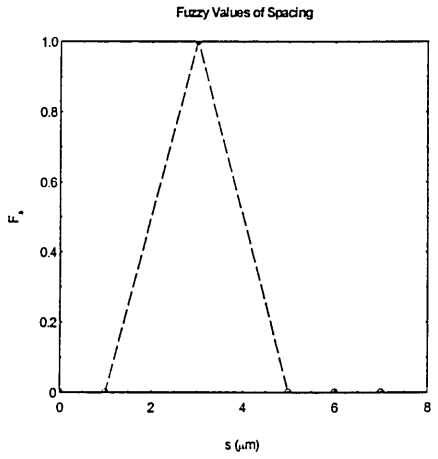

Fig. 8.1(f)

Figure 8.1 Fuzzification of input parameters: (a) C_{gd} (b) dielectric (c) thickness (d) width (e) height (f) spacing.

The α - cuts of all input parameters obtained from Fig. 8.1 are listed in Table 8.2. For a better resolution much smaller values of α - cuts values are recommended.

	α - cuts values				
Input Parameters	**0.2**	**0.4**	**0.6**	**0.8**	**1.0**
Dielectric	[4.2, 9.8]	[5.4, 9.6]	[6.6, 9.4]	[7.8, 9.2]	[9, 9]
Thickness (μm)	[3.4, 6.6]	[3.8, 6.2]	[4.2, 5.8]	[4.6, 5.4]	[5, 5]
Width (μm)	[4.4, 8.4]	[4.8, 7.8]	[5.2, 7.2]	[5.6, 6.6]	[6, 6]
Height (μm)	[8.2, 9.8]	[8.4, 9.6]	[8.6, 9.4]	[8.8, 9.2]	[9, 9]
Spacing (μm)	[1.4, 4.6]	[1.8, 4.2]	[2.2, 3.8]	[2.6, 3.4]	[3, 3]

Table 8.2 α - cuts values of input parameters.

As shown in Fig. 8.2 the process of defuzzification begins by setting the intersection of preferred and induced capacitance curves in order to obtain f^* and C^*_{gd}. Results acquired from the intersection are then analysed to obtain the best possible geometrical configurations of microstrip lines. Samples of three different sets are shown in Table 8.3.

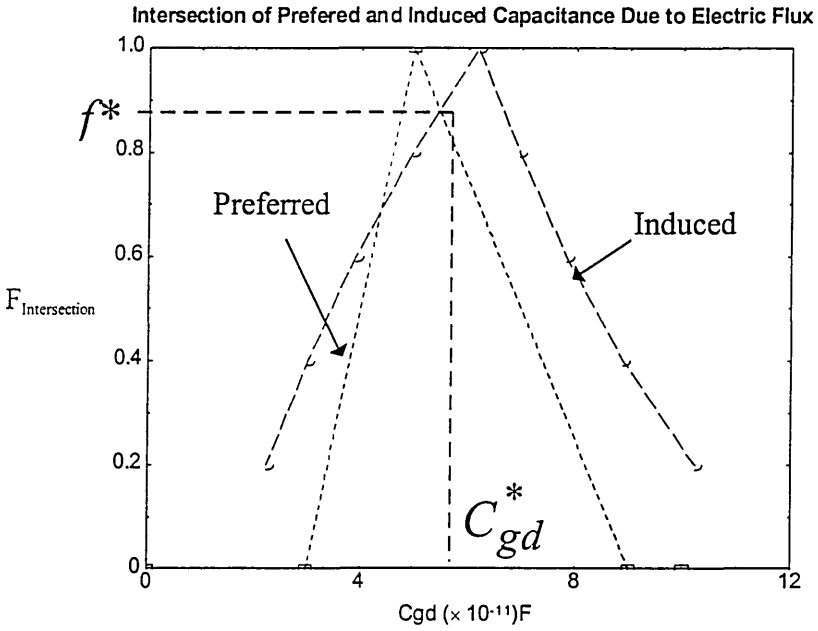

Figure 8.2 Intersection of induced and preferred C_{gd}.

	Initial values (A)			Calculated values (B)			|A -B|/A (%)		
Parameters	**Set 1**	**Set 2**	**Set 3**	**Set 1**	**Set 2**	**Set 3**	**Set 1**	**Set 2**	**Set 3**
C_{gd} (10^{-11})F	5	4	9	5.402	4.281	7.817	8.04	7.02	13.14
Dielectric	9	5	10	8.3	6.614	8.699	7.77	32.28	13.01
Thickness(μm)	5	4	3	5.3	3.677	3.743	6	8.075	24.76
Width(μm)	6	5	4	5.8	6.291	4.299	3.33	25.82	7.47
Height(μm)	9	8	10	8.9	8.645	9.628	1.11	20.35	3.72
Spacing(μm)	3	5	1	3.3	3.708	1.743	10	25.84	74.3

Table 8.3 Preferred and calculated parameters and their difference.

It is clear from Table 8.3 that initial parameters may be of random nature. When fuzzified, it is possible to obtain a set of new calculated values. The normalised difference between the two values are also included. This can be reduced by either

changing the initial input parameters or by selecting α - cut with increment < 0.2. As it can be seen the optimisation model/tool has given the most appropriate values of geometrical parameters. The design optimisation can be further improved by including other input parameters such as crosstalk. This aspect is discussed in the later section.

8.3 Determination of Electrical Parameters

Another application of the algorithms consists of determination of the electrical parameters of microstrip lines. As an example, the mutual capacitance (eqn. 3.18) is adopted as the performance parameters.

The input parameters are given in Table 8.4. A preferred value of a parameter can be any value between minimum and maximum values. Fuzzified values of these input parameters are quoted in Fig. 4. As before, these figures are simple fuzzy numbers where the preferred value is given a the highest membership values and the domain extreme have lowest membership values.

Boundaries	Minimum	Preferred	Maximum
C_{ii}(pF)	6.2	6.6	7
C_{ea}(pF)	5	7	10
C_{et}(pF)	8	15	15
C_{ed}(pF)	2	7	7
C_{ij}(pF)	8	10	13

Table 8.4 Input parameters.

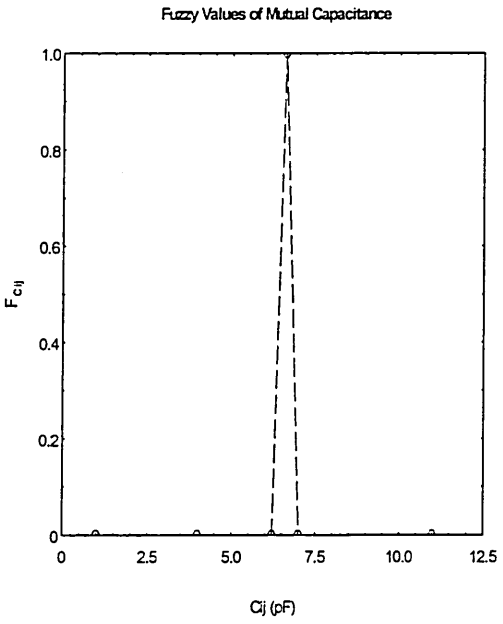

Fig. 8.3(a)

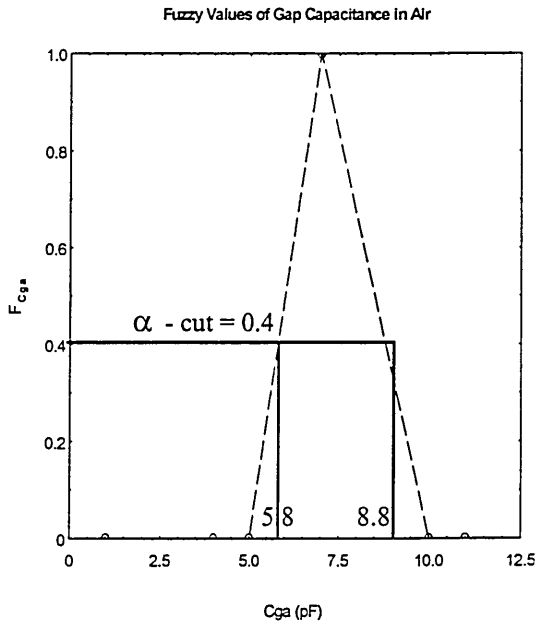

Fig.8.3(b)

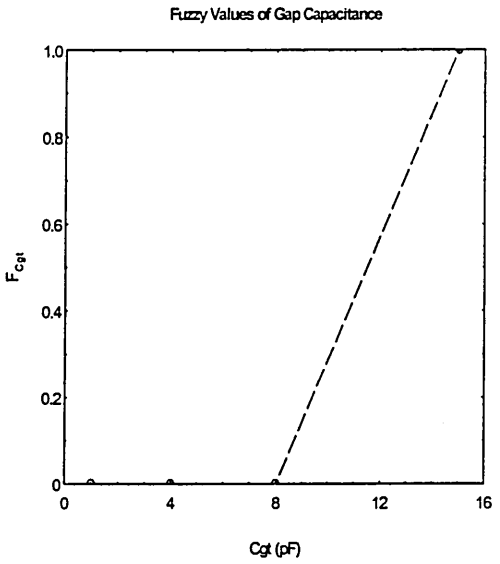

Fig. 8.3(c)

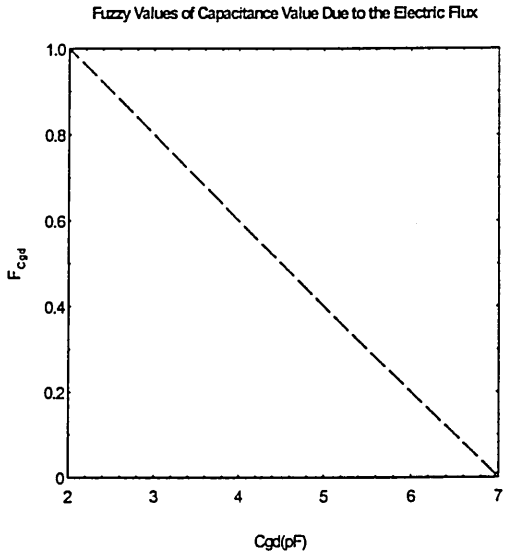

Fig.8.3(d)

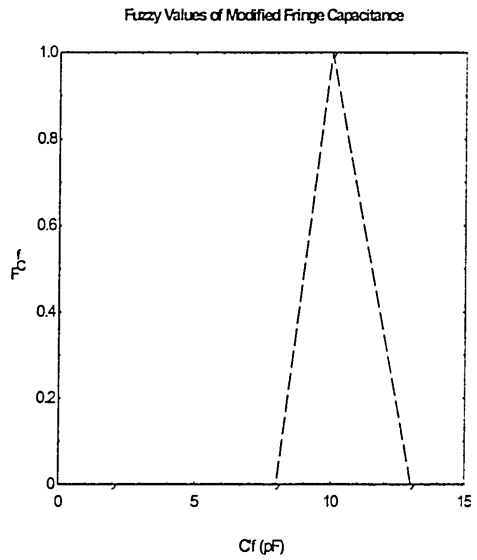

Fig. 8.3(e)

Figure 8.3 Fuzzification of input parameters (a) C_{ij} (b) C_{ga} (c) C_{gt} (d) C_{gd} and (e) C'_f.

The α - cuts of all input parameters, with increment of 0.2, obtained from Fig. 8.3 are listed in Table 8.5.

Fuzzy Values	0.2	0.4	0.6	0.8	1.0
C_{ga} (pF)	[5.4,9.4]	[5.8,8.8]	[6.2,8.2]	[6.6,7.6]	[7,7]
C_{gt} (pF)	[9.4,9.4]	[10.8,10.8]	[12.2,12.2]	[13.6,13.6]	[15,15]
C_{gd} (pF)	[6,6]	[5,5]	[4,4]	[3,3]	[2,2]
C'_f (pF)	[8.4,12.4]	[8.8,11.8]	[9.2,11.2]	[9.6,10.6]	[10,10]

Table 8.5 α - cuts of input parameters

For a better resolution, α - cuts of much smaller value can be used. α - cuts values given in the Table 8.5 are used to calculate the fuzzy values of induced C_{ij} by using the defuzzified algorithm, i.e. F_{ind} and the result is displayed in Fig. 8.4.

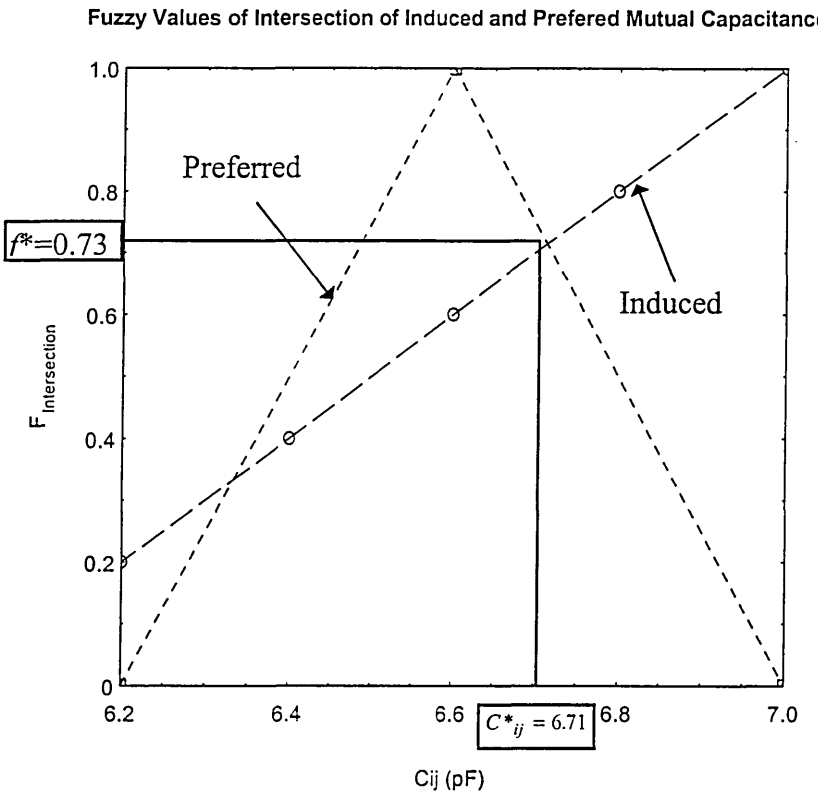

Figure 8.4 Intersection of induced and preferred C_{ij}.

The process of defuzzification begins by setting the intersection of preferred and induced capacitance curves in order to obtain f^* and C^*_{ij}, see Fig. 8.4. These data are then used to obtain the best possible electrical parameters of microstrip lines. Table 8.6 shows the preferred and calculated values together with their percentage of differences.

Parameters	Preferred (A)	Calculated (B)	|A-B|/A (%)
C_{ij} (pF)	6.6	6.71	1.73
C_{ga} (pF)	7	6.42	8.16
C_{gt} (pF)	15	13	13.33
C_{gd} (pF)	7	3.42	51.02
C'_f (pF)	10	9.42	5.71

Table 8.6 Preferred and calculated parameters and their difference.

8.4 Determination of Geometrical and Electrical Parameters with respect to Crosstalk

It has already been established that the effect of spacing on crosstalk is more apparent than any other geometrical parameters (vide Chapter 5). Therefore, the optimisation of spacing with respect to crosstalk is more critically examined than other geometrical parameters.

8.4.1 Spacing optimisation

To illustrate the application of the model for this case, the procedure is described phase by phase. The sample used for this purpose is that from Fig. 5.6.

Phase 1

In the first phase a designer may wish the domain of spacing to lie between 0 and 3500 μm. The preferred value is 2000 μm. With all the other geometrical parameters defined by the designer, the fuzzified line spacing is shown in Fig. 8.5.

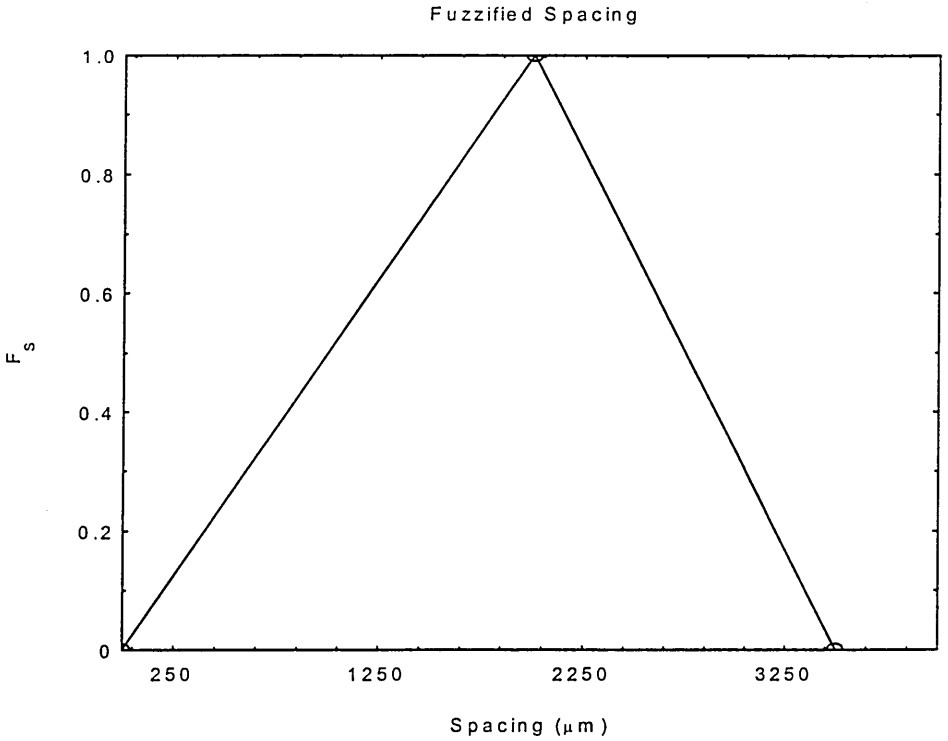

Figure 8.5 Fuzzified spacing.

Similarly, the domain of mutual capacitance lie between -10 pF to 50 pF and the preferred value is 30 pF. The fuzzified mutual capacitance is shown in Fig. 8.6.

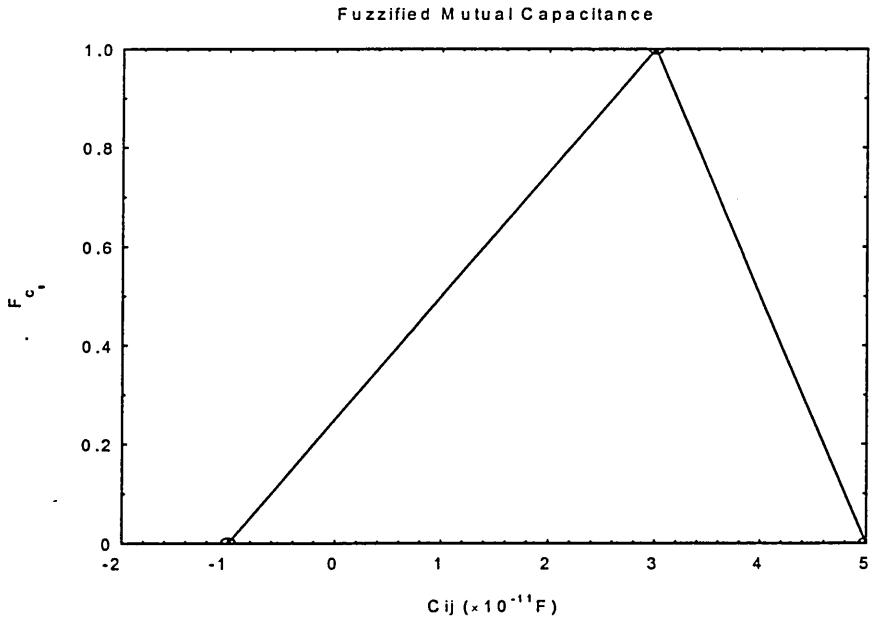

Figure 8.6 Fuzzified mutual capacitance.

The fuzzified crosstalk with respect to spacing is given in Fig. 8.7.

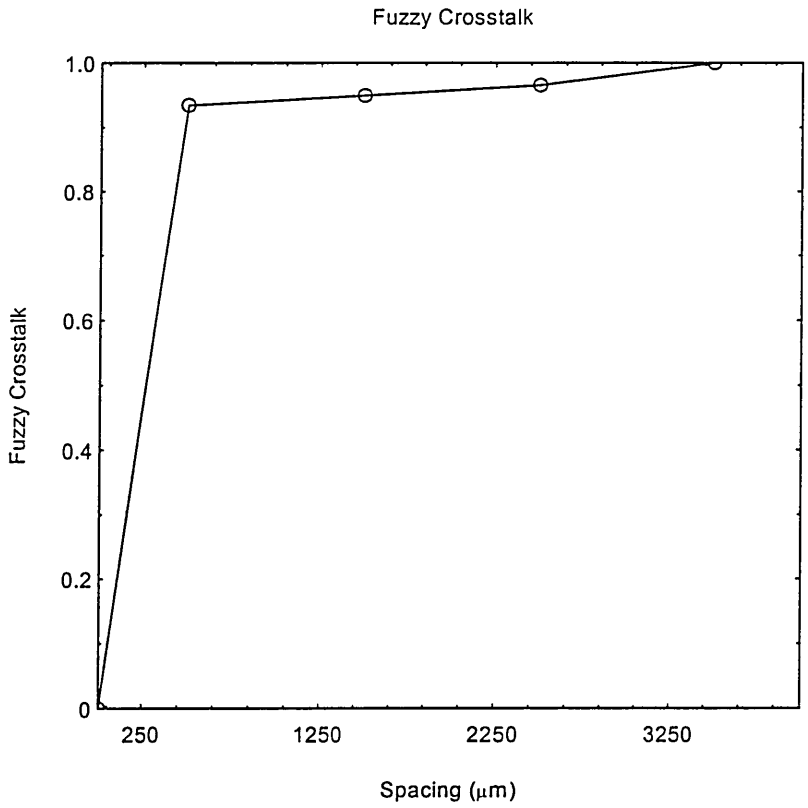

Figure 8.7 Fuzzified crosstalk vs. spacing.

As shown (see Fig. 8.8), the first phase is concluded with the intersection between fuzzified spacing and fuzzified crosstalk. The method of determining the fuzzified interval for spacing is explained in the following phase.

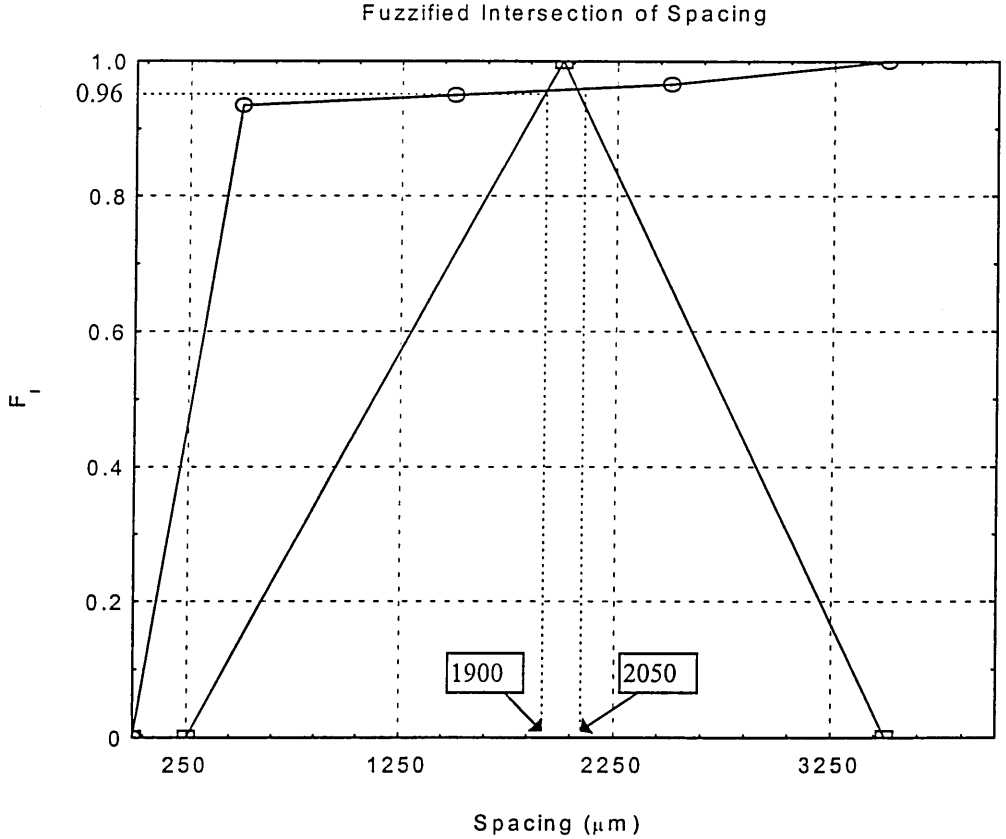

Figure 8.8 Intersection of preferred spacing and fuzzified crosstalk.

Phase 2

In this phase, algorithms I and II (see Sect. 7.4) are applied to produce induced mutual capacitance and its intersection with preferred mutual capacitance. Firstly, α- cuts of the intersection (see Fig. 8.8) are determined and listed in the Table 8.7.

α – cuts	0.2	0.4	0.6	0.8	0.96
Spacing Intervals (μm)	[600,3200]	[950,2900]	[1300,2600]	[1600,2300]	[1900,2050]

Table 8.7 α- cuts of intersection of preferred spacing and fuzzified crosstalk.

Values of induced mutual capacitance are calculated (see Table 8.8) using the above α – cuts values and the corresponding fuzzy graph is shown in Fig. 8.9.

α – cuts	0.2	0.4	0.6	0.8	0.96
C_{ii} (min) $\times 10^{-11}$F	-0.0547284	-0.00390926	0.0590036	0.137952	0.219937
C_{ii} (max) $\times 10^{-11}$F	1.43816	0.928958	0.611267	0.420749	0.278114

Table 8.8 Induced mutual capacitance values.

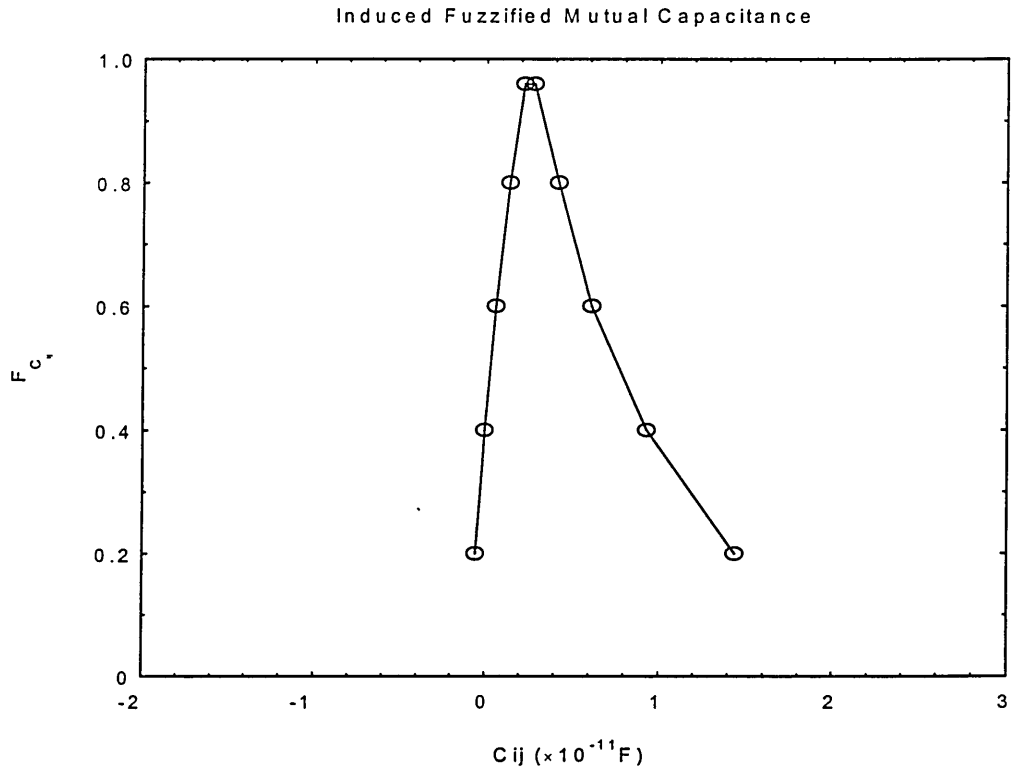

Figure 8.9 Induced mutual capacitance.

Next, algorithm II is applied by considering the intersection of preferred and induced mutual capacitance. This can be graphically described in Fig. 8.10. The supremum C_{ij}^* and its fuzzy membership values f^* are also shown in Fig. 8.10.

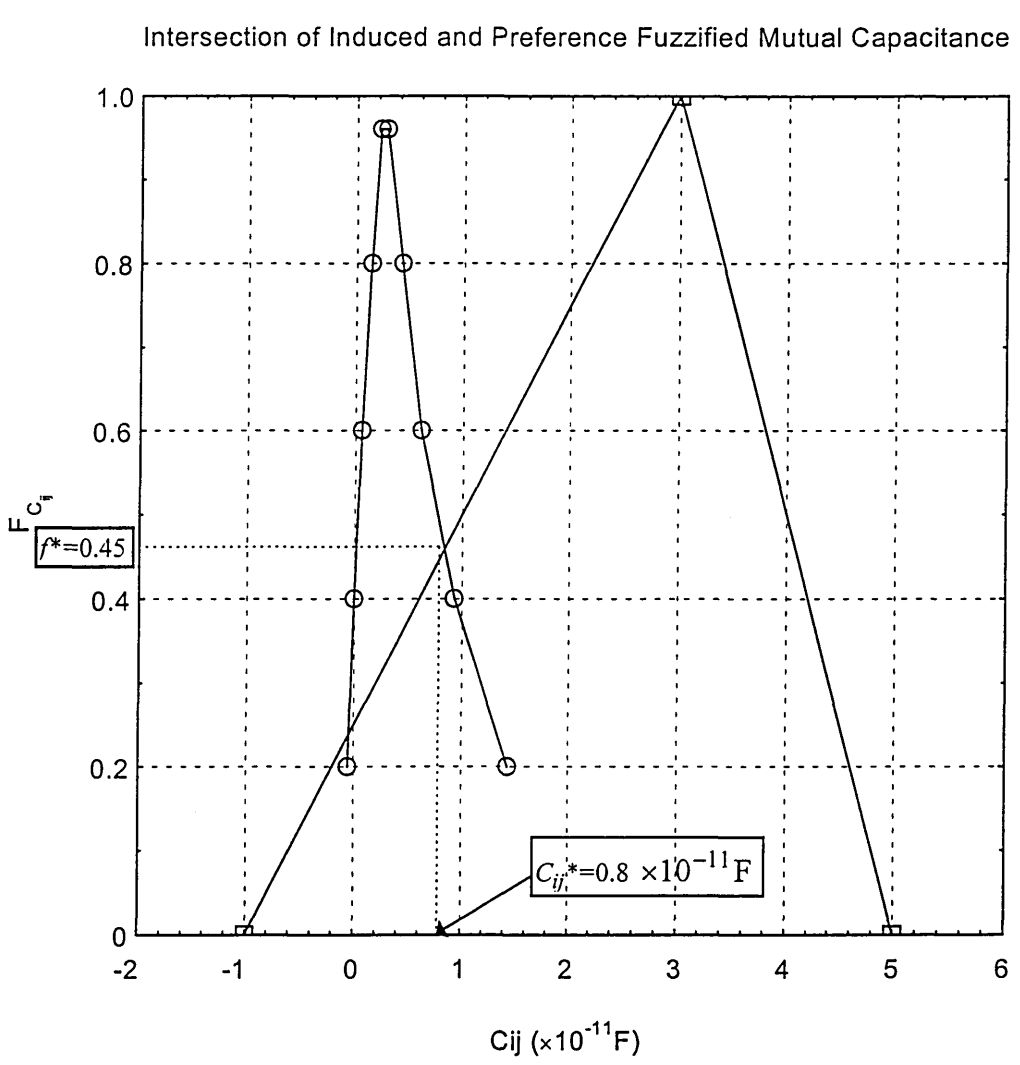

Figure 8.10 Intersection of preferred and induced C_{ij}.

Phase 3

In this phase, the defuzzification is a process to determine the best possible spacing in order to accommodate all geometrical/electrical and crosstalk constraints as defined in Phase 1.

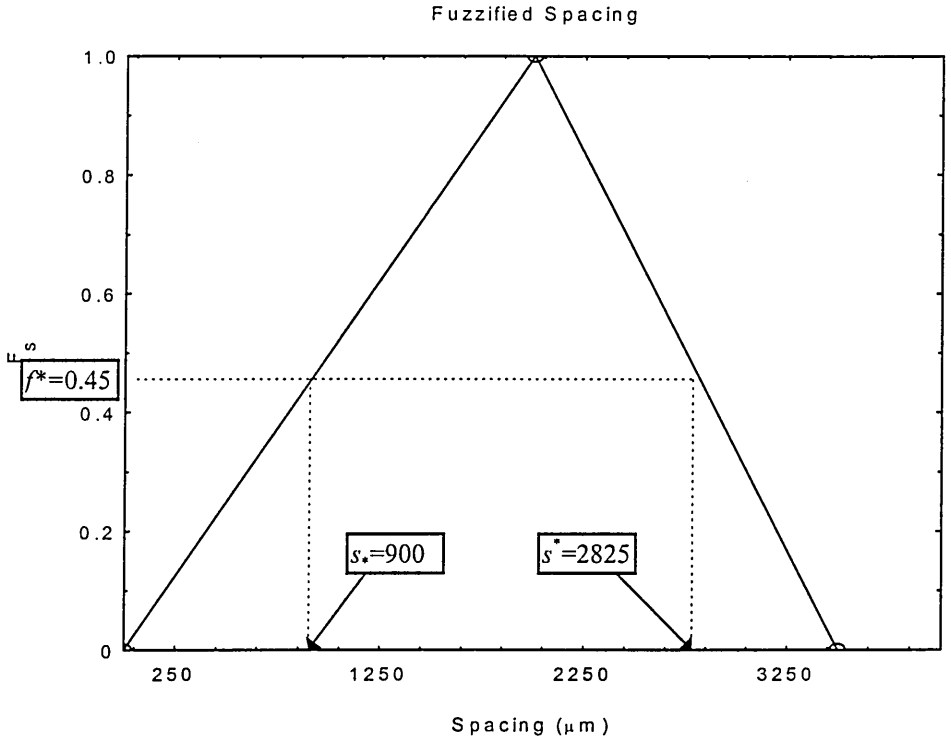

Figure 8.11 Determination of the spacing values.

First, the fuzzy value $f^* = 0.45$ is plotted in Fig. 8.11 in order to determine minimum and maximum values for spacing, s_* and s^*, respectively. Using the equation (see eqn. 3.18), their corresponding mutual capacitances are calculated as:

(s_*, C_{ij}^*)	(s^*, C_{ij}^*)
(900 μm, 0.986604 $\times 10^{-11}$F)	(2825 μm, 0.0105529 $\times 10^{-11}$F)

Table 8.9 Spacings with their respective mutual capacitance values.

The best possible spacing can be determined by applying Theorem 1 in Sect. 7.5.1 to Fig. 8.10. Therefore C_{ij} = max [9.86604 pF, 0.105529 pF] = 9.86604 pF, which corresponds to $s_* = 900$ μm.

A set of 3-coupled microstrip lines with geometrical configurations given in Fig. 5.6 ($\varepsilon_r = 4.7$, t = 35 μm, w = 500 μm, h = 1600 μm and s = 500 μm) is simulated and measured experimentally for crosstalk. Another set of 3-coupled microstrip lines with the same geometrical configurations as above except the spacing is simulated for crosstalk. The optimisation value for spacing (s_* = 900 μm) obtained from the fuzzy model is used for the latter simulation. Time delay and characteristic impedances for the two simulations are calculated using the developed algorithm in Section 4.5 (see Appendix B1 and B2). These lines have been simulated using coupled TEM model implemented on SPICE package (see Sect. 5.4.2). A pulse train of 1 V amplitude is applied to line 1. All the other lines were terminated with 50Ω resistors. The crosstalk are measured at both ends of the lines. The results are presented in Figure 8.12.

Results from the first simulation for crosstalk are in close agreement with those from the experimental work, in particular at line 2 where the difference is just within 2 dB. This fact immediately demonstrates the high accuracy of the mathematical model developed in Section 4.5 to compute the parameters for crosstalk (time delay and characteristic impedance). However, the second simulation using the calculated value of spacing from fuzzy model has the lowest crosstalk compared to the other two.

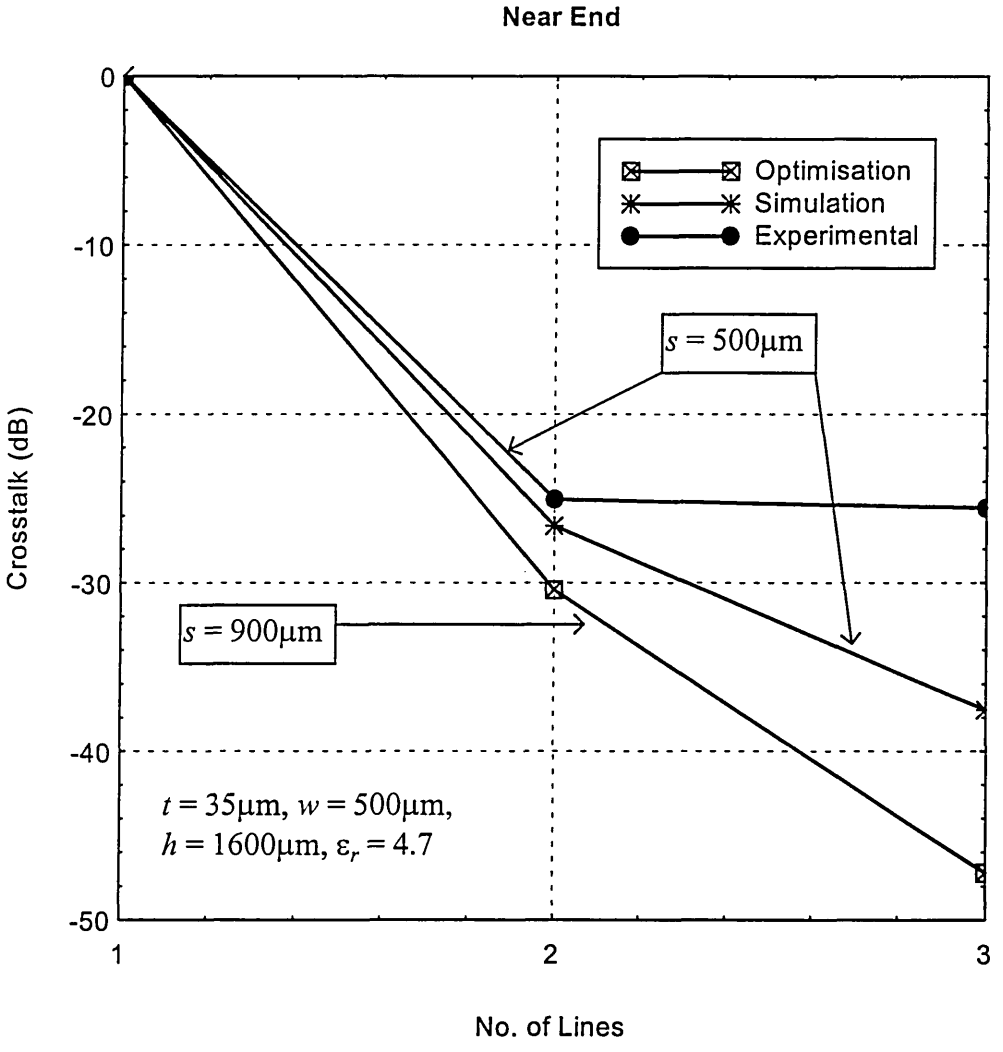
Near End
0
-10
-20
-30
-40
-50
Crosstalk (dB)
1
2
3
No. of Lines
Optimisation
Simulation
Experimental
s = 500μm
s = 900μm
t = 35μm, w = 500μm,
h = 1600μm, εr = 4.7

Fig. 8.12(a)

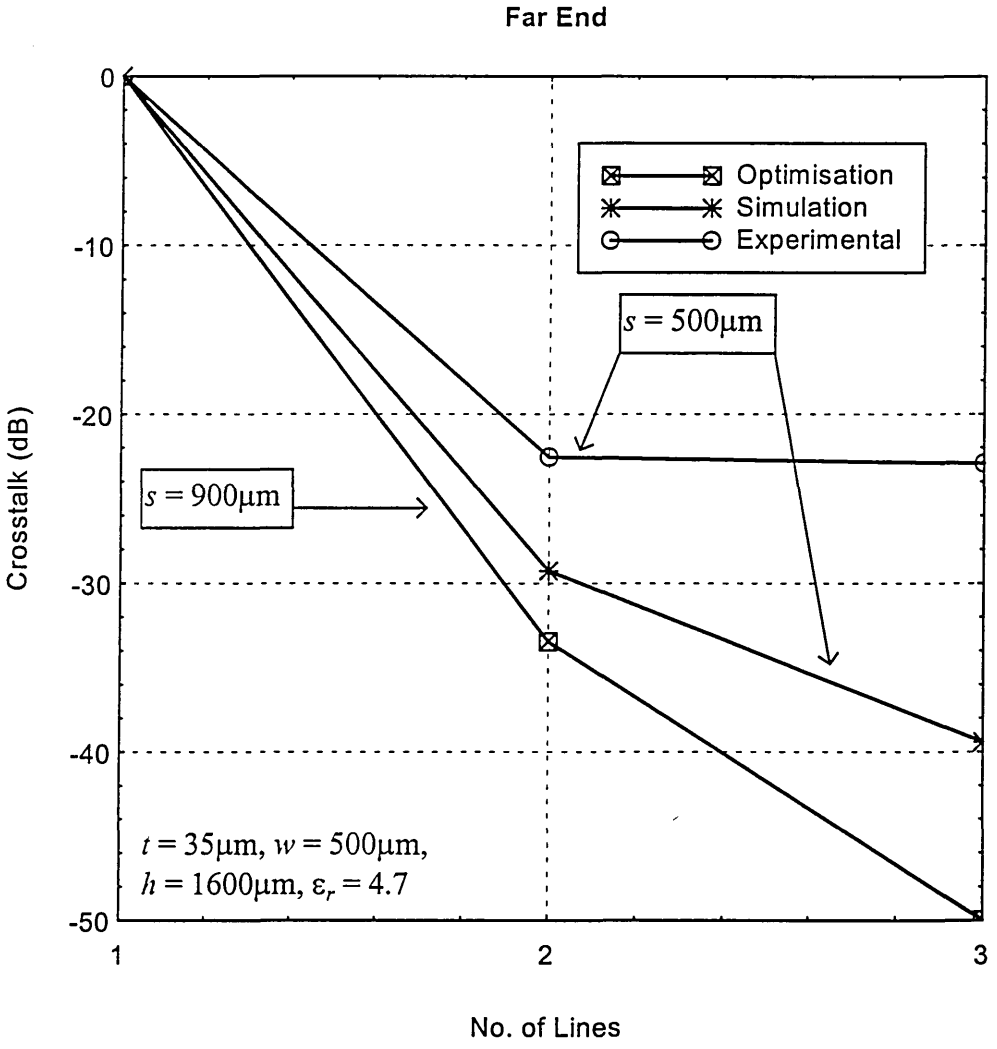

Fig. 8.12(b)

Figure 8.12 Crosstalk (a) near end (b) far end.

The above sample is purposely adopted to demonstrate the scope of application of fuzzy algorithms when only one geometrical parameter, s, and an electrical parameter, C_{ij}, of microstrip lines are varied.

8.4.1.1 Other samples

In addition to the above sample, other cases involving different spacings have been studied and simulated for optimisation. Seven samples with different

domains and preferred mutual capacitances as the initial constraint are listed in Table 8.10. These samples are subjected to the previous domain and preferred value of spacing.

Samples	Preference C_{ii} [min,pref,max] $\times 10^{-11}$F	Fuzzy Values f^*	$C_{ij}f^*$ $\times 10^{-11}$F	Spacing $[s_*, s^*]$ μm
1	[-1,2,4]	0.55	0.58	[1100,2630]
2	[-1,1.5,3]	0.63	0.5	[1260,2750]
3	[-1,0.15,1.5]	0.95	0.23	[1900,2075]
4	[-1,0.09,1.5]	0.92	0.2	[1840,2120]
5	[-1,0.06,1.5]	0.9	0.2	[1800,2150]
6	[-1,-0.07,1.5]	0.85	0.19	[1700,2225]
7	[-1,-0.9,1.5]	0.6	0.06	[1200,2600]

Table 8.10 Samples for optimisation.

The intersection of preferred and induced fuzzy mutual capacitances is obtained for each sample (see Fig. 8.13).

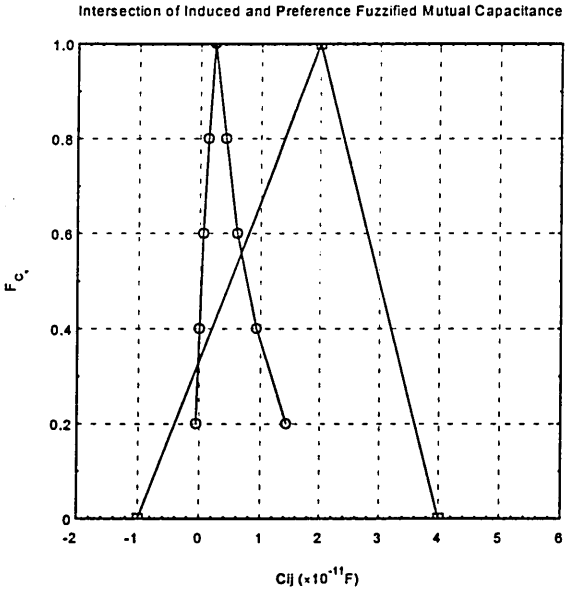

Fig. 8.13(a)

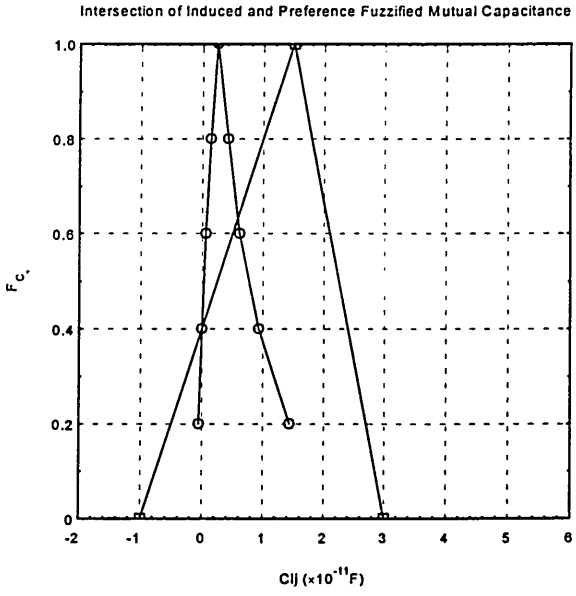

Fig. 8.13(b)

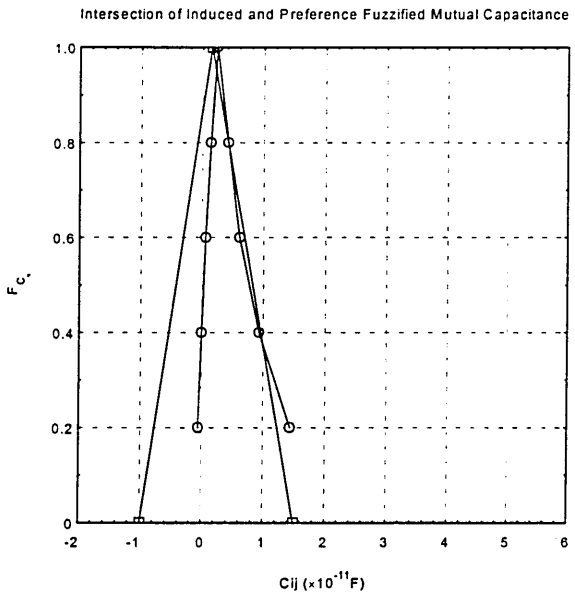

Fig. 8.13(c)

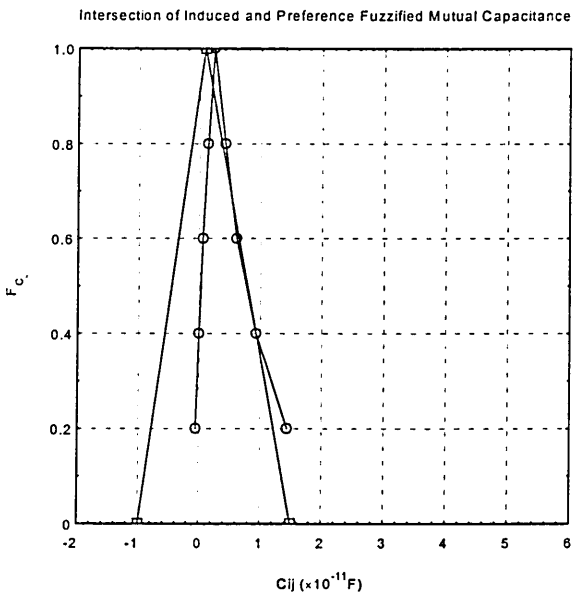

Fig. 8.13(d)

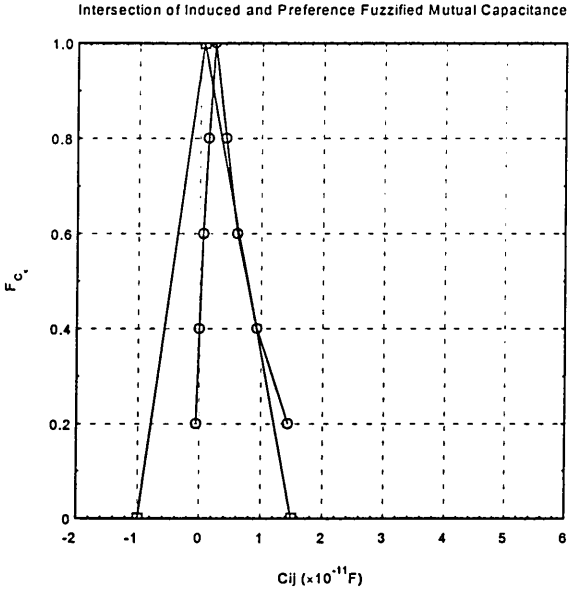

Fig. 8.13(e)

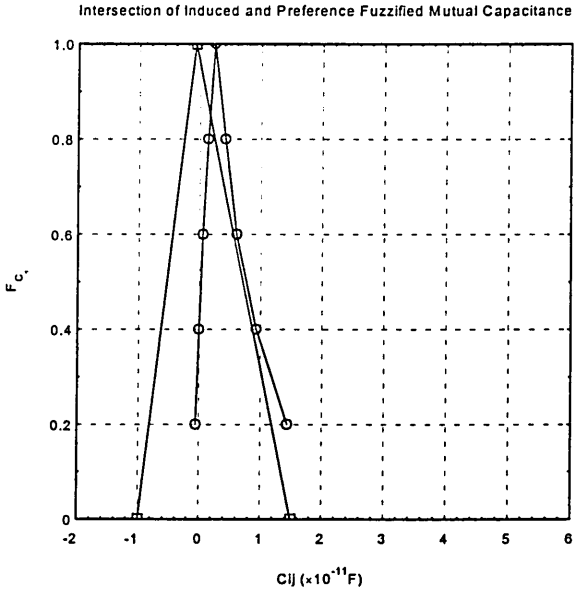

Fig. 8.13(f)

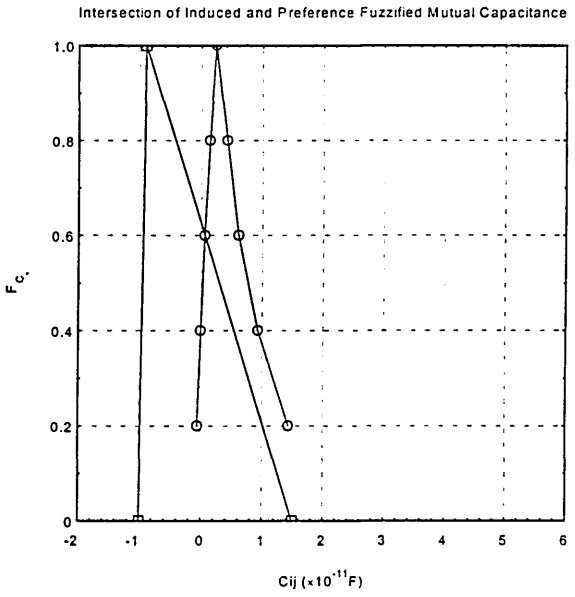

Fig. 8.13(g)

Figure 8.13 Intersection of preferred and induced C_{ij} for sample (a) 1 (b) 2 (c) 3 (d) 4 (e) 5 (f) 6 (g) 7.

In samples 1 and 2 (Fig. 8.13.a-b), the fuzzy preference intersect the maximum side of the induced mutual capacitances. The calculated value of spacing came from the maximum values of mutual capacitances. On the other hand, for samples 3 to 7 (Fig. 8.13.c-g), the fuzzy preference intersect the minimum side of the induced mutual capacitances. Therefore the calculated spacing came from the minimum values of mutual capacitances. Results for each sample are listed in Table 8.11.

Sample	Mutual Capacitances $[C_{ij*}, C_{ij}^{*}]\times10^{-11}$F	Calculated C_{ij} $\times10^{-11}$F	Calculated Spacing μm
1	[0.776612,0.052066]	0.776612	1100
2	[0.641452,0.025819]	0.641452	1260
3	[0.278114,0.210949]	0.210949	2075
4	[0.30361,0.195241]	0.195241	2120
5	[0.321383,0.185093]	0.185093	2150
6	[0.368754,0.1608]	0.1608	2225
7	[0.689287,0.0590036]	0.05900	2600

Table 8.11 Calculated values for each sample.

If all the parameters are varied, then design of microstrip lines will become more complicated and optimisation of constraint and minimisation of crosstalk simultaneously are essential and important.

8.5 Optimisation of Geometrical and Electrical Parameters and Minimisation of Crosstalk

The ultimate application of the fuzzy model is to optimise geometrical and electrical parameters and to minimise crosstalk of coupled microstrip lines at the same time. A set of input parameters with domains and suggested values are listed in Table 8.12.

Parameters	Domain	Suggested
C_{ii}(x 10^{-11})F	-1 - 5	3
Thickness, t (μm)	20 - 40	30
Width, w (μm)	300 - 600	400
Spacing, s (μm)	500 - 800	600

Table 8.12 Input parameters

These parameters are then fuzzified (Fig. 8.14) and calculated for their α - cuts (Table 8.13).

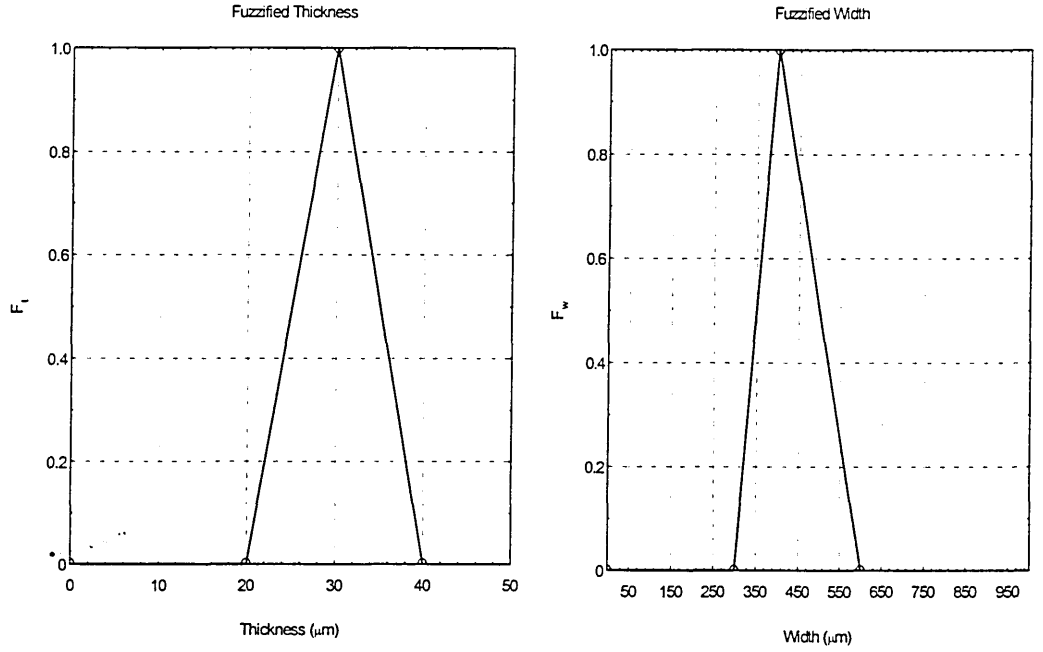

(a) (b)

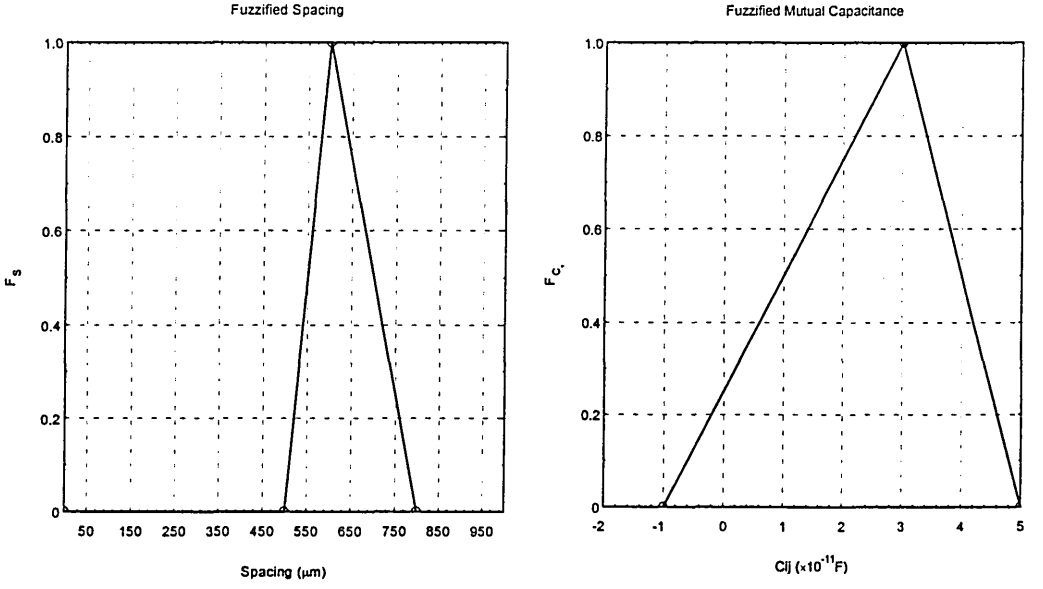

(c) (d)

Figure 8.14 Fuzzification on input parameters (a) thickness (b) width (c) spacing (d) C_{ij}.

The desired interval for spacing is determined from intersection of its suggested/preferred spacing with fuzzified crosstalk (Fig. 8.15).

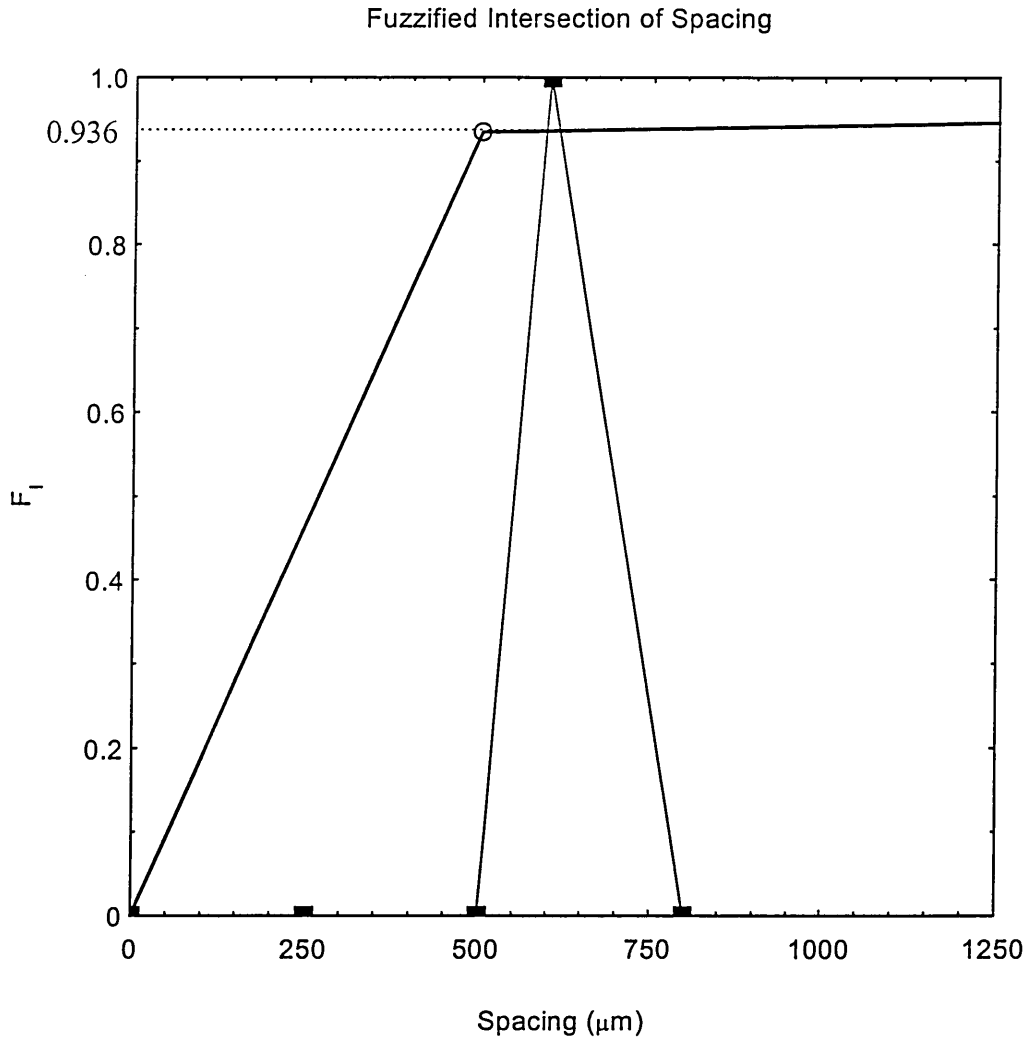

Figure 8.15 Intersection of fuzzified crosstalk and preferred spacing.

All the α - cuts can be determined for the remaining geometrical parameters using the result obtained from the intersection, see Fig.8.13.

	α - cuts values				
Input Parameters	**0.2**	**0.4**	**0.6**	**0.8**	**0.936**
Thickness (μm)	[22, 38]	[24, 36]	[26, 34]	[28, 32]	[29.36,30.64]
Width (μm)	[320,560]	[340,520]	[360,480]	[380,440]	[393.6,412.8]
Spacing (μm)	[520,760]	[540,720]	[560,680]	[580,640]	[612.7,612.7]

Table 8.13 α - cuts of input parameters.

Induced mutual capacitance are calculated using the above α – cuts values and the corresponding fuzzy graph is shown in Fig. 8.16.

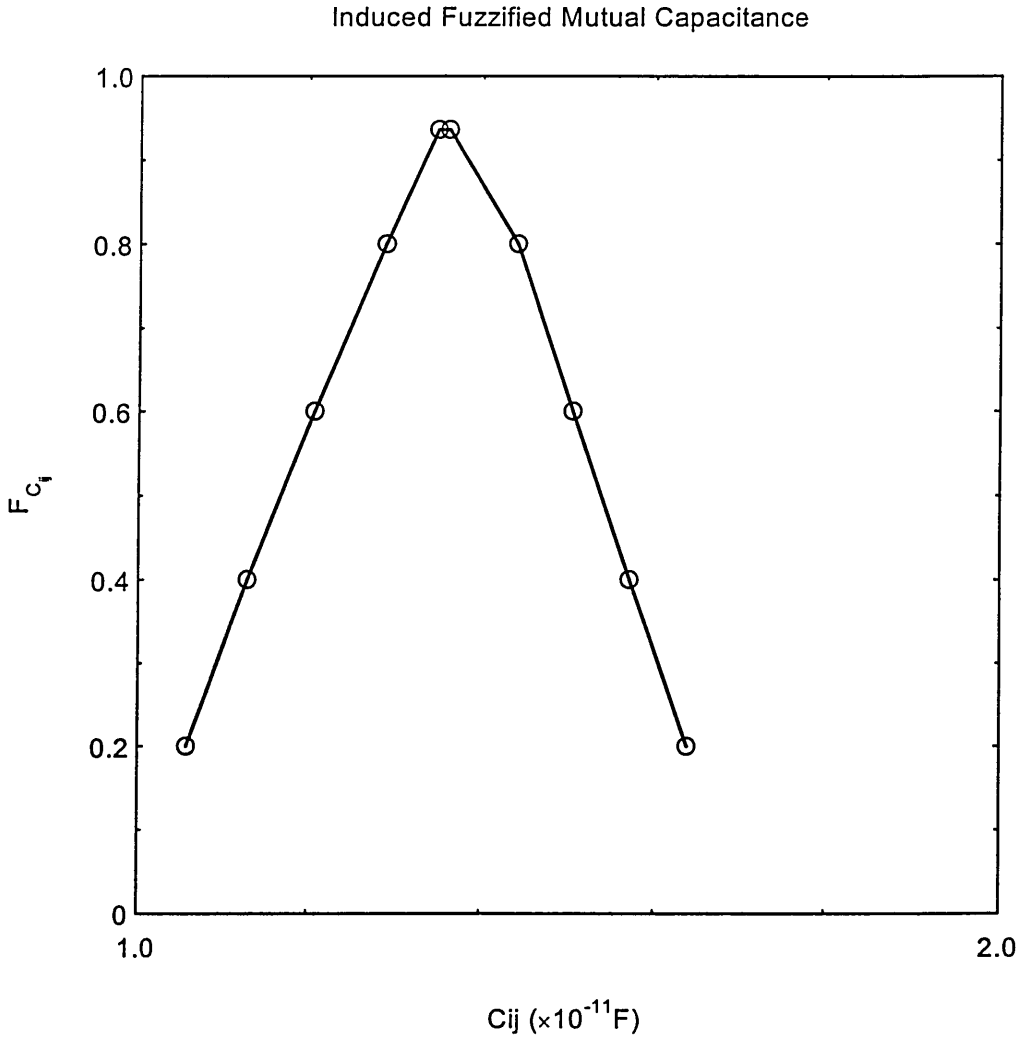

Figure 8.16 Induced mutual capacitance.

The intersection of suggested and induced mutual capacitance (see Fig. 8.17) is performed in order to determine the supremum and its fuzzy membership values. Corresponding fuzzy intervals for the optimised geometrical parameters are also obtained (Table 8.14).

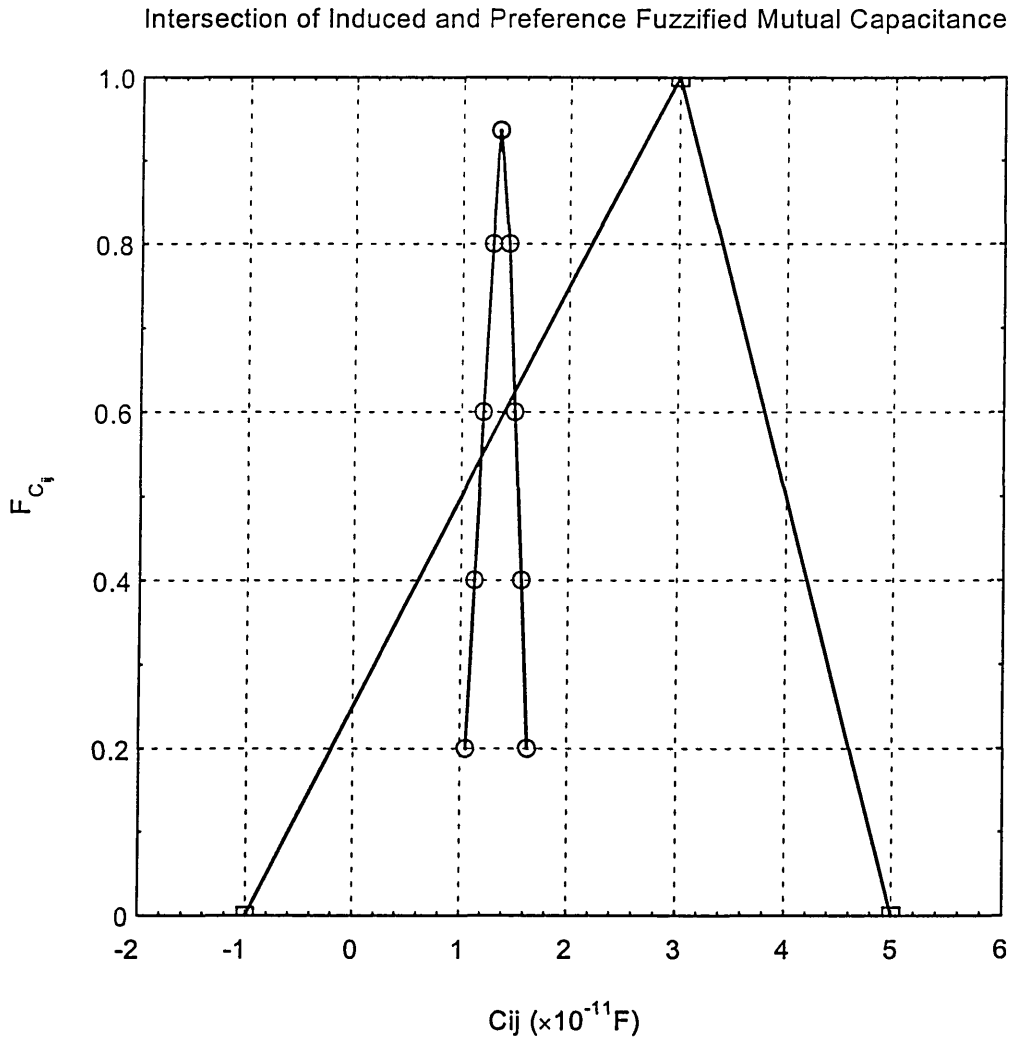

Figure 8.17 Intersection of induced and suggested C_{ij}.

Parameters	Fuzzy intervals (f^*=0.624433)
Cij(x 10^{-11})F	1.49773
Thickness, t (μm)	[26.2443,33.7557]
Width, w (μm)	[362.443,475.113]
Spacing, s (μm)	[562.443,675.113]

Table 8.14 Fuzzy intervals.

Using the equation (see eqn. 3.18), corresponding mutual capacitances are calculated (Appendix B) and the best possible geometrical parameters (optimised) are determined by Theorem 1 (see Table 8.15). The difference between the suggested and optimised parameters are also listed in Table 8.15.

Parameters	Suggested (s)	Optimised (p)	Difference |s-p|/s (%)
C_{ii}(x 10^{-11})F	3	1.49769	50
Thickness, t (μm)	30	33.7557	12.5
Width, w (μm)	400	475.113	18.7
Spacing, s (μm)	600	562.443	6.25

Table 8.15 Optimised parameters.

Once the process of optimisation-minimisation is finalised, the modification is introduced to initial input parameters; the design of coupled microstrip lines takes place. Simulation for crosstalk is then performed using coupled SPICE model presented in Chapter 5. The parameters for the simulation (time delay and characteristic impedance) are calculated using the algorithm developed in Chapter 4.

A set of 3 - coupled microstrip lines (Fig. 8.18) with optimised parameters is adopted as a sample for the simulation.

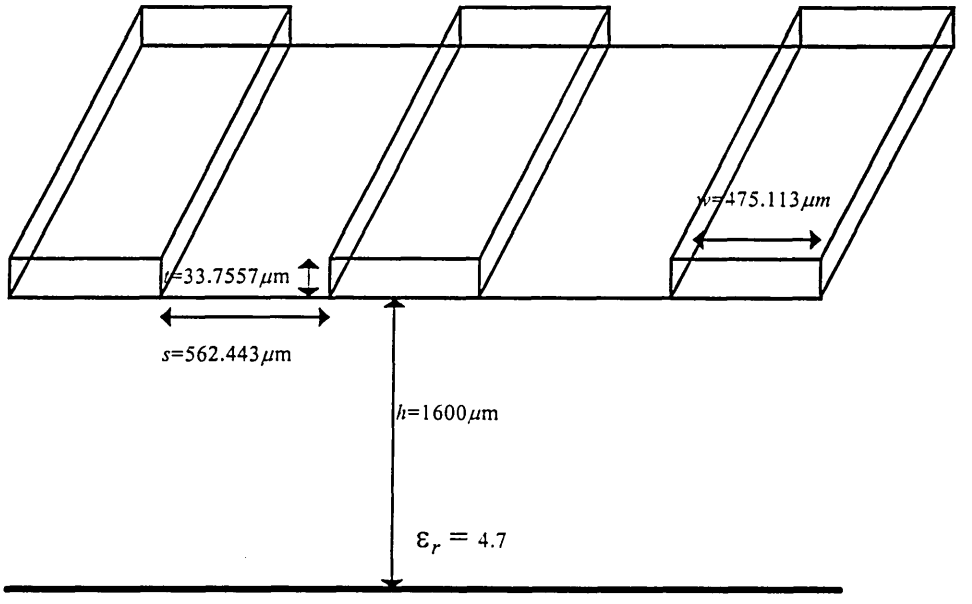

Figure 8.18 Optimised 3-coupled microstrip lines.

Three distinct simulations for crosstalk are performed for each suggested and optimised sets of parameters. A pulse train of 1 V amplitude, is first applied to line 1 and then to line 2 and finally line 3. With other lines terminated with 50Ω resistors the crosstalk for suggested and optimised sets are measured (see Appendix D) at both ends of the lines and presented in Figure 8.19. The near and far ends crosstalk of optimised and suggested sets are very close for all cases with the difference between 1 - 2 dB only. Furthermore, the optimised set has the advantage of compromising all the initial constraints; i.e. geometrical and electrical parameters.

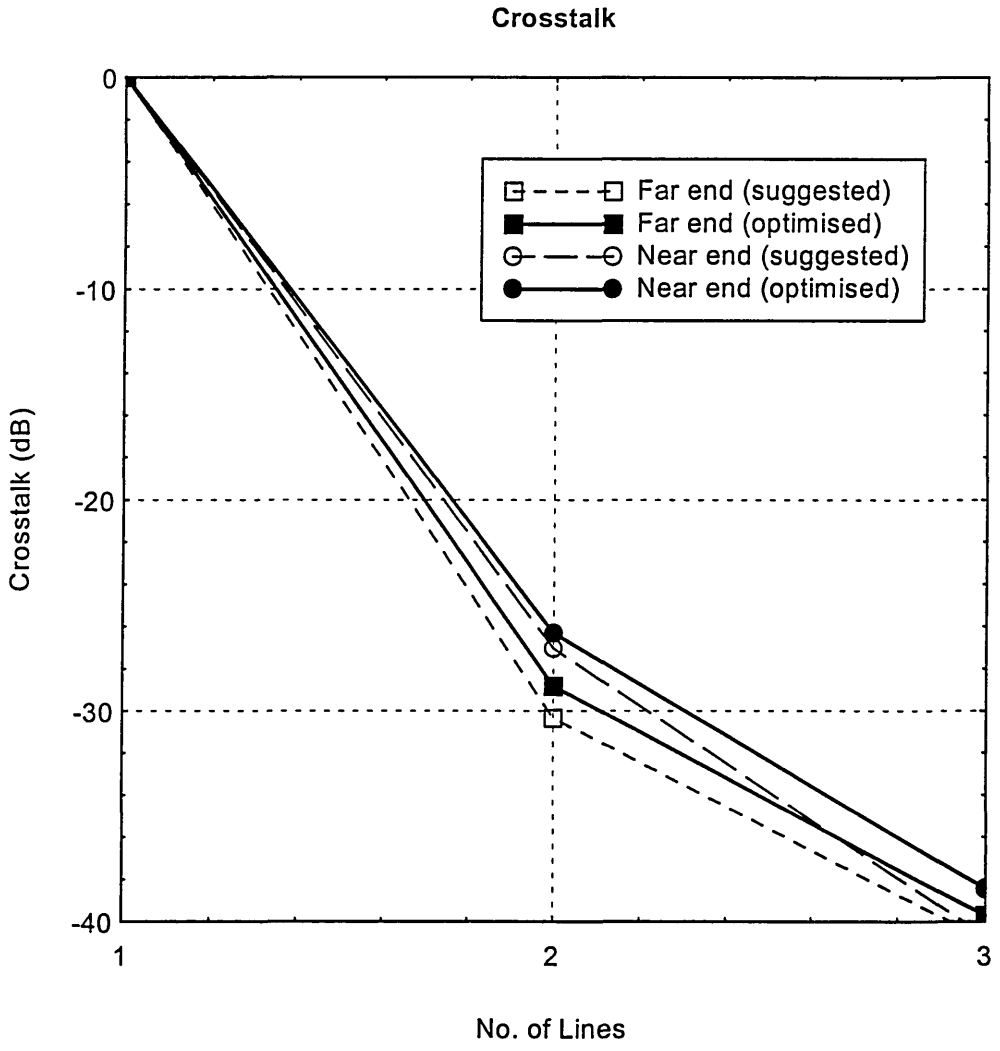
Crosstalk
0
-10
-20
-30
-40
Crosstalk (dB)
1
2
3
No. of Lines
Far end (suggested)
Far end (optimised)
Near end (suggested)
Near end (optimised)

Fig. 8.19(a)

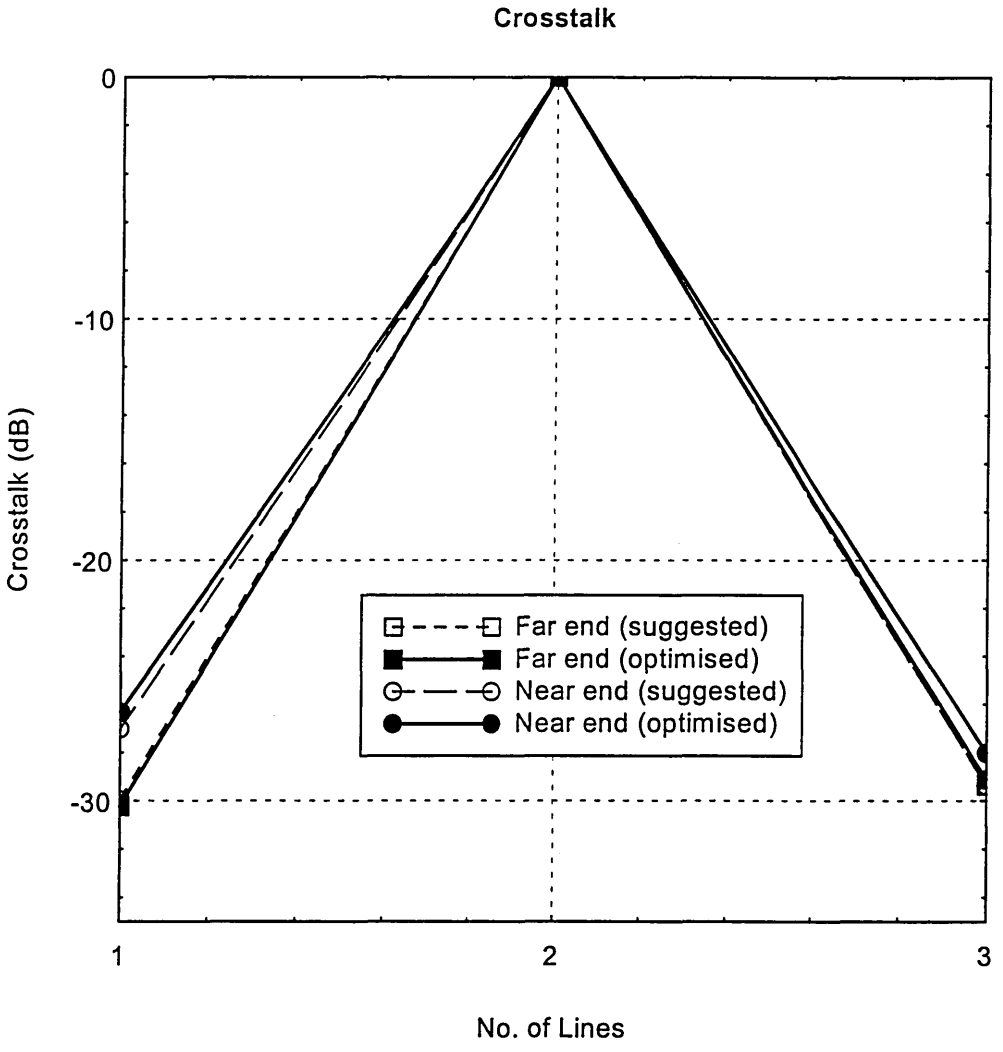
Crosstalk
0
-10
-20
-30
Crosstalk (dB)
1
2
3
No. of Lines
Far end (suggested)
Far end (optimised)
Near end (suggested)
Near end (optimised)

Fig. 8.19(b)

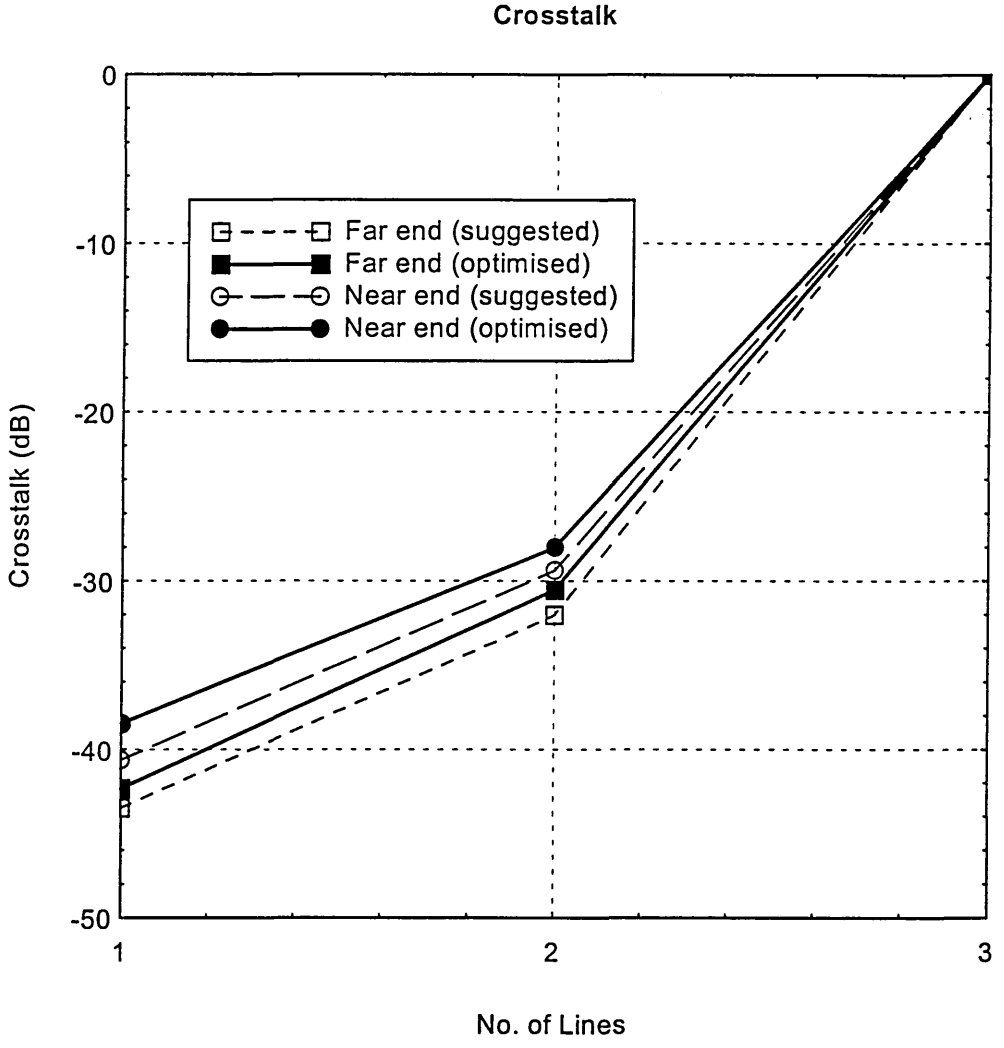

Fig. 8.19(c)

Figure 8.19 Crosstalk vs. line number for 3-coupled optimised and suggested sets with feeder (a) line 1 (b) line 2 (c) line 3.

Finally, if the simulation is satisfactory for a designer, the actual system can be fabricated on a printed circuit board. Otherwise, the process of optimisation-minimisation via fuzzy model can be repeated with other constraints until the designer is fully satisfied with his result.

9. CONCLUSIONS

9.1 Concluding Remarks

This work is concerned with two techniques for simulation of a set of n coupled microstrip lines both mathematical and fuzzy models. It begins with development of a new model for capacitance of nonuniformly spaced, coupled microstrip lines. Several new properties for eigenvalues and eigenvectors are deduced. An algorithm for computation of the time delay and characteristic impedance is also developed. Novel techniques to evaluate the capacitance of strictly nonuniform coupled microstrip lines are introduced. These methods are incorporated into an algorithm to calculate the time delay and characteristic impedance, which eventually becomes a generalised algorithm that can be applied to any coupled microstrip lines.

Output data from the algorithms have been used in the SPICE package to simulate for crosstalk. Experimental results on several sets of coupled microstrip lines for crosstalk prove to be in good agreement with the results obtained from the simulation results of Parker (1994). Furthermore, results obtained from the simulation of uniform and nonuniform coupled microstrip lines show that the spacing between the lines has a more significant effect on crosstalk than other geometrical parameters. Further investigations, using developed Mathematica programs, reveal the effect of geometrical parameters on the electrical parameters of microstrip lines which follows a recognisable pattern.

A novel fuzzy model for microstrip lines is presented. It has the capability as a tool of designing microstrip lines with a given set of parameters for a specific application. The model is also able to minimise crosstalk successfully by optimising the geometrical and electrical parameters of microstrip lines simultaneously.

A major advantage of the approach taken in this research is its flexibility. The model has the flexibility to consider different aspects of input influences such as improvement on performance parameters, design specifications, and technological feasibility for microstrip lines simultaneously.

9.2 Possible Further Works and Recommendations

The future work can be developed in several directions. Firstly, further advances in mathematical modelling may be introduced in order to directly 'estimate' the mutual capacitance of strictly nonuniform coupled microstrip lines. Capacitance and inductance matrices can be constructed from these values. Improvement on the evaluation of eigenvalues and eigenvectors of higher dimensional matrices need to follow concurrently.

Following the discussion in Chapter 5, future work should also examine the effect of microstrip length on crosstalk. The concept of fuzzified crosstalk can be extended to study the similar effects of width, thickness, height, length and dielectric constant.

The theoretical and simulation results obtained suggest that other problems such as skin effect and ringing can also be included in the fuzzy model as new fuzzified input parameters, see Fig. 7.1. Finally, this thesis concludes with an interesting observation as to the relationship between the *principle of incompatibility* (Zadeh 1973) and modelling of the microstrip lines, namely, that whenever the precision and significance concerning complex system behaviour become almost mutually exclusive characteristics, the models may still provide relevant options to the system designer. That is, the crisp mathematical model provides for precision, while the fuzzy model sets focus on minimisation and optimisation.

"Time is not crisp"
Lotfi A. Zadeh
Aachen, Germany
Sept. 9, 1997

REFERENCES

Akhtarzad S., Rowbotham T.R. and Jones P. B., "The Design of Coupled Microstrip Lines", IEEE Trans., MTT-23, No. 6, June **1975**, pp. 486-492.

Altrock C. V., "Industrial Automation and Process Control Applications", Proc. Embedded Systems Conferences, Santa Clara, U.S.A, **1994**, 1995 1nd 1996.

Bahl I. J. and Garg R., "Simple and Accurate Formulas for a Microstrip With Finite Strip Thickness", IEEE Proc., **1977**, Vol. 65, pp. 1611-1612.

Balaban P., "Calculation of the Capacitance Coefficients of Planar Conductors on a Dielectric Surface", IEEE Trans. on Circuit Theory, Vol. CT-20, No. 6, Nov. **1973**, pp. 725-731.

Barrett R.M., "Microwave Printed Circuits - A Historical Survey", IRE Trans. on Microwave Theory and Techn., VMTT-3, No. 2, **1955**, pp. 1-9.

Belahrach H., "Caracterisation Electrique des Interconnexions en Technologies hybrides Multicouches: Modelisation numerique (2D et 3D) et Simulation Temporelle", Thesis for Ph.D, L'Universite de Bordeaux I, France, **1990**.

Bender E.A., "An Introduction to Mathematical Modelling", John Wiley & Sons, **1978**, pp. 1-15, Chap. 1.

Benedek P., "Capacitances of a Planar Multiconductor Configuration on a Dielectric Substrate by a Mixed Order Finite-Element Method", IEEE Trans. on Circuits and Systems, Vol. CAS-23, No. 5, May **1976**, pp. 279-284.

Birkhoff G. and Bartee T. C., "Modern Applied Algebra", McGraw-Hill, New York, **1970**.

Black K. G. and Higgins T. J., "Rigorous Determination of The Parameters of Microstrip Transmission Lines", IRE Trans., MTT-3, **1953**, pp. 93-113.

Brown M. and Harris C., "Neurofuzzy Adaptive Modelling and Control", Prentice Hall, Hertfordshire, **1994**, pp. 361-406, Chap. 10.

Bryant T.G., and Weiss J.A., "Parameters of Microstrip Transmission Lines and of Coupled Pairs of Microstrip Lines", IEEE Trans. on Microwave Theory and Techn., Vol. MTT-16, No. 12, Dec. **1968**, pp. 1021-1027.

Carlin H.J., "A Simplified Circuit Model for Microstrip", IEEE Trans. on Microwave Theory and Techn., short papers, Sep. **1973**, pp. 589-591.

Catania V., Ficili G, Palazzo S. and Panno D., "Using Fuzzy Logic in ATM Source Traffic Control: Lessons and Perspectives", IEEE Comm. Mag., Nov. **1996**, Vol. 34, No. 11, pp. 70-81.

Chang F. Y., "Transient Simulation of Frequency-Dependent Nonuniform Coupled Lossy Transmission Lines", IEEE Trans. on Components, Packaging, and Manufacturing Tech.- Part B: Advanced Packaging, Vol. 17, No. 1, February **1994**, pp. 3-14.

Cheng K.K.M., and Everard J.K.A., "Accurate Formulas for Efficient Calculation of the Characteristic Impedance of Microstrip Lines", IEEE Trans. on Microwave Theory and Techn., Vol. 39, No. 9, Sep. **1991**, pp. 1658-1661.

Chilo J. and Arnaud T., "Coupling Effects in the Time Domain for an Interconnecting Bus in High-Speed GaAs Logic Circuits", IEEE Trans. on Electron Devices, Vol. ED-31, No. 3, March **1984**, pp. 347-352.

Chowdury S., Barkatullah J.S., Zhou D., Bai E.W. and Lonngren K.E., "A Transmission Line Simulator for High-Speed Interconnects", IEEE Trans. on Circuits and Sys.-II: Analog and Digital Signal Processing, Vol. 39, No. 4, April **1992**, pp. 201-211.

Coekin J. A., "High-Speed Pulse Techniques", Pergamon Press, Oxford, **1975**, pp. 203 - 205.

Cottrell P. E. and Buturla E. M., "VLSI Wiring Capacitance", IBM J Res Develop. **1985**, 29(3), pp. 277-288.

Curtins H. and Shah A. V., "Step Response of Lossless Nonuniform Transmission Lines with Power-Law Characteristic Impedance Function", IEEE Trans., MTT-13, No. 11, November **1985**, pp. 1210-1212.

Darney I., "Circuit Modelling for Electromagnetic Compatibility", J. Elect. Comm. Eng., Aug. **1997**, Vol. 9, No. 4, pp. 184-192.

Davidovitz M., "Calculation of Multiconductor Microstrip Line Capacitances using the Semidiscrete Finite Element Method", IEEE Microwave and Guided Wave Letters, Vol. 1, No. 1, January **1991**, pp. 5-7.

Deutsch A., Kopcsay G. V., Ranieri V. A. et-al "High-speed Signal Propagation on Lossy Transmission Lines", IBM J. Res. Develop. Vol. 34, No. 4, July **1990**, pp. 601-615.

Dinh T.V., Cabon B. and Chilo J., "Modelling the Capacitance of Microstrip Line Using Spice", Elec. Letters, Vol. 28, No. 2, Jan. **1992**, pp. 194-196.

Djordjevic A. R. and Sarkar T. K., "Closed-Form Formulas for Frequency-Dependent Resistance and Inductance per Unit Length of

Microstrip and Strip Transmission Lines", IEEE Trans., MTT-13, Vol. 42, No. 2, February **1994**, pp. 241 - 248.

Donath W. E., "Placement and Average Interconnection Lengths of Computer Logic", IEEE Trans. on Circuits and Systems, Vol. CAS-26, No. 4, April **1979**, pp. 272-277.

Dorny C.N., "A Vector Space Approach to Models and Optimization", John Wiley & Sons, **1975**, pp. 1-32, Chap. 1.

Dugundji J., "Topology", Allyn and Bacon, Boston, **1966.**

Dydyk M., "Accurate Design of Microstrip Directional Couplers with Capacitive Compensation", IEEE MTT-S International Microwave Symposium, **1990**, Digest of Papers, pp. 581-584.

Edwards T., "Foundations for Microstrip Circuit Design" 2nd.edition, John Wiley & Sons, Chichester **1992**, pp. 1-221, Chap. 1-6.

Farrar A., "Characteristic Impedance of Microstrip by the Method of Moments", IEEE Trans. on Microwave Theory and Techn., January **1970**, pp. 65-66.

Gao D.S., Yang A. T. and Kang S.M., "Modelling and Simulation of Interconnection Delays and Crosstalks in High-Speed Integrated Circuits", IEEE Trans. on Circuits and Sys., **1990**, Vol. 37, No. 1, pp. 1-9.

Graham A., "Matrix Theory And Applications For Engineers And Mathematicians", John Wiley & Sons, Chichester, **1979.**

Griffith J. R. and Nakhla M. S., "Time-Domain Analysis of Lossy Coupled Transmission Lines", IEEE Trans. Microwave Theory and Techn., Vol. MTT-38, No. 10, Oct. **1990**, pp. 1480-1487.

Grossman S. I., "Calculus" 3rd ed., Int. ed., Academic Press Inc., Florida, **1984**, A17-A18, App.

Gunston M.A.R., and Weale J.R., "Variation of Microstrip Impedance with Strip Thickness", Elec. Letters, Vol. 5, No. 26, Dec. **1969**, pp. 697-698.

Gupta K.C., Garg R. and Bahl I.J., "Microstrip Lines and Slotlines", Artech House, Dedham, MA:USA, **1979**, pp. 1-154, Chap. 1-3; pp. 303-358, Chap. 8.

Hammerstad E.O., "Equations for Microstrip Circuit Design", Proc. Eoropean Microwave Conf., **1975**, pp. 268-272.

Harms P.H. and Mittra R., "Equivalent Circuits for Multiconductor Microstrip Bend Discontinuities", IEEE Trans. on Microwave Theory and Techn., Vol. 41, No. 1, Jan. **1993**, pp. 62-69.

Hill Y.M., Reckord N.O., and Winner D.R., "A General Method for Obtaining Impedance and Coupling Characteristics of Practical

Microstrip and Triplate Transmission Line Configurations", IBM J. Res. Develop., May **1969**, pp. 314-322.

(http1)http://www.cs.cmu.edu/Groups/AI/html/faqs/ai/fuzzy/part1/faq-doc-9.html.

(http2)http://www.neuronet.pitt.edu/~bogdan/research/fuzzy/fvsp/fvsp.html.

John S. and Arlett P., "Simple Method for The Calculation of the Characteristic Impedance of Microstrip", Elec. Letters, Vol. 10, No. 10, May **1974**, pp. 188-190.

Kajfez D. and Govind S., "Effects of Difference in Odd and Even Mode Wavelength on a Parallel-Coupled Bandpass Filter", Elec. Letters, 11, 5, 6 March **1975**, pp. 117 -118.

Kirschning M. and Jansen R. H., "Accurate Wide-Range Design Equations for the Frequency-Dependent Characteristic of Parallel Coupled Microstrip Lines", IEEE Trans., MTT-32, No. 1, January **1984**, pp. 83-89.

Klir G. J. and Folger T. A., "Fuzzy Sets, Uncertainty, and Information", Prentice Hall, Englewood Cliffs, New Jersey, **1988**, pp. 1-103, Chap. 1-3; pp. 231-290, Chap. 6.

Kosanovic B. R., "Signal And System Analysis In Fuzzy Information Space", Thesis for Ph.D, Univ. of Pittsburgh, USA, **1995**.

Kosanovic B. R., Chaparro L. F. and Sclabassi R. J., "Modeling of Quasi-Stationary Signals Using Temporal Fuzzy Sets and Time-Frequency Distributions", Proc. of the IEEE-SP International Sym. on TFTSA-**94**, pp. 425-428.

Kruse R., Gebhardt J. and Klawonn F., "Foundations of Fuzzy Systems", John Wiley & Sons, **1994**, pp. 1-77, Chap. 1-2.

Lange J., "Interdigitated Strip-Line Quadrature Hybrid", **1969** G-MTT Symposium, Digest of Papers, pp. 10 -13.

Linares y M R., Kontorovich V. Y and Jardon H., "Prediction of the Average Power of Crosstalk Effects in Multiconductor Transmission Lines", Micr. and Opt. Tech. Letters, Vol. 10, No. 1, Sep. **1995**, pp. 35-38.

Mao J. F. and Li Z. F., "Analysis of Time Response of Nonuniformly Coupled Multiconductor Transmission Lines with Frequency-Dependent Losses", Elec. Letters, Vol. 27, No. 21, 10th Oct. **1991**, pp. 1941-1943.

Okugawa S. and Hagiwara H., "Analysis and Computation of Crosstalk Noise Between Microstrip Transmission Lines", Electronics and Communications in Japan, No. 7, **1970**, pp. 128 - 138.

Orhanovic N., Tripathi V. K. and Wang P., "Time Domain Simulation of Uniform and Nonuniform Multiconductor Lossy Lines by The Method of Characteristics", IEEE MIT Int. Microwave Symp. Dig., May **1990**, pp. 1191 - 1194.

Palusinski O. A. and Lee A., "Analysis of Transient in Nonuniform and Uniform Multiconductor Transmission Lines", IEEE Trans. on Microwave Theory and Techn., Vol. 37, No. 1, January **1989**, pp. 127-138.

Parker B.H., "Simulation of Interconnections in High-Speed Integrated Circuits", Thesis for Ph.D, Sheffield Hallam University, UK, **1994**.

Parker B.H., Ray A.K. and Ghassemlooy Z., "Crosstalk in the Interconnection Bus for a High-Speed Digital Logic Circuit", Int. Journal Electronics, Vol. 76, No. 2, **1994**, pp. 265-269.

Paul C. R., "Introduction to Electromagnetic Compatibility", Wiley series in Microwave and Optical Engineering, John Wiley & Sons, New York, **1992**, pp. 491-661, Chap. 10.

Pothecary N. M. and Railton C. J., "Analysis of Crosstalk on High-Speed Digital Circuits Using The Finite Difference Time-Domain Method", Int. Journal of Numerical Modelling: Electronic Networks, Devices and Fields, Vol. 4, **1991**, pp. 225-240.

Protonotarios E. N. and Wang O., "Analysis and Intrinsic Properties of the General Nonuniform Transmission Line", IEEE Trans., MTT-15, No. 3, March **1967**, pp. 142-150.

Pucel R.A., Masse' D. J., and Hartwig C.P., "Losses in Microstrip", IEEE Trans. on Microwave Theory and Techn., Vol. MTT-16, June **1968**, pp. 342-350.

Qian Y. and Yamashita E., "Characterization of Picosecond Pulse Crosstalk Between Coupled Microstrip Lines with Arbitrary Conductor Width", IEEE Trans. on Microwave Theory and Techn., Vol. 41, No. 6/7, June/July **1993**, pp. 1011-1016.

Rade L. and Westergren B., "BETA Mathematics Handbook", Chartwell-Bratt, **1988**, pp. 80, Chap. 4.

Rizvi M. and Vetri J. L., "Modelling and Reduction of Crosstalk on Coupled Microstrip Line Structures and Multichip Modules: An FDTD Approach" International Journal of Microwave & Milimeterwave Computer-Aided Engineering, January **1996**, Vol. 6, Pt. 1, pp. 58-68.

Romeo F., and Santomauro M., "Time-Domain Simulation of n Coupled Transmission Lines", IEEE Trans. on Microwave Theory and Techn., Vol. MTT-35, No. 2, Feb. **1987**, pp. 131-136

Ruehli A.E., "Survey of Computer Aided Electrical Analysis of Integrated Circuit Interconnections", IBM. J. Res. Develop., **1979**, Vol. 23, pp. 626-639.

Schneider M.V., "Microstrip Lines for Microwave Intergrated Circuits", The Bell System Technical J., May-June **1969**, pp.1421-1443.

Schutt-Aine J.E. and Mittra R., "Nonlinear Transient Analysis of Coupled Transmission Lines", IEEE Trans. on Circuits and Sys., **1989**, Vol. 36, pp. 959-966.

Schutt-Aine J.E., "Transient Analysis of Nonuniform Transmission Lines", IEEE Trans. on Circuits and Sys.-I: Fundamental Theory and Appl., May **1992**, Vol. 39, No. 5, pp. 378-385.

Science and Technology, "The Middle Age of the Transistor", The Economist, Jan. 3 - 9th, **1998**, pp. 77 - 79.

Seki S. and Hasegawa H., "Analysis of Crosstalk in Very High-Speed LSI/VLSI's Using a Coupled Multiconductor MIS Microstrip Line Model", IEEE Transactions on Microwave Theory and Techn., Vol. MTT-32, No. 12, Dec. **1984**, pp. 1715-1720.

Silvester P. and Benedek P., "Equivalent Capacitances of Microstrip Open Circuits", IEEE Trans. on Microwave Theory and Techn., Vol. MTT-20, No. 8, Aug. **1972**, pp. 511-516.

Snelson J. K., "Propagation of Travelling Waves on Transmission Lines-Frequency Dependent Parameters", PICA Conference, Boston, Mass., May 24-26, **1971**, pp. 85-91.

Son J. H., Wang H. H. Whitaker J. F. and Mourou G. A., "Picosecond Pulse Propagation on Coplanar Striplines Fabricated on Lossy Semiconductor Substrates: Modelling and Experiments", IEEE Trans. on Microwave Theory and Techn., Vol. 41, No. 9, Sep. **1993**, pp. 1574-1579.

Stinehelfer H.E., "An Accurate Calculation of Uniform Microstrip Transmission Lines", IEEE Trans. on Microwave Theory and Techn., Vol. MTT-16, No. 7, July **1968**, pp. 439-444.

Terano T., Asai K., and Sugeno M., "Fuzzy Systems Theory and Its Applications", Academic Press, Inc., **1987**.

Van Deventer T. E. and Katehi L. P. B., "Analysis of Conductor Losses in High-Speed Interconnects", IEEE Trans., MTT-13, Vol. 42, No. 1, January **1994**, pp. 78-83.

Wadell B.C., "Transmission Line Design Handbook", Artech House, **1991**, pp. 431-451, Chap. 9.

Wang P., "Soft Modelling for Intelligent and Complex System", Proc. 5th European Congress on Intelligent Techniques and Soft

Computing, Aachen, Germany, Vol. 2/3, Sep. 8 - 11, **1997**, pp. 891-898.

Weeks W.T., "Calculation of Coefficients of Capacitance of Multiconductor Transmission Lines in the Presence of a Dielectric Interface", IEEE Trans. on Microwave Theory and Techn., Vol. MTT-18, No. 1, Jan. **1970**, pp. 35-43.

Wheeler H. A., "Transmission-line Properties of a Strip on a Dielectric Sheet on a Plane", IEEE Trans. Microwave Theory Techn., Vol. MTT-25, Apr. **1977**, pp. 631-647.

Wheeler H.A., "Transmission-line properties of parallel strips separated by a dielectric sheet", IEEE Trans. Microwave Theory and Techn., Vol. MTT-13, March **1965**, pp.172-185.

Wolfram S., "Mathematica a System for doing Mathematics by Computer", Addison Wesley, **1991.**

Yager R. R., "A Characterization of The Extension Principle", Fuzzy sets and Sys., Vol. 18, **1986**, pp. 205-217.

Yager R., "Implementing Fuzzy Logic Controllers Using Neural Network Framework", Fuzzy Sets and Sys. Vol. 48, **1992**, pp. 53-64.

Yager R.R., and Filev D.P., "Essentials of Fuzzy Modeling and Control", John Wiley and Sons, Inc., **1994**, pp. 1-261, Chap. 1-6.

Yamashita E., "Variational Method for the Analysis of Microstrip-Like Transmission Lines", IEEE Trans. on Microwave Theory and Techn., Vol. MTT-16, No.18, Aug. **1968**, pp. 529-535.

Yamashita E., and Mittra R., "Variational Method for the Analysis of Microstrip Lines", IEEE Trans. Microwave Theory and Techn., Vol. MTT-16, April **1968**, pp. 251-256.

Yuan H.T., Lin Y.T., and Chiang S.Y., "Properties of Interconnection on Silicon, Sapphire, and Semi-Insulating Gallium Arsenide Substrates", IEEE Trans. on Electron Devices, Vol. ED-29, No. 4, April **1982**, pp. 639-644.

Zadeh L. A., "Outline of a New Approach to the Analysis of Complex Systems and Decision Processes", IEEE Trans. on Systems, Man and Cybernetics, 3(1), **1973**, pp. 28-44.

Zadeh L. A., "The Concept of a Linguistic Variable and Its Application to Approximate Reasoning", Information Sciences, Vol 8, **1975**, pp. 199-249.

Zadeh L.A., "Fuzzy Sets", Information and Control, Vol. 8, No. 3, **1965**, pp. 338-353.

Zadeh L.A., "Outline of A New Approach to the Analysis of Complex Systems and Decision Processes", IEEE Trans. Systems, Man., and Cybernetics, SMC-3, **1973**, pp. 28-44.

Zhang Q.J., Lum S. and Nakhla M.S., "Minimization of Delay and Crosstalk in High-Speed VLSI Interconnects", IEEE Trans. on Microwave Theory and Techn., Vol. 40, No. 7, July **1992**, pp. 1555-1563.

Zimmermann H. J., "Fuzzy Set Theory and its Applications", Kluwer Academic Publishers, 2nd rev. edition, **1991**.

Zounon A., Crozat P. and Adde R., "Time Domain CAD and Measurements of Lossy Coupled Lines", Elec. Letters, Vol. 26, No. 7, 29th March **1990**, pp. 473-474.

APPENDIX A

List of Mathematica programs:

A1. Reprogra

Modified program to calculate capacitance and inductance matrices.

A2. Travail

Display the graphs of the electrical parameters.

A3. Met 1&2-c

Calculate the capacitance matrix for nonuniformly coupled microstrip lines using the bound capacitance methods.

A4. Matr2ok

Calculate the new capacitance and inductance matrices for nonuniformly spaced coupled microstrip lines.

A5. Matrdiff

Calculate the new capacitance and inductance matrices for strictly nonuniformly coupled microstrip lines.

```
Off[General::spell]
Off[General::spell1]
Off[Set::setraw]
Off[SetDelayed::write]


BeginPackage["Impedance`"]


Zom::usage = "Zom[Er,t,w,h]
      w is width of line
      h is height of line above ground plane
      t is thickness of line
      er is relative dielectric constant of substrate
      Calculate the impedance of a single microstrip line
      with the above parameters."


Z0::usage = "Z0[Er,t,w,h,s]
      w is width of line
      h is height of line above ground plane
      t is thickness of line
      s is the separation between the lines
      er is relative dielectric constant of substrate
      Calculate the impedance of a pair of microstrip lines
      with the above parameters."


Cm::usage = "Cm[Er,t,w,h,s]
      w is width of line
      h is height of line above ground plane
      t is thickness of line
      s is the separation between the lines
      er is relative dielectric constant of substrate
      Calculates the mutual capacitance of a pair of microstrip lines
      with the above parameters."


Tline::usage = "Tline[Er,t,w,h,s,totln]
      w is width of the lines
      h is height of the lines above the ground plane
      t is thickness of the lines
      s is the separation between adjacent lines
      er is relative dielectric constant of substrate
      totln is the total number of lines
      s, w, and t are the same for all lines
      Calculates the time delay and impedance of a set of
      linen microstrip lines with the above parameters and also
      returns the transformation network control parameters."


Carray::usage = "Carray[Er,t,w,h,s,totln]
      w is width of the lines
```

```
      t is thickness of the lines
      s is the separation between adjacent lines
      er is relative dielectric constant of substrate
      totln is the total number of lines
      s, w, and t are the same for all lines"


Begin["`Private`"]


E0 = 8.854188*10^-12
mu0 = 12.566371*10^-7


MakeRuleConditional[var_, rhs_, condition_] :=
    (var := rhs /; condition)      (* Assigns var = rhs if condition is
true *)


CalcC[er_, t_, w_, h_] :=
    Module[ {c},
        c = (er - 1)*t / 4.6 / Sqrt[w/h] / h;
    c
    ]    (* Correction factor for the effective dielectric *)


We[t_, w_, h_] :=
    Module[ {we},
        MakeRuleConditional[we,
            w+1.25/N[Pi]*t*(1+Log[4*N[Pi]*w/t]),
            w/h <= 1/(2*N[Pi])];
        MakeRuleConditional[we,
            w+1.25/N[Pi]*t*(1+Log[2*h/t]),
            w/h > 1/(2*N[Pi])];
    we
    ]    (* Calculates the effective width of a microstrip line *)


CalcF[w_, h_] :=
    Module[ {conf},
        MakeRuleConditional[conf,
            1/Sqrt[1+12h/w],
            w/h <= 1];
        MakeRuleConditional[conf,
            1/Sqrt[1+12h/w]+0.04(1-w/h)^2,
            w/h > 1];
    conf
    ]    (* Another correction term for the effective dielectric *)


Ere[Er_, t_, w_, h_] :=
    Module[ {ere, c, conf},
        conf = CalcF[w,h];
        c = CalcC[Er,t,w,h];
        ere = (Er+1)/2+conf*(w/h)*(Er-1)/2-c;
    ere
    ]    (* Calculates the effective dielectric constant of the
```

```
Zom[Er_, t_, w_, h_] :=
    Module[ {zom, we, ere},
        we = We[t,w,h];
        ere = Ere[Er,t,w,h];
        MakeRuleConditional[zom,
            60/Sqrt[ere]*Log[8*h/we+0.25*we/h],
            w/h <= 1];
        MakeRuleConditional[zom,

120*N[Pi]/(Sqrt[ere]*(we/h+1.393+0.667*Log[we/h+1.444])),
            w/h > 1];
    N[zom]
    ]   (* Calculates the impedance of a single microstrip lines with
the given parameters *)


Cp[Er_, w_, h_] :=
    Module[ {cp},
        cp = E0*Er*w/h;
    cp
    ]   (* Line to ground plane capacitance *)


Cf[Er_, t_, w_, h_] :=
    Module[ {cf, cp, zom, clight, ere},
        ere = Ere[Er, t, w, h];
        clight = 299792458;
        cp = Cp[Er, w, h];
        zom = Zom[Er, t, w, h];
        cf = (Sqrt[ere]/clight/zom - cp)/2;
    cf
    ]   (* Fringe capacitance for the outside of the lines *)


CalcA[w_, h_] :=
    Module[ {A},
        A = Exp[-0.1*Exp[2.33-2.53*w/h]];
    A
    ]


Cfpri[Er_, t_, w_, h_, s_] :=
    Module[ {cfpri, ere, cf, A},
        ere = Ere[Er, t ,w, h];
        cf = Cf[Er, t, w, h];
        A = CalcA[w, h];
        cfpri = cf*Sqrt[Er/ere]/(1+A*h/s*Tanh[10*s/h]);
    cfpri
    ]   (* Fringe capacitance between the lines *)


Cgd[Er_, t_, w_, h_, s_] :=
    Module[ {cgd, cf},
        cf = Cf[Er, t, w, h];
        cgd = E0*Er*Log[Coth[N[Pi]*s/4/h]]/N[Pi]
```

```
    cgd
    ]    (* Gap capacitance through the dielectric interface *)


Cga[w_, h_, s_] :=
    Module[ {k, kpri, cga},
        k = (s/h)/(s/h + 2*w/h);
        kpri = Sqrt[1-k*k];
        cga = E0*EllipticK[kpri]/EllipticK[k]/2;
    cga
    ]    (* Gap capacitance through the air interface *)


Cgt[t_, s_] :=
    Module[ {cgt},
        cgt = 2*E0*t/s;
    cgt
    ]    (* Capacitance due to the thickness of the line *)


Cm[Er_, t_, w_, h_, s_] :=
    Module[ {cgd, cga, cgt, cfpri, cm},
        cgd = Cgd[Er, t, w, h, s];
        cga = Cga[w, h, s];
        cgt = Cgt[t, s];
        cfpri = Cfpri[Er, t, w, h, s];
        cm = N[(cgd + cga + cgt - cfpri)/2];
    cm
    ](* Calculates the mutual capacitance beween two lines *)


Ci0[Er_, t_, w_, h_] :=
    Module[ {ci0, cp, cf},
        cf = Cf[Er, t, w, h];
        cp = Cp[Er, w, h];
        ci0 = cp + 2*cf;
    ci0
    ](* Calculates the total capacitance of a single line *)


Carray[Er_, t_, w_, h_, s_, totln_] :=
    Module[ {ctemp, ctemp2, diff, seff, carray, i, j},
        Do[
            ctemp = 0;
            Do[If [!(i === j),
                {diff = Abs[N[i-j]];
                seff = diff * (s + w) - w;
                ctemp2 = Cm[Er, t, w, h, seff];
                carray[i,j] = N[- ctemp2];
                ctemp = N[ctemp + ctemp2]}
              ],
            {j, 1, totln}
            ];
            carray[i,i] = N[Ci0[Er, t, w, h] + ctemp],
        {i, 1, totln}
        ];
    Array[carray, {totln, totln}]
```

```
        for the given dielectric and line dimensions *)


Carray[Er_, t_, w_, h_, s_List, totln_] :=
    Module[ {ctemp, ctemp2, seff, carray, i, j, k},
        Do[
            ctemp = 0;
            Do[If [!(i === j),
                {seff = -w;
                Do [seff = seff + s[[k]] + w, {k, j, i-1}];
                Do [seff = seff + s[[k]] + w, {k, i, j-1}];
                ctemp2 = Cm[Er, t, w, h, seff];
                carray[i,j] = N[- ctemp2];
                ctemp = N[ctemp + ctemp2]}
              ],
            {j, 1, totln}
            ];
            carray[i,i] = N[Ci0[Er, t, w, h] + ctemp],
        {i, 1, totln}
        ];
    Array[carray, {totln, totln}]
    ]   (* Constructs the capacitance per unit length matrix
          for the given dielectric and line dimensions *)

Tline[Er_, t_, w_, h_, s_, totln_] :=
    Module[ {L, LC, Mv, Cd, Ld, Wd, Zd, CE0},
        CE0 = Carray[1, t, w, h, s, totln];
            (* Capacitance Matrix without dielectric substrate *)
        L = E0 * mu0 * Inverse[CE0];
            (* Inductance per unit length matrix *)
    (*Print[N[Inverse[CE0].CE0]];*)
        CEr = Carray[Er, t, w, h, s, totln];
            (* Capacitance per unit length matrix *)
        LC = L . CEr;
    (*Chop[LC, 10^-30];*)
        Mv = Transpose[Eigenvectors[LC]];
            (* Transformation matrix obtained from right
eigenvectors of
            LC matrix *)
        Cd = Transpose[Mv].CEr.Mv;
            (* Diagonalised capacitance matrix *)
        Ld = Inverse[Mv].L.Transpose[Inverse[Mv]];
            (* Diagonalised inductance matrix *)
    (*Print[N[Inverse[Mv].Mv]];*)
        Wd = Sqrt[Abs[Ld.Cd]];
            (* Time delay matrix *)
        Zd = Sqrt[Abs[Ld.Cd]].Inverse[Cd];
            (* Impedance matrix *)
    Print[CEr];
    Print[L];
    (*Print[N[Inverse[Cd].Cd]];
        Print[N[Mv]];
        Print[N[Wd]];
        Print[N[Zd]];*)
        {Mv, Wd, Zd}
    ]
```

```
Codd[Er_, t_, w_, h_, s_] :=
    Module[ {codd, cf, cp, cgd, cga, cgt},
        cf = Cf[Er, t, w, h];
        cp = Cp[Er, w, h];
        cgd = Cgd[Er, t, w, h, s];
        cga = Cga[w, h, s];
        cgt = Cgt[t, s];
        codd = cf + cp + cgd + cga + cgt;
    N[codd]
    ]    (* Odd mode capacitance of the lines *)


Ceven[Er_, t_, w_, h_, s_] :=
    Module[ {ceven, cf, cfpri, cp},
        cp = Cp[Er, w, h];
        cf = Cf[Er, t, w, h];
        cfpri = Cfpri[Er, t, w, h, s];
        ceven = cp + cf + cfpri;
    N[ceven]
    ]    (* Even mode capacitance of the lines *)


Zoe[Er_, t_, w_, h_, s_] :=
    Module[ {zoe, cea, ceer},
        cea = Ceven[1, t, w, h, s];
        ceer = Ceven[Er, t, w, h, s];
        zoe = Sqrt[mu0*E0/cea/ceer];
    N[zoe]
    ]    (* Even mode impedance of the lines *)


Zoo[Er_, t_, w_, h_, s_] :=
    Module[ {zoo, coa, coer},
        coa = Codd[1, t, w, h, s];
        coer = Codd[Er, t, w, h, s];
        zoo = Sqrt[mu0*E0/coa/coer];
    N[zoo]
    ]    (* Odd mode impedance of the lines *)


Z0[Er_, t_, w_, h_, s_] :=
    Module[ {z0, zoe, zoo},
        zoe = Zoe[Er, t, w ,h, s];
        zoo = Zoo[Er, t, w, h ,s];
        z0 = Sqrt[zoe*zoo];
    N[z0]
    ]    (* Overall impedance of the pair of lines *)


EndPackage[]
```

```
SaisirCurve[]:=
Module[{rep},
rep =
Input["Wich Curve do you want\r
1 Cga      5 Cij\r
2 Cgd\r
3 Cgt\r
4 Cfpri\r"];
rep
]   (* Choice of the curve you want to draw *)


(*-------------------------------------------------------------------------------*)
SaisirVariable[]:=
Module[{choice},
choice =
Input["According to which variable ?\r
1         w (Width)\r
2         t (Thickness)\r
3         s (Spacing)\r
4         h (Height above substract)\r"];
choice
]  (* Choice of the variable according to which you want to draw the curve *)


(* ================================================================
 Fr :  Saisie des valeurs des variables
       Les valeurs doivent etre des valeurs entieres ou reelles
 Uk : Seize of the values of the variables
       Values must be > 0 and must be Numbers (Except complex Numbers)
================================================================*)


MyNumberQ[number_]:=
Module[{retour},
If[NumberQ[number] == True && Im[number] == 0, retour = True, retour = False];
retour
]         (* Return True if the value is a number (NOT a complex) *)


(*-------------------------------------------------------------------------------*)
Saisirw[]:=
Module[{w},
w=Input["Value for w : "];
While[MyNumberQ[w] == False || w <= 0,
        w=Input["Value for w : "]];
w
]




(*-------------------------------------------------------------------------------*)
Test[repcurve_, t_, er_, w_, h_]:=
Module[{retour},
```

```
    retour = Goodt[t,er,w,h], retour = True];
retour
]   (* If the curve to display can give complex result, there is a verification on the t
value.
        else, return TRUE *)


 (*-------------------------------------------------------------------------------*)
OktVal[t_, h_, w_, er_]:=
Module[{retour, tmax},
If[t<(tmax=N[((2.3 Sqrt[h w]/(er-1))*( er (1+CalcF[w,h])+(1- CalcF[w,h])))]),
  retour = True, retour = False];
If[retour == False, Print["-- OktVal (Er Constraint) -- t must be < ", tmax]];
retour
]   (* Test if t<value, which is calculated to avoid the gain of a complex number
        with Sqrt(Ere) *)


(*-------------------------------------------------------------------------------*)
VerifOft[t_, h_, w_, er_] :=
Module[ { retour },
If[ VerifLn[t, w, h] == True && OktVal[t, h, w, er] == True,
    retour = True, retour = False];
   retour
] (* Test all the constraints on t - Ln and range - *)


(*-------------------------------------------------------------------------------*)
Goodt[t_, er_, w_, h_]:=
Module[{retour, passe=False},
If [ Length[w] == 2,
      passe = True;
         If [ VerifOft[t, h, w[[1]], er] == True  &&
              VerifOft[t, h, w[[2]], er] == True,
         retour = True, retour = False]
  ];
If [ Length[h] == 2,
      passe = True;
         If [ VerifOft[t, h[[1]], w, er] == True  &&
              VerifOft[t, h[[2]], w, er] == True,
         retour = True, retour = False]
  ];
If [ Length[t] == 2,
    passe = True;
    If[VerifOft[t[[2]], h, w, er] == True,
       retour = True, retour = False]
  ];
If [ passe != True,
         If[VerifOft[t, h, w, er] == True,
              retour = True, retour = False]
  ];
(*Print["Retour de Goodt : ",retour];*)
retour
] (* Return True if  t  is Less than the values which give a complex value*)
```

```
(*-------------------------------------------------------------------------------*)
Saisirt[repcurve_,er_, w_, h_]:=
Module[{t},
t=Input["Value for t : "];
While[MyNumberQ[t] == False ||
    t <= 0 ||
    Test[repcurve, t, er, w, h]== False ,
       t=Input["Value for t : "]];
t
] (* seize of t, test if t have a good value = we can't have a complex value later *)


(*-------------------------------------------------------------------------------*)
Saisirs[]:=
Module[{s},
s=Input["Value for s : "];
While[MyNumberQ[s] == False || s <= 0,
      s=Input["Value for s : "]];
s
]


(*-------------------------------------------------------------------------------*)
Saisirh[]:=
Module[{h},
h=Input["Value for h : "];
While[MyNumberQ[h] == False || h <= 0,
      h=Input["Value for h : "]];
h
]


(*-------------------------------------------------------------------------------*)
ValErFalse[er_, repcurve_, repvar_] :=
Module[{retour},
If [ (repcurve == 2 || repcurve == 4 || repcurve ==5 || repvar == 2) && er<= 1,
    retour = False, retour = True];
retour
] (* False if er <= 1, when we are displaying the curves Cgd, Cfpri and Cm
                      and if the variable is t ... because we have to test a constraint
                      where we have 1/(Er-1)*)


(*-------------------------------------------------------------------------------*)
SaisirEr[repcurve_, repvar_]:=
Module[{Er},
Er=Input["Value for Er : "];
While[MyNumberQ[Er] == False || Er <= 0 || ValErFalse[Er, repcurve, repvar]== False,
      Er=Input["Value for Er : "]];
Er
]


(*
================================================================================
*)
VerificationInt[ val_ ]:=
```

```
        If[ Length[val] != 2            ||
          MyNumberQ[ val[[1]] ] == False ||
            MyNumberQ[ val[[2]] ] == False ||
            val[[1]] <= 0  || val[[2]] <= 0 ||
            val[[1]] == val[[2]] ,
             retour = False,
           retour =True];
retour
]   (* Test if the range given in parameter is correct *)



(*-------------------------------------------------------------------------------*)
SaisirRangew[]:=
Module[{w},
w=Input["Value for w : give an interval {min, max} : "];
While[  VerificationInt[w] != True ,
      w=Input["Value for w : give an interval {min, max} : "]];
w
]


(*-------------------------------------------------------------------------------*)
VerifLn[t_, w_, h_]:=
Module[{retour, tmax},
If [ w/h<= N[1/(2 Pi)], If[ t < (tmax=N[4 Pi w]/ 0.367879), retour = True, retour = False
],
                    If[ t < (tmax=N[2 h / 0.367879]), retour = True, retour = False ] ];
If[retour == False,Print["-- VerifLn (Ln Constraint) -- t must be < ", tmax];
                Print[" t, w, h = ",t,",", w," ", h];
];
retour
]   (* Verification of the t value to avoid to have Log of a negative value, which give
       a complex number *)


(*-------------------------------------------------------------------------------*)
Intervallet[t1_, t2_, er_, w_, h_] :=
Module[{m},
If[ t1 > 0 &&  VerifOft[t2, h, w, er] == True,
   m = True,
   m = False
  ];
m
]   (* test of the t value, when t is the variable according to which the curve will be
displayed *)


(*-------------------------------------------------------------------------------*)
SaisirRanget[ er_, w_, h_]:=
Module[{t},
t=Input["Value for t : give an interval {min, max} "];
While[VerificationInt[t] != True ||
      Intervallet[t[[1]], t[[2]], er, w, h] == False,
      t=Input["Value for t : give an interval {min, max} "]];
t
```

```
(*-------------------------------------------------------------------------------*)
SaisirRanges[]:=
Module[{s},
s=Input["Value for s : give an interval {min, max} : "];
While[VerificationInt[s] != True ,
      s=Input["Value for s : give an interval {min, max} : "]];
s
]




(*-------------------------------------------------------------------------------*)
SaisirRangeh[]:=
Module[{h},
h=Input["Value for h : give an interval {min, max} : "];
While[VerificationInt[h] != True ,
      h=Input["Value for h : give an interval {min, max} : "]];
h
]


(*
=================================================================================
AfficheVal[repcurve_, repvar_, er_, t_, w_, h_, s_, min_, max_]:=
Module[{i, inter},
inter = Input["Value of the increment"];
If[ repcurve == 1,
      Print[" Curve : Cga "];
      If[repvar ==1, For[i=min, i<=max, i=i+inter, Print["w= " ,i, "  Cga = ",N[Cga[
i,h,s]]]], (*Nothing*) ];
      If[repvar ==2, For[i=min, i<=max, i=i+inter, Print["t= " ,i, "  Cga = ",
N[Cga[w,h,s]]]], (*Nothing*) ];
      If[repvar ==3, For[i=min, i<=max, i=i+inter, Print["s= " ,i, "  Cga = ", N[Cga[
w,h,i]]]], (*Nothing*) ];
      If[repvar ==4, For[i=min, i<=max, i=i+inter, Print["h= " ,i, "  Cga = ", N[Cga[
w,i,s]]]], (*Nothing*) ];
 , (*Nothing*)];


If[ repcurve == 2,
      If[repvar == 1, For[i=min, i<=max, i=i+inter, Print["w= " ,i, "  Cgd =
",N[Cgd[er, t, i, h, s]]]]  ];
      If[repvar == 2, For[i=min, i<=max, i=i+inter, Print["t= " ,i, "  Cgd = ",N[Cgd[er,
i, w, h, s]]]]   ];
      If[repvar == 3, For[i=min, i<=max, i=i+inter, Print["s= " ,i, "  Cgd = ",N[Cgd[er,
t, w, h, i]]]]   ];
      If[repvar == 4, For[i=min, i<=max, i=i+inter, Print["h= " ,i, "  Cgd = ",N[Cgd[er,
t, w, i, s]]]]   ];
, (*Nothing*)];


If[ repcurve == 3,
```

```
        If[repvar ==2, For[i=min, i<=max, i=i+inter, Print["t= " ,i, "  Cgt = ",N[Cgt[i,
s]]]], (*Nothing*) ];
        If[repvar ==3, For[i=min, i<=max, i=i+inter, Print["s= " ,i, "  Cgt = ",N[Cgt[t,
i]]]], (*Nothing*) ];
        If[repvar ==4, For[i=min, i<=max, i=i+inter, Print["h= " ,i, "  Cgt = ",N[Cgt[t,
s]]]], (*Nothing*) ];
, (*Nothing*)];


If[ repcurve == 4,
        If[repvar ==1, For[ i=min, i<=max, i=i+inter, Print["w= " ,i, "  Cfpri =
",N[Cfpri[er, t, i, h, s]]]]];
        If[repvar ==2, For[i=min, i<=max, i=i+inter, Print["t= " ,i, "  Cfpri =
",N[Cfpri[er, i, w, h, s]]]]];
        If[repvar ==3, For[i=min, i<=max, i=i+inter, Print["s= " ,i, "  Cfpri =
",N[Cfpri[er, t, w, h, i]]]]];
        If[repvar ==4, For[i=min, i<=max, i=i+inter, Print["h= " ,i, "  Cfpri =
",N[Cfpri[er, t, w, i, s]]]]];
, (*Nothing*)];


If[ repcurve == 5,
        If[repvar ==1, For[i=min, i<=max, i=i+inter, Print["w= " ,i, "  Cm = ",N[Cm[er,t,
i, h, s]]]]];
        If[repvar ==2, For[i=min, i<=max, i=i+inter, Print["t= " ,i, "  Cm = ",N[Cm[er,i,
w, h, s]]]]];
        If[repvar ==3, For[i=min, i<=max, i=i+inter, Print["s= " ,i, "  Cm = ",N[Cm[er,t,
w, h, i]]]]];
        If[repvar ==4, For[i=min, i<=max, i=i+inter, Print["h= " ,i, "  Cm = ",N[Cm[er,t,
w, i, s]]]]];
, (*Nothing*)];


] (* Display the values of the calculus, from a start value to an end value, each
increment value.
    (cij(1)= ?, Cij(6) = ? *)


(*
=============================================================================
Lect[]:=
Module[{repcurve, repvar, fini=False, er,  min, max, rep },


While[fini == False,


(* ----------------------------------------------
Fr : Selection de la courbe que je souhaite
Uk : Choice of the curve you want
---------------------------------------------- *)
repcurve = SaisirCurve[];
While[IntegerQ[repcurve] == False || (repcurve>5) || (repcurve<1),
    repcurve = SaisirCurve[]];


(*-------------------------------------------------------------
```

```
Fr : Selection de la variable qui va varier (w, t, h, s)
Uk : Choice of the variable according to which, you
      want to display the curve.
------------------------------------------------------------ *)
repvar = SaisirVariable[];
While[IntegerQ[repvar] == False || repvar >4 || repvar < 1,
    repvar = SaisirVariable[]];


(*-------------------------------------------------
 Fr : Saisie des valeurs des variables fixes
   et de l'intervalle de la variable (qui varie)
 Uk : Seize of the values of the fix values
       and the range for the value which will change
------------------------------------------------------ *)
er = SaisirEr[repcurve, repvar];
If[ repvar != 1 , w = Saisirw[], w = SaisirRangew[]; min = w[[1]]; max=w[[2]]];
If[ repvar != 3 , s = Saisirs[], s = SaisirRanges[]; min = s[[1]]; max=s[[2]]];
If[ repvar != 4 , h = Saisirh[], h = SaisirRangeh[]; min = h[[1]]; max=h[[2]]];
If[ repvar != 2 , t = Saisirt[repcurve,er,w,h], t = SaisirRanget[er,w,h ]; min = t[[1]];
max=t[[2]]];


Print["---------------"];
Print["er = ", er];
Print["w = ", w];
Print["t = ", t];
Print["s = ", s];
Print["h = ", h];


(*-----------------------------------------------------------
Fr : Dessin de la courbe choisie
 Uk : Drawing of the curve choosen
-------------------------------------------------------------*)
AfficheVal[repcurve, repvar, er,t,w,h,s,min,max];  (* Display of the values*)


If[ repcurve == 1,  If[repvar ==1, Plot[Cga[ w,h,s], {w, min, max}, PlotLabel->"Cga/w"
], (*Nothing*) ];
            If[repvar ==2, Plot[Cga[ w,h,s], {t, min, max}, PlotLabel->"Cga/t"],
(*Nothing*) ];
            If[repvar ==3, Plot[Cga[ w,h,s], {s, min, max}, PlotLabel->"Cga/s"],
(*Nothing*) ];
            If[repvar ==4, Plot[Cga[ w,h,s], {h, min, max}, PlotLabel->"Cga/h"],
(*Nothing*) ];
 , (*Nothing*)];


If[ repcurve == 2, If[repvar == 1, Plot[Cgd[er, t, w, h, s], {w, min, max},
PlotLabel->"Cgd/w"], (*Nothing*) ];
            If[repvar == 2, Plot[Cgd[er, t, w, h, s], {t, min, max}, PlotLabel->"Cgd/t"],
(*Nothing*) ];
            If[repvar == 3, Plot[Cgd[er, t, w, h, s], {s, min, max}, PlotLabel->"Cgd/s"],
(*Nothing*) ];
            If[repvar == 4, Plot[Cgd[er, t, w, h, s], {h, min, max}, PlotLabel->"Cgd/h"],
(*Nothing*) ];
```

```
If[ repcurve == 3, If[repvar ==1, Plot[Cgt[t, s], {w, min, max}, PlotLabel->"Cgt/w"],
(*Nothing*) ];
            If[repvar ==2, Plot[Cgt[t, s], {t, min, max}, PlotLabel->"Cgt/t"],
(*Nothing*) ];
            If[repvar ==3, Plot[Cgt[t, s], {s, min, max}, PlotLabel->"Cgt/s"],
(*Nothing*) ];
            If[repvar ==4, Plot[Cgt[t, s], {h, min, max}, PlotLabel->"Cgt/h"],
(*Nothing*) ];
, (*Nothing*)];


If[ repcurve == 4, If[repvar ==1, Plot[Cfpri[er, t, w, h, s], {w, min, max},
PlotLabel->"Cfpri/w"], (*Nothing*) ];
            If[repvar ==2, Plot[Cfpri[er, t, w, h, s], {t, min, max}, PlotLabel->"Cfpri/t"],
(*Nothing*) ];
            If[repvar ==3, Plot[Cfpri[er, t, w, h, s], {s, min, max}, PlotLabel->"Cfpri/s"],
(*Nothing*) ];
            If[repvar ==4, Plot[Cfpri[er, t, w, h, s], {h, min, max},
PlotLabel->"Cfpri/h"], (*Nothing*) ];
, (*Nothing*)];


If[ repcurve == 5, If[repvar ==1, Plot[Cm[er,t, w, h, s], {w, min, max} ,
PlotLabel->"Cm/w"], (*Nothing*) ];
            If[repvar ==2, Plot[Cm[er,t, w, h, s], {t, min, max} , PlotLabel->"Cm/t"],
(*Nothing*) ];
            If[repvar ==3, Plot[Cm[er,t, w, h, s], {s, min, max} , PlotLabel->"Cm/s"],
(*Nothing*) ];
            If[repvar ==4, Plot[Cm[er,t, w, h, s], {h, min, max} , PlotLabel->"Cm/h"],
(*Nothing*) ];
, (*Nothing*)];


rep = Input["Another Curve ?? (y(es) / anything for No"];
fini = Which[rep == y, False, rep != y , True];
]


]
```

```
**********************************************************)

(*-------------------------------------------------------------------------
Cij Matrix (Capacitance) For non uniform coupled lines:
  CarrayMin : to have the minimum Cij, using the following method:


  Calculation of the Cij like if the 2 lines studied are the same.
 We consider first that they have the same characteristic as the line i,
 and that they have the same characteristics than the line j.
 We get a cij min and a cij max. (cij min < cij max)
 We create 2 matrices. (min et Max)
 The comparisons min max are upon Cij = -cij


( CorrectL[t_] : Predicat qui teste tous les elements qui lui sont passes
                 en parametres, pour savoir si se sont des NUMBER.
                 Retourne True ou False selon le resultat.
                 !!! On doit passer une liste, meme pour 1 element
        Uk       : Test all the elements passed as parameters to see if they
                 are numbers


MyNumberQ[number_] : Predicat qui teste que si les nombres sont
                 corrects = non complexes.
        Uk       : Test if the numbers are correct (non complex)
-------------------------------------------------------------------------*)


CorrectL[t_]:=
Module[{i, result},
For[ i=1, i<=Length[t] && MyNumberQ[ t[[i]] ] , i=i+1, ];
If[ i>Length[t] || MyNumberQ[ t[[i]] ], result = True, result = False];
result
]


(* ------------------------------------------------------------------------- *)
MyNumberQ[number_]:=
Module[{retour},
If[NumberQ[number] == True && Im[number] == 0, retour = True, retour = False];
retour
]       (* Return True if the value is a number (NOT a complex) *)


(* ------------------------------------------------------------------------- *)


CarrayMin[Er_, t_List, w_List, h_List, s_List, totln_] :=
Module[ {ctemp, ctempI, ctempJ, ctempMin,
      borneInf, borneMax, seff, carrayMin, i, j, k, cijMin},
  Do[
    ctemp = 0;
    Do[If [!(i === j),
```

```
        If[ i<j, borneInf = i; borneMax = j,
              borneInf = j; borneMax = i ];


      (* Calcul de l'espacement effectif entre la ligne i et j *)

        seff = -w[[borneInf]];
        Do [seff = seff + w[[k]] + s[[k]], {k, borneInf, borneMax-1}];


        ctempI = Cm[Er, t[[i]], w[[i]], h[[i]], seff];
        ctempJ = Cm[Er, t[[j]], w[[j]], h[[j]], seff];


        ctempMin = Min[ {ctempI, ctempJ} ];
        cijMin = Min[ N[-ctempI], N[-ctempJ] ];
        carrayMin[i,j] = cijMin;
        ctemp = N[ctemp + ctempMin]
       }
      ],
     {j, 1, totln}
    ];
    carrayMin[i,i] = N[Ci0[Er, t[[i]], w[[i]], h[[i]]] + ctemp],
    {i, 1, totln}
   ];
   Array[carrayMin, {totln, totln}]
  ]     (* Constructs the capacitance per unit length matrix
          for the given dielectric and line dimensions *)
(* ------------------------------------------------------------------------------ *)


CarrayMax[Er_, t_List, w_List, h_List, s_List, totln_] :=
Module[ {ctemp, ctempI, ctempJ, ctempMax,
      borneInf, borneMax, seff, carrayMax, i, j, k, cijMax},
  Do[
    ctemp = 0;
    Do[If [!(i === j),
      {
       If[ i<j, borneInf = i; borneMax = j,
             borneInf = j; borneMax = i ];

     (* Calcul de l'espacement effectif entre la ligne i et j *)

       seff = -w[[borneInf]];
       Do [seff = seff + w[[k]] + s[[k]], {k, borneInf, borneMax-1}];

       ctempI = Cm[Er, t[[i]], w[[i]], h[[i]], seff];
       ctempJ = Cm[Er, t[[j]], w[[j]], h[[j]], seff];


       ctempMax = Max[ {ctempI, ctempJ} ];
       cijMax = Max[ N[-ctempI], N[-ctempJ] ];
       carrayMax[i,j] =cijMax;
       ctemp = N[ctemp + ctempMax]
      }
     ],
    {j, 1, totln}
```

```
    carrayMax[i,i] = N[Ci0[Er, t[[i]], w[[i]], h[[i]]] + ctemp],
    {i, 1, totln}
   ];
   Array[carrayMax, {totln, totln}]
  ]     (* Constructs the capacitance per unit length matrix
           for the given dielectric and line dimensions *)


(*************************************************************
    Second Method of calcul of the Cij when the parameters are not the sames
*************************************************************)


(*-------------------------------------------------------------------------------
 Cij matrix (capacitance for non uniform coupled lines:
   CarrayMin to have the Cij minimum, using the following method.
      Calculate w = min(w1, w2 ...)
                t = min(t1,t2 ...)
      calculate Cij min, same thing for the max.
-------------------------------------------------------------------------------*)


CarrayMin2[Er_, t_List, w_List, h_List, s_List, totln_] :=
Module[ {ctemp, ctemp2, ctempMin,
      borneInf, borneMax, seff, carrayMin, i, j, k, myt, myw, myh },
  Do[
    ctemp = 0;
    Do[If [!(i === j),
      {
      If[ i<j, borneInf = i; borneMax = j,
            borneInf = j; borneMax = i ];
      (*Print["i: ", i, "j: ", j, "BorneInf : ", borneInf,
          "BorneMax : ", borneMax];*)


    (* Calcul de l'espacement effectif entre la ligne i et j *)

      seff = -w[[borneInf]];
      Do [seff = seff + w[[k]] + s[[k]], {k, borneInf, borneMax-1}];
      (*Print["Seff : ", seff];*)


      myt = Min[ {t[[i]], t[[j]] } ];
      myw = Min[ {w[[i]], w[[j]] } ];
      myh = Min[ {h[[i]], h[[j]] } ];
      ctemp2 = Cm[Er, myt, myw, myh, seff];
      carrayMin[i,j] = N[- ctemp2];
      ctemp = N[ctemp + ctemp2]
     }
    ],
   {j, 1, totln}
  ];
  carrayMin[i,i] = N[Ci0[Er, t[[i]], w[[i]], h[[i]]] + ctemp],  (* ok or not for cii ??? *)
  {i, 1, totln}
 ];
 Array[carrayMin, {totln, totln}]
]     (* Constructs the capacitance per unit length matrix
```

```
(* ------------------------------------------------------------------------------ *)


CarrayMax2[Er_, t_List, w_List, h_List, s_List, totln_] :=
Module[ {ctemp, ctemp2, ctempMax,
      borneInf, borneMax, seff, carrayMax, i, j, k, myt, myw, myh},
  Do[
    ctemp = 0;
    Do[If [!(i === j),
      {
      If[ i<j, borneInf = i; borneMax = j,
            borneInf = j; borneMax = i ];
      (*Print["i: ", i, "j: ", j, "BorneInf : ", borneInf,
          "BorneMax : ", borneMax];*)


     (* Calcul de l'espacement effectif entre la ligne i et j *)

      seff = -w[[borneInf]];
      Do [seff = seff + w[[k]] + s[[k]], {k, borneInf, borneMax-1}];
      (*Print["Seff : ", seff];*)
      myt = Max[ {t[[i]], t[[j]] } ];
      myw = Max[ {w[[i]], w[[j]] } ];
      myh = Max[ {h[[i]], h[[j]] } ];
      ctemp2 = Cm[Er, myt, myw, myh, seff];
      carrayMax[i,j] = N[- ctemp2];
      ctemp = N[ctemp + ctemp2]
     }
    ],
   {j, 1, totln}
  ];
  carrayMax[i,i] = N[Ci0[Er, t[[i]], w[[i]], h[[i]]] + ctemp],
  {i, 1, totln}
 ];
 Array[carrayMax, {totln, totln}]
]     (* Constructs the capacitance per unit length matrix
        for the given dielectric and line dimensions *)


(* ------------------------------------------------------------------------------
  Saisie des caracteristiques des lignes
  Affichage des caracteristiques.
 Selection de la matrice que l'on souhaite afficher.


Uk :    input of the parameters of the lines
        display of the parameters
        choice of the matrix to display
------------------------------------------------------------------------------ *)


Main[]:=
Module[{rep, nb},


nb = Input["Number of lines"];
While[ IntegerQ[nb] == False || nb < 1 ,
```

```
er = Input["Dielectric constant\n\nvalue for er (!=1)"];
While[ MyNumberQ[er] == False ||
        er == 1,
    er = Input["Dielectric constant\n\nvalue for er (<>1)"] ];


w = Input["Width of the lines\n\nvalues for w {w1, w2, ...}"];
While[ CorrectL[w] == False || Length[w]<nb ,
    w = Input["Width of the lines\n\nvalues for w {w1, w2, ...}"] ];


h = Input["Height above the ground plane\n\nvalues for h {h1, h2, ...}"];
While[ CorrectL[h] == False || Length[h]<nb ,
    h = Input["Height above the ground plane\n\nvalues for h {h1, h2, ...}"] ];


s = Input["Spacing between the lines\n\nvalues for s {s1, s2, ...}"];
While[ CorrectL[s] == False || Length[s]<nb ,
    s = Input["Spacing between the lines\n\nvalues for s {s1, s2, ...}"] ];


t = Input["Thickness of the lines\n\nvalues for t {t1, t2, ...}"];
While[ CorrectL[t] == False || Length[t]<nb,
    t = Input["Thickness of the lines\n\nvalues for t {t1, t2, ...}"] ];


(* Re-seize of the values of t if it doesn't respect the constraints *)


For[i=1, i<nb+1, i++,
        If[ VerifOft[ t[[i]], h[[i]], w[[i]], er] != True,
                Print["<",t[[i]],"> Valeur pour t[",i,"]"];
                t[[i]] = Input["Value for t"];
    While[
                        CorrectL[ t[[i]] ] == False || (* On veut un nombre *)
                        VerifOft[ t[[i]], h[[i]], w[[i]],er] ==False,
                        t[[i]] = Input["Value for t"];
                       ];
                ];
        ];


Print["t = ",t];
Print["w = ",w];
Print["h = ",h];
Print["s = ",s];
Print["number of lines = ",nb];


rep = Input["Which Matrix do you want ?\r
1 Min-Method 1 (Cmin <= Cij <= Cmax)\r
2 Max-Method 1\r
3 Min-Method 2 (Cmin(min{w1,w2}, ...))\r
4 Max-Method 2\r"];
Switch[rep, 1, Print[CarrayMin[er,t,w,h,s,nb]],
```

```
        3, Print[CarrayMin2[er,t,w,h,s,nb]],
        4, Print[CarrayMax2[er,t,w,h,s,nb]],
                        5, Print["Bye"]; ];
]




VerifOft[t_, h_, w_, er_] :=
Module[ { retour },
If[ VerifLn[t, w, h] == True && OktVal[t, h, w, er] == True,
    retour = True, retour = False];
   retour
] (* Test all the constraints on t - Ln and range - *)


OktVal[t_, h_, w_, er_]:=
Module[{retour, tmax},
If[t<(tmax=N[((2.3 Sqrt[h w]/(er-1))*( er (1+CalcF[w,h])+(1- CalcF[w,h])))]),
  retour = True, retour = False];
If[retour == False, Print["tokt< ", tmax]];
retour
]   (* Test if t<value, which is calculated to avoid the gain of a complex number
       with Sqrt(Ere) *)


VerifLn[t_, w_, h_]:=
Module[{retour, tmax},
If [ w/h<= N[1/(2 Pi)], If[ t < (tmax=N[4 Pi w]/ 0.367879), retour = True, retour = False
],
                    If[ t < (tmax=N[2 h / 0.367879]), retour = True, retour = False ] ];
If[retour == False,Print["tverifln< ", tmax];
            Print[" t, w, h = ",t,",", w," ", h];
];
retour
]   (* Verification of the t value to avoid to have Log of a negative value, which give
       a complex number *)


(*-------------------------------------------------------------------------------------------------*)


(* Main without test of the values seized : they have to be correct
   MainWithoutTest*)


MainWT[]:=
Module[{rep, nb},


nb = Input["Number of lines"];
While[ IntegerQ[nb] == False || nb < 1 ,
    nb = Input["Number of lines"] ];
```

```
t = Input["values for t {t1, t2, ...}"];
While[ CorrectL[t] == False || Length[t]<nb,
      t = Input["values for t {t1, t2, ...}"] ];


w = Input["values for w {w1, w2, ...}"];
While[ CorrectL[w] == False || Length[w]<nb ,
      w = Input["values for w {w1, w2, ...}"] ];


h = Input["values for h {h1, h2, ...}"];
While[ CorrectL[h] == False || Length[h]<nb ,
      h = Input["values for h {h1, h2, ...}"] ];


s = Input["values for s {s1, s2, ...}"];
While[ CorrectL[s] == False || Length[s]<nb ,
      s = Input["values for s {s1, s2, ...}"] ];




Print["t = ",t];
Print["w = ",w];
Print["h = ",h];
Print["s = ",s];
Print["nb de lignes = ",nb];


rep = Input["Which Matrix do you want ?\r
1 Min-Method 1 (Cmin <= Cij <= Cmax)\r
2 Max-Method 1\r
3 Min-Method 2 (Cmin(min{w1,w2}, ...))\r
4 Max-Method 2\r"];
Switch[rep, 1, Print[CarrayMin[1,t,w,h,s,nb]],
         2, Print[CarrayMax[1,t,w,h,s,nb]],
         3, Print[CarrayMin2[1,t,w,h,s,nb]],
         4, Print[CarrayMax2[1,t,w,h,s,nb]] ];
]
```

```
(*-------------------------------------------------------------
 Val[i_, j_, totln_, cm_]
 on donne la ligne et la colonne de la valeur dans la matrice,
 totln le nombre de lignes de la matrice
 cm le tableau correspondant a la matrice.

 Si on est dans les limites de la matrice,
 - retourne la valeur qui se trouve a la position demandee,
 - sinon, retourne 0
-------------------------------------------------------------*)
Val[i_, j_, totln_, cm_]:=
Module[ {retour},
                If[ i<=0 || j<=0 || i>totln || j>totln,
                   retour = 0,
                         retour = Abs[cm[i,j]]
                ];
retour
]


(*-------------------------------------------------------------*)
(*
 Transfo, retourne la matrice calculee grace a l'algorithme
 Seule 3 colonnes sont differentes de 0 :
 colonnes avant diagonale, diagonale, apres diagonale
-------------------------------------------------------------*)
Transfo[Er_, t_, w_, h_, s_List, totln_]:=
Module[{cm,a, mf, mf2, tet},
   cm = Carray[Er,t,w,h,s,totln];
        Print["cm = ",cm];
        For[i=1, i<= totln, i=i+1,
                For[j=1, j<= totln, j=j+1,
                        If[ j!=i && j!=i-1 && j!=i+1,
                                mf[i,j] = 0; mf2[i,j] = 0,
                                mf[i,j] = cm[[i]][[j]];mf2[i,j] = cm[[i]][[j]]
                        ];
                ];
        ];
mf[1,1] = N[Ci0[Er, t, w, h]] + Val[1,2,totln, mf];
For[i=2, i<= totln, i++,
        mf[i,i] = Val[i-1, i-1, totln, mf]
                        - Val[i-2, i-1, totln, mf]
                        + Val[i  , i+1, totln, mf];
        ];
tet = Array[mf, {totln, totln}];
tet
];


(*----- SAMPLES


Transfo[12,.01,2,20,{3,4},3]
```

```
------*)
(*-----------------------------------------------
  Meme chose que transfo, mais on calcule
  L= E0*mu0*CE0.
-----------------------------------------------*)
TransfoL[Er_, t_, w_, h_, s_List, totln_]:=
Module[{CE0, L, a, mf, mf2, tet},
        CE0 = Carray[1,t,w,h,s,totln];
        L = E0*mu0*Inverse[CE0];
        Print["L = ",L];
        For[i=1, i<= totln, i=i+1,
                For[j=1, j<= totln, j=j+1,
                        If[ j!=i && j!=i-1 && j!=i+1,
                                mf[i,j] = 0; mf2[i,j] = 0,
                                mf[i,j] = L[[i]][[j]];mf2[i,j] = L[[i]][[j]]
                        ];
                ];
        ];
mf[1,1] = N[Ci0[Er, t, w, h]] + Val[1,2,totln, mf];
For[i=2, i<= totln, i++,
        mf[i,i] = Val[i-1, i-1, totln, mf]
                        - Val[i-2, i-1, totln, mf]
                        + Val[i  , i+1, totln, mf];
        ];
tet = Array[mf, {totln, totln}];
tet
];
```

```
(*-----------------------------------------------------------
 Val[i_, j_, totln_, cm_]
 on donne la ligne et la colonne de la valeur dans la matrice,
 totln le nombre de lignes de la matrice
 cm le tableau correspondant a la matrice.

 Si on est dans les limites de la matrice,
 - retourne la valeur qui se trouve a la position demandee,
 - sinon, retourne 0
-----------------------------------------------------------*)
Val[i_, j_, totln_, cm_]:=
Module[ {retour},
                If[ i<=0 || j<=0 || i>totln || j>totln,
                   retour = 0,
                         retour = Abs[cm[i,j]]
                ];
retour
]


(*-----------------------------------------------------------*)
(*
 Transfo, retourne la matrice calculee grace a l'algorithme
 Seule 3 colonnes sont differentes de 0 :
 colonnes avant diagonale, diagonale, apres diagonale


Uk :    Transfo, give the matrix computed with the algorithm
        only 3 rows are different from 0.
        the diagonal, just before, and just after.
-----------------------------------------------------------*)
Transfo[Er_, t_List, w_List, h_List, s_List, totln_]:=
Module[{cm, cm2, mf, mf2, tet, tet2},
   cm  = CarrayMin[Er,t,w,h,s,totln];
   cm2 = CarrayMax[Er,t,w,h,s,totln];
        Print["cm  = ",cm];
        Print["cm2 = ",cm2];
        For[i=1, i<= totln, i=i+1,
                For[j=1, j<= totln, j=j+1,
                        If[ j!=i && j!=i-1 && j!=i+1,
                                mf[i,j] = 0; mf2[i,j] = 0,
                                mf[i,j] = cm[[i]][[j]];mf2[i,j] = cm2[[i]][[j]]
                        ];
                ];
        ];
 mf[1,1] = N[Ci0[Er, t[[1]], w[[1]], h[[1]]]] + Val[1,2,totln, mf];
mf2[1,1] = N[Ci0[Er, t[[1]], w[[1]], h[[1]]]] + Val[1,2,totln, mf2];
For[i=2, i<= totln, i++,
        mf[i,i] = Val[i-1, i-1, totln, mf]
                - Val[i-2, i-1, totln, mf]
                + Val[i  , i+1, totln, mf];
    mf2[i,i] = Val[i-1, i-1, totln, mf2]
                - Val[i-2, i-1, totln, mf2]
```

```
        ];
tet  = Array[mf, {totln, totln}];
tet2 = Array[mf2, {totln, totln}];
{tet, tet2}
];



(*----- SAMPLES


Transfo[12,.01,2,20,{3,4},3]
Transfo[12,.01,2,20,{.3, 4.114, 5.002, 6, 4.7, 8, 9.2, 5.0343, .004},10]


------*)
(*-----------------------------------------------
 Fr : Meme chose que transfo, mais on calcule
Uk : Same thing as Transfo, but we calculate
  L= E0*mu0*CE0.
-----------------------------------------------*)
TransfoL[Er_, t_List, w_List, h_List, s_List, totln_]:=
Module[{CE0, CE02, L, L2, a, mf, mf2, tet},
        CE0   = CarrayMin[1,t,w,h,s,totln];
        L = E0*mu0*Inverse[CE0];
        CE02 = CarrayMax[1,t,w,h,s,totln];
        L2 = E0*mu0*Inverse[CE02];
        Print["L = ",L];
        For[i=1, i<= totln, i=i+1,
                For[j=1, j<= totln, j=j+1,
                        If[ j!=i && j!=i-1 && j!=i+1,
                                mf[i,j] = 0; mf2[i,j] = 0,
                                mf[i,j] = L[[i]][[j]];mf2[i,j] = L2[[i]][[j]]
                        ];
                ];
        ];
 mf[1,1] = N[Ci0[Er, t[[1]], w[[1]], h[[1]]]] + Val[1,2,totln, mf];
mf2[1,1] = N[Ci0[Er, t[[1]], w[[1]], h[[1]]]] + Val[1,2,totln, mf2];
For[i=2, i<= totln, i++,
        mf[i,i] = Val[i-1, i-1, totln, mf]
                - Val[i-2, i-1, totln, mf]
                + Val[i  , i+1, totln, mf];
        mf2[i,i] = Val[i-1, i-1, totln, mf2]
                - Val[i-2, i-1, totln, mf2]
                + Val[i  , i+1, totln, mf2];
        ];
tet = Array[mf, {totln, totln}];
tet2 = Array[mf2, {totln, totln}];
{tet, tet2}
];


(*-------------------------------------------------------------------------
    Same thing with the second Method of calculation of the Cij matrices
-------------------------------------------------------------------------*)
```

```
(*-----------------------------------------------------------*)
(*
 Transfo, retourne la matrice calculee grace a l'algorithme
 Seule 3 colonnes sont differentes de 0 :
 colonnes avant diagonale, diagonale, apres diagonale
-----------------------------------------------------------*)
Transfo2[Er_, t_List, w_List, h_List, s_List, totln_]:=
Module[{cm, cm2, mf, mf2, tet, tet2},
   cm  = CarrayMin2[Er,t,w,h,s,totln];
   cm2 = CarrayMax2[Er,t,w,h,s,totln];
         Print["cm  = ",cm];
         Print["cm2 = ",cm2];
         For[i=1, i<= totln, i=i+1,
                  For[j=1, j<= totln, j=j+1,
                           If[ j!=i && j!=i-1 && j!=i+1,
                                    mf[i,j] = 0; mf2[i,j] = 0,
                                    mf[i,j] = cm[[i]][[j]];mf2[i,j] = cm2[[i]][[j]]
                           ];
                  ];
         ];
 mf[1,1] = N[Ci0[Er, t[[1]], w[[1]], h[[1]]]] + Val[1,2,totln, mf];
mf2[1,1] = N[Ci0[Er, t[[1]], w[[1]], h[[1]]]] + Val[1,2,totln, mf2];
For[i=2, i<= totln, i++,
         mf[i,i] = Val[i-1, i-1, totln, mf]
                  - Val[i-2, i-1, totln, mf]
                  + Val[i  , i+1, totln, mf];
     mf2[i,i] = Val[i-1, i-1, totln, mf2]
                  - Val[i-2, i-1, totln, mf2]
                  + Val[i  , i+1, totln, mf2];
         ];
tet  = Array[mf, {totln, totln}];
tet2 = Array[mf2, {totln, totln}];
{tet, tet2}
];



(*----- SAMPLES


Transfo[12,.01,2,20,{3,4},3]
Transfo[12,.01,2,20,{.3, 4.114, 5.002, 6, 4.7, 8, 9.2, 5.0343, .004},10]


------*)
(*-----------------------------------------------
 Meme chose que transfo, mais on calcule
 L= E0*mu0*CE0.
-----------------------------------------------*)
TransfoL2[Er_, t_List, w_List, h_List, s_List, totln_]:=
Module[{CE0, CE02, L, L2, a, mf, mf2, tet},
         CE0  = CarrayMin2[1,t,w,h,s,totln];
         L = E0*mu0*Inverse[CE0];
         CE02 = CarrayMax2[1,t,w,h,s,totln];
         L2 = E0*mu0*Inverse[CE02];
         Print["L = ",L];
```

```
                For[j=1, j<= totln, j=j+1,
                        If[ j!=i && j!=i-1 && j!=i+1,
                                mf[i,j] = 0; mf2[i,j] = 0,
                                mf[i,j] = L[[i]][[j]];mf2[i,j] = L2[[i]][[j]]
                        ];
                ];
        ];
 mf[1,1] = N[Ci0[Er, t[[1]], w[[1]], h[[1]]]] + Val[1,2,totln, mf];
mf2[1,1] = N[Ci0[Er, t[[1]], w[[1]], h[[1]]]] + Val[1,2,totln, mf2];
For[i=2, i<= totln, i++,
        mf[i,i] = Val[i-1, i-1, totln, mf]
                - Val[i-2, i-1, totln, mf]
                + Val[i  , i+1, totln, mf];
        mf2[i,i] = Val[i-1, i-1, totln, mf2]
                - Val[i-2, i-1, totln, mf2]
                + Val[i  , i+1, totln, mf2];
        ];
tet = Array[mf, {totln, totln}];
tet2 = Array[mf2, {totln, totln}];
{tet, tet2}
];
```

APPENDIX B

List of mathematical calculations using Mathematica:

B1. Nus1

Calculation of the time delay and characteristic impedance for the set of 3-coupled nonuniformly spaced microstrip lines.

B2. Nus2

Calculation of the time delay and characteristic impedance for the set of 3-coupled non-optimised (suggested) microstrip lines in Sect. 8.5.

B3. Final

Calculation of the time delay and characteristic impedance for the set of 3-coupled optimised microstrip lines in Sect. 8.5, see Fig. 8.18

```
a={{6.86293,-1.64943,0},{-1.64943,8.51236,-1.64943},{0,-1.64943,6.86293}}
{{6.86293, -1.64943, 0}, {-1.64943, 8.51236, -1.64943}, {0, -1.64943, 6.86293}}
c=10^-11.a
                -11                -11                  -11              -11              -11
{{6.86293 10    , -1.64943 10    , 0}, {-1.64943 10    , 8.51236 10    , -1.64943 10    },
                  -11                -11
  {0, -1.64943 10    , 6.86293 10    }}
b={{48.0896,9.59195,0},{9.59195,42.9339,9.59195},{0,9.59195,48.0896}}
{{48.0896, 9.59195, 0}, {9.59195, 42.9339, 9.59195}, {0, 9.59195, 48.0896}}
L=10^-8.b
               -7                -8                  -8               -7               -8
{{4.80896 10   , 9.59195 10   , 0}, {9.59195 10   , 4.29339 10   , 9.59195 10   },
                 -8                 -7
  {0, 9.59195 10   , 4.80896 10   }}
L.c
               -17               -19                 -18
{{3.14214 10    , 2.3297 10    , -1.58213 10    },
              -19               -17                 -19
  {-4.98758 10    , 3.33826 10    , -4.98758 10    },
              -18               -19                 -17
  {-1.58213 10    , 2.3297 10    , 3.14214 10    }}
c.L
               -17               -19                 -18
{{3.14214 10    , -4.98758 10    , -1.58213 10    },
              -19               -17                 -19
  {2.3297 10    , 3.33826 10    , 2.3297 10    },
              -18               -19                 -17
  {-1.58213 10    , -4.98758 10    , 3.14214 10    }}
mv=Eigenvectors[L.c]
{{-0.0134705, -0.991403, -0.130148}, {0.997542, -0.0210673, -0.0668282}, {1., 0., 0.}}
```

```
mi=Eigenvectors[c.L]
{{-0.0395695, 0.965515, -0.257323}, {-0.998569, -0.00779015, 0.0529037}, {1., 0., 0.}}
{q,r}=QRDecomposition[N[mv]]
{{{-0.00953636, 0.706204, 0.707944}, {-0.999841, -0.0173831, 0.00387197},
   {-0.0150406, 0.707795, -0.706258}},
  {{1.41254, -0.00542344, -0.0459532}, {0, 0.991612, 0.131289}, {0, 0, -0.0453431}}}
{q,r}=QRDecomposition[N[mi]]
{{{-0.0279889, -0.706324, 0.707336}, {0.999592, -0.0238175, 0.0157699},
   {-0.00570829, -0.707488, -0.706702}},
  {{1.41376, -0.0215213, -0.0301649}, {0, 0.965306, -0.258478}, {0, 0, -0.0359599}}}
MV={{-0.00953636,0.706204,0.707944},{-0.999841,-0.0173831,0.00387197},
{-0.0150406,0.707795,-0.706258}}
{{-0.00953636, 0.706204, 0.707944}, {-0.999841, -0.0173831, 0.00387197},
  {-0.0150406, 0.707795, -0.706258}}
MI={{-0.0279889,-0.706324,0.707336},{0.999592,-0.0238175,0.0157699},
{-0.00570829,-0.707488,-0.706702}}
{{-0.0279889, -0.706324, 0.707336}, {0.999592, -0.0238175, 0.0157699},
  {-0.00570829, -0.707488, -0.706702}}
MV.Transpose[MV]
                 -8              -8              -8                          -8
{{1., -3.3104 10  , -2.07958 10  }, {-3.3104 10  , 0.999999, -7.25082 10  },
               -8              -8
  {-2.07958 10  , -7.25082 10  , 1.}}
MI.Transpose[MI]
                -9              -7              -9                  -8
{{1., 9.3276 10  , -2.43002 10  }, {9.3276 10  , 1., 1.45525 10  },
               -7              -8
  {-2.43002 10  , 1.45525 10  , 1.}}
Inverse[MI]
{{-0.0279889, 0.999592, -0.00570831}, {-0.706323, -0.0238175, -0.707488},
  {0.707335, 0.0157699, -0.706702}}
```

```
Transpose[MV]
{{-0.00953636, -0.999841, -0.0150406}, {0.706204, -0.0173831, 0.707795},
  {0.707944, 0.00387197, -0.706258}}
Cd=Transpose[MV].c.MV
                -11              -11              -14
{{8.43077 10    , 2.35988 10    , -3.4482 10    },
                -11              -11              -14
  {2.35988 10    , 6.94451 10    , -9.09532 10    },
                -14              -14              -11
  {-3.4482 10    , -9.09532 10    , 6.86293 10    }}
Ld=Inverse[MV].L.Transpose[Inverse[MV]]
               -7               -7               -11                -7               -7               -10
{{4.3407 10   , -1.36464 10   , 2.87399 10    }, {-1.36464 10   , 4.76165 10   , 5.25956 10    },
                -11              -10              -7
  {2.87399 10    , 5.25956 10    , 4.80896 10   }}
Wd=Sqrt[Ld.Cd]
               -9               -10                    -11
{{5.77711 10   , 8.75672 10    , 0. + 2.41532 10     I},
                   -10               -9                  -11
  {0. + 5.17697 10     I, 5.46323 10   , 0. + 5.00718 10     I},
                   -11                    -11                -9
  {0. + 4.18009 10     I, 0. + 8.0844 10     I, 5.74487 10   }}
Zd=Wd.Inverse[Cd]
{{71.8268 + 0.000016489 I, -11.7986 + 0.000455333 I, 0.020452 + 0.351937 I},
  {-24.3355 + 6.7861 I, 86.9396 - 2.3051 I, 0.102992 + 0.729952 I},
  {0.00392194 + 0.18782 I, 0.108302 + 1.10032 I, 83.7088 + 0.0015526 I}}
```

```
a={{62.001,-9.86604,0},{-9.866044,71.8671,-9.86604},{0,-9.86604,62.001}}
{{62.001, -9.86604, 0}, {-9.866044, 71.8671, -9.86604}, {0, -9.86604, 62.001}}
c=10^-12.a
            -11              -12                  -12             -11              -12
{{6.2001 10    , -9.86604 10    , 0}, {-9.86604 10    , 7.18671 10    , -9.86604 10    },
                 -12             -11
  {0, -9.86604 10    , 6.2001 10    }}
b={{54.2238,6.76175,0},{6.76175,48.5943,6.76175},{0,6.76175,54.2238}}
{{54.2238, 6.76175, 0}, {6.76175, 48.5943, 6.76175}, {0, 6.76175, 54.2238}}
L=10^-8.b
            -7              -8                  -8              -7              -8
{{5.42238 10   , 6.76175 10   , 0}, {6.76175 10   , 4.85943 10   , 6.76175 10   },
                -8              -7
  {0, 6.76175 10   , 5.42238 10   }}
L.c
             -17              -19              -19
{{3.29522 10    , -4.90268 10    , -6.67117 10    },
               -19              -17              -19
  {-6.01982 10    , 3.35891 10    , -6.0198 10    },
               -19              -19              -17
  {-6.67117 10    , -4.90268 10    , 3.29522 10    }}
c.L
             -17              -19              -19
{{3.29522 10    , -6.0198 10    , -6.67117 10    },
              -19              -17              -19
  {-4.9027 10    , 3.35891 10    , -4.90268 10    },
               -19              -19              -17
  {-6.67117 10    , -6.0198 10    , 3.29522 10    }}
mv=Eigenvectors[L.c]
{{0.152987, -0.882966, 0.443809}, {1., 0., 0.}, {-0.954483, -0.199819, -0.221439}}
```

```
mi=Eigenvectors[c.L]
{{0.159775, -0.83377, 0.528488}, {1., 0., 0.}, {-0.948735, -0.187174, -0.25469}}
{q,r}=QRDecomposition[N[mv]]
{{{-0.109996, -0.718989, 0.686262}, {0.981156, 0.0318036, 0.190583},
   {0.158852, -0.694294, -0.701942}},
  {{-1.39084, -0.0400054, -0.200783}, {0, -0.904409, 0.393244}, {0, 0, 0.225938}}}
{q,r}=QRDecomposition[N[mi]]
{{{-0.115139, -0.720633, 0.68369}, {0.98071, 0.0269794, 0.193597},
   {0.157958, -0.692792, -0.703625}},
  {{-1.38767, -0.0319696, -0.234979}, {0, -0.853923, 0.468987}, {0, 0, 0.262685}}}
MV={{-0.109996,-0.718989,0.686262},{0.981156,0.0318036,0.190583},{0.158852,-0.694294,-0.70194
{{-0.109996, -0.718989, 0.686262}, {0.981156, 0.0318036, 0.190583},
  {0.158852, -0.694294, -0.701942}}
MI={{-0.115139,-0.720633,0.68369},{0.98071,0.0269794,0.193597},{0.157958,-0.692792,-0.703625}
{{-0.115139, -0.720633, 0.68369}, {0.98071, 0.0269794, 0.193597},
  {0.157958, -0.692792, -0.703625}}
MV.Transpose[MV]
                  -7             -7              -7                   -7
{{1., 1.9681 10   , 5.4337 10   }, {1.9681 10   , 1., -6.67932 10   },
             -7              -7
  {5.4337 10   , -6.67932 10   , 1.}}
MI.Transpose[MI]
                  -7             -7              -7                   -7
{{1., 1.1828 10   , 2.74924 10   }, {1.1828 10   , 1., 1.8857 10   },
             -7              -7
  {2.74924 10   , 1.8857 10   , 1.}}
Inverse[MI]
{{-0.115139, 0.98071, 0.157958}, {-0.720632, 0.0269796, -0.692792},
  {0.68369, 0.193597, -0.703625}}
```

Transpose[MV]

```
{{-0.109996, 0.981156, 0.158852}, {-0.718989, 0.0318036, -0.694294},
  {0.686262, 0.190583, -0.701942}}
```

Cd=Transpose[MV].c.MV

```
                -11                -11                -12
{{7.05529 10    , 1.39733 10     , 1.90484 10     },
                -11                -11                -12
  {1.39733 10     , 6.28979 10     , 2.72215 10     },
                -12                -12                -11
  {1.90484 10     , 2.72215 10     , 6.24183 10     }}
```

Ld=Inverse[MV].L.Transpose[Inverse[MV]]

```
               -7                 -8                 -8
{{4.94527 10   , -9.54135 10    , -1.09376 10    },
                -8                 -7                 -8
  {-9.54135 10   , 5.36102 10    , -1.85877 10    },
                -8                 -8                 -7
  {-1.09376 10   , -1.85877 10   , 5.39789 10     }}
```

Wd=Sqrt[Ld.Cd]

```
               -9                 -10                      -11
{{5.79105 10   , 9.37601 10     , 0. + 2.10847 10     I},
                -10                -9                 -10
  {8.50891 10    , 5.68646 10   , 3.42617 10     },
                  -11                  -10                -9
  {0. + 5.65889 10     I, 3.83953 10     , 5.79839 10   }}
```

Zd=Wd.Inverse[Cd]

```
{{82.8163 - 0.00652608 I, -3.38865 - 0.0132032 I, -2.37955 + 0.338572 I},
  {-6.14669, 91.7008, 1.67743}, {-3.05471 + 0.83933 I, 2.76379 - 0.185706 I,
   92.8683 - 0.0175152 I}}
```

In[49]:=

```
a={{6.62081,-1.49769,0},{-1.49769,8.11849,-1.49769},
{0,-1.49769,6.62081}}
```

Out[49]=

```
{{6.62081, -1.49769, 0}, {-1.49769, 8.11849, -1.49769}, {0, -1.49769, 6.62081}}
```

In[50]:=

```
c=10^-11.a
```

Out[50]=

```
                -11              -11                    -11             -11             -11
{{6.62081 10    , -1.49769 10    , 0}, {-1.49769 10    , 8.11849 10    , -1.49769 10    },
                  -11              -11
  {0, -1.49769 10    , 6.62081 10    }}
```

In[51]:=

```
b={{49.9168,9.22541,0},{9.22541,44.6238,9.22541},
{3.93243,9.22541,49.9168}}
```

Out[51]=

```
{{49.9168, 9.22541, 0}, {9.22541, 44.6238, 9.22541}, {3.93243, 9.22541, 49.9168}}
```

In[52]:=

```
L=10^-8.b
```

Out[52]=

```
               -7             -8                   -8             -7             -8
{{4.99168 10   , 9.22541 10   , 0}, {9.22541 10   , 4.46238 10   , 9.22541 10   },
                 -8             -8                  -7
  {3.93243 10   , 9.22541 10   , 4.99168 10   }}
```

In[53]:=

```
L.c
```

Out[53]=

```
                -17              -20              -18
{{3.16673 10    , 1.36507 10    , -1.38168 10    },
                -19              -17              -19
 {-5.75293 10   , 3.34644 10    , -5.75293 10    },
                -18              -19              -17
 {1.22191 10    , -5.75305 10    , 3.16673 10    }}
```

In[54]:=

```
c.L
```

Out[54]=

```
                -17              -19              -18
{{3.16673 10    , -5.75293 10    , -1.38168 10    },
                -19              -17              -20
 {-5.75305 10   , 3.34644 10    , 1.36507 10    },
                -18              -19              -17
 {1.22191 10    , -5.75293 10    , 3.16673 10    }}
```

In[55]:=

```
mv=Eigenvectors[L.c]
```

Out[55]=

```
{{0.72564, 0.432162, -0.535428}, {-0.852667, -0.222548, 0.472685}, {1., 0., 0.}}
```

In[56]:=

```
mi=Eigenvectors[c.L]
```

Out[56]=

```
{{0.217597, 0.815066, -0.536953}, {-0.879959, -0.202358, 0.429794}, {1., 0., 0.}}
```

In[57]:=

```
{q,r}=QRDecomposition[N[mv]]
```

Out[57]=

```
{{{-0.483374, 0.567991, -0.666135}, {-0.767412, 0.091207, 0.634634},
    {-0.421223, -0.817965, -0.391796}},
  {{-1.5012, -0.335301, 0.527293}, {0, -0.351944, 0.454006}, {0, 0, -0.161106}}}
```

In[58]:=

```
{q,r}=QRDecomposition[N[mi]]
```

Out[58]=

```
{{{-0.161219, 0.651969, -0.740908}, {-0.968845, 0.0384614, 0.244662},
    {-0.188009, -0.757269, -0.625456}},
  {{-1.3497, -0.263336, 0.366779}, {0, -0.797456, 0.536755}, {0, 0, -0.224518}}}
```

In[59]:=

```
MV={{-0.483374,0.567991,-0.666135},{-0.767412,0.091207,0.634634},
{-0.421223,-0.817965,-0.391796}}
```

Out[59]=

```
{{-0.483374, 0.567991, -0.666135}, {-0.767412, 0.091207, 0.634634},
  {-0.421223, -0.817965, -0.391796}}
```

In[60]:=

```
MI={{-0.161219,0.651969,-0.740908},{-0.968845,0.0384614,0.244662},
{-0.188009,-0.757269,-0.625456}}
```

Out[60]=

```
{{-0.161219, 0.651969, -0.740908}, {-0.968845, 0.0384614, 0.244662},
  {-0.188009, -0.757269, -0.625456}}
```

In[61]:=

```
MV.Transpose[MV]
```

Out[61]=

$$\begin{pmatrix} 1. & -1.56365\times10^{-7} & 5.16547\times10^{-7} \\ -1.56365\times10^{-7} & 1. & 3.88457\times10^{-7} \\ 5.16547\times10^{-7} & 3.88457\times10^{-7} & 1. \end{pmatrix}$$

In[62]:=

```
MI.Transpose[MI]
```

Out[62]=

```
                    -7             -8                  -7                          -7
{{1., -1.70544 10   , 6.4358 10   }, {-1.70544 10   , 0.999999, 6.37816 10   },
                 -8             -7
  {6.4358 10   , 6.37816 10   , 0.999999}}
```

In[63]:=

```
Inverse[MI]
```

Out[63]=

```
{{-0.161219, -0.968845, -0.188009}, {0.651969, 0.038462, -0.75727},
  {-0.740908, 0.244662, -0.625457}}
```

In[64]:=

```
Transpose[MV]
```

Out[64]=

```
{{-0.483374, -0.767412, -0.421223}, {0.567991, 0.091207, -0.817965},
  {-0.666135, 0.634634, -0.391796}}
```

In[65]:=

```
Cd=Transpose[MV].c.MV
```

Out[65]=

```
                 -11              -12              -11
{{5.42344 10    , -2.68565 10    , -1.08553 10    },
                -12              -11              -12
  {-2.68565 10    , 6.70156 10    , 4.68799 10    },
                -11              -12              -11
  {-1.08553 10    , 4.68799 10    , 9.23511 10    }}
```

In[66]:=

```
Ld=Inverse[MV].L.Transpose[Inverse[MV]]
```

Out[66]=

```
                -7              -9              -8              -8              -7              -9
{{6.04088 10   , 4.38216 10   , 5.87485 10   }, {2.93387 10   , 4.76251 10   , -5.17391 10   },
              -8              -8              -7
  {5.51619 10   , -3.53518 10   , 3.64234 10   }}
```

In[67]:=

```
Wd=Sqrt[Ld.Cd]
```

Out[67]=

```
               -9                  -9                  -9
{{5.66682 10   , 0. + 1.0263 10    I, 0. + 1.05429 10    I},
              -10             -9              -9
  {6.06867 10    , 5.64032 10   , 1.19848 10   },
                 -10                 -10              -9
  {0. + 9.31269 10     I, 0. + 8.99857 10     I, 5.73349 10   }}
```

In[68]:=

```
Zd=Wd.Inverse[Cd]
```

Out[68]=

```
{{107.143 + 2.93099 I, 3.42492 + 14.6611 I, 12.4202 + 11.0164 I},
  {17.5098, 84.1129, 10.7658}, {12.5663 + 18.1514 I, -3.95676 + 14.0557 I,
   63.7616 + 1.42009 I}}
```

APPENDIX C

Experimental results printouts for Experiment 4 of Chapter 5 ($s = w = 500$ μm), see Fig. 5.6.

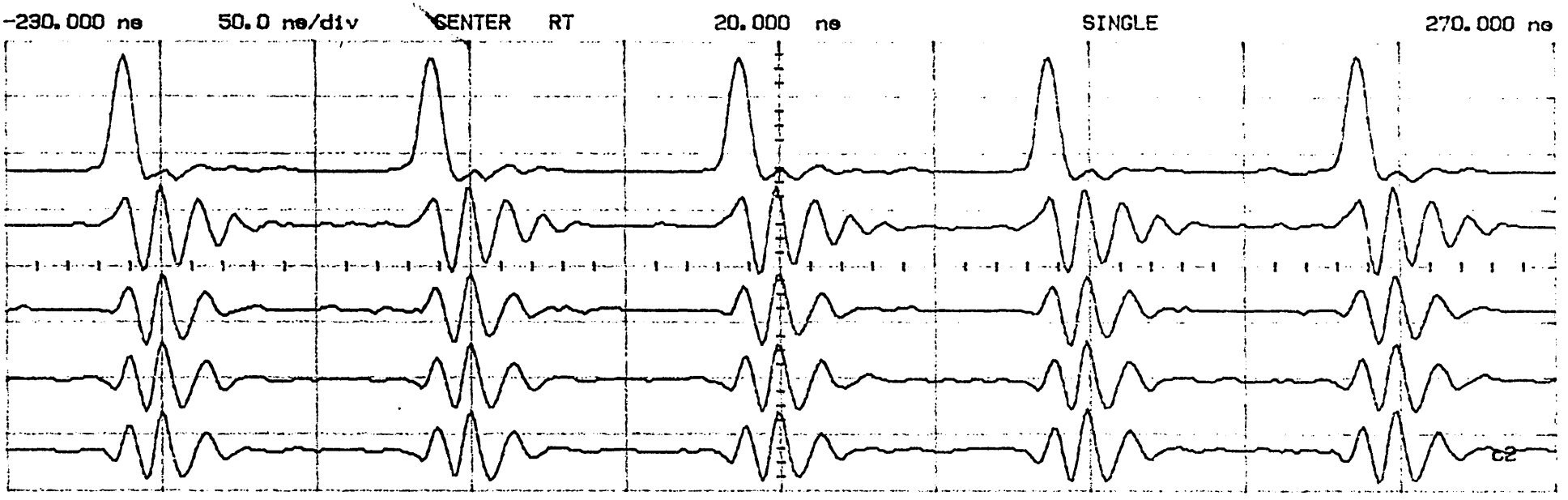

	Sensitivity	Offset	Probe	Coupling	Impedance
Channel 2	99.4 mV/div	322.853 mV	9.937:1	dc	1M ohm
WMemory 1	497 mV/div	-1.38634 V	50.0 ns/div	20.000 ns	RealTime
WMemory 2	99.4 mV/div	-74.5275 mV	50.0 ns/div	20.000 ns	RealTime
WMemory 3	99.4 mV/div	74.5275 mV	50.0 ns/div	20.000 ns	RealTime
WMemory 4	99.4 mV/div	198.740 mV	50.0 ns/div	20.000 ns	RealTime

Trigger Mode: Edge
On the Positive Edge of External
Trigger Level(s)
External = 20.7500 mV (noise reject ON, coupling LFREJ)
Holdoff = 40.000 ns

Printed: 15 APR 1997 at 11:16:00

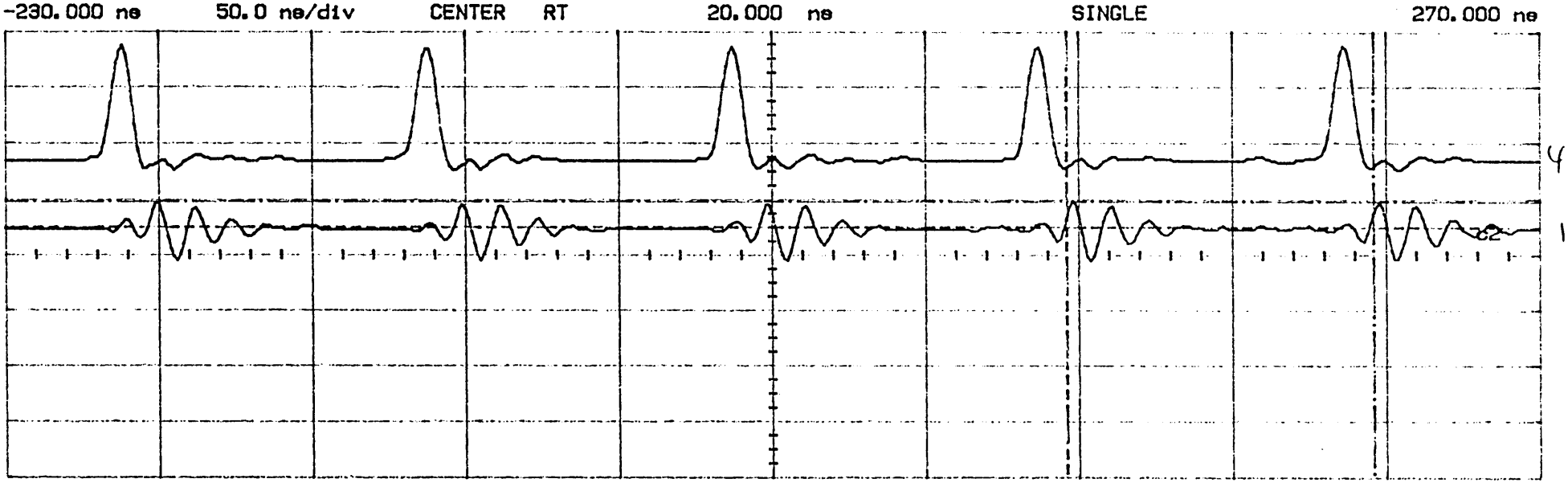

	Sensitivity	Offset	Probe	Coupling	Impedance
Channel 2	99.4 mV/div	-49.6850 mV	9.937:1	dc	1M ohm
WMemory 1	497 mV/div	-1.38634 V	50.0 ns/div	20.000 ns	RealTime

Trigger Mode: Edge
On the Positive Edge of External
Trigger Level(s)
External = 20.7500 mV (noise reject ON, coupling LFREJ)
Holdoff = 40.000 ns

Markers

Y2marker(c2)	=	46.5797 mV
Y1marker(c2)	=	0.00000 V
delta Y	=	46.5797 mV
X2marker(c2)	=	216.000 ns
X1marker(c2)	=	116.000 ns
delta X	=	100.000 ns
1/delta X	=	10.0000 MHz

Printed: 15 APR 1997 at 10:53:08

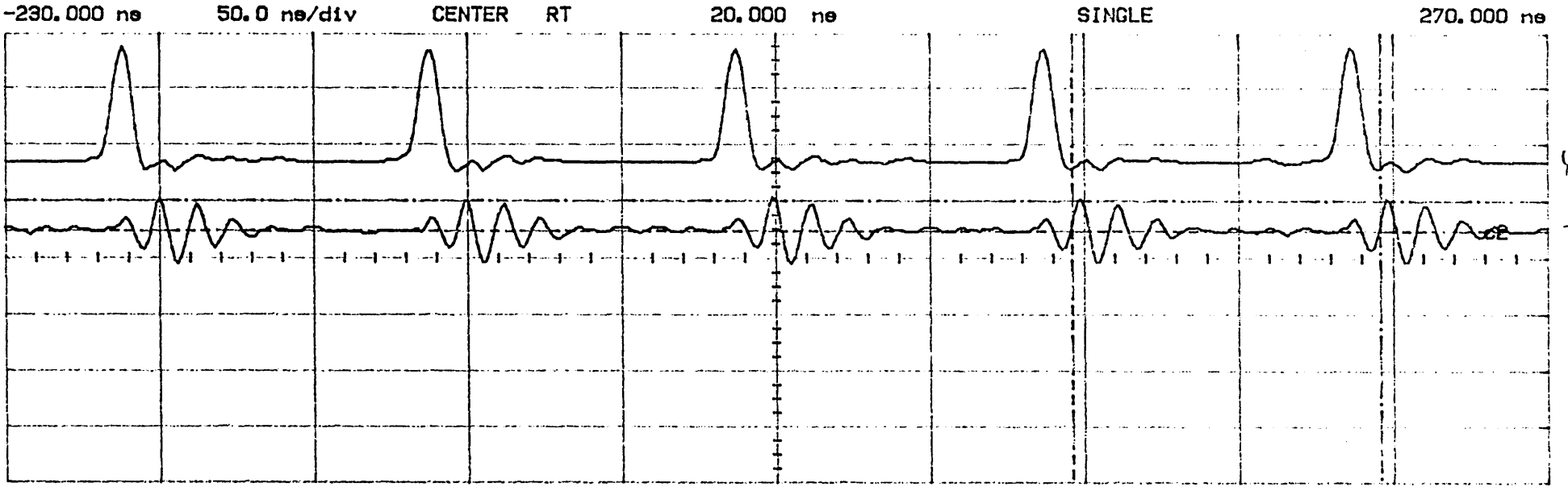

	Sensitivity	Offset	Probe	Coupling	Impedance
Channel 2	99.4 mV/div	-49.6850 mV	9.937:1	dc	1M ohm
WMemory 1	497 mV/div	-1.36634 V	50.0 ns/div	20.000 ns	RealTime

Trigger Mode: Edge
On the Positive Edge of External
Trigger Level(s)
External = 20.7500 mV (noise reject ON, coupling LFREJ)
Holdoff = 40.000 ns

Markers	
Y2marker(c2)	= 49.6850 mV
Y1marker(c2)	= -3.10531 mV
delta Y	= 52.7903 mV
X2marker(c2)	= 216.000 ns
X1marker(c2)	= 116.000 ns
delta X	= 100.000 ns
1/delta X	= 10.0000 MHz

Printed: 15 APR 1997 at 10:42:37

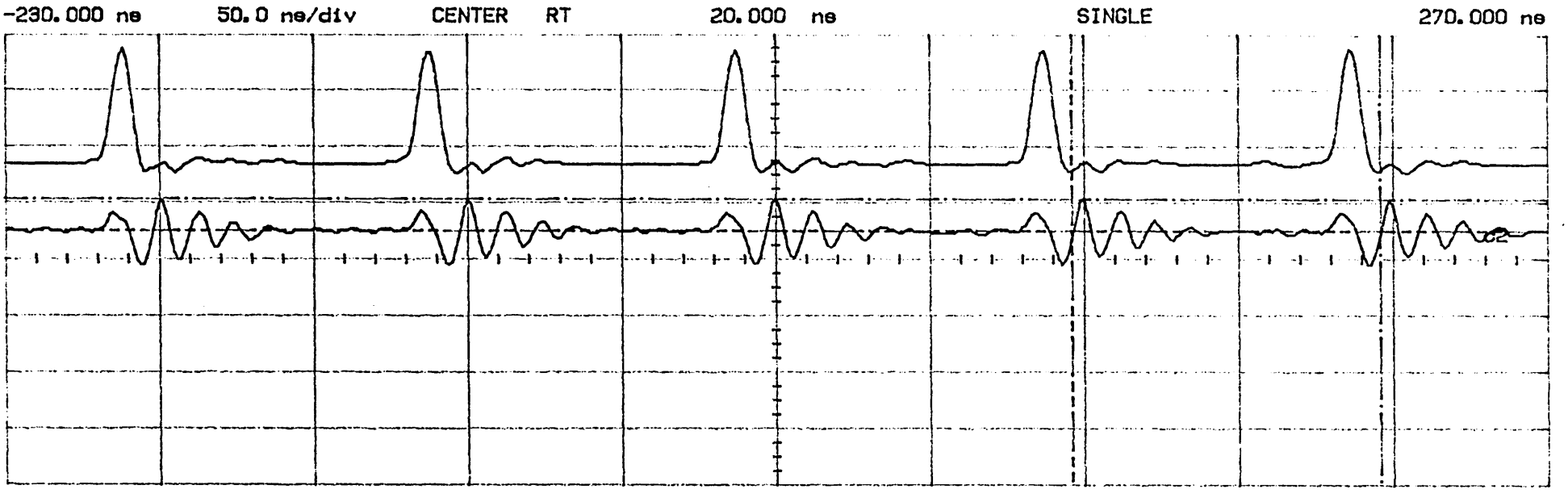

	Sensitivity	Offset	Probe	Coupling	Impedance
Channel 2	99.4 mV/div	-49.6850 mV	9.937:1	dc	1M ohm
WMemory 1	497 mV/div	-1.36634 V	50.0 ns/div	20.000 ns	RealTime

Trigger Mode: Edge
On the Positive Edge of External
Trigger Level(s)
External = 20.7500 mV (noise reject ON, coupling LFREJ)
Holdoff = 40.000 ns

Markers

Y2marker(c2)	=	55.8956 mV
Y1marker(c2)	=	0.00000 V
delta Y	=	55.8956 mV
X2marker(c2)	=	216.000 ns
X1marker(c2)	=	116.000 ns
delta X	=	100.000 ns
1/delta X	=	10.0000 MHz

Printed: 15 APR 1997 at 10:31:34

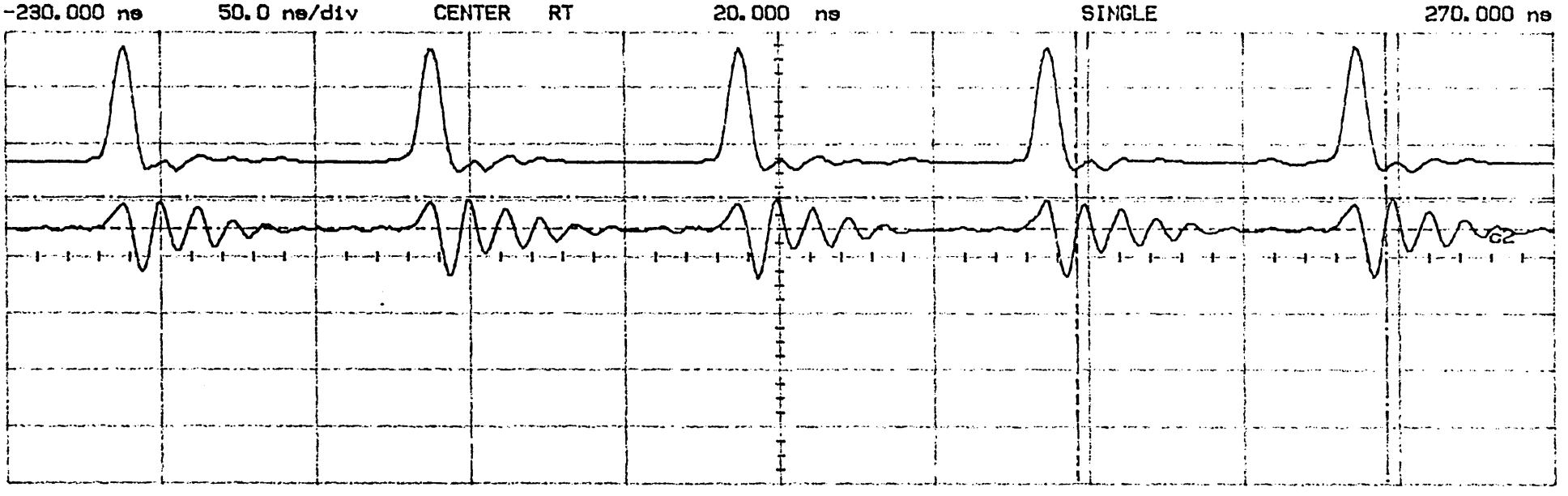

	Sensitivity	Offset	Probe	Coupling	Impedance
Channel 2	99.4 mV/div	-49.6850 mV	9.937:1	dc	1M ohm
WMemory 1	497 mV/div	-1.38634 V	50.0 ns/div	20.000 ns	RealTime

Trigger Mode: Edge
On the Positive Edge of External
Trigger Level(s)
External = 20.7500 mV (noise reject ON, coupling LFREJ)
Holdoff = 40.000 ns

Markers

Y2marker(c2)	=	55.8956 mV
Y1marker(c2)	=	0.00000 V
delta Y	=	55.8956 mV
X2marker(c2)	=	216.000 ns
X1marker(c2)	=	116.000 ns
delta X	=	100.000 ns
1/delta X	=	10.0000 MHz

Printed: 15 APR 1997 at 10:36:59

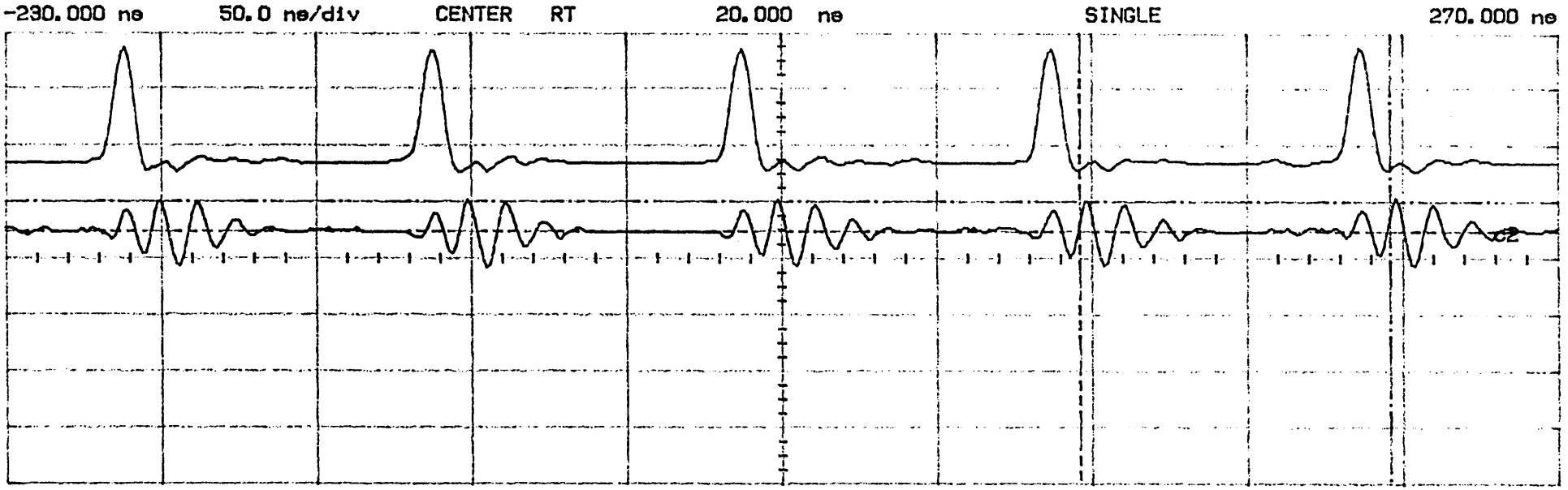

	Sensitivity	Offset	Probe	Coupling	Impedance
Channel 2	99.4 mV/div	-49.6850 mV	9.937:1	dc	1M ohm
WMemory 1	497 mV/div	-1.38834 V	50.0 ns/div	20.000 ns	RealTime

Trigger Mode: Edge
On the Positive Edge of External
Trigger Level(s)
External = 20.7500 mV (noise reject ON, coupling LFREJ)
Holdoff = 40.000 ns

Markers

Y2marker(c2)	=	49.6850 mV
Y1marker(c2)	=	-3.10531 mV
delta Y	=	52.7903 mV
X2marker(c2)	=	216.000 ns
X1marker(c2)	=	116.000 ns
delta X	=	100.000 ns
1/delta X	=	10.0000 MHz

Printed: 15 APR 1997 at 10:48:02

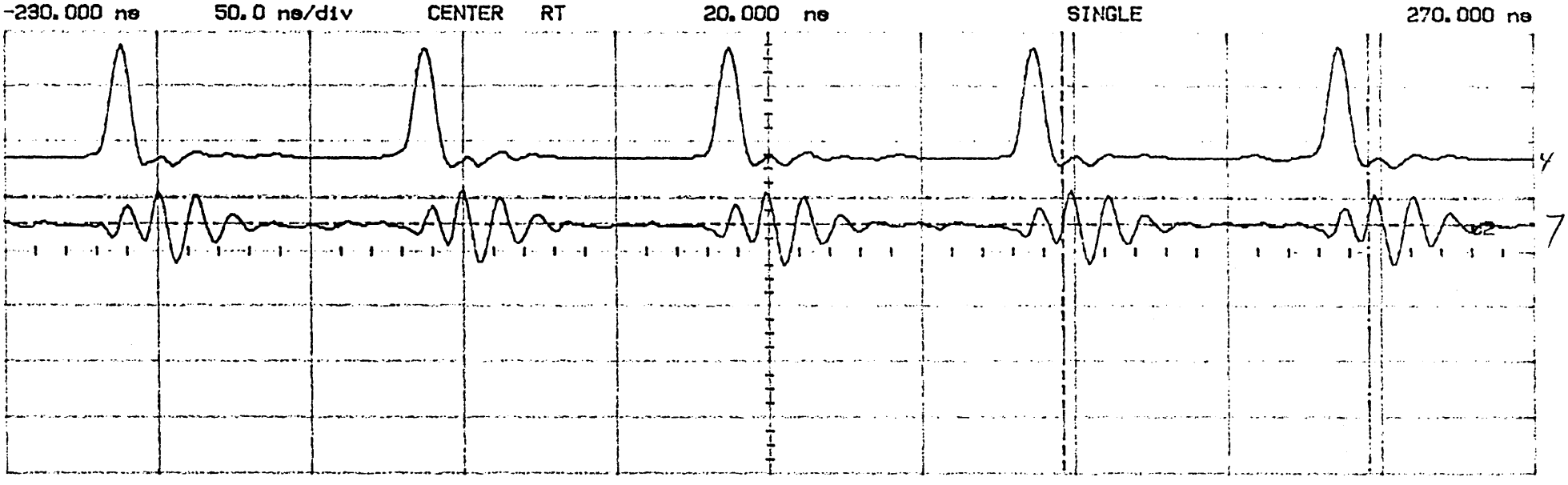

	Sensitivity	Offset	Probe	Coupling	Impedance
Channel 2	99.4 mV/div	-49.6850 mV	9.937:1	dc	1M ohm
WMemory 1	497 mV/div	-1.38634 V	50.0 ns/div	20.000 ns	RealTime

Trigger Mode: Edge
On the Positive Edge of External
Trigger Level(s)
External = 20.7500 mV (noise reject ON, coupling LFREJ)
Holdoff = 40.000 ns

Markers		
Y2marker(c2)	=	46.5797 mV
Y1marker(c2)	=	0.00000 V
delta Y	=	46.5797 mV
X2marker(c2)	=	216.000 ns
X1marker(c2)	=	116.000 ns
delta X	=	100.000 ns
1/delta X	=	10.0000 MHz

Printed: 15 APR 1997 at 11:01:43

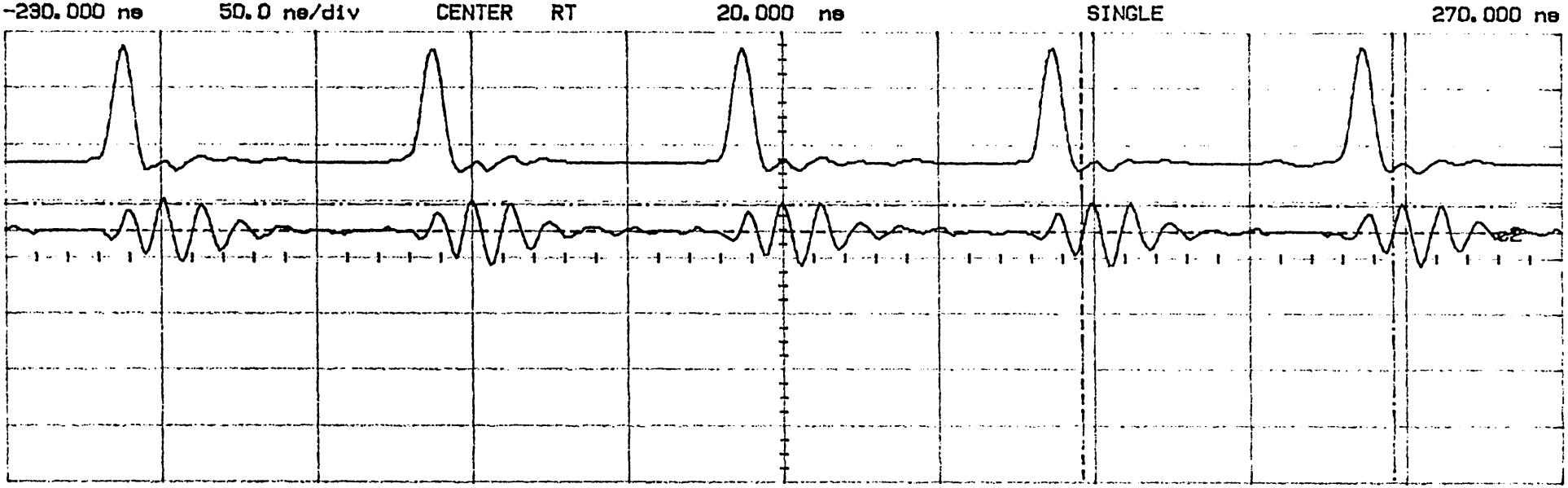

	Sensitivity	Offset	Probe	Coupling	Impedance
Channel 2	99.4 mV/div	-49.6850 mV	9.937:1	dc	1M ohm
WMemory 1	497 mV/div	-1.36834 V	50.0 ns/div	20.000 ns	RealTime

Trigger Mode: Edge
On the Positive Edge of External
Trigger Level(s)
External = 20.7500 mV (noise reject ON, coupling LFREJ)
Holdoff = 40.000 ns

Markers

Y2marker(c2)	=	43.4744 mV
Y1marker(c2)	=	-3.10531 mV
delta Y	=	46.5797 mV
X2marker(c2)	=	216.000 ns
X1marker(c2)	=	116.000 ns
delta X	=	100.000 ns
1/delta X	=	10.0000 MHz

Printed: 15 APR 1997 at 11:07:38

APPENDIX D

List of simulation printouts using SPICE:

D1. Crosstalk simulation for the 3-coupled nonuniformly spaced microstrip lines.

D2. Crosstalk simulation for the 4-coupled strictly nonuniform microstrip lines.

D3. Crosstalk simulation for the optimised 3-coupled microstrip lines.

* C:\MSIMEV63\GAIN.SCH

Date/Time run: 12/17/97 16:46:21 Temperature: 27.0

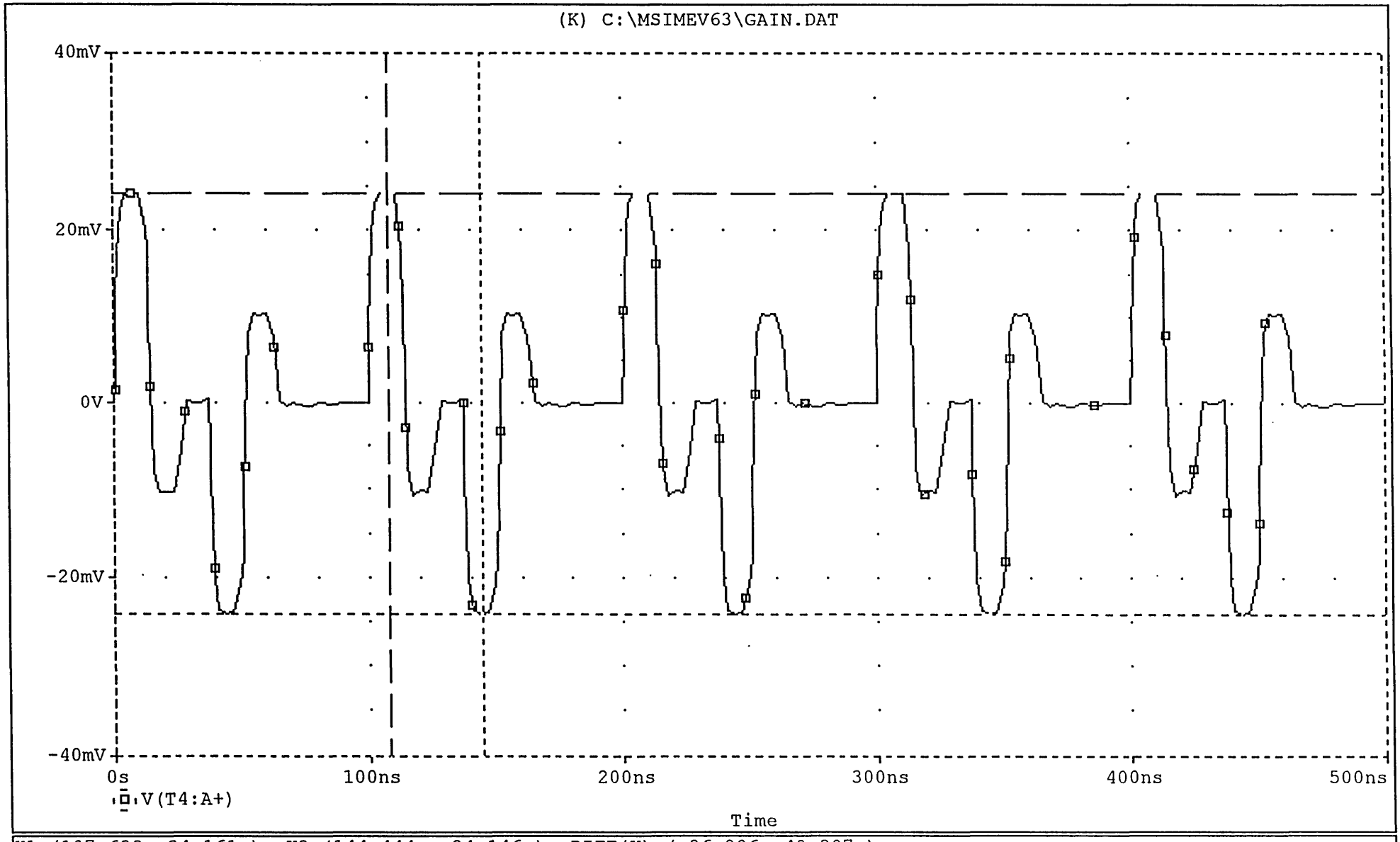

K1:(107.639n,24.161m) K2:(144.444n,-24.146m) DIFF(K):(-36.806n,48.307m)

Date: December 17, 1997 Page 1 Time: 16:47:33

* C:\MSIMEV63\GAIN.SCH

Date/Time run: 12/17/97 16:46:21

Temperature: 27.0

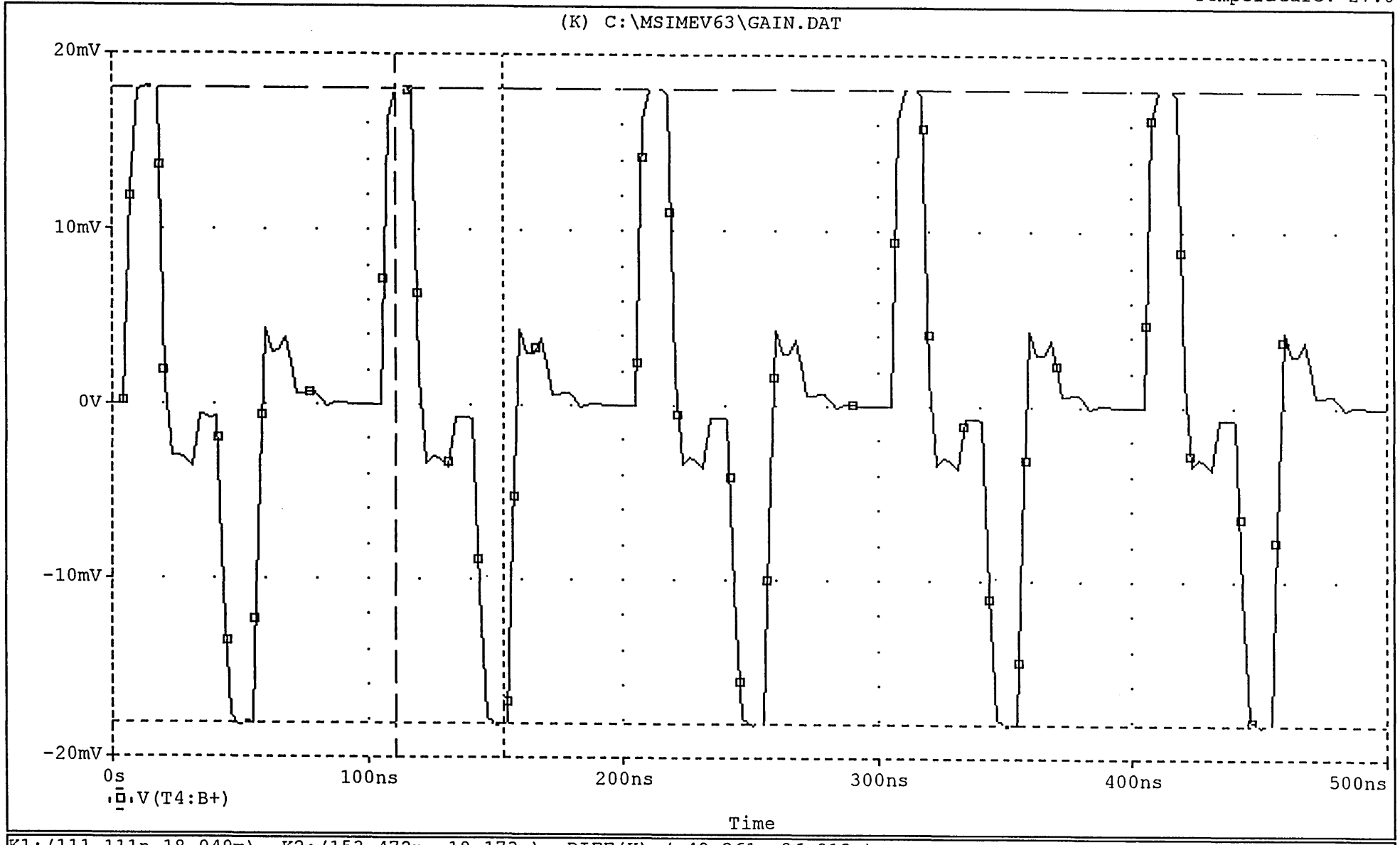

K1:(111.111n,18.040m) K2:(153.472n,-18.173m) DIFF(K):(-42.361n,36.213m)

Date: December 17, 1997

Time: 16:49:16

* C:\MSIMEV63\GAIN.SCH

Date/Time run: 12/17/97 16:51:55

Temperature: 27.0

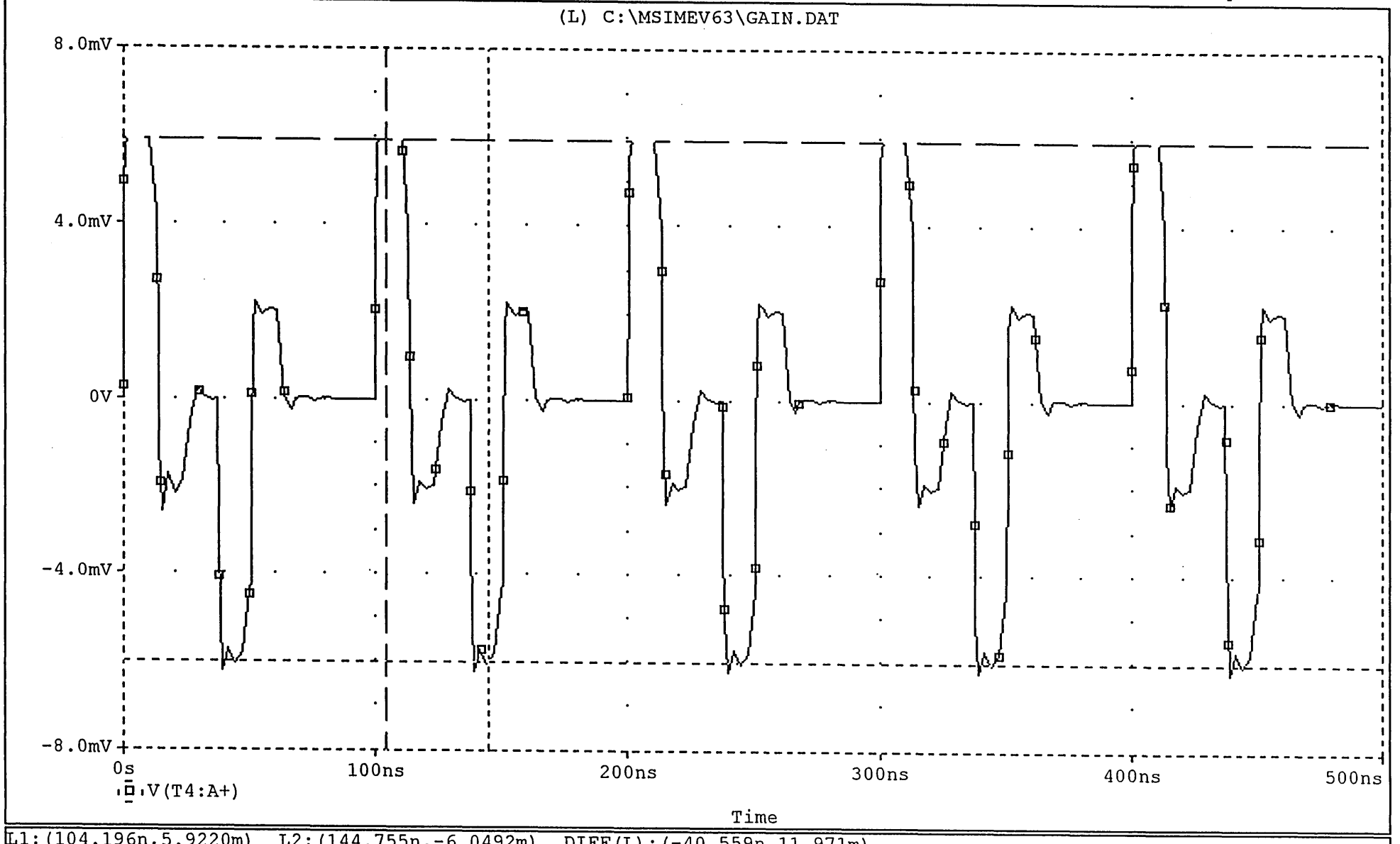

L1:(104.196n,5.9220m) L2:(144.755n,-6.0492m) DIFF(L):(-40.559n,11.971m)

Date: December 17, 1997

Time: 16:52:27

* C:\MSIMEV63\GAIN.SCH

Date/Time run: 12/17/97 16:51:55 Temperature: 27.0

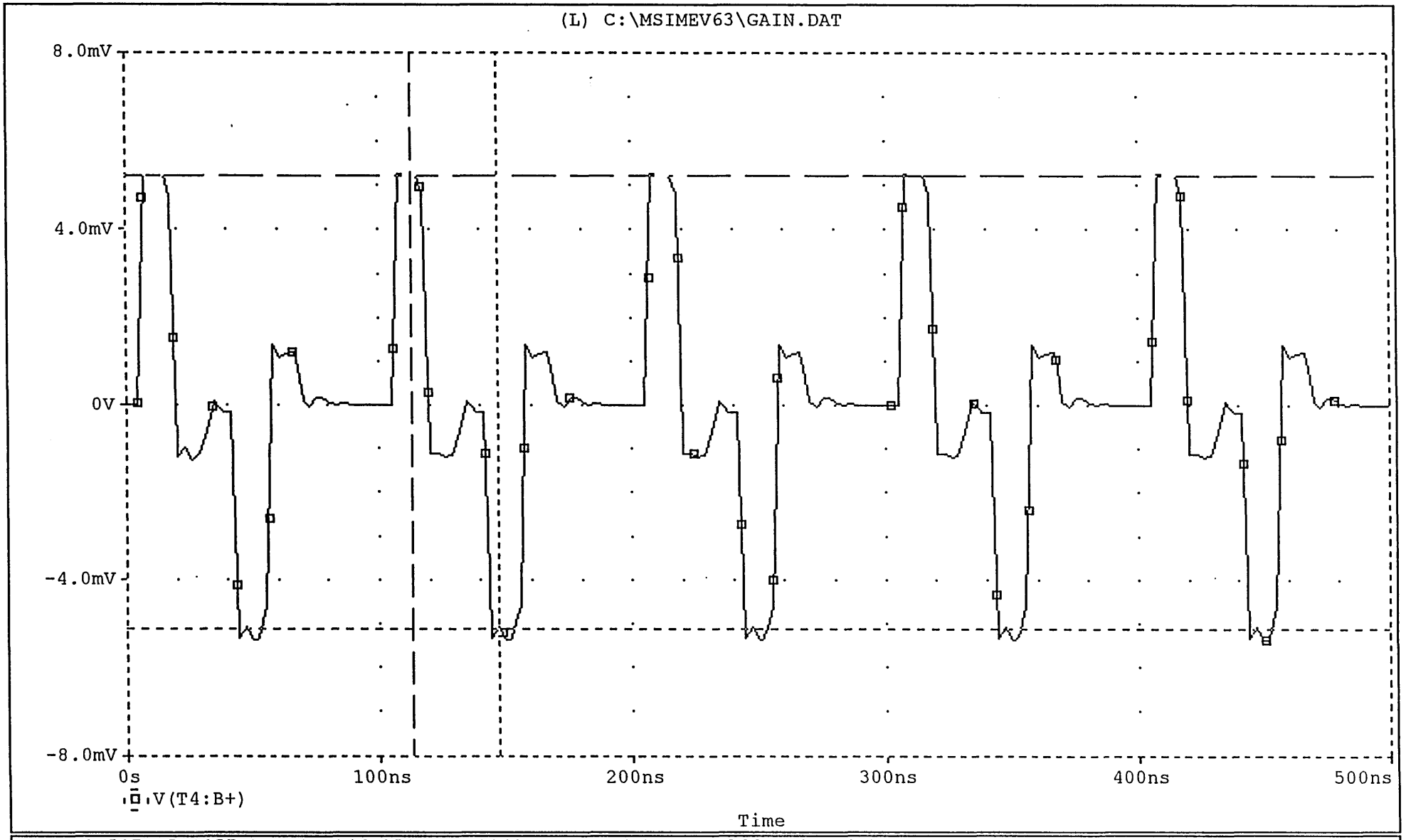

L1:(112.587n,5.2057m) L2:(146.853n,-5.1142m) DIFF(L):(-34.266n,10.320m)

* C:\MSIMEV63\GAIN.SCH

Date/Time run: 12/17/97 16:57:21 Temperature: 27.0

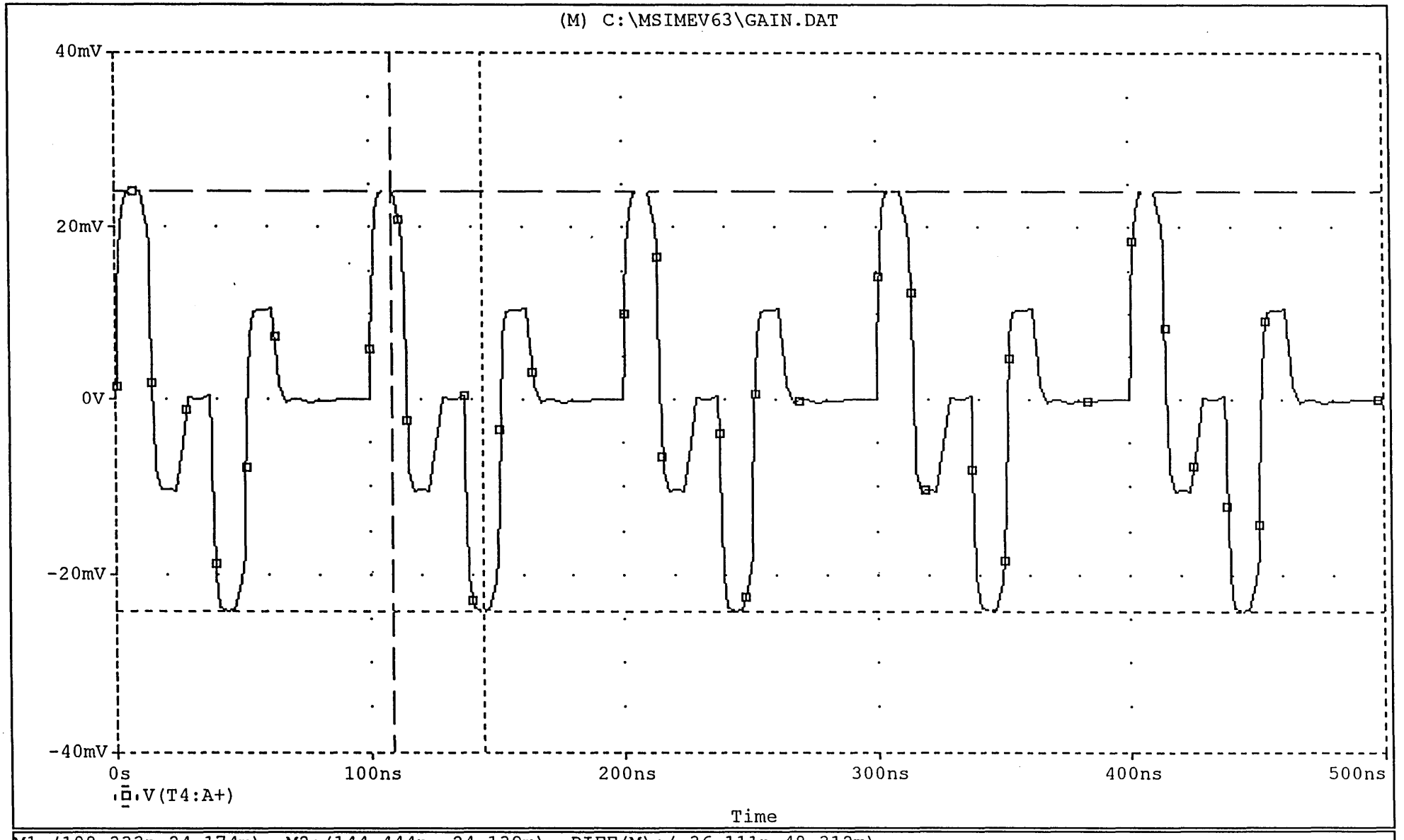

M1:(108.333n,24.174m) M2:(144.444n,-24.139m) DIFF(M):(-36.111n,48.312m)

Date: December 17, 1997 Page 1 Time: 16:58:06

* C:\MSIMEV63\GAIN.SCH

Date/Time run: 12/17/97 16:57:21 Temperature: 27.0

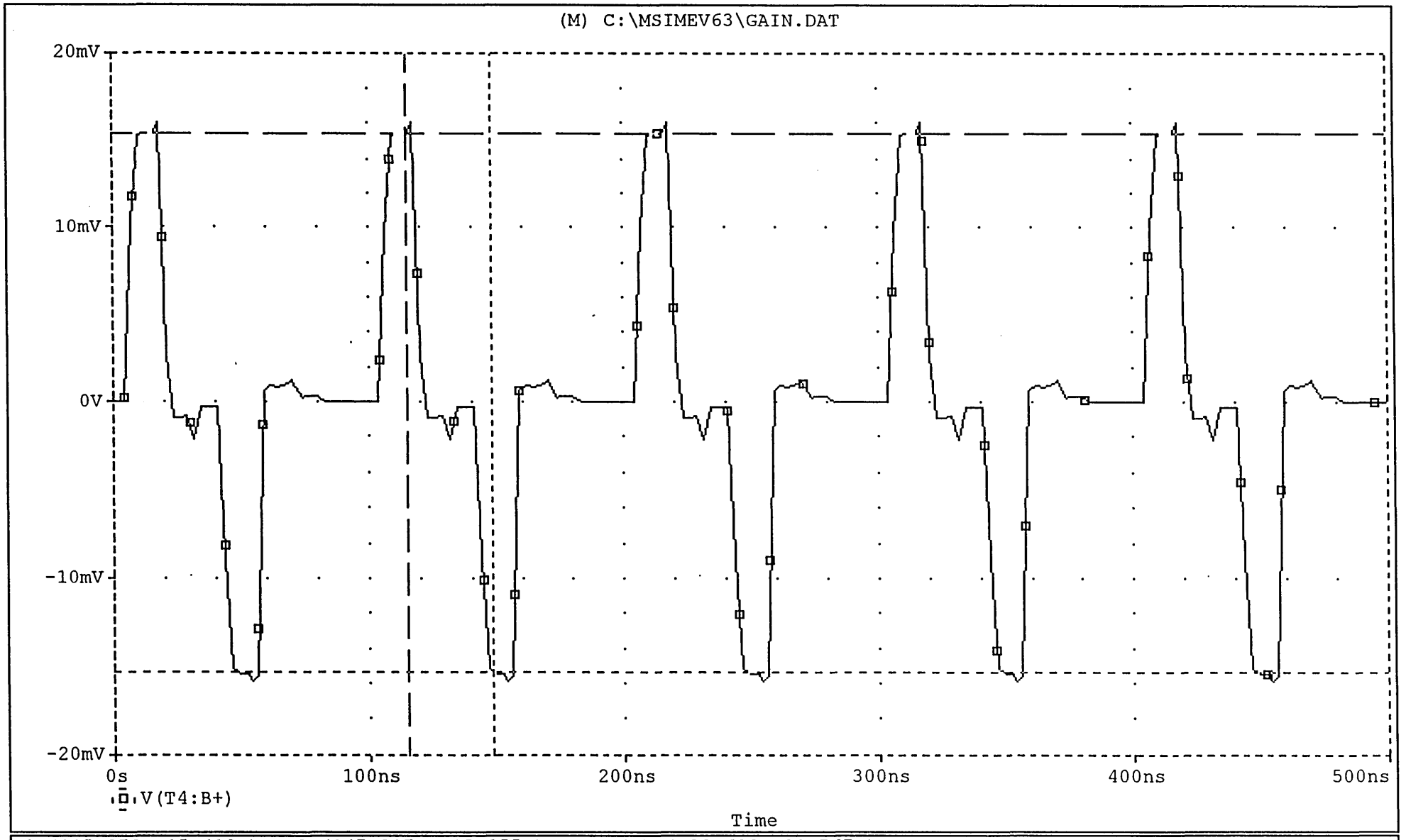

M1:(115.278n,15.412m) M2:(147.917n,-15.355m) DIFF(M):(-32.639n,30.767m)

* C:\MSIMEV63\GAIN.SCH

Date/Time run: 12/17/97 17:02:46 Temperature: 27.0

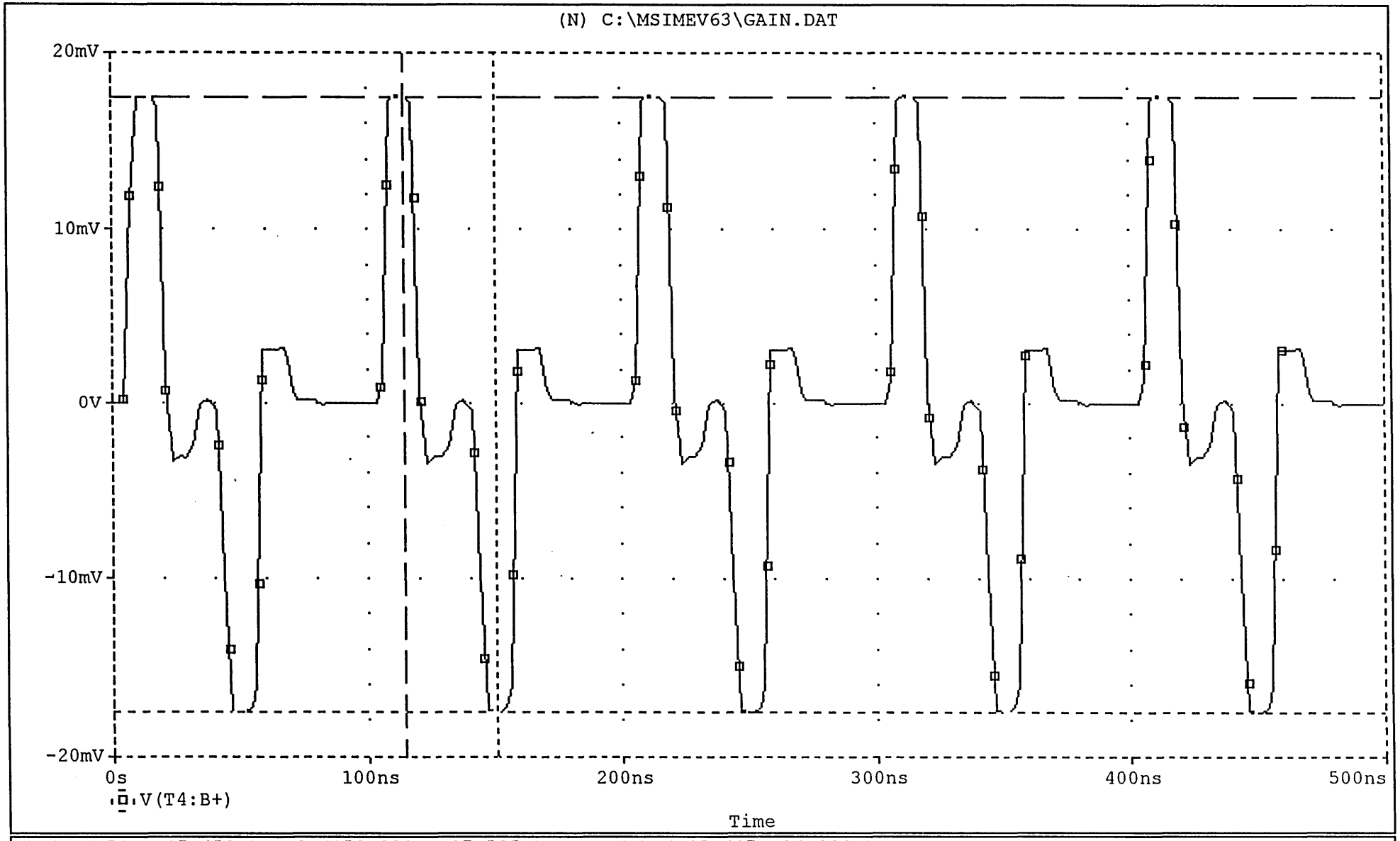

N1:(114.583n,17.459m) N2:(150.000n,-17.535m) DIFF(N):(-35.417n,34.993m)

Date: December 17, 1997 Page 1 Time: 17:04:04

* C:\MSIMEV63\GAIN.SCH

Date/Time run: 12/17/97 16:41:02 Temperature: 27.0

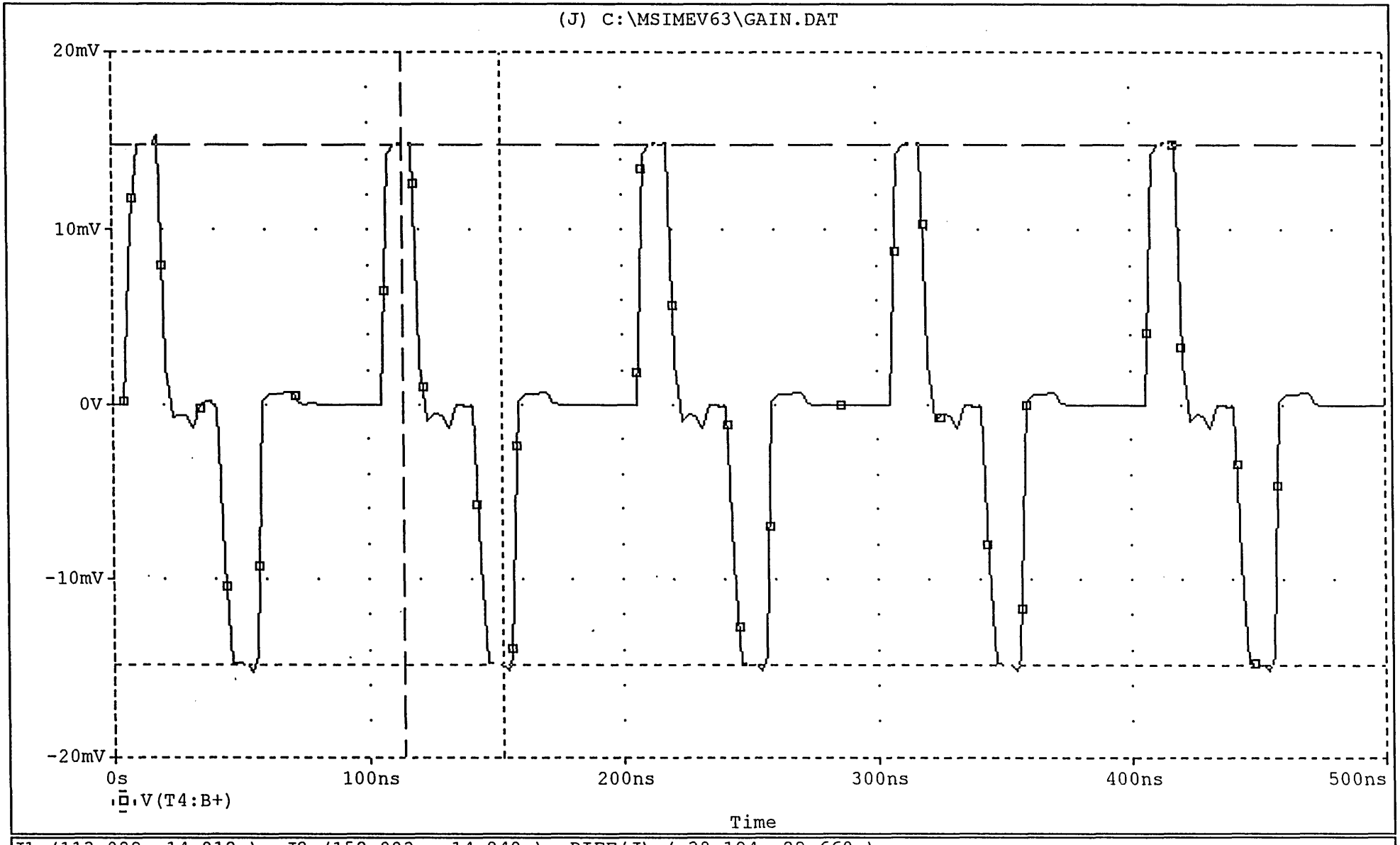

J1:(113.889n,14.812m) J2:(152.083n,-14.848m) DIFF(J):(-38.194n,29.660m)

Date: December 17, 1997 Page 1 Time: 16:43:32

* C:\MSIMEV63\GAIN.SCH

Date/Time run: 12/17/97 16:41:02

Temperature: 27.0

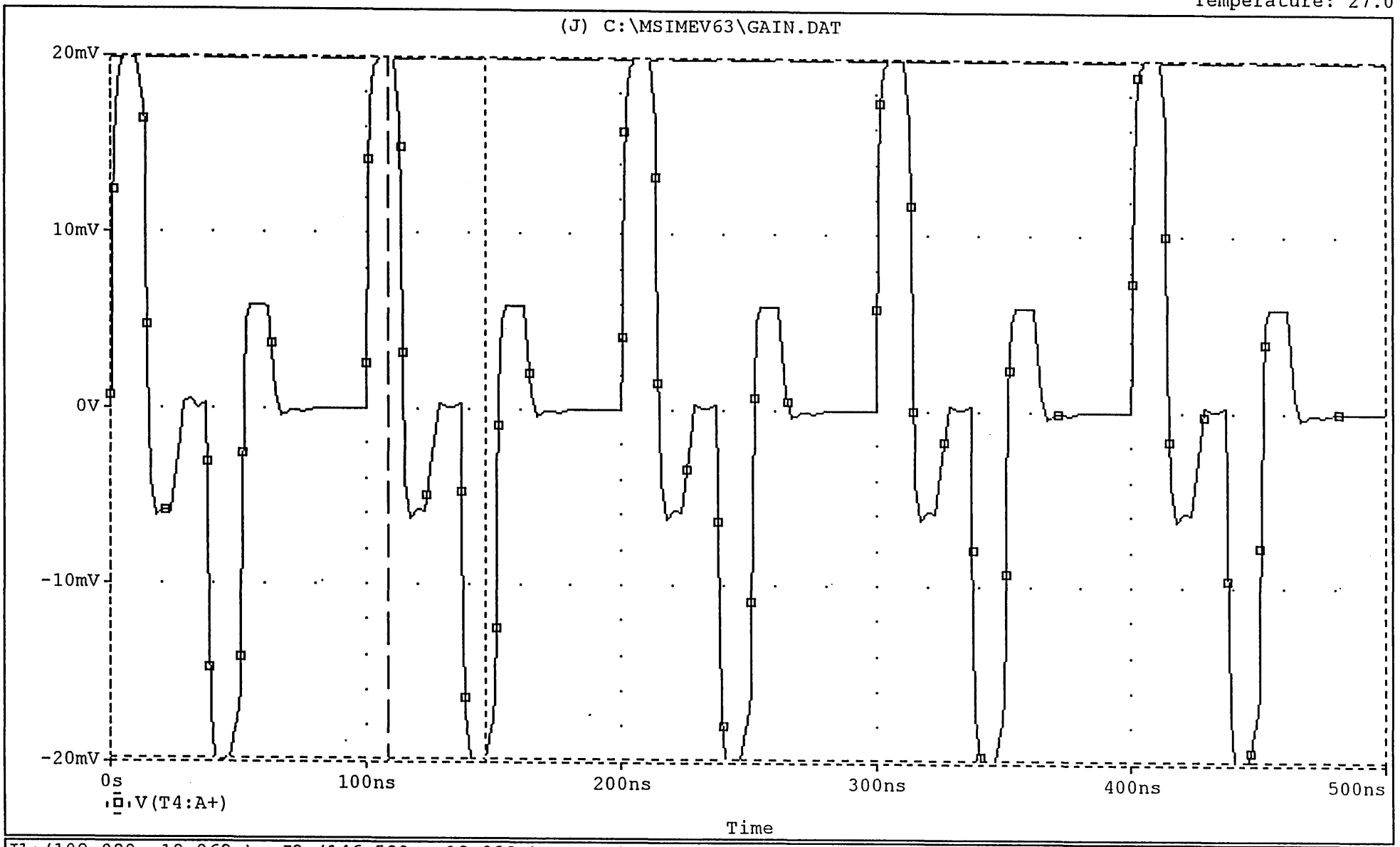

J1:(109.028n,19.862m) J2:(146.528n,-19.838m) DIFF(J):(-37.500n,39.699m)

* C:\MSIMEV63\GAIN.SCH

Date/Time run: 12/17/97 16:33:19

Temperature: 27.0

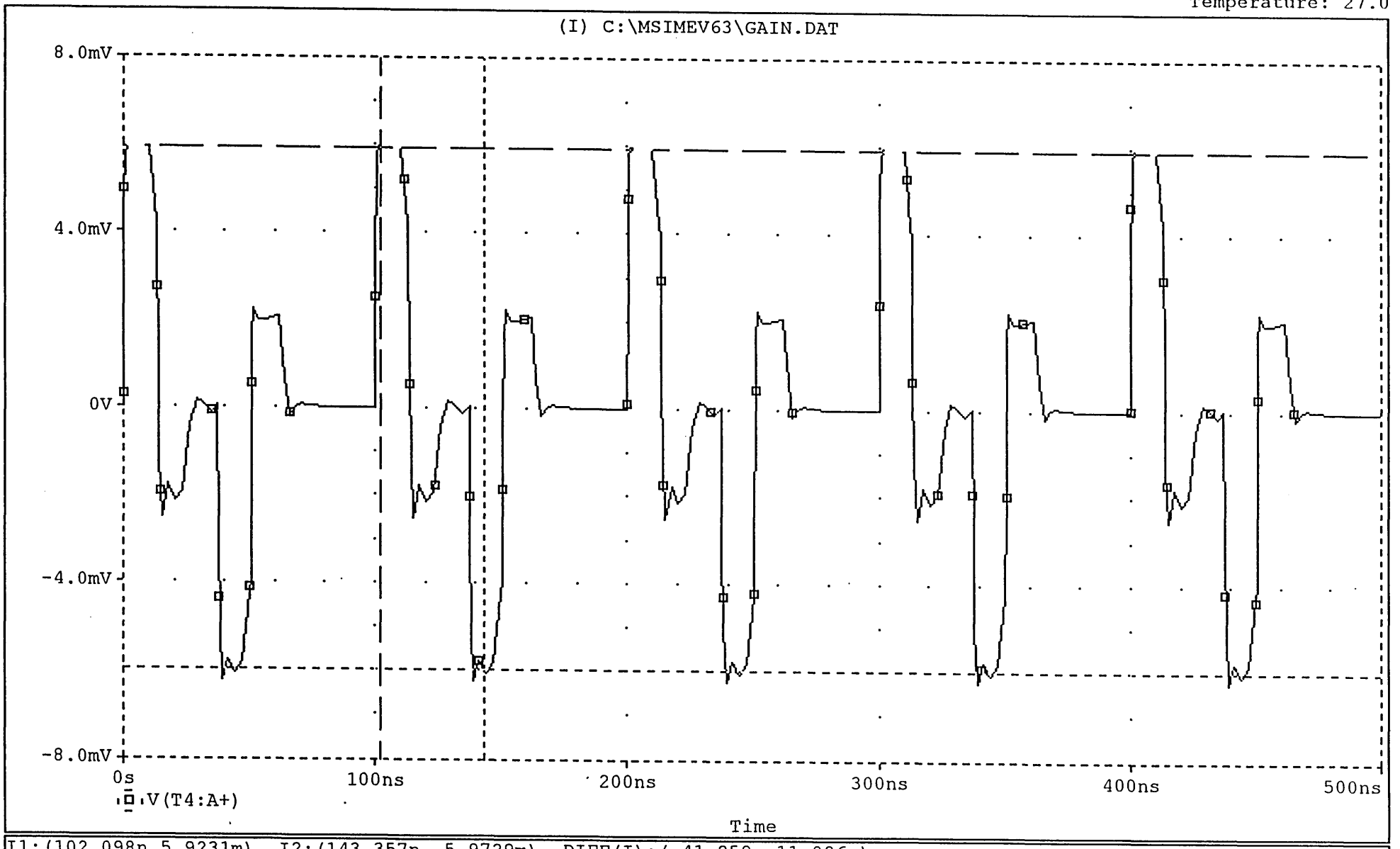

I1:(102.098n,5.9231m) I2:(143.357n,-5.9729m) DIFF(I):(-41.259n,11.896m)

Date: December 17, 1997

Time: 16:38:34

* C:\MSIMEV63\GAIN.SCH

Date/Time run: 12/17/97 16:33:19 Temperature: 27.0

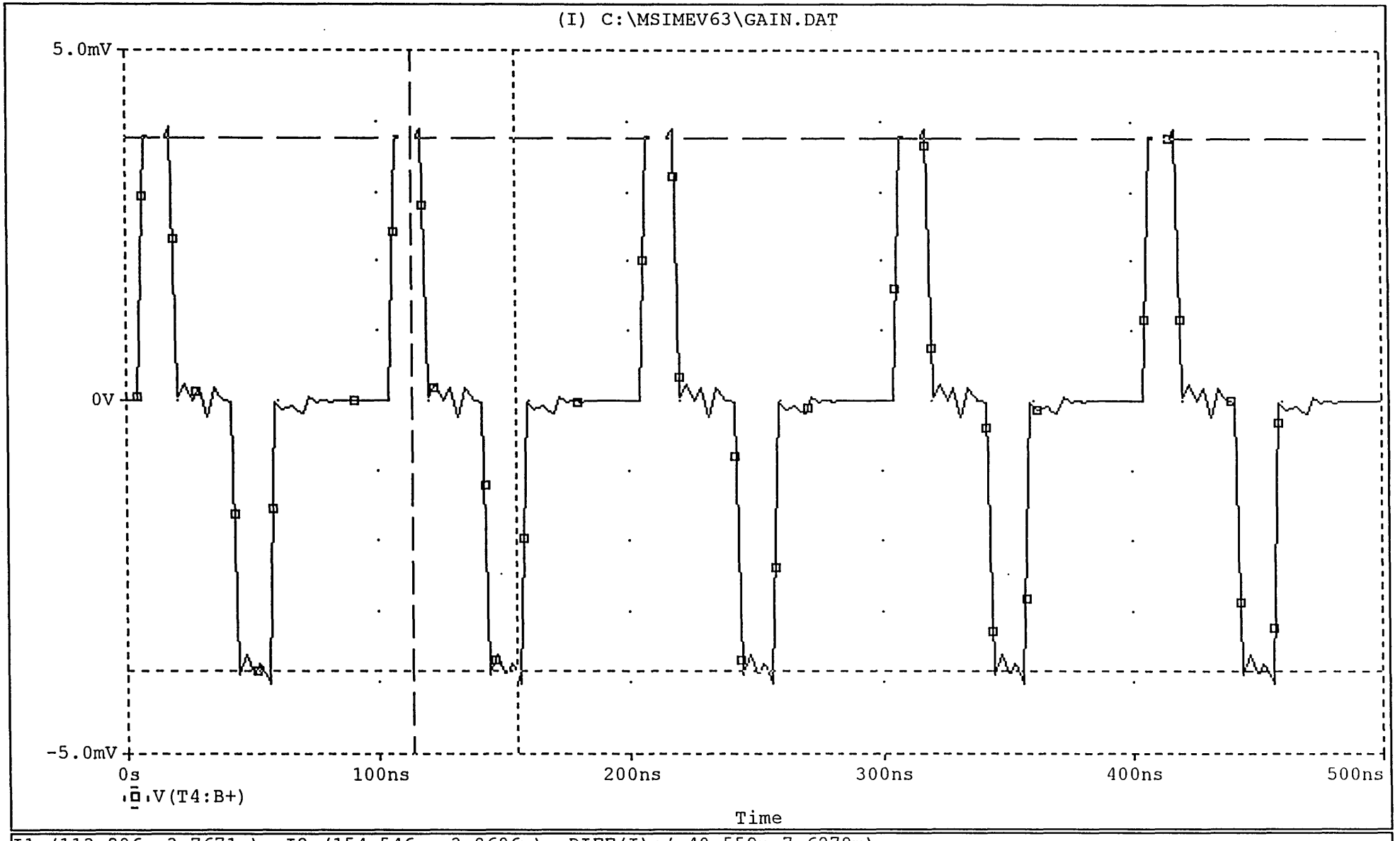

I1:(113.986n,3.7671m) I2:(154.546n,-3.8606m) DIFF(I):(-40.559n,7.6278m)

Date: December 17, 1997 Page 1 Time: 16:35:29

APPENDIX E

List of publications (chronological order):

E1. "On The Analysis of Three Nonuniform Coupled Microstrip Lines"

T. Ahmad[1], Z. Ghassemlooy[1], A. K. Ray[1], B. Parker[2] and Y. M. Moyal[3]

[1] Physical Electronics & Fibre Optics Research Group, Sheffield Hallam Univ., UK

[2] Dept. of Elec. Engineering, Brunel Univ., Uxbridge, UK

[3] Ecole Nationale Superieure en Electronique et Radioelectricite de Bodeaux, Talence, France

Proceeding Third Communication Networks Symposium

Centre for Communication Networks Research

Department of Electrical and Electronic Engineering

Manchester Metropolitan University, and

The Institute of Electrical and Electronics Engineers

8 - 9 July 1996

E2. "Analisis Gandingan Mikrojalur Tidak Seragam"(*in Malay*)

T. Ahmad[1], Z. Ghassemlooy[1], A. K. Ray[1], B. Parker[2] and Y. M. Moyal[3]

[1] Physical Electronics & Fibre Optics Research Group, Sheffield Hallam Univ., UK

[2] Dept. of Elec. Engineering, Brunel Univ., Uxbridge, UK

[3] Ecole Nationale Superieure en Electronique et Radioelectricite de Bodeaux, Talence, France

Proceeding National Symposium of Mathematics VII

Kuala Lumpur, Malaysia, 3 - 5 December 1996

E3. "Fuzzified Crosstalk in Microstrip Lines"

T. Ahmad[1], Z. Ghassemlooy[1], A. K. Ray[1] and N. Sarma[2]

[1] Physical Electronics & Fibre Optics Research Group, Sheffield Hallam Univ., UK

[2] Dept. of Elec. & Elec. Engineering, Warangal, India

Proceeding Fourth Communication Networks Symposium, Manchester, UK, 7-8 July 1997.

E4. "Determination of Electrical Parameters for Microstrip Lines by Fuzzy Method" (invited session)

T. Ahmad, Z. Ghassemlooy and A. K. Ray

Physical Electronics & Fibre Optics Research Group, Sheffield Hallam Univ., UK

Proceeding World Multiconference On Systemics, Cybernetics and Informatics, Caracas, Venezuela, 7-11 July, 1997.

E5. "A Fuzzy Approach in Designing Microstrip Lines"

T. Ahmad, Z. Ghassemlooy and A. K. Ray

Physical Electronics & Fibre Optics Research Group, Sheffield Hallam Univ., UK

Proceeding 5th European Congress on Intelligent Techniques and Soft Computing (Eufit 97), Aachen, Germany, 8-12 Sep. 1997

E6. "Determination of Physical Parameters for Microstrip Lines by Fuzzy Method"

T. Ahmad, Z. Ghassemlooy and A. K. Ray

Physical Electronics & Fibre Optics Research Group, Sheffield Hallam Univ., UK

Proceeding of Second International ICSC Symposium on SOFT COMPUTING, Nimes, France, 17-19 Sep. 1997.

(Fuzzy Logic, Artificial Neural Networks, Genetic Algorithms)

at Nimes France, 17-19 September 1997

E7. "Application of Fuzzy Method for Design Optimisation of High-Speed Interconnects" (to be published)

T. Ahmad, Z. Ghassemlooy , A. K. Ray and A. Razzaly

Physical Electronics & Fibre Optics Research Group, Sheffield Hallam Univ., UK

Proceeding 1st International Symposium on Communications Systems and Digital Signal Processing, Sheffield, UK, 6-8 Apr. 1998

*T. Ahmad, *Z. Ghassemlooy, ^B. Parker, *A. K. Ray, and `Y. M. Moyal

* *Electronics & Communications Research Group, School of Engineering Technology, Sheffield Hallam University , Sheffield , UK.*

^ *Department of Electrical Engineering, Brunel University, Uxbridge, Middlesex, UK.*

`*Ecole Nationale Superieure en Electronique et Radioelectricite de Bordeaux, Talence, France.*

Abstract

In this paper, a study of three parallel coupled microstrip lines is presented. The model consists of three identical geometrical configurations of coupled microstrip lines with non-uniform line spacing. The coupling model is presented by capacitance and inductance matrices. Predicted results are compared with simulation data obtained using Mathematica.

I. Introduction

There is an ever increasing demand for high speed communication links which requires access to ultra fast switching circuits with high density onchip and interchip interconnections. The recent advances in integrated circuit technology has increased the single device speed to multi-giga hertz region. In such environment the transmission line property of the IC interconnection play a major role which cannot be ignored. The advances being made in circuit density and speed, both at the chip and package levels, are placing increasing demands on the performance of interconnection technology. Accurate modelling and simulation of such interconnection have become more important in studying these lines.

The planar geometry used in IC technology allows the on-chip and interchip interconnections to be modelled as microstrip lines, which can be best described by the well known Telegraph equations. There were numerous mathematical models for uniform coupled microstrip lines. The extension of a single line model to two coupled lines is fairly simple. However the generalization to more than two coupled lines is not straightforward. Because of this reason, the study of nonuniform coupled microstrip lines are more complicated. Thus it is of interest to investigate three coupled lines[10] to n-coupled lines.

The three coupled microstrip lines have many applications in communication systems and microwave components. Among these applications are coupler structures, the six-port reflectometer, and dc blocks[1].

The aim of this paper is to derive some of mathematical properties from the study on three coupled microstrip lines to n coupled microstrip lines with different spacing which will give some flexibility and options in designing microstrip lines and perhaps to minimize some of the problems such as crosstalks[3,6].

II. Line Spacing

Spacing between coupled microstrip lines have a direct impact on mutual capacitance and thus on the capacitance matrix. The equation of mutual capacitance of a coupled microstrip lines is given as [3]:

$$C_{ij} = C_{m(i,j)} = \frac{1}{2}[C_{ga} + C_{gd} + C_{gt} - C'_f] \quad (1)$$

such that C_{ga} is gap capacitance in air, C_{gd} is capacitance value due to the electric flux, C_{gt} is gap capacitance and C'_f is modification of fringe capacitance of a single line due to the presence of another line[7].

Three different line configurations were investigated. Using the parameters in Table 1 the results for the mutual and fringe capacitances are shown in Fig. 1.

Table 1

Line Spacing	S_1	S_2	S_3
Dielectric Constant	12	11	9
Thickness (μm)	0.01	0.006	0.05
Width (μm)	2	0.004	3
Height (μm)	20	5	15

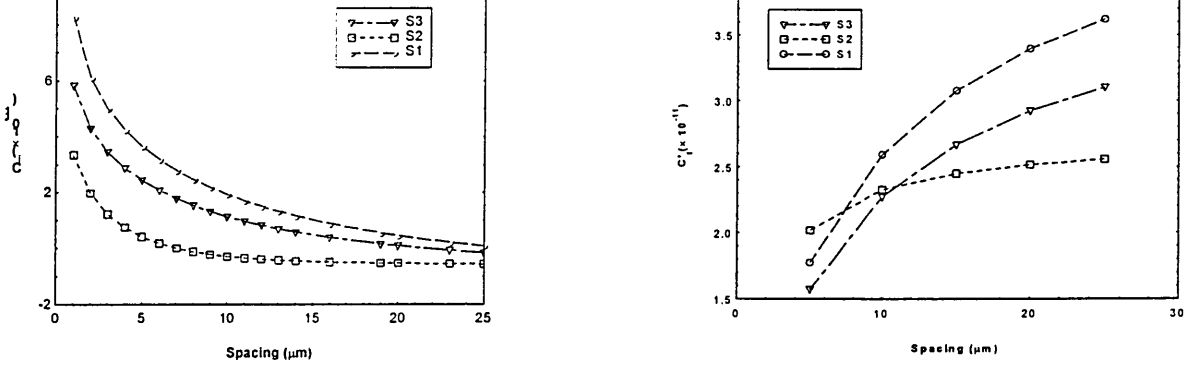

(a) (b)

Fig. 1 Mutual and fringe capacitances for three different line spacings.

From Fig. 1.a. it can be seen that the mutual capacitance decreases as the spacing between a coupled lines, S, increases. Thus varifying the assumptions made by Gao et al [5] and experimental result obtained by Cottrell and Buturla[11].

The result can also be proven analytically by taking the limit on C_{ij} as $s \to \infty$, where $\lim_{s\to\infty} C_{ij} = -\infty$.

Furthermore, as $C_{ij} \to -\infty$ we can see clearly from (1) that $C_{ga} + C_{gd} + C_{gt}$ is decreasing whereas the fringe capacitance, C_f, is increasing as $s \to \infty$ (Fig.1.b) which is in close agreement with experimental results obtained by Cottrell and Buturla [11].

III. Mathematical Formulation

Let us consider a set of any three identical coupled microstrip lines with different spacing between them, say $S_1 \neq S_2$; where S_1 is the spacing between line 1 and line 2 and S_2 is the spacing between line 2 and line 3.

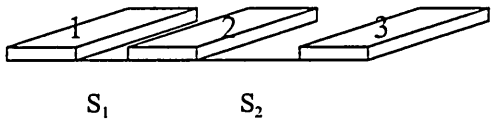

With the assumptions of the *tranverse electromagnetic* (TEM) mode of wave propagation, the distribution of voltages and currents along the lines is given by the generalized telegraphists' equations:

$$\begin{bmatrix} v^x(x,t) \\ i^x(x,t) \end{bmatrix} = -\begin{bmatrix} 0 & L \\ C & 0 \end{bmatrix}\begin{bmatrix} v^t(x,t) \\ i^t(x,t) \end{bmatrix} \tag{2}$$

where vectors $v(x,t)$ and $i(x,t)$ denote voltages and currents, respectively. L is the PUL inductance matrix and on the other hand C is the PUL capacitance matrix. Superscripts x and t denote differentiation of signals with respect to space and time, respectively. Distance and time are denoted by x and t and [2,4]:

$$C = \begin{bmatrix} c_{11} & -c_{12} & \cdots & -c_{1n} \\ -c_{21} & c_{22} & \cdots & -c_{2n} \\ \vdots & \vdots & \vdots & \vdots \\ -c_{n1} & -c_{n2} & \cdots & c_{nn} \end{bmatrix} \text{ such that } c_{ii} = c_{i0} + \sum_{\substack{j=1 \\ j\neq i}}^{n} c_{ij} \tag{3}$$

where c_{i0} is the capacitance PUL of line i with respect to ground, c_{ij} is the capacitance PUL between line i and c_{ii} is the self capacitance PUL of line i. Thus the capacitance matrix C may be written as:

$$C = \begin{bmatrix} -a_{12} & a_{22} & -a_{23} \\ 0 & -a_{23} & a_{33} \end{bmatrix} \qquad (4)$$

where

(i) each line is coupled directly only to adjacent line,[5]
(ii) all lines are identical, not equally spaced and side effects are neglible,
(iii) the length of the lines are equal and have the same reference point,
(iii) the dielectric and the material of the lines are the same.

Note: *All the minus signs in the C matrix can be ignored since they do not effect calculations and proof.*

From (3) and (4) we can have;

$a_{11} = a_{10} + a_{12} + a_{13} = a_{10} + a_{12} + 0$, $a_{22} = a_{20} + a_{21} + a_{23} = a_{10} + a_{12} + a_{23}$, and $a_{33} = a_{30} + a_{31} + a_{32} = a_{10} + 0 + a_{23}$.

Furthermore, we can simplify

$a_{22} = a_{11} + a_{23}$, and $a_{10} = a_{11} - a_{12}$ *thus* $a_{33} = a_{10} + a_{23} = (a_{11} - a_{12}) + a_{23} = (a_{11} + a_{23}) - a_{12}$

Therefore, the new *C* matrix is represented as:

$$C = \begin{bmatrix} a_{11} & -a_{12} & 0 \\ -a_{12} & a_{11} + a_{23} & -a_{23} \\ 0 & -a_{23} & a_{11} + a_{23} - a_{12} \end{bmatrix} \qquad (5)$$

which is tridiagonal and symmetric.

Equation 5 indicates that; (i) the self capacitance of line 2 depends only on the self capacitance of line 1 and the mutual capacitance of line 2 and 3, and (ii) the self capacitance of line 3 depends only on the self capacitance of line 1, the mutual capacitance of line 2 and 3, and the mutual capacitance of line 1 and line 2.

IV. n-Coupled Microstrip Lines

It is also of interest to look at more complicated lines. The results obtained above can be extended to n-coupled microstrip lines with a theorem:

Theorem: For n-coupled identical microstrip lines with different spacing such that $n \geq 3$, see Fig. 2, the capacitance matrix can be written as:

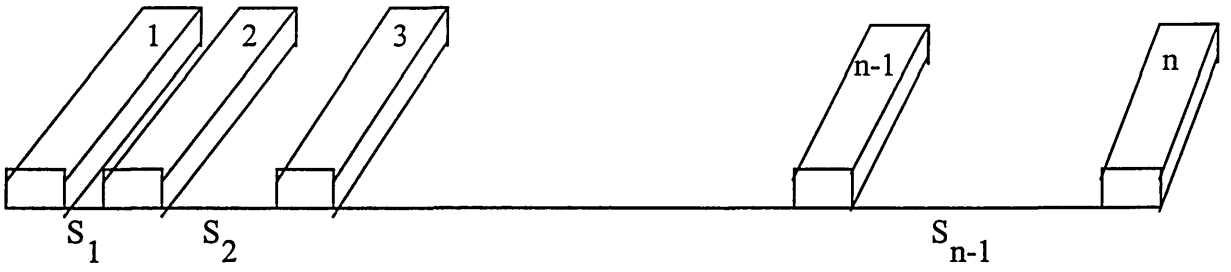

Fig. 2 Nonuniform n-coupled micropsrip lines.

$$C = \begin{bmatrix} a_{11} & -a_{12} & 0 & \dots & 0 & 0 \\ -a_{12} & a_{22} & -a_{23} & \dots & 0 & 0 \\ . & . & . & . & . & . \\ . & . & . & . & . & . \\ 0 & 0 & 0 & \dots & -a_{n(n-1)} & a_{nn} \end{bmatrix} \qquad (6)$$

where $a_{11} = a_{10} + a_{12}$, and $a_{ii} = a_{(i-1)(i-1)} - a_{(i-2)(i-1)} + a_{i(i+1)}$ for $2 \leq i \leq n$.

For n=2, $a_{22} = a_{11} - a_{01} + a_{23} = a_{11} + a_{23}$ ($a_{01} = 0$ since this term does not exist)

$= a_{10} + a_{12} + a_{23}$ which satisfies (5).

Suppose that $a_{nn} = a_{(n-1)(n-1)} - a_{(n-2)(n-1)} + a_{n(n+1)}$, then we need to show

$$a_{(n+1)(n+1)} = a_{nn} - a_{(n-1)n} + a_{(n+1)(n+2)} = a_{nn} - a_{(n-1)n}$$

since $a_{(n+1)(n+2)} = 0$ (this term does not exist) for

$$C = \begin{bmatrix} a_{11} & -a_{12} & 0 & 0 & \dots & 0 & 0 \\ -a_{12} & & & & & & \vdots \\ 0 & & & & & -a_{(n-1)n} & 0 \\ \vdots & \vdots & \vdots & & -a_{(n-1)n} & a_{nn} & -a_{n(n+1)} \\ 0 & 0 & 0 & \dots & 0 & -a_{n(n+1)} & a_{(n-1)(n-1)} \end{bmatrix} \quad (7)$$

Now,

$$a_{(n+1)(n+1)} = a_{(n+1)0} + 0 + \dots\dots\dots + 0 + a_{(n+1)n} = a_{(n+1)0} + a_{(n+1)n} = a_{10} + a_{n(n+1)}$$

$$= a_{10} + a_{(n+1)n} = a_{10} + a_{nn} - a_{(n-1)(n-1)} + a_{(n-2)(n-1)} = a_{nn} + a_{10} - a_{(n-1)(n-1)} + a_{(n-2)(n-1)}$$

and since $a_{(n-1)(n-1)} = a_{(n-1)0} + a_{(n-1)1} + \dots\dots\dots + a_{(n-1)(n-2)} + a_{(n-1)n}$

$$= a_{10} + 0 + \dots\dots\dots 0 + a_{(n-1)(n-2)} + a_{(n-1)n} = a_{10} + a_{(n-1)(n-2)} + a_{(n-1)n}$$

then, $a_{(n+1)(n+1)} = a_{nn} + a_{10} - (a_{10} + a_{(n-1)(n-2)} + a_{(n-1)n}) + a_{(n-2)(n-1)}$

$= a_{nn} - a_{(n-1)n}$ because $a_{(n-1)(n-2)} = a_{(n-2)(n-1)}$.#

We have just shown that the self capacitance of line i, where $2 \le i \le n$, of n-coupled microstrip lines with different spacing is given by $a_{ii} = a_{(i-1)(i-1)} - a_{(i-2)(i-1)} + a_{i(i+1)}$.

V. Simulation Results

A modified mathematica program [3,8] is used to verify the above theorem. Below are two examples of coupled microstrip lines with different spacing. In both examples, different values are used to produce the capacitance matrices. The matrices obtained from these simulation results are then compared to those predicted by the theorem.

i)3 coupled microstrip lines

Dieletric constant of substrate = 12, thickness of line = 0.01 μm, width of line = 2 μm, height of line = 20 μm, $S_1 = 3\mu m$ and $S_2 = 4\mu m$.

$$C = \begin{bmatrix} 155.2(133.4) & -50(-50) & -21.79(0) \\ -50(-50) & 175.8(175.8) & -42.4(42.4) \\ -217.9(0) & -42.44(-42.4) & 147.6(125.8) \end{bmatrix} \text{ pF} \quad (8)$$

ii)10 coupled microstrip lines

Dielectric constant of substrate = 12, thickness of line = 0.01 μm, width of line = 2 μm and height of line = 20 μm. $S_1 = 0.3\mu m$, $S_2 = 4.114\mu m$, $S_3 = 5.002\mu m$, $S_4 = 6\mu m$, $S_5 = 4.7\mu m$, $S_6 = 8\mu m$, $S_7 = 9.2\mu m$, $S_8 = 5.0343\mu m$ and $S_9 = 0.004\mu m$.

$$C = \begin{bmatrix} -30.2 & -41.7 & 189(161) & -36.6 & -13.2 & -4.78 & 1.68 & 5.17 & 6.41 & 6.68 \\ -12.5 & -16.7 & -36.6 & 183(151) & -31.9 & -13.7 & -2.31 & 3.29 & 5.18 & 5.58 \\ -3.30 & -5.34 & -13.2 & -31.9 & 179(153) & -38.2 & -10.5 & -0.232 & 2.96 & 3.63 \\ 0.948 & -0.281 & -4.78 & -13.7 & -38.2 & 168(146) & -24.6 & -5.26 & -4.20 & 1.00 \\ 4.52 & 3.89 & 1.68 & -2.31 & -10.5 & -24.6 & 146(129) & -21.2 & -8.52 & -6.23 \\ 6.60 & 6.27 & 5.17 & 3.29 & -0.232 & -5.26 & -21.2 & 153(141) & -36.4 & -27.8 \\ 7.39 & 7.16 & 6.41 & 5.18 & 2.96 & -0.0420 & -8.52 & -36.4 & 4380(4400) & -4280 \\ 7.57 & 7.37 & 6.68 & 5.58 & 3.63 & 1.00 & -6.23 & -27.8 & -4280 & 4370(4360) \end{bmatrix} \text{pF} \quad (9)$$

In both cases, self capacitances, a_{ii}, are very close to what the theorem predicted (listed in brackets).

VI. Conclusions

A mathematical proof on relations of self capacitance of n-coupled microstrip lines with different spacing has been presented. The proof is based on four assumptions in which they are usually satisfied for microstrip lines constructed on multilayer printed circuit board. The capacitance matrix is tridiagonal, symmetric and non-teoplitz for any n-coupled microstrip lines with different spacing. The self capacitance of line i for n-coupled microstrip lines with different spacing was given. The simulations results obtained for three and ten coupled microstrip lines with different spacing show excellent agreement with the predicted results.

VII. Acknowledgment

One of the authors (Tahir Ahmad) is financially assisted by Faculty of Science, University of Technology Malaysia, Locked Bag 791, 80990 Johor Bahru, Johor Darul Takzim, Malaysia.

VIII. References

[1] E.A.F. Abdallah and N.A.El-Deeb, "On the analysis and design of three coupled microstrip lines", IEEE Trans. Microwave Theory and Techniques, 1985, vol. MTT-33, No.11, pp. 1217-1222
[2] F.Rameo and M. Santomauro, "Time-Domain Simulation of n Coupled Transmission Lines", IEEE, Trans. Microwave Theory and Techniques, 1987, vol. MTT-35, No.2, pp. 131-136
[3] B.H.Parker, "Simulation of Interconnections in High-Speed Integrated Circuits", Thesis for Ph.D, Sheffield Hallam University, UK, 1994.
[4] F.Y.Chang, "Transient Analysis of Lossless Coupled Transmission Lines in a Nonhomogenous Dielectric Medium", IEEE Trans. Microwave Theory & Techniq., 1970, vol. MTT-18, No.9, pp. 616-626
[5] D.S.Gao, A.T.Yang and S.M.Kang, "Modelling and Simulation of Interconnection Delays and Crosstalks in High-Speed Integrated Circuits", IEEE Trans. on Circuits and Sys., 1990, 37(1), pp. 1-9
[6] Y.C.E. Yang, J.A.Kong and Q.Gu "Time-domain Pertubational Analysis of Nonuniformly Coupled Transmission Lines", IEEE Trans. Microwave Theory and Techq., 1985, vol. MTT-33, pp. 1120-1130
[7] K.C. Gupta, R. Garg and I.J. Bahl, "Microstrip Lines and Slotlines", Artech House, Dedham, MA:USA.
[8] S. Wolfram, "Mathematica a system for doing mathematics by computer", Addison Wesley, 1991.
[9] L.Rade and B. Westergren, "BETA Mathematics Handbook", Chartwell-Bratt, 1988.
[10] B.C. Wadell, "Transmission Line Design Handbook", Artech House, 1991.
[11] P.E. Cottrell and E.M.Buturla, "VLSI wiring capacitance", IBM J Res Develop. 1985, 29(3), pp.277-288

*T. Ahmad, *Z. Ghassemlooy, ^B. Parker, *A. K. Ray, and `Y. M. Moyal

* *Electronics & Communications Research Group, School of Engineering Technology, Sheffield Hallam University, Sheffield, UK.*

^ *Department of Electrical Engineering, Brunel University, Uxbridge, Middlesex, UK.*

`*Ecole Nationale Superieure en Electronique et Radioelectricite de Bordeaux, Talence, France.*

Abstrak

Dalam kertas ini, dipaparkan hasil penyelidikan yang dibuat ke atas gandingan tiga selari mikrojalur. Sistem yang dipaparkan mengandungi tiga tatarajah yang serupa gandingan mikrojalur dengan jarak yang berbeza. Model gandingan tersebut diberi oleh matriks kemuatan dan kearuhan. Keputusan yang diperolehi dipadankan kepada gandingan n selari mikrojalur melalui sebuah teorem serta dibandingkan dengan hasil penyalakuan menggunakan perisian Mathematica. Beberapa ciri matematik matriks kemuatan yang terhasil di ketengahkan menerusi sebuah teorem dan dua korolari kemudiannya.

I. Pengenalan

Peningkatan serta permintaan yang begitu ketara dalam perhubungan berkelajuan tinggi memerlukan litar pensuisan ultra laju dengan berketumpatan tinggi dalam dan antara racik saling hubungan. Kemajuan terkini dalam teknologi litar bersepadu telah menaikan peranti berkelajuan tunggal kepada multi -giga hertz. Di dalam suasana tersebut, ciri-ciri talian penghantaran litar bersepadu memainkan peranan penting serta tidak dapat dinafikan lagi. Kemajuan dalam ketumpatan dan kelajuan litar, pada tahap racik dan perisian, meminta prestasi tinggi dalam teknologi hubungan. Oleh demikian, pemodelan dan penyalakuan yang tepat dalam talian hubungan tersebut menjadi semakin penting.

Pensatahan dalam teknologi litar bersepadu membuka ruang hubungan dalam dan antara racik dimodelkan sebagai mikrojalur dimana ia dapat diperihalkan melalui persamaan Telegraf. Kini terdapat beberapa model matematik yang telah dihasilkan bagi sepasang mikrojalur seragam. Bagi menghasilkan model untuk satu talian seragam kepada sepasang talian adalah mudah, tetapi pengitlakan talian seragam untuk lebih dari sepasang talian adalah sukar sekali. Justru itu, kajian ke atas gandingan talian tidak seragam adalah lebih rumit lagi mencabar.

Gandingan tiga mikrojalur [10] banyak digunakan dalam sistem perhubungan dan komponen gelombang mikro, di antaranya ialah struktur pengganding, enam liang meter pantulan dan blok arus terus[1].

Lantaran itu, tujuan utama kertas kerja ini ditulis ialah untuk menerbitkan ciri-ciri matematik dalam kajian gandingan tiga mikrojalur kepada gandingan n mikrojalur dengan jarak yang berbeza semoga dapat memberi kebolehlenturan serta pilihan dalam merekabentuk mikrojalur lantas mengurangkan masalah yang akan timbul seperti cakap silang [3,6].

II. Kesan Jarak

Jarak di antara dua mikrojalur memberi kesan secara langsung kepada kemuatan saling talian dan seterusnya kepada matriks kemuatan yang diperolehi dari sistem yang direka bentuk. Persamaan kemuatan saling untuk sesuatu sistem gandingan mikrojalur adalah diberi seperti di bawah; [3]:

$$C_{ij} = C_{m(i,j)} = \frac{1}{2}[C_{ga} + C_{gd} + C_{gt} - C'_f] \qquad (1)$$

dengan C_{ga} ialah kemuatan jurang diudara, C_{gd} ialah nilai kemuatan yang bergantung terhadap fluks elektrik, C_{gt} ialah kemuatan jurang dan C'_f ialah kemuatan pinggir yang diubahsuai [7].

Bagi menggambarkan kesan jarak ini, tiga gandingan mikrojalur yang berlainan tatarajah dikaji. Parameter di dalam jadual 1 digunakan dan hasil kajian terhadap kemuatan saling dan pinggirnya dipamerkan pada rajah 1.

Gandingan	S_1	S_2	S_3
Pemalar dielektrik	12	11	9
Ketebalan (μm)	0.01	0.006	0.05
Keluasan (μm)	2	0.004	3
Ketinggian (μm)	20	5	15

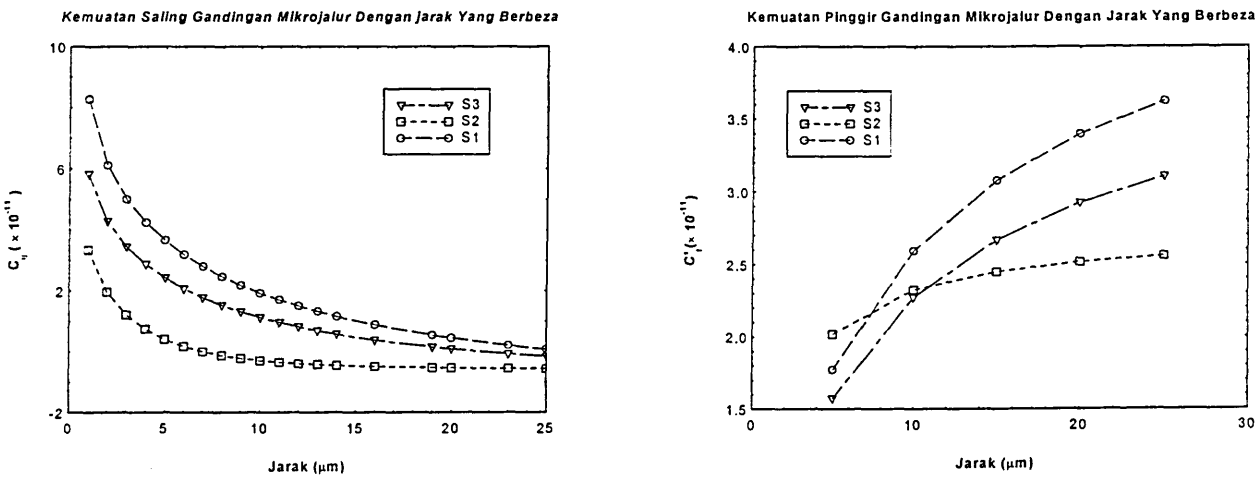

(a) (b)

Rajah 1. Kemuatan saling dan pinggir untuk tiga gandingan yang berlainan

Dari Raj. 1.a jelas dapat dperhatikan bahawa kemuatan saling gandingan mikrojalur berkurangan apabila jarak, *S*, di antaranya semakin bertambah, lantas mentahkikan andaian yang di ambil oleh Gao dan rakannya [5] serta hasil ujikaji yang didapati oleh Cottrell dan Buturla[11].
Keputusan di atas juga dapat ditunjukkan dengan mengambil limit C_{ij} apabila $s \to \infty$, dimana

$$\lim_{s\to\infty} C_{ij} = -\infty .$$

Seterusnya, apabila $C_{ij} \to -\infty$, jelas didapati dari (1) bahawa $C_{ga} + C_{gd} + C_{gt}$ akan menurun manakala kemuatan pinggir pula, C'_f, akan menaik apabila $s \to \infty$ (Raj.1.b). Fenomena ini bertepatan dengan hasil ujikaji yang diperolehi oleh Cottrell dan Buturla [11].

III. Formulasi Matematik

Pertimbangkan sebarang set gandingan tiga mikrojalur yang serupa dengan ukuran jarak yang berbeza di antara talian tersebut, katakanlah $S_1 \neq S_2$; dengan S_1 ialah ukuran jarak di antara talian 1 dengan talian 2 dan S_2 ialah ukuran jarak di antara talian 2 dengan talian 3.

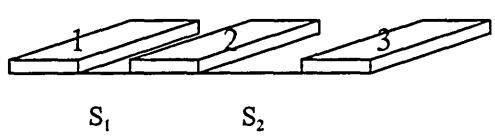

Rajah 2. Gandingan tiga mikrojalur dengan jarak berbeza

Dengan mengambil andaian mod melintang elektromagnet; *tranverse electromagnetic mode* (TEM), untuk perambatan gelombang, maka agihan voltan dan arus pada talian di atas diberi oleh persamaan telegraf am di bawah.

$$\begin{bmatrix} v^x(x,t) \\ i^x(x,t) \end{bmatrix} = -\begin{bmatrix} 0 & L \\ C & 0 \end{bmatrix}\begin{bmatrix} v^t(x,t) \\ i^t(x,t) \end{bmatrix} \qquad (2)$$

dan masa. Jarak dan masa diwakili oleh x dan t sementara [2,4]:

$$C = \begin{bmatrix} c_{11} & -c_{12} & \cdots & -c_{1n} \\ -c_{21} & c_{22} & \cdots & -c_{2n} \\ \vdots & \vdots & \vdots & \vdots \\ -c_{n1} & -c_{n2} & \cdots & c_{nn} \end{bmatrix} \quad \text{dengan } c_{ii} = c_{i0} + \sum_{\substack{j=1 \\ j \neq i}}^{n} c_{ij} \tag{3}$$

c_{i0} ialah kemuatan PPU talian i terhadap bumi, c_{ij} ialah kemuatan saling PPU di antara talian i dengan talian j dan c_{ii} ialah kemuatan diri PPU talian i. Oleh demikian matriks kemuatan C (lihat Raj. 2) dapat diungkapan sebagai:

$$C = \begin{bmatrix} a_{11} & -a_{12} & 0 \\ -a_{12} & a_{22} & -a_{23} \\ 0 & -a_{23} & a_{33} \end{bmatrix} \tag{4}$$

dimana

(i) setiap talian hanya dan hanya digandingkan dengan talian yang bersebelahan/terdekat [5]
(ii) setiap talian adalah serupa dengan jarak yang berbeza
(iii) panjang talian adalah sama serta mempunyai titik rujukan yang serupa
(iii) dielektrik serta bahan bagi setiap talian adalah sama.

Nota: *Tatatanda negatif di dalam matriks kemuatan C boleh diabaikan kerana ia tidak akan memberi kesan terhadap pengiraan serta pembuktian seterusnya.*

Seterusnya (3) dan (4) akan memberi;

$a_{11} = a_{10} + a_{12} + a_{13} = a_{10} + a_{12} + 0$, $a_{22} = a_{20} + a_{21} + a_{23} = a_{10} + a_{12} + a_{23}$, and $a_{33} = a_{30} + a_{31} + a_{32} = a_{10} + 0 + a_{23}$.

serta dapat dipermudahkan

$a_{22} = a_{11} + a_{23}$, and $a_{10} = a_{11} - a_{12}$ dan $a_{33} = a_{10} + a_{23} = (a_{11} - a_{12}) + a_{23} = (a_{11} + a_{23}) - a_{12}$.

Oleh demikian matriks C yang baru dapat ditulis sebagai:

$$C = \begin{bmatrix} a_{11} & -a_{12} & 0 \\ -a_{12} & a_{11} + a_{23} & -a_{23} \\ 0 & -a_{23} & a_{11} + a_{23} - a_{12} \end{bmatrix} \tag{5}$$

iaitu bertiga pepenjuru serta simetri.

Lantaran itu (5) memberi penunjuk bahawa; (i) kemuatan diri talian 2 hanya bergantung kepada kemuatan diri talian 1 dan kemuatan saling talian 2 dan 3 (ii) kemuatan diri talian 3 hanya bergantung kepada kemuatan diri talian 1, kemuatan saling talian 2 dan 3, serta kemuatan saling talian 1 dan 2.

IV. Gandingan n Mikrojalur

Objektif utama kertas ini ditulis ialah untuk menyelidiki serta memberi perhatian kepada talian yang lebih mencabar. Bahagian III di atas membuka laluan supaya keputusannya dapat dipadankan kepada gandingan n mikrojalur melalui teorem di sebelah:

Rajah 3. Gandingan n mikrojalur dengan jarak berbeza.

$$C = \begin{bmatrix} a_{11} & -a_{12} & 0 & \dots & 0 & 0 \\ -a_{12} & a_{22} & -a_{23} & \dots & 0 & 0 \\ . & . & . & . & . & . \\ . & . & . & . & . & . \\ 0 & 0 & 0 & \dots & -a_{n(n-1)} & a_{nn} \end{bmatrix} \qquad (6)$$

dengan $a_{11} = a_{10} + a_{12}$, dan $a_{ii} = a_{(i-1)(i-1)} - a_{(i-2)(i-1)} + a_{i(i+1)}$ untuk $2 \le i \le n$.

bukti:

Keputusan di atas dapat dibuktikan menggunakan aruhan matematik[9].

Untuk n=2, $a_{22} = a_{11} - a_{01} + a_{23} = a_{11} + a_{23}$ ($a_{01} = 0$; ungkapan ini tidak wujud)

$= a_{10} + a_{12} + a_{23}$ lantas memuaskan (5).

Andaikanlah $a_{nn} = a_{(n-1)(n-1)} - a_{(n-2)(n-1)} + a_{n(n+1)}$, maka perlu ditunjukkan bahawa

$$a_{(n+1)(n+1)} = a_{nn} - a_{(n-1)n} + a_{(n+1)(n+2)} = a_{nn} - a_{(n-1)n}$$

kerana $a_{(n+1)(n+2)} = 0$ (ungkapan ini tidak wujud) untuk

$$C = \begin{bmatrix} a_{11} & -a_{12} & 0 & 0 & \dots & 0 & 0 \\ -a_{12} & & & & & & \vdots \\ 0 & & & & & -a_{(n-1)n} & 0 \\ \vdots & \vdots & \vdots & & -a_{(n-1)n} & a_{nn} & -a_{n(n+1)} \\ 0 & 0 & 0 & \dots & 0 & -a_{n(n+1)} & a_{(n+1)(n+1)} \end{bmatrix} \qquad (7)$$

Sekarang,

$$a_{(n+1)(n+1)} = a_{(n+1)0} + 0 + \dots\dots\dots + 0 + a_{(n+1)n} = a_{(n+1)0} + a_{(n+1)n} = a_{10} + a_{n(n+1)}$$

$$= a_{10} + a_{(n+1)n} = a_{10} + a_{nn} - a_{(n-1)(n-1)} + a_{(n-2)(n-1)} = a_{nn} + a_{10} - a_{(n-1)(n-1)} + a_{(n-2)(n-1)}$$

tetapi $a_{(n-1)(n-1)} = a_{(n-1)0} + a_{(n-1)1} + \dots\dots\dots + a_{(n-1)(n-2)} + a_{(n-1)n}$

$$= a_{10} + 0 + \dots\dots\dots 0 + a_{(n-1)(n-2)} + a_{(n-1)n} = a_{10} + a_{(n-1)(n-2)} + a_{(n-1)n}$$

lantaran itu, $a_{(n+1)(n+1)} = a_{nn} + a_{10} - (a_{10} + a_{(n-1)(n-2)} + a_{(n-1)n}) + a_{(n-2)(n-1)}$

$= a_{nn} - a_{(n-1)n}$ kerana $a_{(n-1)(n-2)} = a_{(n-2)(n-1)}$.#

Oleh demikian tertunjuklah bahawa kemuatan diri talian i, dengan $2 \le i \le n$, untuk gandingan n mikrojalur diberi oleh $a_{ii} = a_{(i-1)(i-1)} - a_{(i-2)(i-1)} + a_{i(i+1)}$.

V. Penyalakuan

Satu aturcara Mathematica yang telah diubah suai [3,8] digunakan untuk mentahkikkan teorem di atas. Dua contoh gandingan mikrojalur dengan jarak yang bebeza dipaparkan. Pada setiap contoh,

i)Gandingan 3 mikrojalurs

Pemalar dielektrik = 12, ketabalan talian = 0.01 μm, keluasan talian = 2 μm, ketinggian talian = 20 μm, $S_1 = 3\mu m$ dan $S_2 = 4\mu m$.

$$C = \begin{bmatrix} 155.2(133.4) & -50(-50) & -21.79(0) \\ -50(-50) & 175.8(175.8) & -42.4(42.4) \\ -217.9(0) & -42.44(-42.4) & 147.6(125.8) \end{bmatrix} \text{ pF} \qquad (8)$$

ii)Gandingan 10 mikrojalur

Pemalar dielektrik = 12, ketebalan talian = 0.01 μm, keluasan talian = 2 μm dan ketinggian talian = 20 μm. $S_1 = 0.3\mu m$, $S_2 = 4.114\mu m$, $S_3 = 5.002\mu m$, $S_4 = 6\mu m$, $S_5 = 4.7\mu m$, $S_6 = 8\mu m$, $S_7 = 9.2\mu m$, $S_8 = 5.0343\mu m$ dan $S_9 = 0.004\mu m$.

$$C = \begin{bmatrix} 245(226) & -143 & -30.2 & -12.5 & -3.30 & 0.948 & 4.52 & 6.60 & 7.39 & 75.7 \\ -143 & 266(268) & -41.7 & -16.7 & -5.34 & -0.281 & 3.89 & 6.27 & 7.16 & 7.37 \\ -30.2 & -41.7 & 189(161) & -36.6 & -13.2 & -4.78 & 1.68 & 5.17 & 6.41 & 6.68 \\ -12.5 & -16.7 & -36.6 & 183(151) & -31.9 & -13.7 & -2.31 & 3.29 & 5.18 & 5.58 \\ -3.30 & -5.34 & -13.2 & -31.9 & 179(153) & -38.2 & -10.5 & -0.232 & 2.96 & 3.63 \\ 0.948 & -0.281 & -4.78 & -13.7 & -38.2 & 168(146) & -24.6 & -5.26 & -4.20 & 1.00 \\ 4.52 & 3.89 & 1.68 & -2.31 & -10.5 & -24.6 & 146(129) & -21.2 & -8.52 & -6.23 \\ 6.60 & 6.27 & 5.17 & 3.29 & -0.232 & -5.26 & -21.2 & 153(141) & -36.4 & -27.8 \\ 7.39 & 7.16 & 6.41 & 5.18 & 2.96 & -0.0420 & -8.52 & -36.4 & 4380(4400) & -4280 \\ 7.57 & 7.37 & 6.68 & 5.58 & 3.63 & 1.00 & -6.23 & -27.8 & -4280 & 4370(4360) \end{bmatrix} \text{ pF} \qquad (9)$$

Didapati bahawa pada setiap kes, kemuatan diri talian, a_{ii}, adalah begitu hampir kepada nilai yang telah diramalkan oleh teorem (ditulis dalam kurungan).

VI. Nilai dan vektor eigen

Seterusnya, matriks kemuatan C yang baru (6) dapat diungkapkan sebagai:

$$C = \begin{bmatrix} a_{11} & a_{12} & 0 & \dots & 0 & 0 \\ a_{12} & a_{22} & a_{23} & \dots & 0 & 0 \\ . & . & . & . & . & . \\ . & . & . & . & . & . \\ 0 & 0 & 0 & \dots & a_{n(n-1)} & a_{nn} \end{bmatrix}$$

$$= \begin{bmatrix} a_{10} + a_{12} & a_{12} & 0 & \dots & 0 & 0 \\ a_{12} & a_{10} + a_{12} + a_{23} & a_{23} & \dots & 0 & 0 \\ . & . & . & . & . & . \\ . & . & . & . & . & . \\ 0 & 0 & 0 & \dots & a_{n(n-1)} & a_{(n-1)(n-1)} - a_{(n-2)(n-1)} + a_{n(n+1)} \end{bmatrix}$$

$$= \begin{bmatrix} a_{10} + a_{12} & a_{12} & 0 & \dots & 0 & 0 \\ a_{12} & a_{10} + a_{12} + b_2 a_{12} & b_2 a_{12} & \dots & 0 & 0 \\ . & . & . & . & . & . \\ . & . & . & . & . & . \\ 0 & 0 & 0 & \dots & b_{n-1} a_{12} & a_{10} + b_{n-1} a_{12} \end{bmatrix}$$

$$= \begin{bmatrix} \cdot & & \cdot & \cdot & \cdot & \cdot \\ \cdot & & \cdot & \cdot & \cdot & \cdot \\ 0 & & 0 & 0 & \ldots & b_{n-1}a_{12} \quad a_{10}+b_{n-1}a_{12} \end{bmatrix}$$

$$= a_{10}\begin{bmatrix} 1 & 0 & 0 & . & . & . & 0 \\ 0 & 1 & 0 & . & . & . & 0 \\ . & . & . & . & . & . & . \\ . & . & . & . & . & . & . \\ . & . & . & . & . & . & . \\ 0 & 0 & 0 & . & . & 1 & 0 \\ 0 & 0 & 0 & . & . & 0 & 1 \end{bmatrix} + a_{12}\begin{bmatrix} 1 & 1 & 0 & . & . & . & 0 \\ 1 & (1+b_2) & b_2 & . & . & . & 0 \\ 0 & b_2 & (b_2+b_3) & b_3 & . & . & 0 \\ . & . & . & . & . & . & . \\ . & . & . & . & . & . & . \\ 0 & 0 & 0 & . & . & . & b_{n-1} \\ 0 & 0 & 0 & . & . & b_{n-1} & b_{n-1} \end{bmatrix}$$

$$= a_{10}\mathrm{I} + a_{12}\mathrm{S_n}\text{; dimana, } b_i = \frac{a_{i(i+1)}}{a_{12}} \text{ untuk } i = 2,\ldots,n. \qquad (10)$$

Nota: *Tatatanda negatif di dalam matriks kemuatan C boleh diabaikan kerana ia tidak akan memberi kesan terhadap pembuktian seterusnya.*

Justru itu, nilai eigen untuk C dapat dicari dengan mudah setelah ia dapat diungkapkan seperti (10). Nilai eigen ini tidak bergantung pada a_{ii}, dengan erti kata yang lain, nilai eigen untuk gandingan n mikrojalur yang serupa dengan jarak berbeza boleh diperolehi tanpa sebarang maklumat mengenai kemuatan diri talian-taliannya.

Teorem 6.1: Bagi gandingan n mikrojalur yang serupa dengan jarak yang berbeza untuk n ≥ 3, lihat Raj.3, maka nilai eigen untuk C diberi oleh;

$$\lambda_j = a_{10} + a_{12}\theta_j(\mathrm{S_n}) \text{ dimana } \mathrm{S_n} = \begin{bmatrix} 1 & 1 & 0 & . & . & . & 0 \\ 1 & (1+b_2) & b_2 & . & . & . & 0 \\ 0 & b_2 & (b_2+b_3) & b_3 & . & . & 0 \\ . & . & . & . & . & . & . \\ . & . & . & . & . & . & . \\ 0 & 0 & 0 & . & . & . & b_{n-1} \\ 0 & 0 & 0 & . & . & b_{n-1} & b_{n-1} \end{bmatrix} \text{ dengan,}$$

$b_i = \frac{a_{i(i+1)}}{a_{12}}$ untuk $i = 2,\ldots,n$ dan $\theta_j(\mathrm{S_n})$ ialah nilai eigen $\mathrm{S_n}$.

bukti:

$$\det[C-\lambda\mathrm{I}] = \det[a_{10}\mathrm{I} + a_{12}\mathrm{S_n} - \lambda\mathrm{I}] = \det[(a_{10}-\lambda)\mathrm{I} + a_{12}\mathrm{S_n}] = \det a_{12}\left[\frac{(a_{10}-\lambda)}{a_{12}}\mathrm{I} + \mathrm{S_n}\right].$$

Biarkan $\lambda = a_{10} + a_{12}\theta(\mathrm{S_n})$ dimana $\theta(\mathrm{S_n})$ ialah nilai eigen $\mathrm{S_n}$, oleh demikian

$$= \det a_{12}\left[\frac{\left(a_{10}-a_{10}-a_{12}\theta(\mathrm{S_n})\right)}{a_{12}}\mathrm{I} + \mathrm{S_n}\right]$$

$$= \det a_{12}\left[\frac{\left(-a_{12}\theta(\mathrm{S_n})\right)}{a_{12}}\mathrm{I} + \mathrm{S_n}\right]$$

$$= \det a_{12}\left[-\theta(\mathrm{S_n})\mathrm{I} + \mathrm{S_n}\right]$$

Keputusan ini menjurus secara langsung kepada korolari berikut:

Korolari 6.2: Untuk sebarang gandingan tiga mikrojalur dengan jarak yang berbeza dengan $C = \begin{bmatrix} a_{11} & a_{12} & 0 \\ a_{12} & a_{22} & ba_{12} \\ 0 & ba_{12} & a_{33} \end{bmatrix}$, maka nilai eigennya ialah $\lambda = a_{10} + a_{12}\left\{0, (b+1) \pm \sqrt{b^2 - b + 1}\right\}$ dimana $b = \frac{a_{23}}{a_{12}}$.

Tambahan dari itu, vektor eigen matriks C diberi oleh korolari seterusnya.

Korolari 6.3: Matriks C dan S_n mempunyai vektor eigen yang sama.

bukti:

$$[C - \lambda I]x = [a_{10}I + a_{12}S_n - \lambda I]x = [a_{12}S_n - (\lambda - a_{10})I]x = a_{12}[S_n - \frac{(\lambda - a_{10})}{a_{12}}I]x$$

$$= a_{12}[S_n - \theta\ (S_n)I]x. \quad \#$$

VII. Rumusan

Suatu pembuktian tentang hubungan kemuatan diri gandingan n talian mikrojalur dengan jarak yang berbeza telah diberi. Pembuktian tersebut berdasarkan kepada empat andaian awal dimana andaian-andaian ini selalu digunakan/memuaskan dalam rekabentuk talian mikrojalur di atas multilapisan papan litar. Matriks kemuatannya adalah tiga segi pepenjuru, simetri dan bukan teoplitz untuk sebarang gandingan n mikrojalur dengan jarak yang berbeza. Nilai kemuatan saling gandingan mikrojalur berkurangan apabila jarak di antaranya semakin bertambah. Kemuatan diri talian i mikrojalur dengan jarak yang berbeza diberi oleh $a_{ii} = a_{(i\text{-}1)(i\text{-}1)} - a_{(i\text{-}2)(i\text{-}1)} + a_{i(i+1)}$ untuk $2 \le i \le n$.

Penyalakuan terhadap dua sistem, menggunakan gandingan tiga dan sepuluh mikrojalur dengan jarak yang berbeza menunjukkan persetujuan dengan apa yang telah diramalkan oleh teorem. Nilai dan vektor eigen matriks C boleh diterbitkan menerusi S_n.

VIII. Penghargaan

Penulis utama kertas ini (Tahir Ahmad) mendapat bantuan kewangan (biasiswa) dari Fakulti Sains, Universiti Technologi Malaysia, Karung Berkunci 791, 80990 Johor Bahru, Johor Darul Takzim, Malaysia.
Y.M. Moyal adalah pelajar Erasmus di bawah penyelian Tahir Ahmad mendapat bantuan dari E.N.S.E.R.B., France.
Puan Siti Rahmah Awang telah membantu dalam lakaran grafik serta terjemahan teknikal di dalam kertas kerja ini.

VIV. Rujukan

[1] E.A.F. Abdallah and N.A.El-Deeb, "On the analysis and design of three coupled microstrip lines", IEEE Trans. Microwave Theory and Techniques, 1985, vol. MTT-33, No.11, pp. 1217-1222
[2] F.Rameo and M. Santomauro, "Time-Domain Simulation of n Coupled Transmission Lines", IEEE, Trans. Microwave Theory and Techniques, 1987, vol. MTT-35, No.2, pp. 131-136
[3] B.H.Parker, "Simulation of Interconnections in High-Speed Integrated Circuits", Thesis for Ph.D, Sheffield Hallam University, UK, 1994.
[4] F.Y.Chang, "Transient Analysis of Lossless Coupled Transmission Lines in a Nonhomogenous Dielectric Medium", IEEE Trans. Microwave Theory & Techniq., 1970, vol. MTT-18, No.9, pp. 616-626
[5] D.S.Gao, A.T.Yang and S.M.Kang, "Modelling and Simulation of Interconnection Delays and Crosstalks in High-Speed Integrated Circuits", IEEE Trans. on Circuits and Sys., 1990, 37(1), pp. 1-9
[6] Y.C.E. Yang, J.A.Kong and Q.Gu "Time-domain Pertubational Analysis of Nonuniformly Coupled Transmission Lines", IEEE Trans. Microwave Theory and Techq., 1985, vol. MTT-33, pp. 1120-1130
[7] K.C. Gupta, R. Garg and I.J. Bahl, "Microstrip Lines and Slotlines", Artech House, Dedham, MA:USA.
[8] S. Wolfram, "Mathematica a system for doing mathematics by computer", Addison Wesley, 1991.
[9] L.Rade and B. Westergren, "BETA Mathematics Handbook", Chartwell-Bratt, 1988.

Fuzzified Crosstalk in Microstrip Lines

T. Ahmad, Z. Ghassemlooy, A. K. Ray, and *N. Sarma
Physical Electronics & Fibre Optics Research Laboratories, Electronics Research Group, School of Engineering, Sheffield Hallam University, Sheffield, UK.
**Dept. of Electronics & Communication Engineering, Regional Engineering College Warangal, India*

Abstract

In microstrip lines crosstalk and spacing between the lines is of prime importance. An attempt has been made to describe the correlation between crosstalk and line spacing by employing fuzzy logic. In this paper, an experimental crosstalk results for a set of eight identical geometrical configurations coupled microstrip lines together with fuzified crosstalk are presented.

I. Introduction

Recent advances in integrated circuit technology have reduced the single device switching time to ten picoseconds or less. Unfortunately, the electrical performance of the interconnection does not scale as well, and this results in many unexpected problems such as delay, reflection, ringing and particularly crosstalk. Studies have shown that length, spacing, and termination conditions of interconnection and output impedance of gates have major effects on crosstalk [2,3]. In order to design high speed logic circuitry with an optimum interconnection configuration it is essential that crosstalk levels are reduced as much as possible. To accomplish this, it is necessary to relate electrical parameters and physical configurations of line to the crosstalk phenomena.

The aim of this paper is to derive correlation between crosstalk and spacing of lines via fuzzy logic approach. This is an initial step towards fuzzy modelling of microstrip lines with an aim to minimise crosstalk [1].

II. Crosstalk

The study of crosstalk between the interconnection lines on high-speed digital circuits is important because it may lead to the distortion of desired logic functions. The crosstalk (ξ) in dB is defined as:

$$\xi = 20\log_{10}[V_e(t) / V_i(t)] \qquad (1)$$

where V_i is the voltage source on the activated line at time t, and V_e is the voltage at the same time t at a particular position on the line [4]. There are two kinds of crosstalk, far end and near end. The former is measured at the end of line whereas the later is measured at the start of line.

III. Experimental Results

The effect of microstrip line spacing on electrical parameters has been reported both experimentally [8] and by modelling [5,6]. The effect of line spacing on crosstalk has also been noted by various researchers [2,3,4]. However, the direct relation between the line spacing and crosstalk (crosstalk as a function of spacing) has not been dealt with and it therefor requires further investigation.

To investigate this relation a set of 8-coupled microstrip lines of uniform spacing, width, thickness and length, see Fig. 1, is fabricated.

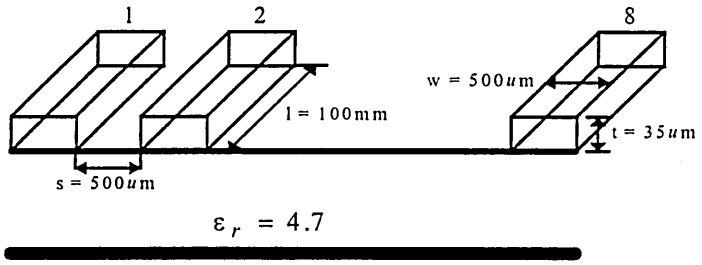

Fig. 1 Eight coupled microstrip lines.

The schematic diagram of Fig. 1 is illustrated in Fig. 2.

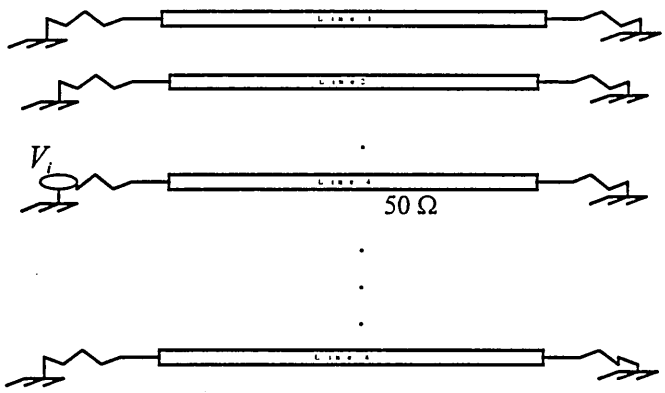

Fig. 2 Schematic diagram of eight coupled microstrip lines.

A pulse train of 1 V amplitude, 10 MHz frequency and 8% duty cycle is applied to the line 4. With all the lines terminated with 50Ω resistor the crosstalk measured at both ends of the lines is shown in Fig. 3.

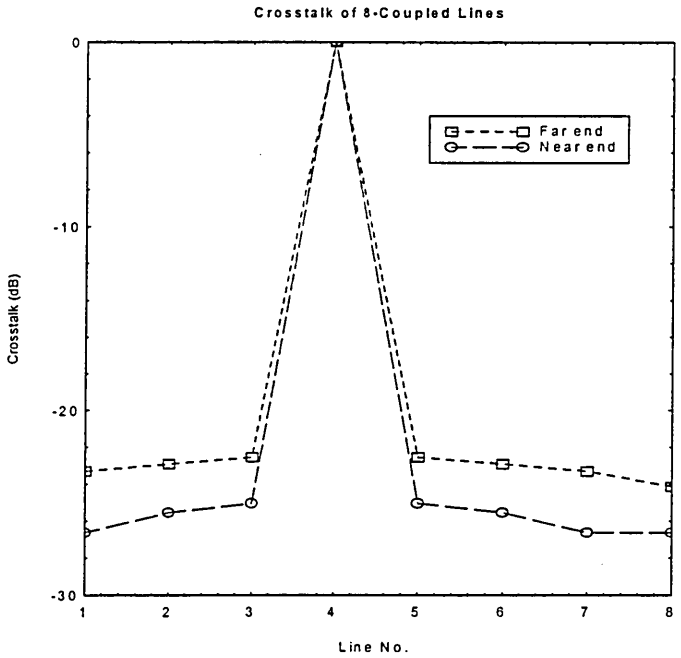

Fig. 3 Crosstalk of 8-coupled lines.

As can be seen from Fig. 3, the far end and near end crosstalk decreases rapidly when moving away from the feeder line (line 4) to the adjacent lines i.e. 3 & 5. Beyond these crosstalk decreases gradually. This is in close agreement with the simulation results reported by Parker et al [4]. It is important to note that crosstalk at the far end is about 2.5 dB higher than that of the near end. This is mainly due to mutual field interaction (proximity effect) between the lines as signal propagation along the line and the corresponding phase delays.

IV. Fuzzy Membership

Crosstalk being a complex phenomenon depends on various factors. Therefore, to obtain sufficient information from measurement alone is impossible and it is also fairly complex to express it mathematically. To assist designers in overcoming these difficulties an alternative approach based on fuzzy logic may be adopted. This is because the choice of a certain precise membership function (i.e. line parameters) is less significant in fuzzy applications since only the qualitative properties of functions are often needed [7].

From section III, Fig. 3, the following statements can be concluded:

(i) spacing effect the crosstalk

(ii) $\lim_{s\to\infty} \xi(s) = -\infty$

(iii) crosstalk between lines decreases monotically as spacing increases;
i.e.: $\xi(a) \geq \xi(s) \geq \xi(b),\ \forall s \in [a,b]$

(iv) all the values of ξ appear in the fourth quadrant

(v) crosstalk is symmetrical about the feeder line (line 4)

(vi) length of lines also affect the crosstalk.

These properties are the basis of acquisition for membership function of fuzzy crosstalk. This is done by a single direct physical measurement method [9]. For a given line spacing $S=[a,b]$, where a and b are the possible range of values for line spacing, the crosstalk for such a configuration is given as $\xi(s)$. This is valid for the interval $(\forall s \in S)$. The crosstalk preference membership function μ mapped $S \rightarrow [0,1]$ with respect to spacing between lines is defined as:

$$\mu_{\xi}(s) = \begin{cases} 1, & s = b \\ \dfrac{\xi(s)}{\xi(b)}, & s \neq b \end{cases} \qquad (2)$$

and a set of fuzzified crosstalk is also defined as $F_{\xi} = \{(s, \mu_{\xi}): s \in S\}$.

By the property of (v), the crosstalk versus line spacing is shown in Fig. 4.a. Because of symmetry only the spacing between lines 4 to 8 are shown. Using the defined membership function (Eqn. 2) the measured crosstalk, as given in Fig 4.a. is then transformed into the fuzzified crosstalk and the results are presented in Fig. 4.b. The novel fuzzified crosstalk always carry the factor of preference with respect to spacing which indicates that as the spacing between the lines increases the crosstalk decrease and the fuzzy value approaches unity. Fuzzy value of one is what the designer really wants. Therefore, fuzzified results, obtained from a single set of practical measurement, can then be used to design any other lines as long as the physical parameters are within the fuzzy set.

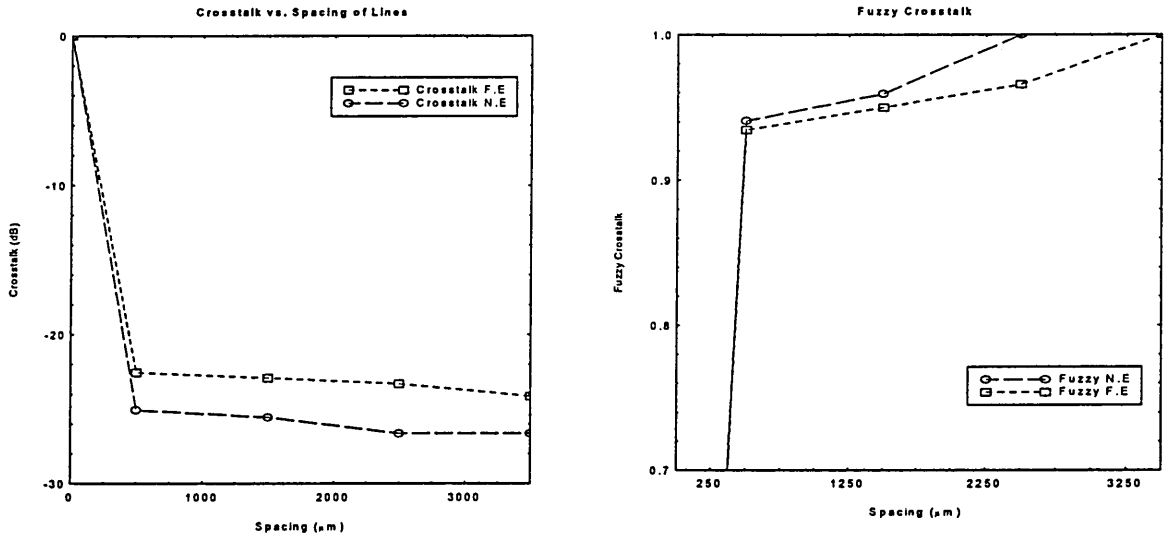

Fig. 4 Crosstalk versus line spacing, (a) measured and (b) fuzzified.

V. Conclusion

In this paper, we have investigated the crosstalk phenomenon of 8-coupled microstrip lines. Experimental data shows that the effect of spacing on the crosstalk. Fuzzy logic is used to describe the correlation between crosstalk and spacing of lines. Similarly, the same procedure can be applied to make the

correlation between crosstalk and other geometric parameters. This correlation is an initial stage and one of the components in building fuzzy modelling of microstrip lines.

VI. Acknowledgements

Tahir Ahmad is financially assisted by Faculty of Science, University of Technology Malaysia, Locked Bag 791, 80990 Johor Bahru, Johor Darul Takzim, Malaysia. Dr. N. Sarma is a visiting researcher to Sheffield Hallam University from Regional Engineering College, Warangal, India. He is sponsored by The British Council.

VII. References

[1] T. Ahmad, Z. Ghassemlooy and A. K. Ray, "Determination of Physical Parameters for Microstrip Lines by Fuzzy Method", to be published in Proc. Second International ICSC Symposia on Soft Computing/SOCO'97 on Sep. 17-19, 1997 in Nimes, France.

[2] S. Seki and H. Hasegawa, "Analysis of Crosstalk in Very High-speed LSI/VLSI's Using a Coupled Multiconductor MIS Microstrip Line Model", IEEE Trans. Microwave Theory and Techniques, 1984, vol. MTT-32, No. 12, pp. 1715-1720.

[3] Q. J. Zhang, S. Lum and M. S. Nakhla, "Minimization of Delay and Crosstalk in High-Speed VLSI Interconnects", IEEE Trans. Microwave Theory and Techniques, 1992, vol. 40, No. 7, pp. 1555-1563.

[4] B. H. Parker, A. K. Ray and Z. Ghassemlooy, "Crosstalk in the Interconnection Bus for a High-Speed Digital Logic Circuit", Int. J. Electronics, 1994, vol. 76, No. 2, pp. 265-269.

[5] T. Ahmad, Z. Ghassemlooy, B. Parker, A. K. Ray and Y. M. Moyal, "On The Analysis of Three Nonuniform Coupled Microstrip Lines", Proc. Third Communication Networks Symposium on July 8-9, 1996 in Manchester, England, pp. 141-145.

[6] T. Ahmad, Z. Ghassemlooy, B. Parker, A. K. Ray and Y. M. Moyal, "Analisis Gandingan Mikrojalur Tidak Seragam", (in Malay) Proc. National Sym. of Mathematics VII, Kuala Lumpur on Dec 3-5, 1996 in Kuala Lumpur, Malaysia, pp. 206-212.

[7] T. Terano, K. Asai and M. Sugeno, "Fuzzy Systems Theory and Its Applications", 1987, Academic Press Inc., Tokyo, Japan.

[8] P. E. Cottrell and E. M. Buturla, "VLSI Wiring Capacitance", IBM J Res Develop. 1985, 29(3), pp. 277-288.

[9] http://www.cs.cmu.edu/Groups/AI/html/faqs/ai/fuzzy/part!/faq-doc-9.html

Determination of Electrical Parameters for Microstrip Lines by Fuzzy Method

T. Ahmad, Z. Ghassemlooy and A. K. Ray
Physical Electronics & Fibre Optics Research Laboratories
Electronic Research Group, School of Engineering
Sheffield Hallam University, City Campus, Pond Street
Sheffield S1 1WB, UK

Abstract - **A novel and flexible method based on fuzzy logic for design optimisation of electrical parameters of microstrip lines in high speed integrated circuit technology is developed. The method is summarized into two fuzzy algorithms. All the electrical parameters are identified and specified. Membership functions based on preference for these parameters are established to create a fuzzy environment. The environment is then processed to produce the optimized electrical parameters of microstrip lines. An example is presented to illustrate the execution of this technique.**

I. INTRODUCTION

Recent advances in integrated circuit technology have reduced the single device switching time to tens of picoseconds or less. Unfortunately, the electrical performance of the interconnect do not scale as well, and this results in many unexpected problems such as delay, reflection, ringing, crosstalk [1] and false switching. In many cases the interconnection delay time is often significantly longer than the devices switching time. In such cases the transmission line property of the lines can not be neglected. Therefore, accurate selection of electrical parameters as well as geometrical parameters [2], modelling and simulation of such lines have become very important.

In a large scale circuits the relation between the design criteria and a large number of circuit parameters becomes very complicated. Since there is no direct connection between various parameters then establishing a trade-offs between them is desirable. Recently, Lu and Ungvichian [3] have introduced a multivariable optimization technique based on spectral domain approach in multi-layered multi-conductor microstrip lines (see Fig. 1) board of high speed digital circuits.

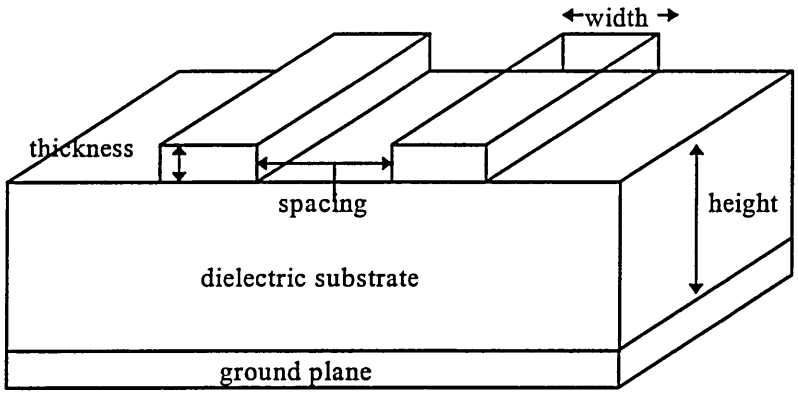

Figure 1

The approach adopted in this work is based on fuzzy theory which best expresses inherent uncertainty, vagueness, and imprecision in a relationship encountered in real world [4]. Fuzzy control is carried out by programming the rules of selection used by skilled individual, $A_i \rightarrow B_i$ (i =1, 2, ...n), in which the judgement on manipulated valuable B for a given state A is best made by a computer.

In this paper, we report how fuzzy concept can be extended to microstrip lines. Performance and electrical specifications (obtained from theoritical and experimental data, current state of technology, and consumers) are fuzzified to create fuzzy environment. This is then processed by the extension principle to produce the best and the most appropriate output data. The output data produced contains the best possible electrical parameters of microstrip lines, which a designer wishes to use, is then defuzzified.

II. PARAMETERS

Variables involved in an engineering design are usually referred to as parameters. These parameters are input, output and performance parameters [5]. The specifications of each parameters is presented in the Table 1:

Input Paramaters (design parameters)	*Output Parameters*	*Performance Parameters*
• independent • values is determined during the design process	• involve in design process • functionally dependent on the input parametes and possibly on some performance parameters • not subject to any specified functional requirement	• subject to some functional requirement

Table 1

Functional requirement is refer to a value or range of values that is specified for a performance parameter and independent of the design process

The electrical parameters for microstrip lines [6,7,8] are very complicated mathematical expressions. They are best describe by equation of mutual capacitance of a coupled microstrip lines between line *i* and *j*:

$$C_{ij} = \frac{1}{2}[C_{ga} + C_{gd} + C_{gt} - C'_f] \quad (1)$$

such that C_{ga} is the gap capacitance in air, C_{gd} is the capacitance value due to the electric flux, C_{gt} is the gap capacitance with the inclusion of finite thickness, C'_f is the modified fringe capacitance of a single line due to the presence of another line.

Some of these parameters are shown in Fig. 2. C_f and C_p are the fringe and parallel plate capacitances, respectively [8].

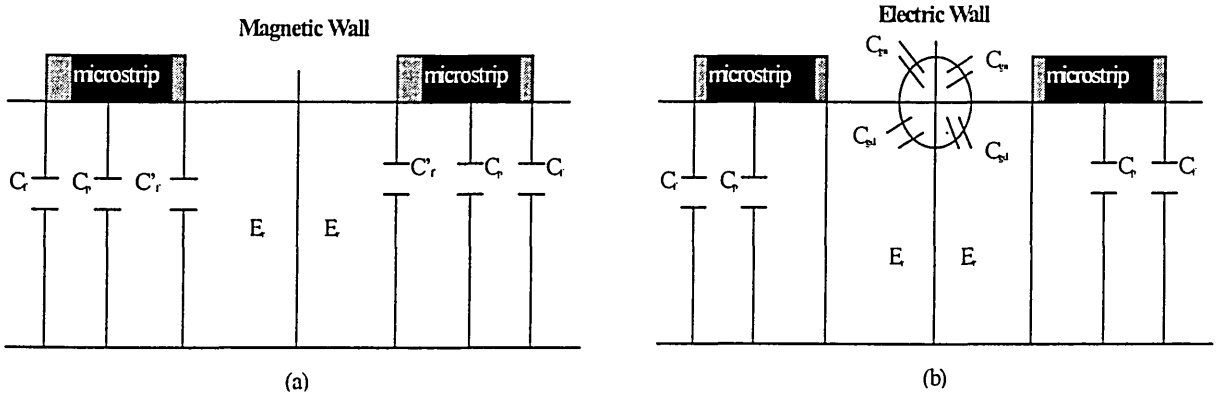

Figure 2 Capacitances (a) even mode (b) odd mode

All the electrical parameters of microstrip lines can be performance parameters or output parameters once their range of values have been specified. They are predetermined by the designer, consumer or the current state of technology and experimentally.

III. FUZZY ENVIRONMENT

The main part of this technique is to incorporate all the electrical parameters available through theoretical or experimental results, consumer and technology specifications into the fuzzy environment/fuzzification (see Fig.3). In other words, we need to establish the proper membership functions for fuzzy set of all the input parameters. Once determined, they are employed for calculating the associated fuzzy sets for performance parameters.

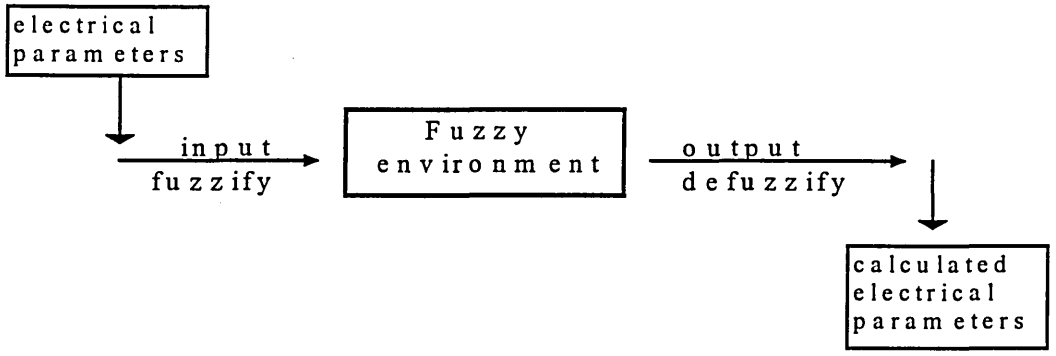

Figure 3 Fuzzy Environment

All the input together with the performance parameters which have been fuzzified are ready to be processed by the extension principle [3] in the fuzzy environment to produce the best and most appropriate output data. The output data produced contains the best electrical parameters of microstrip lines.

IV. FUZZY ALGORITHMS

All the fuzzy sets F_{I_i} expressing preferences of all input parameters $g_i \in I_i \subset R^+ \ (i \in N)$ are determined, normalized and convex. I is a close interval of positive reals. Let C_g is a performance parameter which takes all takes all the input parameters as its variables and is presented by fuzzy set F_{C_g}. The algorithm to determine a fuzzy set F_{ind}, that is induced on C_g has the following steps:

1. Let $C_g: I_1 \times I_2 \times ... \times I_i \rightarrow R$ is the performance parameter $(i \in N)$ such that $r = C_g(g_1, g_2, g_3, ..., g_n)$.

2. Select appropriate values for α - cut, such that $\alpha_1, \alpha_2, \alpha_3, ..., \alpha_k \in (0,1]$ which are equally spaced.

3. Determine all the α_k - cuts of all F_{I_i} $(i \in N)$.

4. Generate all 2^n combinations of the endpoints of intervals representing α_k - cuts of all F_{I_i} $(i \in N)$. Each combination is an n-tuple $(g_1, g_2, g_3, ..., g_n)$.

5. Determine $r_j = C_g(g_1, g_2, g_3, ..., g_n)$ for each n-tuple $j \in 1,2,3,...,2^n$.

6. Set $F_{j_{ind}} = [\min r_j, \max r_j]$ for all $j \in 1,2,3,...,2^n$.

The process of defuzzification has the following steps:

1. Set $F_{C_g} \cap F_{ind}$.

2. Find the membership value of supremum of step 1, say $f^* = \sup [F_{C_g} \cap F_{ind}]$.

3. Find the C_g value of f^*, say C_g^*.

4. Find f^*- cut of all F_{I_i} $(i \in N)$.

5. Generate all 2^n combinations of the endpoints of interval representing f^*- cut of all F_{I_i} $(i \in N)$. Each combination is an n-tuple $(g_1^*, g_2^*, g_3^*, ..., g_n^*)$.

6. Determine $r_j^* = C_g^*(g_1^*, g_2^*, g_3^*, ..., g_n^*)$ for each n-tuple $j \in 1,2,3,...,2^n$.

V. NUMERICAL EXAMPLE

As an example of results obtained by the technique, the mutual capacitance (eqn. 1) is used as the performance parameters [7,8,9].

The input parameters are given in Table 2. A prefered value of a parameter could be any value between minimun and maximum. The fuzzified values of these input parameters are given in Figure 4. These figures are simple fuzzy numbers [5] where the prefered and minimum/maximum are set to have the highest and lowest membership values, respectively.

Boundaries	Minimum	Prefered	Maximum
Cij (pF)	6.2	6.6	7
Cga (pF)	5	7	10
Cgt (pF)	8	15	15
Cgd (pF)	2	7	7
C'f (pF)	8	10	13

Table 2 Preference Input Parameters

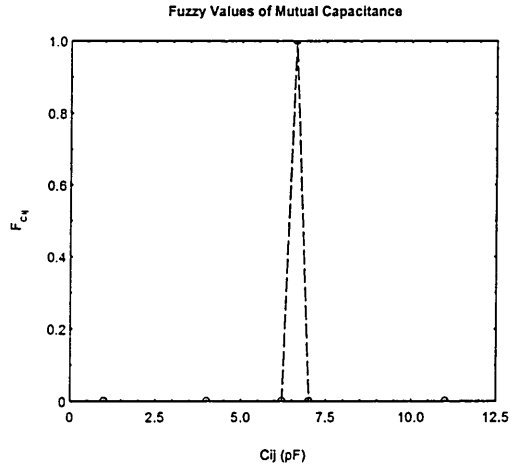

(a)

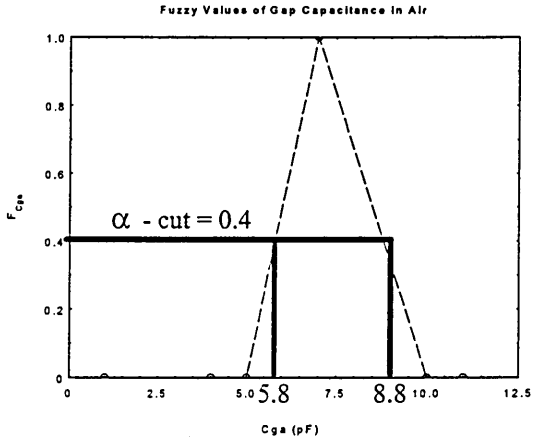

(b)

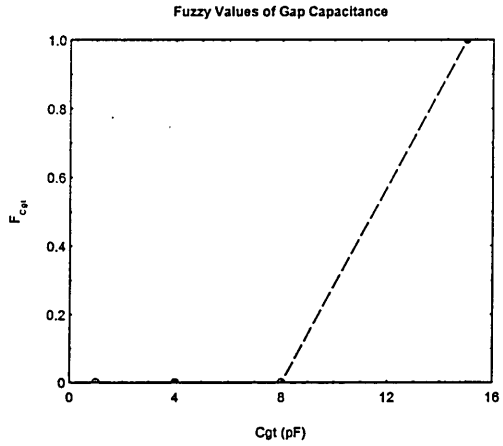

(c)

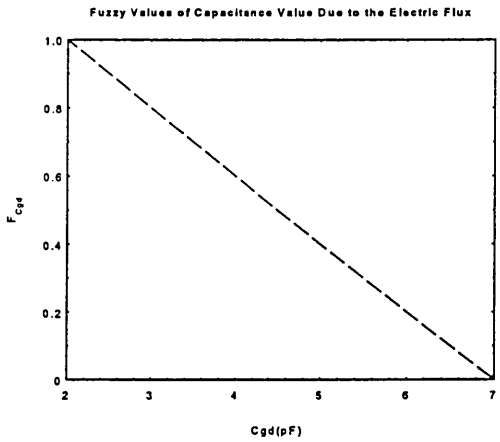

(d)

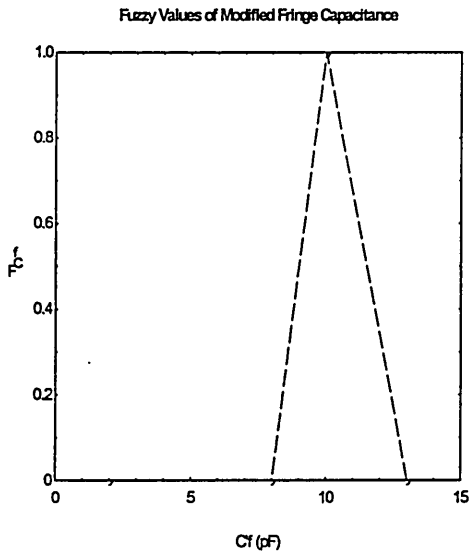

(e)

Figure 4 Fuzzification (a) Cij (b) Cga (c) Cgt (d) Cgd (e) C'f

The α - cuts of all input parameters, with increment of 0.2, obtained from Fig. 4 are listed in Table 3. For a better resolution α - cuts of much smaller value can be used. Using the defuzzified algorithm α - cuts values given in Table 3 are used to calculate the fuzzy values of induced C_{ij} : i.e. F_{ind} and the result is displayed in Fig. 5.a.

The process of defuzzification begins by setting the intersection of preferred and induced capacitance curves in order to obtain f^* and C^*_{ij} (see Fig. 5.b).

These data are then used to obtain the best possible electrical parameters of microstrip lines with the results (calculated) shown in Table 4. Also shown are the prefered values together with the percentage of difference between them.

Fuzzy Values	0.2	0.4	0.6	0.8	1.0
Cga (pF)	[5.4,9.4]	[5.8,8.8]	[6.2,8.2]	[6.6,7.6]	[7.7]
Cgt (pF)	[9.4,9.4]	[10.8,10.8]	[12.2,12.2]	[13.6,13.6]	[15.15]
Cgd (pF)	[6,6]	[5,5]	[4,4]	[3,3]	[2,2]
C'f (pF)	[8.4,12.4]	[8.8,11.8]	[9.2,11.2]	[9.6,10.6]	[10.10]

Table 3 α - cuts of input parameters

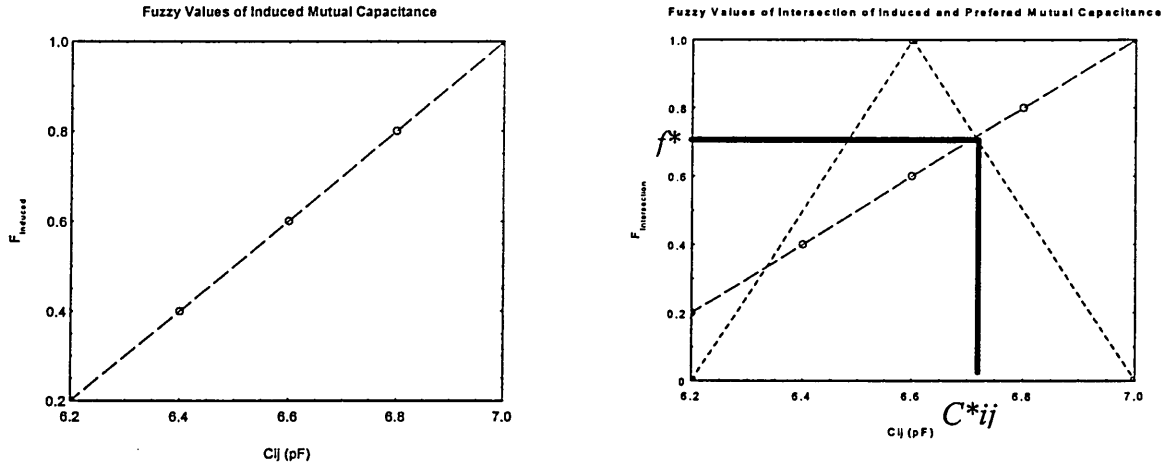

(a) (b)

Figure 5 (a) Induced C_{gd} (b) Intersection of induced and prefered C_{gd}

Parameters	Prefered (A)	Calculated (B)	|A-B|/A .(%)
Cij (pF)	6.6	6.71429	1.73
Cga (pF)	7	6.42857	8.16
Cgt (pF)	15	13	13.33
Cgd (pF)	7	3.42857	51.02
C'f (pF)	10	9.42857	5.71

Table 4 Calculated Values

VI. CONCLUSIONS

A novel technique based on fuzzy logic was presented for optimisation of electrical parameters of microstrip lines. In this approach we fuzzified all the input parameters to create a fuzzy environment. This is then processed by the extension principle to produce the output data. The output data is then defuzzified to extract the best electrical parameters of the microstrip lines. Algorithms for the processed by the extension principle and defuzzication are presented.

An example was included to illustrate the application of the proposed technique.

VII. ACKNOWLEDGMENTS

Tahir Ahmad is financially assisted by Faculty of Science, University of Technology Malaysia, Locked Bag 791, 80990 Johor Bahru, Johor Darul Takzim, Malaysia.
Thanks are due to Dr. N. Sarma and Dr. R. Saatchi of Regional Engineering College, Warangal, India and Sheffield Hallam University, UK, respectively for fruitful discussions.

REFERENCES

[1] Q.J. Zhang, S. Lum and M.S. Nakhla, "Minimization of Delay and Crosstalk in High-Speed VLSI Interconnects", IEEE Trans. Microwave Theory and Techniques, vol. 40, no. 7, July 1992, pp. 1555 - 1563.

2] T. Ahmad, Z. Ghassemlooy and A. K. Ray, "Determination of Physical Parameters for Microstrip Lines by Fuzzy Method", Proc. Second International ICSC Symposia on Intelligent Industrial Automation and Soft Computing, Nimes, France, Sep. 16-19, will be published.

[3] L. Lu and V. Ungvichian, "An Optimization Technique to Minimize Crosstalk in Multi-Layered and Multi-Microstrip-Line Board of High-Speed Digital Circuits", Proc. IEEE Int. Symp. on Electromagnetic Compatibility, Santa Clara, CA, USA, Aug. 19-23, 1996, pp. 442 - 447

[4] T. Terano, K. Asai and M. Sugeno, "Fuzzy Systems Theory and Its Applications", Academic Press Inc., 1987

[5] R. Kruse, J. Gebhardt and F. Klawonn, "Foundations of Fuzzy Systems", John Wiley & Sons, 1994

[6] T. Ahmad, Z. Ghassemlooy, B. Parker, A.K. Ray, and Y.M. Moyal, "On the Analysis of Three Nonuniform Coupled Microstrip Lines", Proc. Third Communication Networks Symposium, Manchester, July 8-9, 1996, pp. 141-145

[7] K.C. Gupta, R. Garg and I.J. Bahl, "Microstrip Lines and Slotlines", Artech House, Dedham, MA:USA

[8] B.H. Parker, "Simulation of Interconnections in High-Speed Integrated Circuits", Thesis for Ph.D, Sheffield Hallam University, UK, 1994

[9] T. Ahmad, Z. Ghassemlooy, A. K. Ray and N. Sarma, "Integration of Fuzzy Logic Into The Experimental Assesment of Coupled Microstrip Lines", submitted.

A Fuzzy Approach in Designing Microstrip Line

T. Ahmad, Z. Ghassemlooy and A. K. Ray
Physical Electronics & Fibre Optics Research Laboratories
Electronics Research Group
School of Engineering
Sheffield Hallam University
Pond Street
Sheffield S1 1WB
England
e-mails: T.Ahmad@shu.ac.uk, Z.F.Ghassemlooy@shu.ac.uk, A.K.Ray@shu.ac.uk
Fax: 0114-2533306

ABSTRACT: This paper presents a new and flexible approach based on fuzzy logic for design optimisation of geometrical parameters of microstrip lines in high speed integrated circuit technology. For all different input conditions optimum parameters are calculated at the output.

I. INTRODUCTION

Recent advances in integrated circuit technology have reduced the single device switching time to tens of picoseconds or less. Unfortunately, the electrical performance of the interconnect do not scale as well, and this results in many unexpected problems such as delay, reflection, ringing and false switching. In many cases the interconnection delay time is often significantly longer than the devices switching time. In such cases the transmission line property of the lines can not be neglected. Therefore, accurate selection of geometrical and electrical parameters, modelling and simulation of such lines in particular their delay and cross-talk have become very important.

2. CROSSTALK

An obvious solution to the problem of delay and reflection is to decrease the length of the interconnections by increasing the density. This solution, however, leads to increase crosstalk [1]. Since there is not a direct relationship between many parameters trade-offs are to be made between various conflicting parameters or factors which in turn will depend on the line geometrical parameters. When working with a large circuits the relationship between the design criteria and a large number of circuit parameters becomes very complicated. For example, to minimise interline crosstalk and at the same time to decrease the delay time, fuzzy theory can be used as a tool for determining the appropriate geometrical parameters of microstrip lines; width, thickness, spacing and height (see Fig. 1) as well as electrical parameters [2,3].

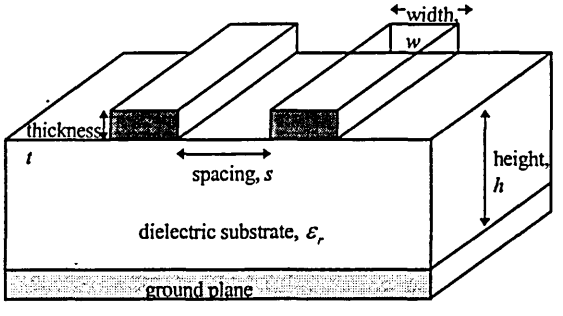

Figure 1.

3. THE APPROACH

The approach (see Fig. 2) adopted in this work is based on fuzzy theory which best expresses inherent uncertainty, vagueness, and imprecision in a relationship encountered in real world [4], hence in microstrip lines. Fuzzy control is carried out by programming the rules of selection used by skilled individual, $A_i \rightarrow B_i$ (i =1, 2, ...n), in which the judgement on manipulated valuable B for a given state A is best made by a computer.

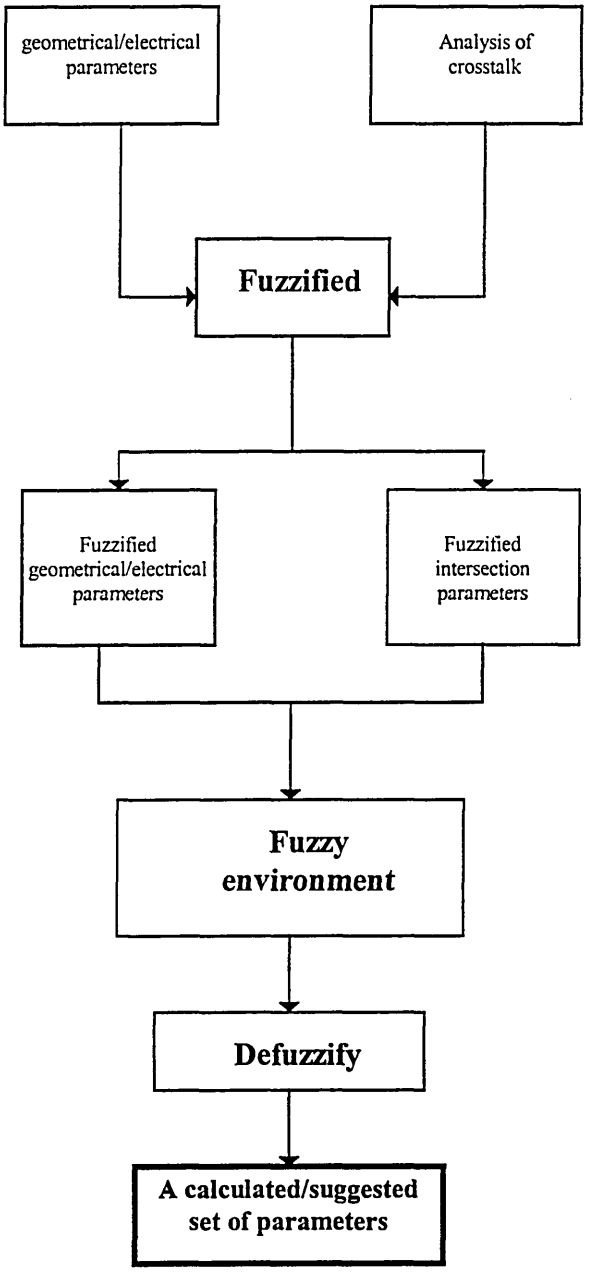

Figure 2. Flow chart of fuzzy algorithm

4. FUZZY ALGORITHM

All the fuzzy sets F_{I_i} expressing preferences of all input parameters $g_i \in I_i \subset R^+ \ (i \in N)$ are determined, normalised and convex. I is a close interval of positive real numbers. Let C_g be a

performance parameter which takes all the input parameters as its variables and is presented by fuzzy set F_{C_g}.

The algorithm to determine a fuzzy set induced on C_g, F_{ind}, has the following steps:

1. Let $C_g: I_1 \times I_2 \times ... \times I_i \rightarrow R$ is the performance parameter $(i \in N)$ such that $r = C_g(g_1, g_2, g_3, ..., g_n)$.
2. Select appropriate values for α - cut, such that $\alpha_1, \alpha_2, \alpha_3, ..., \alpha_k \in (0,1]$ which are equally spaced.
3. Determine all the α_k- cuts for all F_{I_i} $(i \in N)$.
4. Generate all 2^n combinations of the endpoints of intervals representing α_k - cuts for all F_{I_i} $(i \in N)$. Each combination is an n-tuple $(g_1, g_2, g_3, ..., g_n)$.
5. Determine $r_j = C_g(g_1, g_2, g_3, ..., g_n)$ for each n-tuple $j \in 1,2,3,...,2^n$.
6. Set $F_{jind} = [\min r_j, \max r_j]$ for all $j \in 1,2,3,...,2^n$.

For defuzzification the following steps are required:

1. Set $F_{C_g} \cap F_{ind}$.
2. Find the membership value of supremum of step 1, say $f^* = \sup [F_{C_g} \cap F_{ind}]$.
3. Find the C_g value of f^*, say C_g^*.
4. Find f^*- cut of all F_{I_i} $(i \in N)$.
5. Generate all 2^n combinations of the endpoints of interval representing f^*- cut of all F_{I_i} $(i \in N)$. Each combination is an n-tuple $(g_1^*, g_2^*, g_3^*, ..., g_n^*)$.
6. Determine $r_j^* = C_g^*(g_1^*, g_2^*, g_3^*, ..., g_n^*)$ for each n-tuple $j \in 1,2,3,...,2^n$.

5. NUMERICAL SAMPLES

To illustrate the approach, two types of numerical samples are presented. Table 1 and table 2 show when the algorithm is applied to geometrical [5] and electrical [6] parametes of microstrip lines respectively.

	Initial values (A)			Calculated values (B)			|A -B|/A (%)		
Parameters	**Set 1**	**Set 2**	**Set 3**	**Set 1**	**Set 2**	**Set 3**	**Set 1**	**Set 2**	**Set 3**
***Cgd*(10^{-11})F**	5	4	9	5.402	4.281	7.817	8.04	7.02	13.14
Dielectric	9	5	10	8.3	6.614	8.699	7.77	32.28	13.01
Thickness(*um*)	5	4	3	5.3	3.677	3.743	6	8.075	24.76
Width(*um*)	6	5	4	5.8	6.291	4.299	3.33	25.82	7.47
Height(*um*)	9	8	10	8.9	8.645	9.628	1.11	20.35	3.72
Spacing(*um*)	3	5	1	3.3	3.708	1.743	10	25.84	74.3

Table 1. Algorithm applied on geometrical parameters

Parameters	[Min, Prefered (A), Max]	Calculated (B)	|A-B|/A (%)
Cij (pF)	[6.2, 6.6, 7]	6.71429	1.73
Cga (pF)	[5, 7, 10]	6.42857	8.16
Cgt (pF)	[8, 15, 15]	13	13.33
Cgd (pF)	[2, 7, 7]	3.42857	51.02
C'f (pF)	[8, 10, 13]	9.42857	5.71

Table 2. Algorithm applied on electrical parameters

6. CONCLUSION

A novel approach based on fuzzy logic was presented for optimisation of electrical and geometrical parameters of microstrip lines. In this approach we fuzzified all the input parameters to create a fuzzy environment. This is then processed by the extension principle to produce the output data. The output data is then defuzzified to extract the best electrical parameters of the microstrip lines. Algorithm for the processed is presented.

Examples were included to illustrate the application of the proposed technique. It can be incorporated with fuzzified crosstalk [7] information which in turn can produce the best design that can minimize crosstalk.

REFERENCES

[1] Q.J. Zhang, S. Lum and M.S. Nakhla, "Minimization of Delay and Crosstalk in High-Speed VLSI Interconnects", IEEE Trans. Microwave Theory and Techniques, vol. 40, no. 7, July 1992, pp. 1555 - 1563

[2] K.C. Gupta, R. Garg and I.J. Bahl, "Microstrip Lines and Slotlines", Artech House, Dedham, MA:USA

[3] B.H. Parker, "Simulation of Interconnections in High-Speed Integrated Circuits", Thesis for Ph.D, Sheffield Hallam University, UK, 1994.

[4] T. Terano, K. Asai and M. Sugeno, "Fuzzy Systems Theory and Its Applications", Academic Press, Inc., 1987

[5] T. Ahmad, Z. Ghassemlooy and A. K. Ray, "Determination of Physical Parameters for Microstrip Lines by Fuzzy Method", Proc. Second International ICSC Symposia on Intelligent Industrial Automation and Soft Computing, Nimes, France, Sep. 16-19, 1997, will be published.

[6] T. Ahmad, Z. Ghassemlooy and A. K. Ray, "Determination of Electrical Parameters for Microstrip Lines by Fuzzy Method", Proc. World Multiconference on Systemics, Cybernetics and Informatics, Caracas, Venezuela, July 7-11, 1997, will be published.

[7] T. Ahmad, Z. Ghassemlooy, A. K. Ray and N. Sarma "Fuzzified Crosstalk in Microstrip Lines", Proc. Fourth Communication Networks Symposium, Manchester, July 7-8, 1997, will be published.

Determination of Physical Parameters for Microstrip Lines by Fuzzy Method

T. Ahmad, Z. Ghassemlooy and A. K. Ray
Physical Electronics & Fibre Optics Research Laboratories
Electronic Research Group, School of Engineering
Sheffield Hallam University, City Campus, Pond Street
Sheffield S1 1WB, UK

Abstract - **Fuzzy logic is an attractive alternative for design optimisation of geometrical parameters of microstrip lines in high speed integrated circuit technology. In this paper two sets of fuzzy algorithms are presented. Membership functions based on preference/suggested of a given geometrical parameters are fuzzified to create a fuzzy environment. The environment is then processed to produce the optimised geometrical configurations of microstrip lines. An example is presented to illustrate the execution of this technique.**

I. INTRODUCTION

Although single chip devices are now capable of switching at extremely fast rate, but when used in high density PCB interconnects the small line physical geometry will result in many unexpected problems such as delay, reflection, ringing, crosstalk and false switching. In many cases the interconnection delay time is often significantly longer than the devices switching time. In such cases the transmission line property of the lines can not be neglected. Therefore, to minimise signal degradation and crosstalk [1] accurate selection of geometrical parameters, see Fig. 1, modelling and simulation of lines have become very important.

In a large scale circuits the relation between the design criteria and a large number of circuit parameters becomes very complicated. Since there is no direct relation between many parameters then establishing a trade-offs between them is desirable. Recently, Lu and Ungvichian [2] have introduced a multivariable optimisation technique based on spectral domain approach in multi-layered multi-conductor microstrip lines board of high speed digital circuits.

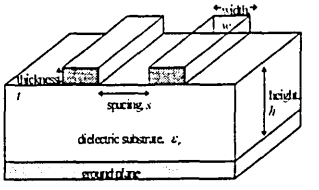

Figure 1

In this paper, we report how fuzzy concept can be used as a design optimisation technique for calculating the physical parameters of microstrip lines. The technique is based on two fuzzy algorithms. In the first algorithm, the geometrical parameters are fuzzified to create fuzzy environment, see Fig. 2. These are then used to calculate the associated fuzzy sets for a performance parameter. The input together with the fuzzified performance parameters are then processed by the extension principle to produce the best and the most appropriate output data. The second algorithm is employed to defuzzified the output data in order to obtain the best possible physical/geometrical configurations of the lines. The developed technique is an important step toward flexible design with an aim to minimise interline crosstalk.

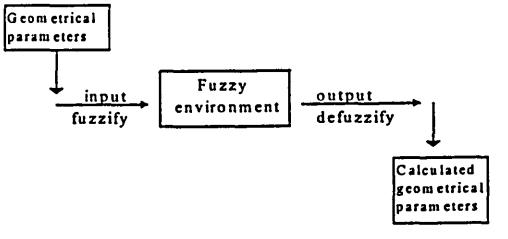

Figure 2 Fuzzy environment

II. PARAMETERS

Variables involved in an engineering design are usually referred to as parameters. These are input, output and performance parameters [4]. The specifications of each of parameters is presented in the Table 1. Functional requirement is assigned to a value or range of values specified for a performance parameter and independent of the design process.

The electrical parameters for microstrip lines [5,6,7,8] have complex mathematical expressions. However, they are best describe by the equation of mutual capacitance of a coupled microstrip lines between line i and j is given as:

$$C_{ij} = \frac{1}{2}[C_{ga} + C_{gd} + C_{gt} - C'_f] \qquad (1)$$

such that C_{ga} is the gap capacitance in air, C_{gd} is the capacitance value due to the electric flux, C_{gt} is the gap capacitance with the inclusion of finite thickness, C'_f is the modified fringe capacitance of a single line due to the presence of another line.

Some of these parameters are shown in Fig. 3. C_f and C_p are the fringe and parallel plate capacitances, respectively [7].

All the electrical parameters of microstrip lines can be considered as performance parameters or output parameters. For this particular example, the former is adopted. On the other hand, all the geometrical parameters of the microstrip lines are input parameters which are predetermined by the designer, consumer or the current state of technology.

Input Parameters *(design parameters)*	**Output Parameters**	**Performance Parameters**
• Independent values are determined during the design process.	• Involve in design process. • Functionally dependent on the input parameters and possibly on some performance parameters. • Not subject to any specified functional requirement.	• Subject to some functional requirement.

Table 1. Type of parameters in engineering design

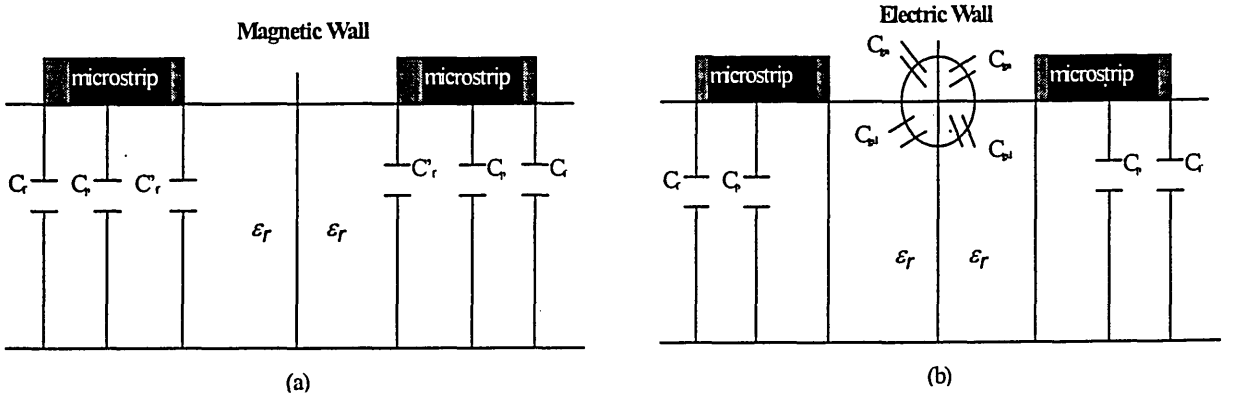

Figure 3 Capacitance (a) even mode (b) odd mode.

III. FUZZY ALGORITHMS

All the fuzzy sets F_{I_i} expressing preferences of all input parameters $g_i \in I_i \subset R^+ \ (i \in N)$ are determined, normalised and convex. I is a close interval of positive real numbers. Let C_g be a performance parameter which takes all the input parameters as its variables and is presented by fuzzy set F_{C_g}.

The algorithm to determine a fuzzy set induced on C_g, F_{ind}, has the following steps:

1. Let $C_g : I_1 \times I_2 \times ... \times I_i \rightarrow R$ is the performance parameter $(i \in N)$ such that $r = C_g(g_1, g_2, g_3, ..., g_n)$.
2. Select appropriate values for α- cut, such that $\alpha_1, \alpha_2, \alpha_3, ..., \alpha_k \in (0,1]$ which are equally spaced.
3. Determine all the α_k- cuts for all $F_{I_i} \ (i \in N)$.
4. Generate all 2^n combinations of the endpoints of intervals representing α_k - cuts for all $F_{I_i} \ (i \in N)$. Each combination is an n-tuple $(g_1, g_2, g_3, ..., g_n)$.
5. Determine $r_j = C_g(g_1, g_2, g_3, ..., g_n)$ for each n-tuple $j \in 1,2,3,...,2^n$.
6. Set $F_{jind} = [\min r_j, \max r_j]$ for all $j \in 1,2,3,...,2^n$.

For defuzzification the following steps are required:

1. Set $F_{C_g} \cap F_{ind}$.
2. Find the membership value of supremum of step 1, say $f^* = \sup [F_{C_g} \cap F_{ind}]$.
3. Find the C_g value of f^*, say C_g^*.
4. Find f^*- cut of all $F_{I_i} \ (i \in N)$.
5. Generate all 2^n combinations of the endpoints of interval representing f^*- cut of all $F_{I_i} \ (i \in N)$. Each combination is an n-tuple $(g_1^*, g_2^*, g_3^*, ..., g_n^*)$.
6. Determine $r_j^* = C_g^*(g_1^*, g_2^*, g_3^*, ..., g_n^*)$ for each n-tuple $j \in 1,2,3,...,2^n$.

IV. NUMERICAL EXAMPLE

To test the validity of these algorithms, the capacitance value due to the electric flux is used as the performance parameter [6,7].

$$C_{gd}(\varepsilon_r, t, w, h, s) = \frac{\varepsilon_0 \varepsilon_r}{\pi} \ln\left[\coth\left(\frac{\pi s}{4h}\right)\right] + 0.65 C_f \left[\frac{0.02}{s/h}\sqrt{\varepsilon_r} + \left(1 - \frac{1}{\varepsilon_r^2}\right)\right] \quad (2)$$

such that $C_f = 0.5\left\{\frac{\sqrt{\varepsilon_{re}}}{cZ_{om}} - \varepsilon_0 \varepsilon_r \frac{w}{h}\right\}$ (3)

where ε_0 and ε_r are permitivity of free space and dielectric, respectively. Z_{om} is the characteristic impedance,

$$Z_{om} = \frac{60}{\sqrt{\varepsilon_{re}}} \ln\left(\frac{8h}{w} + 0.25\frac{w}{h}\right) \quad \text{for } \frac{w}{h} \leq 1 \quad (4)$$

$$Z_{om} = \frac{120\pi}{\sqrt{\varepsilon_{re}}}\left[\frac{w}{h} + 1.393 + 0.667 \ln\left(\frac{w}{h} + 1.444\right)\right]^{-1} \quad \text{for } \frac{w}{h} \geq 1 \quad (5)$$

where $\varepsilon_{re} = \frac{\varepsilon_r + 1}{2} + \frac{\varepsilon_r - 1}{2} F(w/h)$ (6)

and

$$F(w/h) = \begin{cases} (1 + 12h/w)^{-1/2} + 0.04(1 - w/h)^2 & \text{for } \frac{w}{h} \geq 1 \\ (1 + 12h/w)^{-1/2} & \text{for } \frac{w}{h} \leq 1 \end{cases} \quad (7)$$

The domain and suggested set of input parameters are given in Table 2. The suggested value could be any value within the domain. The fuzzified values of these input parameters given shown in Fig. 4. These figures are simple fuzzy numbers [4] where the suggested and minimum/maximum of the domain parameters are set to have the highest and lowest membership values, respectively.

Parameters	Domain	Suggested
Cgd (x 10^{-11})F	3 - 9	5
Dielectric	3 - 10	9
Thickness, *t* (*u*m)	3 - 7	5
Width, *w* (*u*m)	4 - 9	6
Height, *h* (*u*m)	8 - 10	9
Spacing, *s* (*u*m)	1 - 5	3

Table 2 Input parameters.

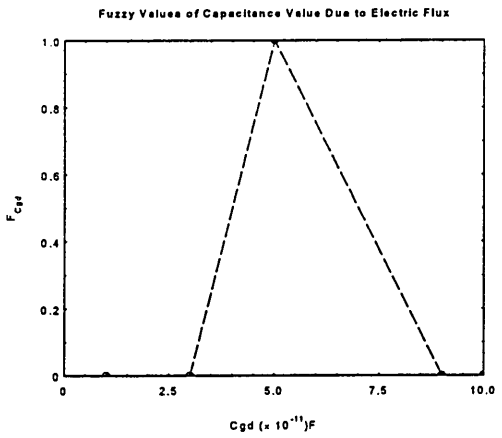

(a)

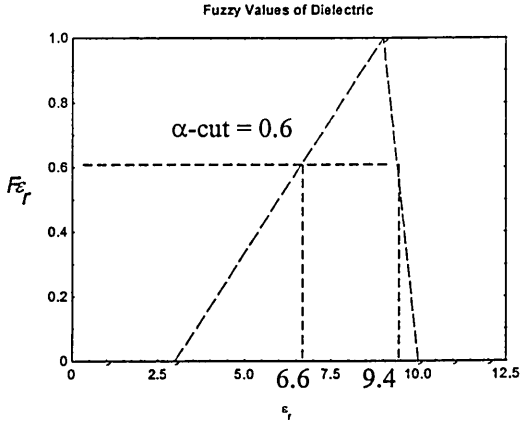

(b)

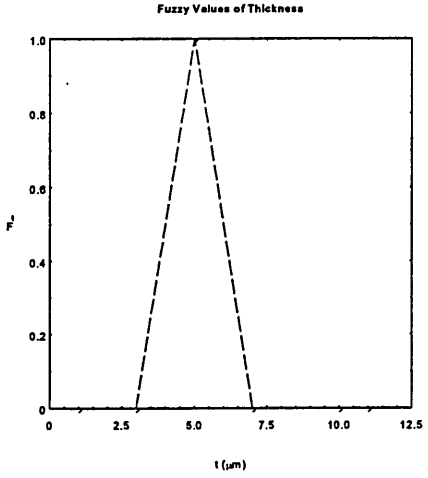

(c)

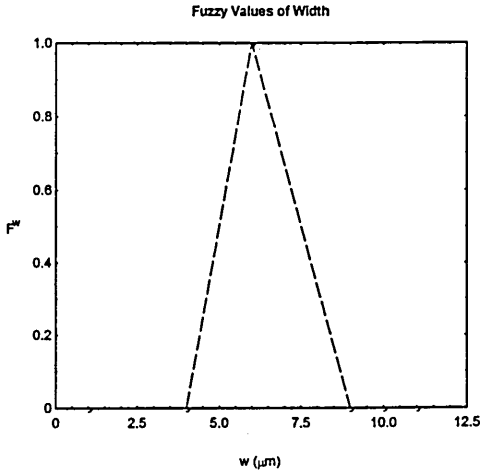

(d)

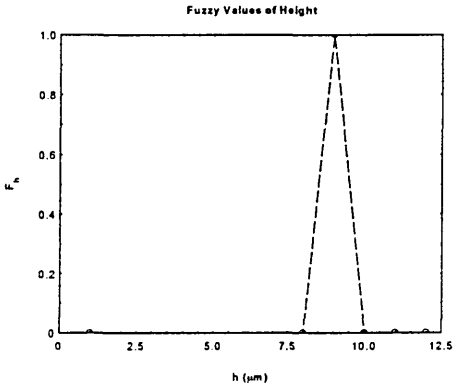

(e)

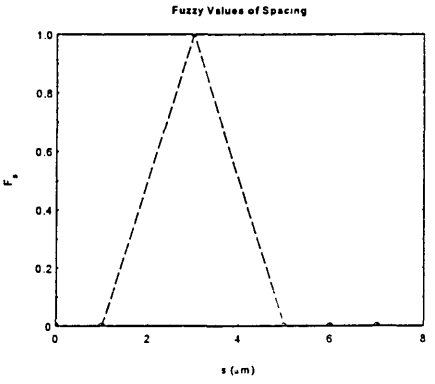

(f)

Figure 4 Fuzzification (a) C_{gd} (b) dielectric (c) thickness (d) Width (e) height (f) spacing.

The α - cuts of all input parameters, with increment of 0.2, obtained from Fig. 4 are listed in Table 3. For a better resolution α - cuts of much smaller value can be used. Using the defuzzified algorithm α - cuts values given in Table 3 are used to calculate the fuzzy values of induced C_{gd}: i.e. F_{ind} and the result is displayed in Fig. 5.a.

The process of defuzzification begins by setting the intersection of preferred and induced capacitance curves in order to obtain f^* and C^*_{gd} (see Fig. 5.b).

These data are then used to obtain the best possible geometrical configurations of microstrip lines with the results shown in Table 4 for three calculated values of C_{gd} . Also shown are the initial input parameters together and the percentage of difference between them.

	α - cuts values				
Input Parameters	**0.2**	**0.4**	**0.6**	**0.8**	**1.0**
Dielectric	[4.2, 9.8]	[5.4, 9.6]	[6.6, 9.4]	[7.8, 9.2]	[9, 9]
Thickness (um)	[3.4, 6.6]	[3.8, 6.2]	[4.2, 5.8]	[4.6, 5.4]	[5, 5]
Width (um)	[4.4, 8.4]	[4.8, 7.8]	[5.2, 7.2]	[5.6, 6.6]	[6, 6]
Height (um)	[8.2, 9.8]	[8.4, 9.6]	[8.6, 9.4]	[8.8, 9.2]	[9, 9]
Spacing (um)	[1.4, 4.6]	[1.8, 4.2]	[2.2, 3.8]	[2.6, 3.4]	[3, 3]

Table 3 α - cuts values of input parameters.

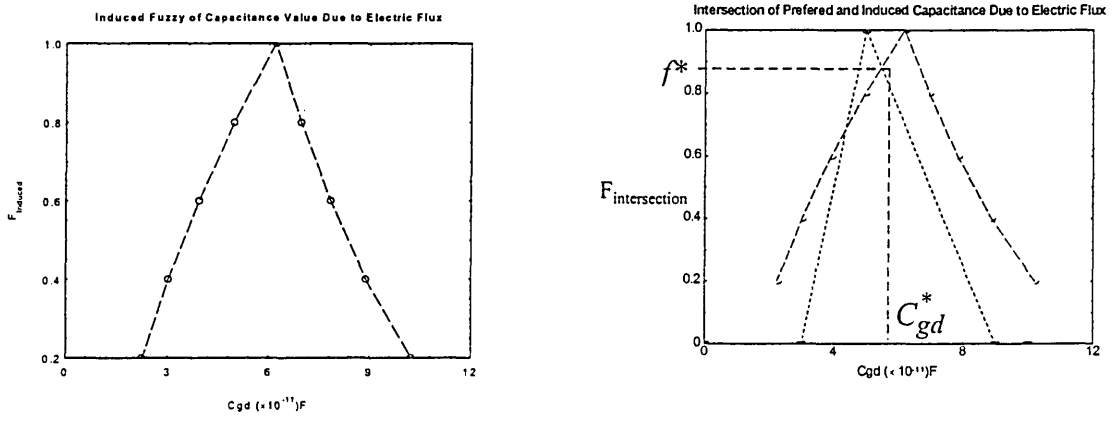

(a) (b)

Figure 5 (a) Induced C_{gd} (b) intersection of induced and preferred C_{gd}.

	Initial values (A)			Calculated values (B)			|A -B|/A (%)		
Parameters	Set 1	Set 2	Set 3	Set 1	Set 2	Set 3	Set 1	Set 2	Set 3
Cgd(10^{-11})F	5	4	9	5.402	4.281	7.817	8.04	7.02	13.14
Dielectric	9	5	10	8.3	6.614	8.699	7.77	32.28	13.01
Thickness(*um*)	5	4	3	5.3	3.677	3.743	6	8.075	24.76
Width(*um*)	6	5	4	5.8	6.291	4.299	3.33	25.82	7.47
Height(*um*)	9	8	10	8.9	8.645	9.628	1.11	20.35	3.72
Spacing(*um*)	3	5	1	3.3	3.708	1.743	10	25.84	74.3

Table 4. Output parameters.

The results shown in Table 4 are the worst possible case where the designer starts off with an initial random input parameters. What this design optimisation tool does is to come up with the most appropriate geometrical parameters. The percentage of difference between the initial and calculated values can be reduced by either changing the initial input parameters or by selecting α - cut increment of < 0.2. This novel technique provides a promising tool in optimisation of geometrical configurations of microstrip lines. The design optimisation can be further improved by including other input parameters such as crosstalk, line delay, skin effect, etc, which is the topic of our current research programme.

V. CONCLUSIONS

A novel technique based on fuzzy logic has been presented for optimisation of geometrical parameters of microstrip lines. In this approach all the input parameters are fuzzified to create a fuzzy environment. This is then processed by the extension principle to produce the output data.

This data is then defuzzified to extract the best geometrical configurations of the microstrip lines. Algorithms to create fuzzy environment and defuzzication are presented.

An example was included to illustrate the application of the proposed technique.

VI. ACKNOWLEDGEMENTS

Tahir Ahmad is financially assisted by Faculty of Science, University of Technology Malaysia, Locked Bag 791, 80990 Johor Bahru, Johor Darul Takzim, Malaysia.
Thanks are due to Dr. N. Sarma and Dr. R. Saatchi of Regional Engineering College, Warangal, India and Sheffield Hallam University, UK, respectively for their fruitful discussions.

REFERENCES

[1] Q.J. Zhang, S. Lum and M.S. Nakhla, "Minimization of Delay and Crosstalk in High-Speed VLSI Interconnects", IEEE Trans. Microwave Theory and Techniques, vol. 40, no. 7, July 1992, pp. 1555 - 1563.
[2] L. Lu and V. Ungvichian, "An Optimisation Technique to Minimise Crosstalk in Multi-Layered and Multi-Microstrip-Line Board of High-Speed Digital Circuits", Proc. IEEE Int. Symp. on Electromagnetic Compatibility, Santa Clara, CA, USA, Aug. 19-23, 1996, pp. 442 - 447.
[3] T. Terano, K. Asai and M. Sugeno, "Fuzzy Systems Theory and Its Applications", Academic Press Inc., 1987.
[4] R. Kruse, J. Gebhardt and F. Klawonn, "Foundations of Fuzzy Systems", John Wiley & Sons, 1994.
[5] T. Ahmad, Z. Ghassemlooy, B. Parker, A.K. Ray, and Y.M. Moyal, "On the Analysis of Three Nonuniform Coupled Microstrip Lines", Proc. Third Communication Networks Symposium, Manchester, July 8-9, 1996, pp. 141-145.
[6] K.C. Gupta, R. Garg and I.J. Bahl, "Microstrip Lines and Slotlines", Artech House, Dedham, MA:USA
[7] B.H. Parker, "Simulation of Interconnections in High-Speed Integrated Circuits", Thesis for Ph.D, Sheffield Hallam University, UK, 1994.
[8] T. Ahmad, Z. Ghassemlooy, B. Parker, A.K. Ray, and Y.M. Moyal, "Analisis Gandingan Mikrojalur Tidak Seragam", (in Malay) Proc. National Sym. of Mathematics VII, Kuala Lumpur, Dec 5-9, 1996, pp. 206-212.

Application of Fuzzy Method for Design Optimisation of High-Speed Interconnects

T. Ahmad, Z. Ghassemlooy, A. K. Ray, and A. Razzaly
Electronics Research Group, School of Engineering
Sheffield Hallam University, City Campus, Pond Street
Sheffield S1 1WB, UK
E-mails:T.Ahmad@shu.ac.uk, Z.F.Ghassemlooy@shu.ac.uk, A.K.Ray@shu.ac.uk
Fax: 0114-2533306

Abstract

In this paper a novel technique for design optimisation of high speed interconnections has been introduced. Optimisation of all geometrical/electrical parameters with the system performance, such as minimum cross-talk, has been implemented using fuzzy method. Membership functions based on preference/suggested geometrical/electrical parameters and cross-talk performance are fuzzified to create a fuzzy environment. The environment is then processed to produce the optimised geometrical configurations for the microstrip lines. An example is presented which illustrates the potential of this technique. To confirm the validity of the proposed technique experimental and simulated results are compared.

1. Introduction

Geometrical parameters of microstrip lines , see Fig. 1, such as the length, spacing, substrate thickness [1] and width [2] have large and complicated effects on cross-talk performance. Several techniques such as the use of shielded/screened lines and multiple dielectric substrates [3], pulse shaping [4] and the idea of building several small simple processors on a chip [5] have been proposed in order to minimise cross-talk. However, these techniques contribute to other problem such as ringing , limited wiring capacity and distortion of the signals [6], and have a complex design procedures. However, some (if not all) of the problems associated with existing techniques may be overcome by implementing the design optimisation in fuzzy logic. This paper demonstrates the potential of fuzzy logic in optimisation of geometrical parameters of a microstrip line with cross-talk performance. Optimised parameters are incorporated into the developed mathematical model. The model is then used to carry out for experimental and simulation measurements. Simulation is carried out by using both P-SPICE and MATHEMATICA [7].

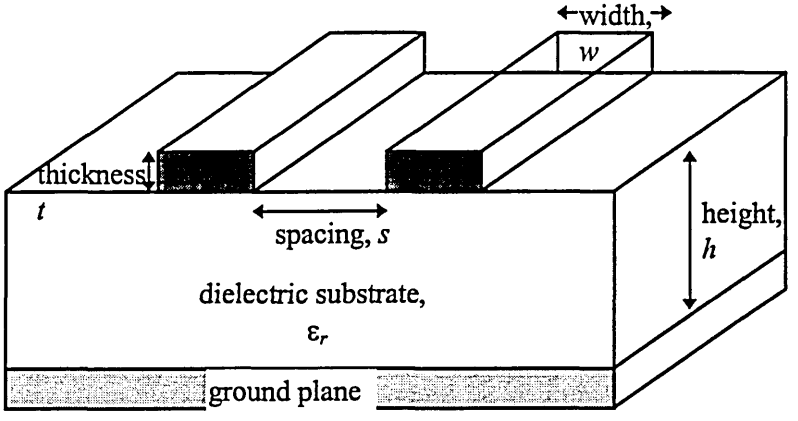

Fig. 1 A coupled of microstrip lines.

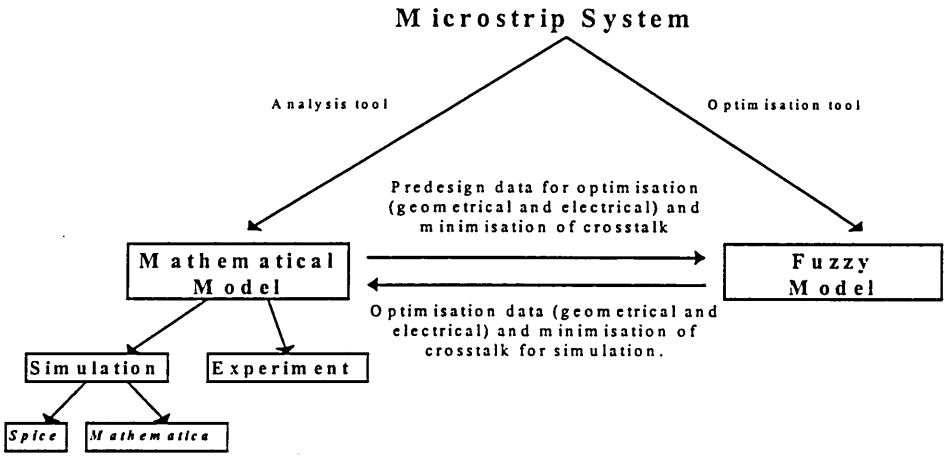

Fig. 2 Mathematical and fuzzy models of microstrip lines.

2. Fuzzy Modelling

The fuzzy model adopted for optimisation is shown in Fig. 3, where three different algorithms [8] has been developed for this purpose, see Fig. 4. The firs algorithms represent the fuzzification of all the input parameters, for this case there are: line spacing s, line mutual capacitance and the measured cross-talk. The fuzzified parameters are then processed in the fuzzy environment by fuzzy intersections, which is carried out by the second algorithm. Finally, the third algorithm is used to implement the defuzzification of the processed data by the extension principle [9] in order to obtain the optimise output parameters.

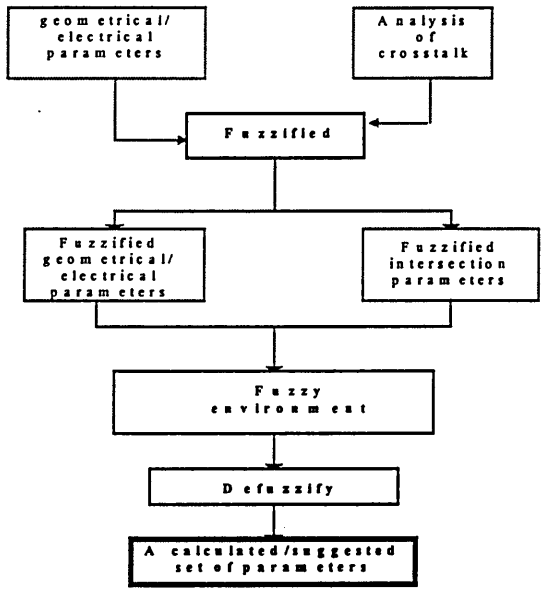

Fig. 3 Fuzzy flow chart.

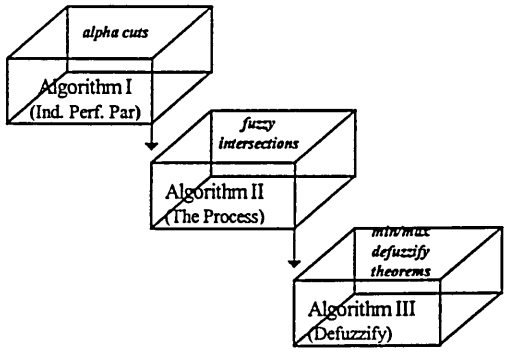

Fig. 4 Fuzzy algorithms blocks.

3. Simulation & Experimental Results

To illustrate the application of the fuzzy model, a set of 8-coupled microstrip lines with geometrical configurations of $\varepsilon_r = 4.7$, $t = 35$ μm, $w = 500$ μm and $h = 1600$ μm, see Fig. 1, was design and a set of cross-talk measurement were carried out. The input parameters include: (i) measured cross-talk values in a range of 0 to -28 dB, (ii) line spacing in a range of 0 to 3500 μm with the preferred value of 2000 μm and (iii) the mutual capacitance in a range of -10 pF to 50 pF with the preferred value of 30 pF. After fuzzification the fuzzified spacing and mutual capacitance are shown in Figs. 5 and 6, respectively.

The figures show that the fuzzy number for minimum and maximum parameters are both zero , whereas the for preferred values it unity. In Figure 5, for fuzzified membership value (or α cut) of 0.45 the spacing intervals are 900 and 2825. How this is obtained is explained as follow:

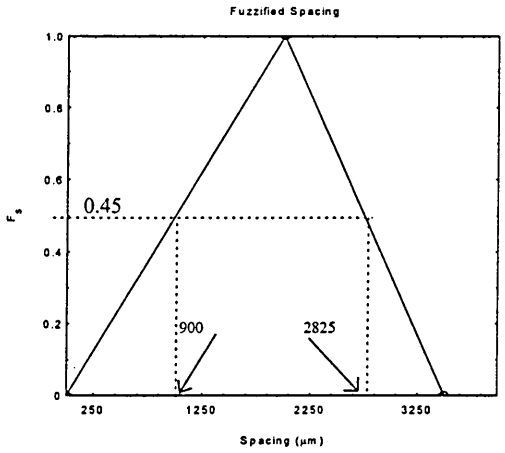

Fig. 5 Fuzzified spacing.

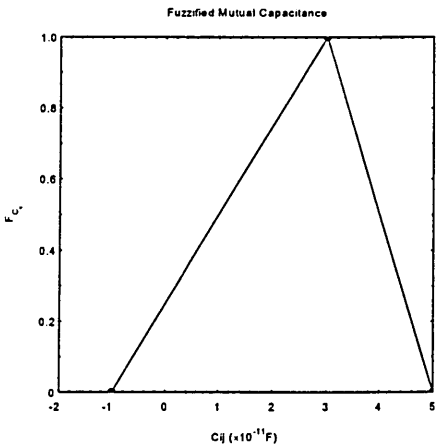

Fig. 6 Fuzzified mutual capacitance.

Figure 7 shows the fuzzified spacing and fuzzified cross-talk [10], where the intersection between them is performed, by using the second algorithm, in order to obtain the fuzzified spacing of 1900 and 2050 corresponding to the fuzified membership value of 0.96. Using the fuzzified interval F_I the induced mutual capacitance are calculated and the results together with fuzzified mutual capacitance are illustrated in Fig. 8. Algorithm three has been use to obtained the intersection between two graphs in order to determine the supremum of the mutual capacitance C_{ij}^* and its fuzzy membership value f^* of 8 pF and 0.45, respectively. Having obtained the fuzzy membership 0f 0.45, it is then applied to the Fig. 5 to obtained the optimum values of the line spacing. As shown in Fig. 5 the intersection gives two of candidate optimised value for the line spacing at of 900 μm and 2828 μm. The corresponding mutual capacitance is then obtained from:

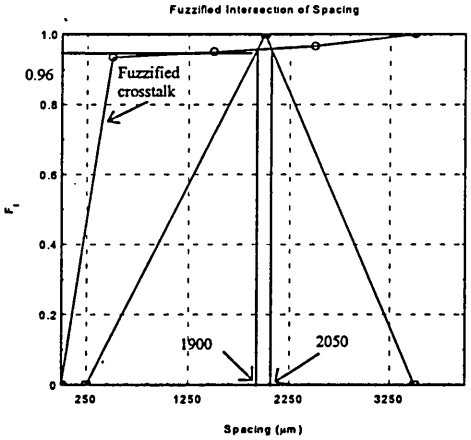

Fig. 7 Intersection between fuzzified spacing and fuzzified cross-talk.

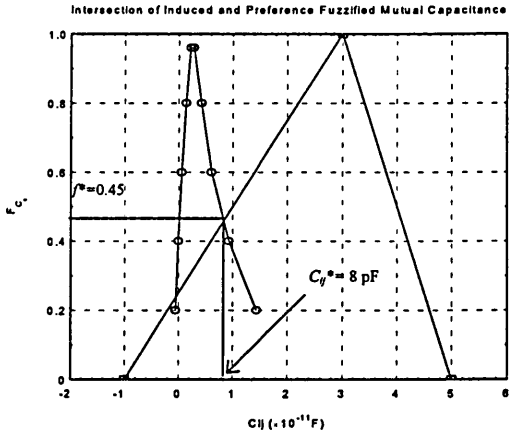

Fig. 8 Intersection of induced and fuzzified mutual capacitance.

$$C_{ij}(\varepsilon_r, t, w, h, s) = \frac{1}{2}\left[C_{ga} + C_{gd} + C_{gt} + C_f'\right] \quad (1)$$

Where, C_{ga} is the gap capacitance in air, C_{gd} is the capacitance due to electric flux, C_{gt} is the gap capacitance s the and C'_f is the modified fringe capacitance.

The difference between the preferred and calculated candidates for line spacing and mutual capacitance are presented in Table 1. The best possible spacing is determined when the difference for the mutual capacitance is at its the lowest value of $s = 900\,\mu m$.

Table 1 Preferred and calculated parameters and their difference.

Optimised Parameters	Domain	Preferred (p)	Calculated (c)	|c-p|/p (%)
Spacing (s) μm	0 - 3500	2000	900 & 2825	55 & 41.3
Mutual Capacitance (C_{ij}) pF	-10 – 50	30	9.8 & 0.1	67 & 99.6

To verify our model a set of 3-coupled microstrip lines with geometrical configurations given as above and spacing of 500 μm were designed and also simulated using coupled TEM model implemented on SPICE package. Time delay and characteristic impedance for the set was also calculated using a developed mathematical model [7]. For both simulation and practical cases, a pulse train of 1 V amplitude was applied to line 1, with all the other lines being terminated with $50\,\Omega$ impedance, and the cross-talk was measured at both ends of the lines. The experimental and simulated results for near and far ends are presented in Figs. 9 and 10, respectively, showing close agreement, in the line 2, to within 2 dB, thus demonstrating the accuracy of the simulation model. The measured cross-talk value of -25 dB was then used as a fuzzy input parameter together with line spacing and the mutual capacitance. The optimised values of the s and C_{ij} were then incorporated into the simulation model and the results for cross-talk is displayed in Fig. 9 and 10, respectively. As expected for optimised values of geometrical and electrical parameters the cross-talk is at its lowest value compared to non-optimised experimental and simulated results. Here, only one geometrical and electrical and performance parameters have been included in the model. However, the model can accommodate multiple of input parameters. This paper illustrates the validity of our model, and the potential of fuzzy logic application in design optimisation of microstrip lines.

3. Conclusions

A novel technique based on fuzzy logic has been presented for optimisation of geometrical/electrical parameters of the microstrip lines with the aim of minimising the cross-talk. In this approach all the input parameters are fuzzified to create a fuzzy environment. The environment is then processed to produce the optimised geometrical configurations of microstrip lines. An example was included to illustrate the validity of the developed model. The optimised results are compared to non-optimised experimental and simulation data, showing improved cross-talk performance. The paper demonstrates the potential use of fuzzy logic in designing high speed in integrated circuits.

4. References

1 SEKI, S. and HASEGAWA, H.: "Analysis of Cross-talk in Very High-Speed LSI/VLSI's Using a Coupled Multiconductor MIS Microstrip Line Model", IEEE Transactions on Microwave Theory and Techn., Vol. MTT-32, No. 12, Dec. 1984, pp. 1715-1720.

2 QIAN, Y. and YAMASHITA, E.: "Characterisation of Picosecond Pulse Crosstalk Between Coupled Microstrip Lines with Arbitrary Conductor Width", IEEE Trans. on Microwave Theory and Techn., Vol. 41, No. 6/7, June/July 1993, pp. 1011-1016.

3 RIZVI, M., and VETRI, J. L.: "Modelling and Reduction of Crosstalk on Coupled Microstrip Line Structures and Multichip Modules: An FDTD Approach" International Journal of Microwave & Milimeterwave Computer-Aided Engineering, January 1996, Vol. 6, Pt. 1, pp. 58-68.

4 POTHECARY, N. M. and RAILTON, C. J.: "Analysis of Crosstalk on High-Speed Digital Circuits Using The Finite Difference Time-Domain Method", Int. Journal of Numerical Modelling: Electronic Networks, Devices and Fields, Vol. 4, 1991, pp. 225-240.

5 SCIENCE AND TECHNOLOGY: "The Middle Age of the Transistor", The Economist, Jan. 3 - 9th, 1998, pp. 77-79.

6 CHILO, J., and ARNAUD, T.: "Coupling Effects in the Time Domain for an Interconnecting Bus in High-Speed GaAs Logic Circuits", IEEE Trans. on Electron Devices, Vol. ED-31, No. 3, March 1984, pp. 347-352.

7 AHMAD, T.: "Mathematical and Fuzzy Modelling of Interconnection in Integrated Circuit", Thesis for Ph.D, Sheffield Hallam University, UK, 1998 (submitted).

8 AHMAD, T., GHASSEMLOOY, Z., and RAY, A. K.: "Determination of Physical Parameters for Microstrip Lines by Fuzzy Method", Proc. of the Second Int. ICSC Symp., Nimes, France., 17-19 Sep 1997, pp. 25-31.
9 KRUSE, J. G., and KLAWONN, F.: "Foundations of Fuzzy Systems", John Wiley & Sons, 1994, pp. 1-77, Chap. 1-2.
10 AHMAD, T., GHASSEMLOOY, Z., RAY, A. K., and SARMA, N.: "Fuzzified Crosstalk in Microstrip Lines", Proc. Fourth Comm. Netw. Symp., Manchester, UK., 7-8 July 1997, pp. 34-38.

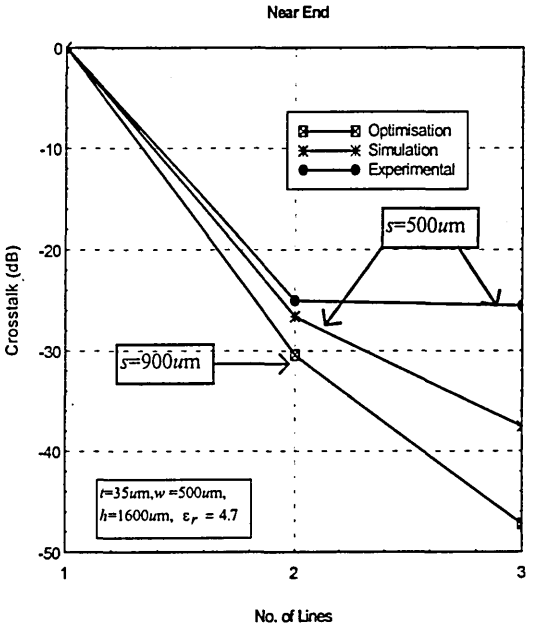

Fig. 9 Cross-talk near ends.

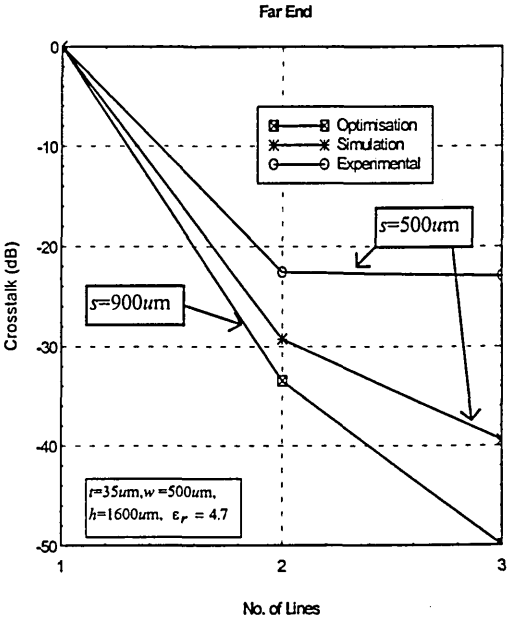

Fig. 10 Cross-talk far ends.